Université du Québec

Institut National de la Recherche Scientifique

Centre Eau Terre Environnement

Le devenir et l'élimination de la ciprofloxacine et de ses complexes métalliques dans les stations d'épuration

Par

Agnieszka Cuprys

Thèse présentée pour l'obtention du grade de

Philosophiae Doctor (Ph.D.)

en sciences de l'Eau

Jury d'évaluation

Examinateur externe	Safia Hamoudi, Professeure *Université Laval*
Examinateur externe	Ahmad Abdel-Mawgoud Saleh, Professeur *Université Laval*
Examinateur interne	Yann LeBihan, Chercheur *CRIQ, Québec, Canada*
Codirecteur de recherche	Tarek Rouissi, *GS Impact Global Solutions,* *Québec, Canada*
Directeur de recherche	Satinder Kaur Brar, Professeure *INRS-ETE, Québec, Canada*
Codirecteur de recherche	Patrick Drogui, Professeur *INRS- ETE, Québec, Canada*

© Droits réservés de *(Agnieszka Cuprys)*, 13 décembre 2019

RÉMERCIEMENTS

I sincerely thank my Ph.D. supervisor, Professor Satinder Kaur Brar for her guidance and suggestions during my doctoral training. Her constant support and encouragement kept me motivated and helped me to become a better researcher.

I would like to thank my co-supervisor, Professor Patrick Drogui, for his suggestions and advice that have guided me to improve my work for this Ph.D. project. I would like to express my gratitude for my co-supervisor, Dr. Tarek Rouissi for a great scientific support and constructive discussions. I am also extremely thankful for their help in preparation of my doctoral examination.

I would like to thank my jury members, Dr. Yann Le Bihan (CRIQ, Canada), Professor Safia Hamoudi (Laval University, Canada) and Professor Ahmad Abdel-Mawgoud Saleh (Laval University, Canada). Despite their busy schedules, they agreed to provide me the guidance, advice and comments.

I sincerely thank INRS Emeritus Professor, Prof. P.G.C. Campbell whose discussion and thoughts helped me understand the essentials of my work. I am very grateful to François Proulx, Professeur associé at Laval University and the director of the Division de la qualité de l'eau, Quebec for his help in investigating the water quality in Quebec City area. I would like to thank all the laboratory personnel form INSR, especially Sebastien Duval, for rescuing me every time I needed it, and Stéfane Moïse, for fighting alongside me to understand the logic behind ciprofloxacin's behaviour.

I would like to express my gratitude to Water, Environment, Sanitation and Health (WESH) research team at Norwegian University of Life Sciences (NMBU), Norway, especially Dr. Zakhar Maletskyi and Dr. Harsha Ratnaweera for accepting me for the internship at their laboratory. I would like to thank Sven Andreas Högfeldt, MSc, for technical and scientific support during my stay at NMBU.

During my studies, I had a great support of my teammates, who always helped me with apiece of advice or encouragement. Hence, I would thank from the bottom of my heart to all my colleagues, especially Dr. Krishnamoorthy Hegde, Dr. Tayssir Kadri, Dr. Mitra Naghdi, Dr. Merhdad Taheran, Javier Fernandez Reynes, Pratik Kumar, Joseph Sebastian, Carlos Osorio, Mariana Valdez, Saba Miri and Rahul Sani. Special thank for Mona Chaali who enormously helped me with the French part of this thesis. I owe special thanks to people who adopted me to their Indo-Canadian family, supported me scientifically and personally, and never let me give up: Gayatri Suresh, Akhil Soman and Rama Pulicharla, Dr. Vinayak Pachapur and Preetika Pachapur. Also, I would like to thank Dr. Joanna Lecka for always being ready to listen.

Finally, I would like to give my sincerest thanks to my parents, grandmothers and my sister for their constant support and encouragement. I wouldn't reach here without them.

RÉSUMÉ

La ciprofloxacine (CIP) est un antibiotique à large spectre appartenant à la famille des fluoroquinolones. Son utilisation fréquente a contribué à sa détection répandue dans l'environnement à de très faibles concentrations. Les processus de traitement actuels de l'usine de traitement des eaux usées (STEP) ne permettent pas d'éliminer efficacement les contaminants à l'état de traces. Les objectifs principaux de cette thèse étaient d'étudier le devenir de la CIP dans l'environnement et au cours du traitement des eaux usées, ainsi que de tester de nouvelles techniques d'enlèvement. Premièrement, la stabilité de cinq complexes de CIP-métal (CIP-Me) a été étudiée. Les ions métalliques visés étaient Al^{3+}, Co^{2+}, Cu^{2+}, Fe^{3+} et Mg^{2+} en raison de leur prévalence dans les eaux usées et les boues d'épuration. Les complexes de CIP-Al sont les plus stables, suivis de CIP-Cu et CIP-Co. Les complexes entre CIP et Fe3 + et Mg2 + présentaient les plus grandes variations de la stabilité des complexes. La présence de substances humiques (HS) a diminué la stabilité de tous les complexes. La toxicité des complexes CIP-Me a également été évaluée. Dans l'eau ultrapure, les complexes CIP-Me présentent une toxicité plus élevée vis-à-vis d'*Enterobacter aeruginosa* à Gram négatif, la toxicité vis-à-vis de *Bacillus subtilis* à Gram positif étant constante pour les complexes (avec l'exception CIP-Mg) et le CIP seul. La présence de HS réduit l'activité antimicrobienne des complexes CIP-Me d'au moins 2 fois vis-à-vis de *E. aeruginosa*. Cependant, la toxicité vis-à-vis de *B. subtilis* est restée pratiquement inchangée.

La complexation des antibiotiques avec des ions métalliques peut affecter leur distribution dans la station d'épuration, ce qui n'est généralement pas pris en compte. L'étude analytique a été menée pour évaluer la concentration de CIP, de chlorotétracycline (CTC) et d'autres ions choisis dans la station d'épuration. Plus de 70% des CTC ont été récupérés lors du traitement des eaux usées lorsque la concentration de CIP était légèrement supérieure dans les effluents par rapport aux eaux usées de l'affluent. De plus, une concentration élevée de CIP et de CTC, soit 3,9 mg/kg, respectivement 11 mg/kg, a été détectée dans les fractions solides de boues. Cette concentration élevée pourrait être due aux interactions avec les ions métalliques dans les boues. Par conséquent, la spéciation des ions dans les boues a été effectuée pour les localiser plus précisément. La concentration correspondante d'antibiotiques dans chaque fraction de boues a également été évaluée. L'introduction d'antibiotiques dans l'environnement peut contribuer à la pression sélective et à l'expansion de la résistance bactérienne. L'enquête sur les bactéries résistantes au CTC/CIP dans les eaux du Québec a été étudiée. La réaction en chaîne de la polymérase a été utilisée pour vérifier la présence de trois agents pathogènes d'origine hydrique les plus fréquents, à savoir *Salmonella sp., Shigella sp.* ou *Campylobacter jejuni* dans l'eau de la région de Québec.

Pour minimiser le problème ci-dessus, l'amélioration de la station d'épuration est nécessaire. Dans le cadre de la thèse, trois systèmes ont été testés: l'oxydation électro-enzymatique ultérieure, l'oxydation enzymatique via un extrait de laccase brute et l'adsorption sur du biochar fonctionnalisé. La combinaison d'une électro-oxydation suivie d'une oxydation enzymatique a conduit à une élimination de la CIP de 97 à 99% en environ 6 heures. Dans le même temps, l'oxydation brute médiée par la laccase ne réduisait la

concentration de l’antibiotique qu’à 68%. L'adsorption sur du biochar fonctionnalisé avec du chitosane a entraîné l'élimination de CIP à 36%, ainsi que 10% d'As, 98% de Cd et 73% de Pb.

Abstract

Ciprofloxacin (CIP) is a broad-spectrum antibiotic, belonging to the fluoroquinolone family. The frequent usage of CIP has contributed to its widespread detection in the environment at very low concentrations. The current treatment processes of the wastewater treatment plant (WWTP) are not efficient in removing trace concentration contaminants. The main objectives of this thesis were to investigate the fate of CIP in the environment and during the wastewater treatment, as well as to test novel techniques for its removal. Firstly, the stability of five CIP-metal complexes (CIP-Me) was investigated. The targeted metal ions were Al^{3+}, Co^{2+}, Cu^{2+}, $Fe^{3+,}$ and Mg^{2+} due to their prevalence in wastewater and wastewater sludge. The complexes of CIP-Al were found to be the most stable, followed by CIP-Cu and CIP-Co. The complexes between CIP and Fe^{3+} and Mg^{2+} exhibited the greatest variations in the stability of the complexes.. The presence of humic substances (HS) decreased the stability of all complexes. In addition, the antimicrobial activity of CIP-Me complexes was also evaluated. In ultrapure water, CIP-Me complexes exhibit higher toxicity towards Gram-negative *Enterobacter aeruginosa,* where the toxicity against Gram-positive, *Bacillus subtilis* was constant for complexes (except CIP-Mg) and CIP alone. The presence of HS reduced the antimicrobial activity of CIP-Me complexes by at least 2-fold towards *E. aeruginosa*. However, the toxicity towards B. subtilis remained almost unchanged.

The complexation of antibiotics with metal ions may affect their distribution in WWTP, which is usually not taken into consideration. Hence, the analytical study was conducted to evaluate the concentration of CIP, chlortetracycline (CTC) and other chosen ions in the WWTP. More than 70% of CTC was recovered during wastewater treatment where the concentration of CIP was slightly higher in effluent than the influent wastewater. Additionally, a high concentration of CIP and CTC, 3.9 mg/kg 11 mg/kg respectively, was detected in the solid fractions of sludge. This elevated concentration might have been due to interactions with metal ions in sludge. Hence, the ion speciation in sludge was performed to localize them more precisely. The corresponding concentration of antibiotics in each sludge fraction was also evaluated. The introduction of antibiotics to the environment may contribute to the exertion of selective pressure and expansion of bacterial resistance. The investigation of CTC/CIP-resistant bacteria in Quebec waters was investigated. Polymerase Chain Reaction was used to verify the presence of three most common waterborne pathogens, i.e. *Salmonella* sp., *Shigella* sp. and *Campylobacter jejuni* in water from Quebec area.

To minimize the above problem, the improvement of WWTP is needed. As a part of the thesis, three systems were tested for CIP removal: subsequent electro-enzymatic oxidation, enzymatic oxidation via crude laccase extract and adsorption onto functionalized biochar. The combination of electrooxidation followed by enzymatic oxidation led to 97-99 % removal of CIP in around 6 hours. At the same time, crude laccase-mediated oxidation decreased the antibiotic's concentration only to 68%. The adsorption on chitosan-functionalized biochar led to 36% removal of CIP, along with 10% of As, 98% of Cd and

73% of Pb. The tested methods have the potential for their application in wastewater treatment, however, further studies are needed.

PUBLICATIONS DE CETTE THÈSE

1. **Cuprys A.,** Pulicharla R. Brar S.K, Drogui P., Verma M., Surampalli R.Y. Fluoroquinolones metal complexation and its environmental impacts; *Coordination Chemistry Reviews,* Volume 376, 2018, Pages 46-61
2. **Cuprys A.,** Pulicharla R., Lecka J., Brar S.K., Drogui P., Surampalli R.Y., Ciprofloxacin-metal complexes –stability and toxicity tests in the presence of humic substances, *Chemosphere*, 2018, doi.org/10.1016/j.chemosphere.2018.03.117
3. **Cuprys A.,** Lecka J., Proulx F., Brar S.K., Drogui P., Appearance of ciprofloxacin/chlortetracycline-resistant bacteria in waters of Québec City in Canada, *Journal of Infection and Public Health*, 2019, doi.org/10.1016/j.jiph.2019.04.012
4. **Cuprys A.,** Lecka J., Brar S.K., Rouissi T., Drogui P., Speciation of ions and its influence on antibiotics distribution in wastewater sludge, *(*to be submitted*)*
5. **Cuprys A.,** Thompson P., Ouarda Y., Suresh G., Rouissi T., Brar S.K., Drogui P., Surampalli R.Y., Novel approach for ciprofloxacin removal via sequential electrooxidation and enzymatic oxidation, *Journal of Hazardous Materials* (accepted)
6. **Cuprys A.,** Thompson P., Suresh G., Rouissi T., Brar S.K., Drogui P., Potential of agro-industrial produced laccase to remove ciprofloxacin, (to be submitted)
7. **Cuprys A.,** Sebastian J., Maletskyi Z., Rouissi T., Högfeldt S.A., Ratnaweera H., Brar S.K., Drogui P., Functionalized adsorbent for simultaneous removal of heavy metal ions and ciprofloxacin, (to be submitted)

PUBLICATION EN DEHORS DE CETTE THÈSE

1. Kadri T., **Cuprys A.,** Rouissi T., Brar S.K., Daghrir R., Lauzon J-M., Nanoencapsulation and release study of enzymes from *Alkanivorax borkumensis* in chitosan-tripolyphosphate formulation, Biochemical Engineering Journal, Volume 137, 2018, P: 1-10
2. Suresh G., Cabezudo I., Pulicharla R., **Cuprys A.**, Rouissi T., S.K. Brar, Biodegradation of Aflatoxin B_1 with cell-free extracts of *Trametes versicolor* and *Bacillus subtilis*. *Food Control* (2019). (Submitted)

CONFÉRENCES

1. **Cuprys A.,** Pulicharla R. Brar S.K, Drogui P., Verma M., Surampalli R.Y. (2018). Fluoroquinolones metal complexation and its environmental impacts. International Symposium on Metal Complexes, June 3-5, 2018, Florence, Italy
2. **Cuprys A.,** Brar S.K., Drogui P. (2018). Ciprofloxacin: its distribution during wastewater treatment and its potential removal improvement. The 2nd International Conference on Advanced Materials and Processes for Environment, Energy and Health. October 31- November 02, 2018, Montreal, Canada

TABLE DES MATIÈRES

LISTE DES TABLEAUX

LISTE DES FIGURES

LISTE DES ÉQUATIONS

LISTE DES SIGLES ET ABRÉVIATIONS

ABTS	2,2'-azino-bis(3-ethylbenzothiazoline-6-sulphonic acid
AOP	Advanced oxidation process
ARB	Antibiotic-resistant bacteria
ARG	Antibiotic-resistance genes
AS-BC	Almond shell biochar
ASE	Accelerated solvent extractor
BDD	Boron-doped diamond
CH-BB	Chitosan-biochar bead
CIP	Ciprofloxacin
CMI	= MIC
CTC	Chlortetracycline
dNTP	Deoxynucleotide
EDTA	Ethylenediaminetetraacetic acid
ENR	Enrofloxacin
FQs	Fluoroquinolones
FTIR	Fourier-Transform Infrared Spectroscopy
GAC	granulated activated carbon
GTI	Gatifloxacin
HS	Humic substances
ICP-AES	Inductively Coupled Plasma Atomic Emission Spectroscopy
LC-MS/MS	liquid chromatography coupled with tandem mass spectrometry
LOME	lomefloxacin
Me	Metal
MI	Metal Ion
MIC	Minimal inhibitory concentration
MMO	Mixed metal oxides

NOR	Norfloxacin
OFL	Ofloxacin
PCR	Polymerase chain reaction
PM-BC	Pig-manure biochar
PW-BC	Pine wood biochar
SA	syringaldehyde
SDS	Sodium dodecyl sulfate
SEM	Scanning electron microscopy
SS	suspended solids
STEP	Station d'épuration de eaux usée
TEU	Traitement de eaux usée
TOC	total organic carbon
TS	total solids
VS	volatile solids
WW	Wastewater
WWS	Wastewater sludge
WWTP	Wastewater treatment plant

CHAPTER ONE

SYNTHÈSE

INTRODUCTION

La découverte de la pénicilline par Alexander Fleming dans les années 1920 marqua une étape décisive pour le médicament qui déclencha la révolution des antibiotiques. Cependant, l'utilisation fréquente et le développement rapide d'antimicrobiens ont contribué à leur détection répandue dans les compartiments environnementaux [1-3]. Leur apparition a conduit à exercer une pression sélective sur les microorganismes présents dans les écosystèmes contaminés. Cela a abouti à la sélection et à la dissémination de bactéries résistantes aux antibiotiques (ARB) et aux gènes (ARG) [4].

La ciprofloxacine (CIP) est un FQ à large spectre efficace contre les bactéries à Gram négatif et à Gram positif, utilisé pour le traitement des infections des voies respiratoires et urinaires, des infections de la peau et des structures cutanées, des infections des os et des articulations, de la diarrhée infectieuse et de la fièvre typhoïde. La CIP a été classée parmi les antimicrobiens les plus couramment prescrits au Canada entre 2012 et 2017 [5]. Son utilisation fréquente a permis la détection de la CIP dans divers compartiments environnementaux, tels que les effluents des stations de traitement des eaux usées (STEP) (42-721 ng/L) [6, 7], les eaux des rivières (30-77 ng/L) [8], les sédiments. (1,65-156 ng/g) [8, 9] et des eaux usées (200 à 650 ng/L) [10].

La présence de CIP dans les écosystèmes exerce une pression sélective sur les communautés bactériennes, ce qui entraîne une augmentation des souches résistantes à la CIP. Par exemple, la CIP est connue comme antimicrobien pour le traitement des infections à *Neisseria gonorrhoeae* [11]. Au Canada, en 2014, l'apparence élevée d'isolats de *N. gonorrhoeae* résistants à la CIP a été rapportée (34%), alors qu'en 2004, son niveau était d'environ 5%. La présence accrue de souches d'*Escherichia coli* multirésistantes (FQ, céphalosporines de troisième génération et aminoglycosides) a été observée dans les pays de l'Union européenne entre 2013 et 2016, ce qui a été signalé comme une tendance les années précédentes [12]. De plus, le CIP, comme d'autres FQ, a la capacité de former des complexes stables avec des ions métalliques (MI) [13]. La formation de complexes CIP-métaux est un phénomène répandu dans tous les compartiments environnementaux, en raison de la prévalence de métaux (Me) dans l'eau et le sol [13]. Cette propriété modifie les propriétés physico-chimiques du CIP, c'est-à-dire la solubilité, l'affinité d'adsorption, mais aussi son activité antimicrobienne.

La raison de l'augmentation de la concentration de CIP et d'autres antibiotiques dans l'environnement est principalement due à leur métabolisme incomplet et à leur élimination inappropriée. En fait, de 8% (trovafloxacine) à 83% (gatifloxacine) d'antibiotique peuvent être libérés dans l'urine et les matières fécales sous forme active dans l'environnement [14]. Par exemple, la CIP sous forme inchangée est excrétée à 65% dans l'urine et à 25% dans les matières fécales [15]. Les médicaments sont introduits dans l'eau, puis se retrouve dans la station d'épuration. Cependant, ces installations ne sont pas conçues pour éliminer les faibles quantités de composés organiques. L'élimination inefficace par les stations

d'épuration entraîne une accumulation d'antibiotiques dans l'eau et le sol. Ces dernières années, de nombreuses études ont été menées pour améliorer le taux de dégradation des antimicrobiens. La CIP s'est révélé être un médicament persistant et difficilement biodégradable; le taux de dégradation variait entre 37 et 86% [16]. Malgré la forte hydrophilie de la CIP (logK_{OW} = 0,28), celle-ci a une forte affinité avec les boues; même 39% de la CIP peut être absorbée par les boues d'épuration non traitées [16].

Plusieurs techniques ont été testées pour augmenter le taux d'élimination de la CIP pendant le traitement des eaux usées (TEU). Les méthodes d'oxydation se sont révélées efficaces pour la dégradation du CIP. Les études précédentes ont montré que la CIP est sensible à la présence de radicaux libres, à savoir $^{\cdot}OH$, $^{\cdot}N_3$ ou $SO_4^{\cdot-}$ [17, 18]. Toutefois, des problèmes tels que la formation de sous-produits liée à l'oxydation, ou les couts plus élevés sont imprévisibles [19, 20]. Les méthodes d'oxydation écologique, c'est-à-dire l'utilisation d'enzymes microbiennes, ont également prouvé leur efficacité pour éliminer la CIP [21, 22]. Cependant, la transformation du composé est généralement un processus lent. L'autre méthode prometteuse pour l'élimination de la CIP est l'adsorption [23-25]. Les principaux avantages de cette méthode sont le faible coût de l'adsorbant et l'absence de génération de sous-produits. Cependant, l'influence de divers facteurs sur le traitement de l'eau, tels que la présence d'ions métalliques, n'est généralement pas prise en compte. Il est donc nécessaire d'étudier plus leurs effets possibles sur les taux de dégradation du CIP.

Références

1. Berkner, S., S. Konradi, and J. Schönfeld, *Antibiotic resistance and the environment—there and back again.* EMBO Reports, 2014. **15**(7): p. 740-744.

2. Xu, J., et al., *Occurrence of antibiotics and antibiotic resistance genes in a sewage treatment plant and its effluent-receiving river.* Chemosphere, 2015. **119**: p. 1379-85.

3. Koba, O., et al., *Antibiotics degradation in soil: A case of clindamycin, trimethoprim, sulfamethoxazole and their transformation products.* Environ Pollut, 2017. **220**(Pt B): p. 1251-1263.

4. Sharma, C., et al., *Antimicrobial Resistance: Its Surveillance, Impact, and Alternative Management Strategies in Dairy Animals.* Front Vet Sci, 2017. **4**: p. 237.

5. Canada, P.H.A.o., *CANADIAN ANTIMICROBIAL RESISTANCE SURVEILLANCE SYSTEM UPDATE 2018*. 2018, Public Health Agency of Canada.

6. Miao, X.S., et al., *Occurrence of antimicrobials in the final effluents of wastewater treatment plants in Canada.* Environ Sci Technol, 2004. **38**(13): p. 3533-41.

7. Lee, H.B., T.E. Peart, and M.L. Svoboda, *Determination of ofloxacin, norfloxacin, and ciprofloxacin in sewage by selective solid-phase extraction, liquid chromatography with fluorescence detection, and liquid chromatography--tandem mass spectrometry.* J Chromatogr A, 2007. **1139**(1): p. 45-52.

8. Gibs, J., et al., *Occurrence and partitioning of antibiotic compounds found in the water column and bottom sediments from a stream receiving two wastewater treatment plant effluents in Northern New Jersey, 2008.* Sci Total Environ, 2013. **458**: p. 107-116.

9. Zhou, L.J., et al., *Trends in the occurrence of human and veterinary antibiotics in the sediments of the Yellow River, Hai River and Liao River in northern China.* Environ Pollut, 2011. **159**(7): p. 1877-85.

10. Vieno, N.M., T. Tuhkanen, and L. Kronberg, *Analysis of neutral and basic pharmaceuticals in sewage treatment plants and in recipient rivers using solid phase extraction and liquid chromatography–tandem mass spectrometry detection.* J Chromatogr A, 2006. **1134**(1): p. 101-111.

11. Fenton, K.A., et al., *Ciprofloxacin resistance in Neisseria gonorrhoeae in England and Wales in 2002.* The Lancet, 2003. **361**(9372): p. 1867-1869.

12. Control, E.C.f.D.P.a., *Surveillance of antimicrobial resistance in Europe 2016. Annual Report of the European Antimicrobial Resistance Surveillance Network (EARS-Net)*, in *Surveillance of antimicrobial resistance in Europe*. 2017, Stockholm: EDCD.

13. Uivarosi, V., *Metal complexes of quinolone antibiotics and their applications: an update.* Molecules, 2013. **18**(9): p. 11153-97.

14. Zhanel, G.G., et al., *The new fluoroquinolones: A critical review.* Can J Infect Dis, 1999. **10**(3): p. 207-38.

15. Frade, V.M.F., et al., *Environmental contamination by fluoroquinolones.* Braz J Pharm Sci, 2014. **50**: p. 41-54.

16. Jia, A., et al., *Occurrence and fate of quinolone and fluoroquinolone antibiotics in a municipal sewage treatment plant.* Water Res, 2012. **46**(2): p. 387-94.

17. An, T., et al., *Kinetics and mechanism of advanced oxidation processes (AOPs) in degradation of ciprofloxacin in water.* Applied Catalysis B: Environmental, 2010. **94**(3): p. 288-294.

18. Sui, M., et al., *Heterogeneous catalytic ozonation of ciprofloxacin in water with carbon nanotube supported manganese oxides as catalyst.* J Hazard Mater, 2012. **227-228**: p. 227-36.

19. Zhou, Z. and J.Q. Jiang, *Reaction kinetics and oxidation products formation in the degradation of ciprofloxacin and ibuprofen by ferrate(VI).* Chemosphere, 2015. **119 Suppl**: p. S95-100.

20. Rajasulochana, P. and V. Preethy, *Comparison on efficiency of various techniques in treatment of waste and sewage water – A comprehensive review.* Resource-Efficient Technologies, 2016. **2**(4): p. 175-184.

21. Parra Guardado, A.L., et al., *Effect of redox mediators in pharmaceuticals degradation by laccase: A comparative study.* Process Biochemistry, 2019. **78**: p. 123-131.

22. Prieto, A., et al., *Degradation of the antibiotics norfloxacin and ciprofloxacin by a white-rot fungus and identification of degradation products.* Bioresour Technol, 2011. **102**(23): p. 10987-95.

23. Carabineiro, S.A.C., et al., *Adsorption of ciprofloxacin on surface-modified carbon materials.* Water Research, 2011. **45**(15): p. 4583-4591.

24. Wu, S., et al., *Adsorption of ciprofloxacin onto biocomposite fibers of graphene oxide/calcium alginate.* Chemical engineering journal, 2013. **230**: p. 389-395.

25. Mekhamer, W. and S. Al-Tamimi, *Removal of ciprofloxacin from simulated wastewater by pomegranate peels.* Environmental Science and Pollution Research, 2019. **26**(3): p. 2297-2304.

1. REVUE DE LITTÉRATURE

Une partie de ce chapitre est basée sur l'article de synthèse publié (Annexe 1) et a été mise à jour avec les données récentes de la littérature.

1.1. Présence de fluoroquinolones dans l'environnement

Les fluoroquinolones (FQ) sont une famille d'antibiotiques de synthèse à large – spectre d'application et qui ont été développés dans les années 1970 [1]. Ils font partie des antibiotiques quinolones étant donné la structure de la quinine antipaludique. La caractéristique principale de FQ est un atome de fluor attaché au système cyclique central. Les antibiotiques FQ les plus courants sont présentés dans le Tableau 1.1.

L'un des FQs les plus utilisés est ciprofloxacine (CIP). Il est souvent détecté dans différents compartiments environnementaux. Par exemple, il est largement présent dans les eaux usées municipales non traitées: dans le Maryland, aux États-Unis, la concentration de CIP était de l'ordre de 1900 ng/L; celle d'ofloxacine (OFL) était de 600 ng/L [2]. De plus, la fréquence de détection de CIP était de 100%, sur tous les sites d'échantillonnage. En Finlande, parmi toutes les produits pharmaceutiques cibles (FQ, bêta-bloquants, antiépileptiques) les FQ, en particulier la CIP (200-650 ng/L), étaient les composés les plus fréquemment détectés dans les eaux d'égout [3]. Lors du traitement des eaux usées, les FQs ont tendance à s'adsorber aux boues. Par exemple, la CIP était l'antibiotique le plus répandu dans les boues de station d'épuration suédoise (1.6-11 mg/kg) [4]. Miao et al. (2004) ont étudié les effluents finaux dans les stations d'épuration dans cinq villes canadiennes (i.e. Le district régional du Grand Vancouver, Colombie - Britannique, Calgary, Alberta, Burlington, Peterborough et Windsor en Ontario), ils ont détecté principalement les: CIP, norfloxacine (NOR) et OFL avec des concentrations moyennes de 118, 50 et 94 ng/L, respectivement [5]. Lee et al. (2007) ont étudié une station d'épuration en Ontario, au Canada, et ont découvert que la concentration de CIP dans les effluents entre l'entrée et la sortie variait entre 42 et 721 ng/L [6].

Outre que les échantillons d'eaux usées, les autres compartiments de l'environnement ont été également étudiés. Selon l'étude de Gibs et al. (2013), dans le New Jersey, aux États-Unis, la concentration de CIP dans les eaux de Hohokus Brook (en aval de la station d'épuration) a augmenté de 0,03 µg/L à 0,077 µg/L entre 2001 et 2008 [7]. En outre, sur le même site d'échantillonnage, deux antibiotiques FQs ont été détectés dans les sédiments: OFL (21 µg/kg) et CIP (10 µg/kg), qui étaient le deuxième et troisième concentrations les plus élevées d'antibiotiques, après l'antibiotique macrolide l'azithromycine (44 µg/kg). Dans les rivières chinoises, les FQs (CIP, NOR, OFL, lomefloxacine) ont présenté la plus forte concentration dans leurs sédiments (comprise entre 1,67-156 ng/g) parmi les quatre classes d'antibiotiques ciblées [8].

De nos jours, une attention particulière a été portée à la co-contamination par des antibiotiques avec des ions métalliques. De nombreux produits pharmaceutiques, y compris les FQs, possèdent la capacité de former des complexes métalliques qui peuvent modifier les propriétés des FQs, c'est-à - dire modifier l'activité antimicrobienne de l'antibiotique [9-11], la solubilité [12] ou la biodisponibilité [13]. Des études plus approfondies ont été effectuées pour de nombreux complexes pharmaceutiques -métalliques, à savoir les tétracyclines, les quinolones ou les β- lactames [11, 14-17]. Il a été prouvé que la présence des ions métalliques modifie l'adsorption et la désorption d'antibiotique [18-20], la photolyse [21-23] ou l'absorption [17, 24].

1.2. Fluoroquinolones: usage médical, structure, propriétés physicochimiques

L'efficacité de la première génération du FQ était principalement contre les bactéries Gram–négatives [25]. Cependant, en raison des modifications de leur structure, la nouvelle génération de FQs possède un effet antimicrobien à large spectre vis -à - vis des souches Gram-positives et Gram-négatives. Les FQs sont principalement utilisés pour traiter les infections au niveau de la peau, des voies urinaires, gastro-intestinales et respiratoires ou les maladies sexuellement transmissibles [26, 27]. Leur structure diffère des quinolones en raison d'un atome de fluor fixé au noyau central de la C-6 anneau de position et de la pipérazine (ou un autre N-hétérocycle) à la position C-7 (Tableau 1.1). L'addition de ces deux groupes a amélioré l'activité des antibiotiques et les propriétés pharmacocinétiques [28]. Deux groupes ionisables sont présents dans la structure des FQs, à savoir un groupe carboxylique en C-3 et un groupe pipérazinyle en C-7, avec deux constantes de dissociation macroscopiques pK_{a1} et $pK_{a2,}$ respectivement, comme représenté sur la Figure 1.1.

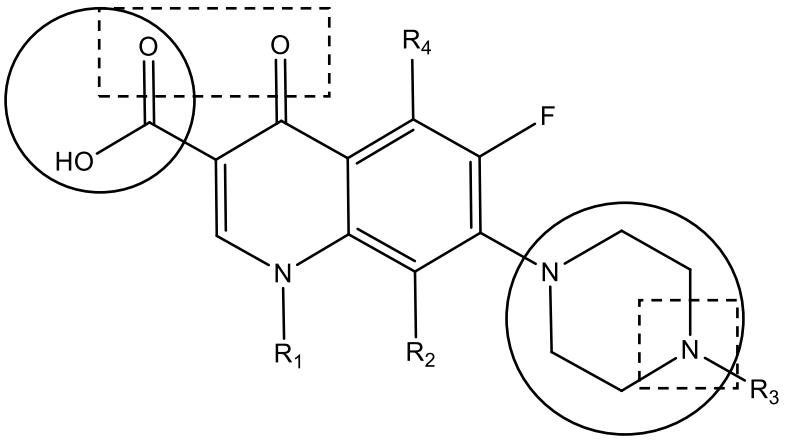

Figure 1. 1 Structure de la fluoroquinolone ceux avec des sites de liaison possibles (encadré en rectangles) et la position des groupes ionisables, responsable de valeurs du pK_a (encadré en cercles)

Différents substituants modifient les caractéristiques du composé, à savoir un atome de fluor supplémentaire (lomefloxacine (LOME)) ou un groupe méthoxy (GTI) en C-8, groupe cyclopropane (CIP, sparfloxacine) et un groupe éthyle (NOR, LOME) en N-1 dans le noyau central, groupe amine en

C-5 (sparfloxacine), divers N-hétérocycles en C-7, [1, 25]. Cependant, les groupes en C-4 (groupe carbonyle), ainsi qu'en C-2 (atome d'hydrogène) et C-3 (groupe carboxyle) restent inchangés en raison de leur rôle clé dans l'activité antibactérienne [25, 29]. En milieu aqueux, la FQ peut exister dans la forme protonée lorsque le pH est acide (H_2FQ^+). À pH égal à 1, cette forme est présente à près de 100%. La forme zwitterionique (HFQ^{+-}) ou non chargée (HFQ^0) se produit à pH légèrement acide ou neutre et prend la forme anionique lorsque le pH est alcalin (FQ^-) [30-32]. En général, les FQs existent sous forme de zwitterion, dans un large spectre de pH (le pH peut varier entre 3 et 11) [32].

Les FQs ciblent deux enzymes bactériennes, essentielles à la réplication et/ou à la transcription de l'ADN qui sont l'ADN gyrase et la topoisomérase IV [25, 33]. L'ADN gyrase est une enzyme bactérienne qui catalyse le superenroulement négatif de l'ADN double brin. La topoisomérase IV est responsable de la partition de l'ADN chromosomique après la réplication de l'ADN. Les FQs forment un complexe ternaire stable comprenant l'antibiotique, l'enzyme et le segment d'ADN. Les FQs se lient à l'ADN via des atomes d'oxygène se trouvant dans les groupements carbonyle et carboxylate par des liaisons hydrogène, comme le montre la Figure 1.2A, tandis que l'atome de fluor, le groupe N-hétérocycle en C-7 et l'ion carboxylate sont liés à l'enzyme [1]. Ceci conduit à la restriction de l'activité enzymatique et bloque la régulation des changements conformationnels dans le chromosome bactérien lors de la réplication et la transcription de l'ADN. Il provoque probablement le clivage de l'ADN et la libération d'extrémités d'ADN double brin, suivies par la mort cellulaire [33].

La présence de Mg^{2+} est essentielle en raison de son rôle de médiateur entre les FQ, l'ADN et les enzymes ciblées. L'importance des ions magnésium dans le déroulement de l'ADN, en présence de FQ, a été observée par Tornaletti et Pedrini (1988) [34]. Plus tard, le rôle médiateur de Mg^{2+} a été confirmé par Palu et al. (1992) [35]. Par la suite, les chercheurs se sont concentrés sur l'étude de l'interaction FQ-Mg-ADN-enzyme; Sur la base de la structure cristalline, il a été prouvé que les ions magnésium sont chélatés par les FQs via deux atomes d'oxygène dans les groupements carboxylique et carboxyle des FQs [36-39]. D'autres travaux, portant sur les complexes CIP-Me, ont suggéré que le complexe CIP-Mg est lié à l'ADN, principalement au groupement phosphate [40]. Deux groupes de chercheurs ont réussi à obtenir la structure cristalline du complexe entre les FQs et la topoisomérase IV médiée par les ions magnésium [29, 41]. Il a été prouvé que les ions magnésium sont coordonnés par la molécule FQ via des atomes d'oxygène du groupe carboxylique (C-3) et un groupe carboxyle (C-4) (fig. 1.2 B) [29, 41].

Tableau 1. 1 Structures, usage médical et propriétés physico-chimiques des représentants des fluoroquinolones. Données obtenues de la base de données de composés PubChem

Structure de quinolone	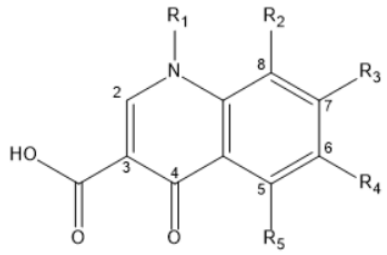									
Nom du composé	R_1	R_2	R_3	R_4	R_5	PubChem CID	Poids moléculaire [g/mol]	$logK_{ow}$	pK_a	Solubilité (dans l'eau) [mg/L]
Ciprofloxacine (CIP)		-H	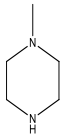	-F	-H	2764	331.347	0.28	pK_{a1}=6.09 pK_{a2}=8.74	30.0 (20°C)
Gatifloxacine (GTI)		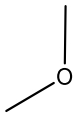	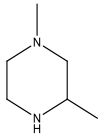	-F	-H	5379	375.4	2.6	pK_{a1}=5.69** pK_{a2}=8.73**	60 (at pH4)
Norfloxacine (NOR)	$-CH_2CH_3$	-H	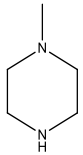	-F	-H	4539	319.336	0.46	pK_{a1}= 6.34 pK_{a2}=8.75	0.28 (25 ° C) *La solubilité dans l'eau dépend du pH et augmente fortement à pH <5 ou pH> 10*

Ofloxacine (OFL)	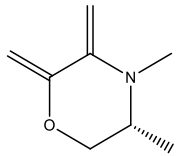	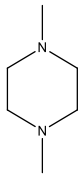	-F	-H	4583	361.373	-0.39	pK_{a1}= 5.97 pK_{a2}=9.28	28.3

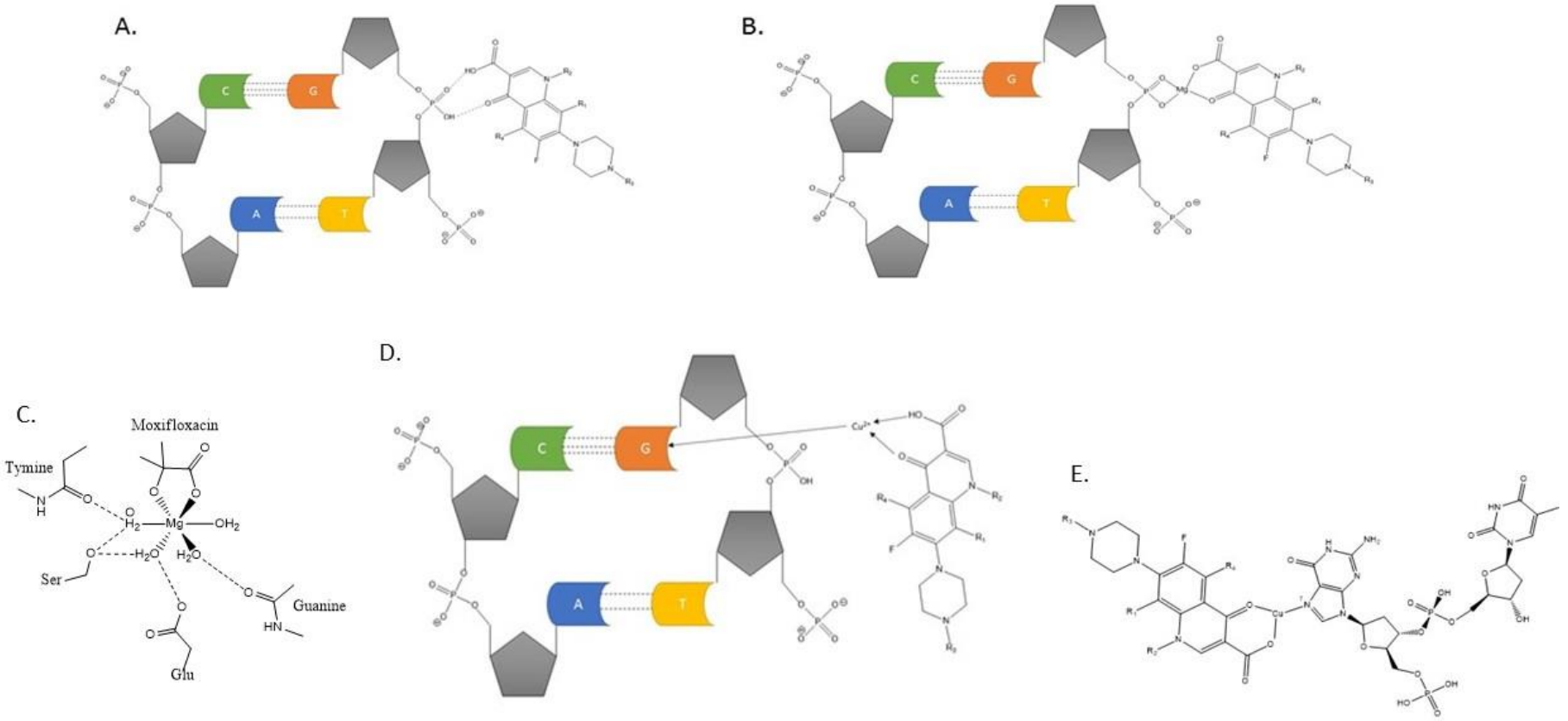

Figure 1. 2 Liaison schématique entre l'ADN et A. fluoroquinolone; B. fluoroquinolone via un pont de magnésium; C. Sphère de coordination autour de Mg^{2+} basée sur la structure cristalline du complexe moxifloxacine, ADN et ions magnésium [29] ; D. fluoroquinolone via un ion de transition en tant que médiateur; E. liaison entre N-7 au niveau de la guanine et de la fluoroquinolone, lorsqu'un ion de transition agit comme médiateur - la présence d'installations ioniques la liaison de la fluoroquinolone

Plus tard, les ions Mg^{2+} coordonnées avec des molécules d'eau se lient à l'un des enzymes par des liaisons hydrogène (fig. 1.2 C), tandis que les groupes en C-1 et C-8 FQ s'intercalent avec l'ADN. Il a été observé que les bases entourant l'antibiotique adaptent la molécule FQ et dirigent les atomes polaires de base Mg^{2+} et ses molécules d'eau coordonnées [29]. Le groupe N-hétérocyclique en C-7 ouvre la poche entre la sous-unité enzymatique et l'ADN. La Figure 1.2 C présente la sphère de coordination autour de l'ion magnésium, qui montre l'importance du Mg^{2+} dans l'interaction entre la moxifloxacine, l'ADN et l'ion métallique - comme décrit ci-dessus, en raison des molécules d'eau coordonnées, le complexe moxifloxacine-Mg peut se lier à bases d'ADN et enzyme. Cependant, les études sur la GTI ont confirmé que le Mg^{2+} en se liant au groupe phosphate de l'ADN, pourrait également jouer le rôle de pont dans l'interaction FQ - ADN [42]. En outre, différents ions divalents, à avoir Cu^{2+}, Cd^{2+}, et Co^{2+}, peuvent augmenter capacité de liaison de GTI à l'ADN - ions de transition se lient avec une N-7 de la base de purine de l'ADN, qui est à l'intérieur de sa molécule (fig. 1.2 D). Ils facilitent la liaison du FQ en jouant le rôle d'intermédiaire entre GTI et l'ADN (fig. 1.2 E) [42]. Les propriétés médiatrices des ions dans l'interaction FQ-ADN ont également été confirmées pour OFL et Cu^{2+},' loméfloxacine et Cu^{2+}, Ni^{2+},' Co^{2+}, Zn^{2+} [43].

En général, les ions de magnésium sont considérés comme étant les plus puissant dans les liaisons ADN-enzyme-FQ, même si sa constante déformation logβ avec FQ est relativement faible si on la compare par rapport à d'autres ions métalliques (l$og\beta_{Mg}$ peut être comprise entre 10 et 12, $log\beta_{Cu}$ = 13-29, $log\beta_{Zn}$ = 11-26, Tableau 1.3.. Parmi les complexes testés, le Mg^{2+} a la capacité la plus faible de se lier aux bases de l'ADN, mais il se lie fortement au groupe phosphate de l'ADN. Cependant, il n'y a pas assez de données sur l'influence exacte des ions métalliques sur l'interaction FQ – enzyme – ADN. Par conséquent, des études approfondies doivent être effectuées pour comprendre l'importance de complexation FQ-métal au niveau moléculaire.

1.3. Complexation des métaux aux fluoroquinolones

La formation de complexes FQ-métal altère généralement les propriétés du composé en question. Le premier rapport concernait la mauvaise absorption de la CIP en présence d'un antiacide contenant du magnésium/aluminium [13]. La diminution de l'absorption est due à la formation de CIP et de chélate de métal ionique. Depuis, des études approfondies de complexation métallique FQ ont été effectuées.

1.3.1. La capacité des FQ à former des complexes

La structure des FQs leur permet de former des complexes métalliques. La Figure 1.1 présente les sites de liaison potentiels FQ-métalliques. Une description détaillée des propriétés de liaison FQs comme présenté par Turel (2002) [44], mis à jour par Serafin et Stanczak (2009) [45] et plus récemment par Uivarosi V. (2013) [32]. Habituellement, ils agissent en tant que ligand via l'un des atomes d'oxygène présent dans le groupe carboxylique et l'un des atomes d'oxygène du cycle carbonyle [9, 46, 47]. Ils

peuvent également coordonner les ions dans une manière unidentée par l'intermédiaire d'un atome d'azote terminal dans le groupe pipérazinyle [46]. Rarement, il est possible de former un complexe FQs-métal par deux atomes d'oxygène carboxyle ou par deux atomes d'azote pipéraziniques [48, 49]. Par conséquent, on peut constater que les FQs peuvent se complexer de plusieurs manières avec les métaux. Cela rend difficile l'étude des complexes FQs-Me.

L'étude thermodynamique de la décomposition a été proposée pour avoir une meilleure idée sur le mécanisme de complexation. L'énergie d'activation (E^*), l'entropie d'activation (ΔS^*), l'enthalpie d'activation (ΔH^*) et l'énergie libre de Gibbs (ΔG^*) des complexes NOR-Me sont présentés dans Tableau 1.2 [50-52]. Ils ont été calculés graphiquement en adaptant les équations de Coats – Redfern comme indiqué en Eq. 1-3 [53]:

$$\Delta S^* = R \cdot ln(Ah/kT) \qquad Eq.\ 1$$

$$\Delta H^* = E^* - RT \qquad Eq.\ 2$$

$$\Delta G^* = \Delta H^* - T\,\Delta S^* \qquad Eq.\ 3$$

où R est la constante des gaz, A est la constante de Arrhenius, h est la constante de Planck, k est la constante de Boltzmann, T est la température maximale de décomposition. Les valeurs d'énergie d'activation de décomposition sont relativement élevées et montrent la stabilité thermique du complexe. Tous les complexes présentent des valeurs négatives de ΔS^*, ce qui augmente de la valeur globale de ΔG^*. Cela indique que le processus de décomposition est non spontané et que la réaction est désavantagée. Les valeurs positives de ΔH^* indiquent que le processus est endothermique - le système nécessite de l'énergie pour que la réaction se poursuive. Globalement, les données présentées dans le Tableau 1.2 prouve que FQs forment des complexes stables avec les ions métaux.

Tableau 1. 2 Paramètres thermodynamiques de la procédure de décomposition de la norfloxacine (NOR) complexation métallique

Composé	Gamme de température [K]	E^* [kJ mol^{-1}]	ΔS^* [JK^{-1}mol^{-1}]	ΔH^* [kJ mol^{-1}]	ΔG^* [kJ mol^{-1}]	Ref.
NOR	336–458	4.43	-1.78	4.11	1.1	[50]
	537–735	12.6	-1.73	12.1	2.25	
	844–996	17.5	-1.74	16.7	3.28	
[Mn(NOR)$_2$](OAc)$_2$· 8H$_2$O	305–369	3.65	-1.74	3.38	0.91	
	727–827	24.5	-0.26	23.9	2.19	

Composé	Gamme de température [K]	E^* [kJ mol^{-1}]	ΔS^* [JK^{-1}mol^{-1}]	ΔH^* [kJ mol^{-1}]	ΔG^* [kJ mol^{-1}]	Ref.
$[Fe(NOR)_3]Cl_3 \cdot 12H_2O$	316-383	9.33	-0.007	9.05	0.903	
	597-694	15.3	-0.526	14.8	1.81	
$[Co(NOR)_2]SO_4\ 8H_2O$	312-372	8.02	-0.399	7.44	0.907	
	706-909	11.1	-1.63	10.04	2.4	
$[Cd(NOR)_2]Cl_2 \cdot 2H_2O$	303-413	37.98	-129.2	37.48	45.23	[52]
	413-843	27.96	-87.45	25.31	53.30	
	843-1273	71.28	-104.4	65.29	140.5	
$[Cd(NOR)_2](NO_3)_2$	373-696	71.66	-133.0	68.67	116.6	
	696-1173	56.79	-96.26	51.14	116.6	
$[Hg(NOR)_2]Cl_2$	323-423	116.2	-83.50	115.6	109.7	
	423-693	59.40	-146.8	57.15	96.79	
	693-923	49.82	-69.82	45.74	93.18	
$[Hg(NOR)_2](NO_3)_2$	323-773	17.24	-67.41	14.17	39.11	
$[Zn(NOR)_2]Cl_2 \cdot 2H_2O$	303-413	46.75	-116.5	46.21	53.78	
	473-583	113.6	-80.39	111.0	136.7	
$[Zn(NOR)_2]Br_2$	423–1273	205.0	-67.52	16.34	50.10	

1.3.2. Équilibre des complexes FQs-métaux

Les FQs se lient avec les ions divalents dans un rapport 1: 1 ou 1: 2 (métal: ligand) et avec les ions trivalents dans un rapport 1: 1 ou 1: 3, rarement 1: 2 [9, 32], Ces rapports molaires sont également dépendant du pH. Par exemple, lors de la complexation CIP-Cu, le rapport est de 1:1 est à pH acides, mais à pH plus élevé, il se forme un complexe à un rapport de 1:2 [54]. De plus, il a été découvert que les FQs forment des complexes plus stables avec les cations trivalents qu'avec les divalents. Les complexes FQs les moins stables sont ceux contenant du magnésium (II) et du calcium (II) [55, 56]. Le facteur qui influence également la stabilité du complexe est la constante diélectrique du solvant [57]. La

constante diélectrique ε (permittivité relative) est la capacité du support à isoler les charges. Elle est également liée à la polarité chimique des médias. Dans les solutions, lorsque la constante diélectrique est élevée (par exemple, l'eau, ε = 78), il n'y a pas d'association d'ions en raison de la polarisation élevée du milieu, les ions métalliques et les FQs sous forme ionique existeraient sous forme d'ions libres. Cependant, lorsque ε est plus faible (par exemple, MeOH, ε = 32,6), le complexe peut être formé via un appariement ionique [57]. Par conséquent, plus la constante diélectrique est faible, plus le composé est stable en raison de la plus forte apparition d'association d'ions. Cependant, la formation de complexes métalliques est une réaction privilégiée et le composé créé présente une stabilité élevée, ce qui entraîne la formation de complexes même dans l'eau (constante diélectrique élevée). La formation de complexes dépend également du pH en raison de l'ionisation du composé [58]. Les FQs sont zwitterioniques, en raison de la présence d'un groupement acide carboxylique et du groupement pipérazinyle basique. Lorsque le pH est faible (acide), le groupe basique sera ionisé plus fortement. Avec l'augmentation du pH, l'ionisation du groupe basique s'affaiblit, mais l'ionisation du groupe acide augmente. Par conséquent, l'affinité des FQs envers les ions diffère selon la forme d'ionisation de l'antibiotique. L'affinité de la loméfloxacine pour deux ions divalents (Mg^{2+}, Ca^{2+}) diminue dans l'ordre anion> zwitterion >> cation [32].

Des études approfondies ont été réalisées pour établir des constantes de stabilité ($log\beta$) de complexes FQs- métaux. Cependant, les valeurs de $log\beta$ peuvent différer les uns des autres dépendamment des méthodes conditions et expérimentales qui ont été utilisées (en particulier le pH). Le Tableau 1.3 présente la des constantes globales de stabilité des complexes FQs-métaaux obtenus par Urbaniak et al. (2009) [56]. Les expériences de titration potentiométrique ont été réalisées à des pH variant de 2 à11 gamme et une force ionique I = 0,1 M NaCl, de sorte que toutes les valeurs de $log\ \beta$ soient déterminées dans les mêmes conditions. Par la suite, les données obtenues ont été analysées par le programme Hyperquad. Les valeurs les plus élevées de $log\ \beta$ correspondaient aux complexes avec les ions trivalents, comprise entre 15,8 et 51,6, ce qui confirment qu'ils sont les plus stables. Les valeurs les plus basses de $log\ \beta$ peuvent être observées pour les complexes avec Mg (II) et Ca (II) - les valeurs ont varié de 9,39 à 11,88. Il s'agit donc des complexes FQs les moins stables [55, 56].

Tableau 1. 3 Constantes de stabilité globale logβ des complexes FQs-métaux obtenues via l'expérience de titration potentiométrique, pH 2-11, force ionique I = 0,1 M NaCl, sous atmosphère d'azote gazeux, à 22 °C, et analysés par le programme Hyperquad. Données obtenues de [56]

$pMe + qFQ + rH \rightarrow Me_pFQ_qH_r$					$log\beta = \frac{[Me_pFQ_qH_r]}{[Me]^p[FQ]^q[H^r]}$	
Ions métalliques	Ca^{2+}	Cu^{2+}	Mg^{2+}	Zn^{2+}	Fe^{3+}	Al^{3+}
CIP						
Me(FQ)H	11.24	14.89	11,88	12,74	18.86	16,27
$Me(FQ)_2H_2$	-	29.06	-	24.84	-	29.67
$Me(FQ)_3H_3$	-	-	-	-	48,63	43,53
NOR						
Me(FQ)H	10.65	14,75	11.80	12.90	15.80	15,36
$Me(FQ)_2H_2$	-	28.45	-	25,35	-	29.47
$Me(FQ)_3H_3$	-	-	-	-	47.80	42.79
OFL						
Me(FQ)H	9,89	14.21	11.11	14.64	20.32	17,56
$Me(FQ)_2H_2$	-	26.25	-	24.40	-	28.84
$Me(FQ)_3H_3$	-	-	-	-	48.32	41.11

Park et al. (2000) ont étudié la complexation de cations divalents avec OFL et NOR [15]. Les valeurs des constantes de formation de complexe pour les cations appartenant au groupe du béryllium diminuent de la même manière que $Mg^{2+}>Ca^{2+}>Ba^{2+}$ en raison de l'augmentation des rayons cationiques. Si les valeurs des constantes de transition des ions de métaux à sont comparées, ils sont

plus faibles pour Mn^{2+} et Zn^{2+} que pour Ni^{2+} et Co^{2+}. Ces constantes sont faibles à cause de l'occupation du d - orbital par des électrons. Par exemple, d - orbitale de Zn^{2+}est entièrement remplie, de sorte que l'interaction entre les orbitales des ions métalliques et des FQ est faible et que la valeur constante est principalement déterminée par une interaction ion-dipôle. Les cations, Ni^{2+} ou Co^{2+} forment des complexes plus stables que Mn^{2+} et $Zn^{2+,}$ en raison des interactions d'autres électron-électron entre le métal ionique et les ligands. En conclusion, la valeur de la constante de formation du complexe augmente avec l'augmentation de la charge nucléaire des ions métalliques. Ainsi, les ions de métaux alcalino-terreux généralement présents dans l'eau et les sols forment des complexes moins stables. Cependant, les ions métalliques qui sont considérés comme des ions de métaux lourds, ont une charge nucléaire plus élevée, forment des complexes plus persistants et constituent une plus grande menace pour l'environnement [10, 59].

1.4. Impact de la complexation métallique de la ciprofloxacine et d'autres fluoroquinolones sur le traitement des eaux usées

Au cours des dernières années, la communauté scientifique s'est concentrée sur l'investigation du sort des FQs dans les usines de traitement des eaux usées. Cependant, les données concernant l'influence de la complexation des métaux des FQs sur les stations d'épuration sont encore rares. Généralement, les FQs sont principalement éliminés par adsorption sur les boues, avec une efficacité d'élimination de 80 à 90% [60, 61]. Il a été observé que la présence de Mg^{2+} et de Ca^{2+} inhibait la sorption de la CIP ainsi que de la NOR et de la OFL dans les eaux usées salines [60]. Comme mentionné précédemment, Mg^{2+} et Ca^{2+} génèrent les complexes les moins stables, il est donc possible que les ions métalliques, comme le Cu^{2+} ou les ions trivalents, présentent un effet différent. Les complexes formés peuvent augmenter l'affinité des FQs avec la boue ou les rendre plus résistantes à une dégradation supplémentaire, qui peut être une digestion anaérobie/aérobie par voie bactérienne. Des études ont montré que la biodégradation des FQs est généralement négligeable en raison du faible temps de rétention hydraulique des FQs dans le système et/ou de la prédominance de l'adsorption en tant que méthode d'élimination [60, 61].

Comme présenté dans la section suivante , les complexes FQs-Me peuvent présenter une toxicité envers les bactéries. Cela peut entraîner une réduction de la communauté bactérienne présente dans les boues activées. Ainsi, le traitement biologique des eaux usées serait moins efficace. De plus, la CIP s'est avérée difficile à dégrader dans les systèmes aqueux, mais dans les sols, la minéralisation a été observée [62]. Do et al. (2019) ont étudié le devenir et l'élimination du CIP dans un réacteur à membrane anaérobie [63]. Étonnamment, la biodégradation était la principale méthode d'élimination, lorsqu'une petite fraction du CIP était adsorbée sur les boues. Liao et al. (2016) ont étudié deux cultures bactériennes mixtes pour la biodégradation potentielle en CIP [64]. Les microorganismes provenant de biofiltre d'eau potable et de bactéries acclimatées au CIP ont pu utiliser le CIP comme source de carbone/d'azote. Cependant, si le CIP génère des complexes métalliques stables, il est possible que la

minéralisation soit plus lente, donc l'exposition de l'antibiotique dans l'environnement est plus longue. Par conséquent, en dehors de la présence des FQs, des variables doivent être prises en compte lors du traitement des eaux usées, telles que la présence d'autres composés susceptibles de réagir avec eux, notamment les ions métalliques.

De nombreuses études ont été menées pour déterminer l'efficacité de la dégradation des FQs lors du traitement physico-chimique. Les méthodes les plus prometteuses sont les procédés d'oxydation avancés (AOP). Par exemple, il a été prouvé que la CIP peut être efficacement éliminée par oxydation à l'aide de dioxyde de titane [65, 66]. Pour traiter les eaux usées hospitalières, les nanotubes de ZnO présentaient une activité photocatalytique supérieure à celle du TiO_2 utilisé dans le commerce [67]. L'efficacité du procédé Fenton a également été testée. Diao et al. (2017) ont développé un système dans lequel des microsphères FeS_2/SiO_2 étaient utilisées comme catalyseur de Fenton [68]. En conséquence, presque 100% de la CIP s'est dégradée en moins de 60 minutes. Le persulfate activé par le fer solide a permis d'éliminer la CIP (95%) après 15 min, ainsi que ses produits de transformation (90%) [69]. De plus, Feng et al. (2018) ont récemment décrit l'influence de l'oxydation des FQs par les métaux [70]. En général, on a constaté que la présence des métaux améliore l'oxydation de FQ due à une production accrue de radicaux (·OH and $SO_4^{-\cdot}$).

L'influence des ions métalliques sur l'élimination des FQs a été étudiée de manière plus approfondie dans le cas des méthodes d'adsorption. Par exemple, la présence de Cu (II) a entraîné une augmentation de la capacité d'adsorption CIP de l'oxyde de graphène magnétique fonctionnalisé par l'acide nitrilotriacétique en raison du pontage du métal [71]. Une autre étude menée par Ma et al. (2020), a révélé que la présence de Cu (II) à faible concentration augmente légèrement d'adsorption de CIP sur hydrogel de graphène [72]. Cependant, lorsque la concentration de Cu (II) est élevée, il entre en concurrence d avec les antibiotiques sur les sites de liaison. Une microsphère magnétique fonctionnalisée de $NiFe_2O_4$ a été développée et testée par Liu et al. (2018) [73]. Il a été découvert que l'adsorbant produit était capable d'éliminer simultanément CIP, ENR et NOR ainsi que les métaux lourds, à savoir Cu^{2+}, Cd^{2+}, Cr^{3+} et Zn^{2+}. Cependant, les deux types de contaminants présentaient des mécanismes d'adsorption différents, leur présence n'affectait donc pas l'efficacité d'élimination.

1.5. Impact de la complexation métallique de la ciprofloxacine et d'autres fluoroquinolones sur les microorganismes présents dans l'environnement

1.5.1. Activité antimicrobienne des complexes fluoroquinolone-métal

La présence de FQs et sa persistance dans les compartiments de l'environnement peuvent avoir un effet toxique sur les microorganismes vivant dans le sol et dans l'eau [62, 74]. Il a été prouvé que la CIP conservait son activité antimicrobienne dans les deux systèmes, le pouvoir d'inhibition étant plus

fort dans l'eau que dans les sols. De plus, le CIP est capable de former des complexes stables avec des ions métalliques et des substances humiques, en préservant leur pouvoir antimicrobien [75].

Les facteurs qui influencent sur l'efficacité complexe contre les micro-organismes sont: (1) la nature de l'ion métallique; (2) la nature des ligands; (3) l'effet chélatant, c'est-à-dire des complexes avec des ligands chélateurs bidentés (FQs) et des ligands N,N'-donneur, présente une puissance antimicrobienne accrue; (4) la charge globale du complexe - généralement l'activité antimicrobienne suit l'ordre: complexe cationique> zwitterionique> anionique; (5) la nature et l'existence de l'ion neutralisant le complexe ionique; (6) le nombre d'atomes de métaux centraux réunis dans le composé de coordination (noyau) - en général, les complexes dinucléaires sont plus puissants que ceux mononucléés [16].

Le Tableau 1.4 présente l'activité antimicrobienne exprimée par la concentration minimale inhibitrice (CMI) [μg/ml] - la plus faible concentration de composé empêchant la croissance visible des bactéries. Le Tableau 1.5 présente les résultats obtenus par la méthode de diffusion, test qualitatif de sensibilité aux antimicrobiens. Dans certains cas, l'efficacité à inhiber les micro-organismes est inférieure à celle du ligand lui-même. Cependant, en général, les complexes métalliques FQ présentent une activité antimicrobienne similaire ou plus élevée, en comparaison avec les ligands libres. En fait, la composition du milieu utilisé et les conditions expérimentales peuvent affecter les résultats des tests de toxicité [76]. L'interaction entre le complexe antibiotique-métal et les composants du milieu peut entraîner une altération du complexe, c'est-à-dire une hydrolyse. Ainsi, le composé actif qui présente un effet toxique vis-à-vis du microorganisme, peut-être une substance non testée.

Tableau 1. 4 Concentration minimale d'inhibition des complexes fluoroquinolone- métal [μg/mL]

Composé	Concentration minimale d'inhibition [μg/mL]											Ref.
	Bacteria Gram+					Bacteria Gram-						
	S.aureus	*M.luteus*	*B. subtilis*	*S. epidermidis*	*E. faecalis*	*E. coli*	*P. aeugrinosa*	*S. enteriditis*	*K..pneumoniae*	*S. liquefaciens*	*C. freundii*	
CIP	0.25	-	0.03	0.12	1	0.12	0.12	-	0.12	0.004	0.004	[9]
$[Co(CIP)_2(H_2O)_2]\cdot 9H_2O$	0.25	-	0.06	0.06	1	0.03	0.12	-	0.12	0.008	0.12	
$[Zn(CIP)_2(H_2O)_2]\cdot 8H_2O$	0.25	-	0.03	0.12	1	0.03	0.12	-	0.06	0.008	0.004	
$Ni(CIP)_2\cdot 10H_2O$	0.5	-	0.03	0.12	1	0.03	0.12	-	0.12	0.001	0.004	
$Cu(CIP)_2\cdot 6H_2O$	0.25	-	0.03	0.06	1	0.12	0.12	-	0.06	0.004	0.001	
NOR	0.06	-	-	0.04	-	0.05	-	-	0.08	-	-	[77]
$Bi(NOR)_4(H_2O)_2$	0.045	-	-	0.03	-	0.025	-	-	0.06	-	-	
OFL	-	12	0.5	0.75	10	0.2	7	0.75	0.7	-	-	[39]
$[Mg(R/S\text{-}OFL)(H_2O)_2]\cdot 2H_2O$	-	20	0.8	1	15	0.25	10	1	1	-	-	

Tableau 1. 5 Activité antimicrobienne testée via le Test de diffusion de plat

Composé	Bacteria Gram+			Bacteria Gram-					Fungi	
	S.aureus	*C. hoffmannii*	*B. subtilis*	*P. mirabilis*	*E. coli*	*P. aeugrinosa*	*S. enteriditis*	*K..pneumoniae*	*C. albicans*	*S. cerevisiae*
Diamètre de la zone d'inhibition [mm/mL échantillon] [78]										
LOME	48	-	-	-	43	-	-	-	11	-
[Cr(LOME)(H_2O)$_4$]·Cl_3	38	-	-	-	36	-	-	-	12	-
[Mn(LOME)(H_2O)$_4$]·Cl_2	48	-	-	-	43	-	-	-	11	-
[Fe(LOME)(H_2O)$_4$]Cl_3·H_2O	46	-	-	-	40	-	-	-	13	-
[Co(LOME)(H_2O)$_4$]·Cl_2	44	-	-	-	40	-	-	-	20	-
[Ni(LOME)(H_2O)$_4$]Cl_2·H_2O	40	-	-	-	40	-	-	-	21	-
[Cu(LOME)(H_2O)$_4$]Cl_2·$2H_2O$	43	-	-	-	42	-	-	-	12	-
[Zn(LOME)(H_2O)$_4$]·Cl_2	47	-	-	-	42	-	-	-	12	-

[79]; Activité du composé: +++++ = 150–200% d'inhibition; ++++, inhibition de 90 à 100%; +++, inhibition de 75–85%; ++, inhibition de 50 à 60%; +, Inhibition de 20-30%

GTI	++++	-	++++	++++	++++	++++	-	++++	++++	NA
$Mg(GTI)_2$	++++	-	++++	++++	++++	++++	-	++++	NA	NA

Composé	Bacteria Gram+			Bacteria Gram-					Fungi	
	S.aureus	*C. hoffmannii*	*B. subtilis*	*P. mirabilis*	*E. coli*	*P. aeugrinosa*	*S. enteriditis*	*K..pneumoniae*	*C. albicans*	*S. cerevisiae*
$Ca(GTI)_2$	++++	-	++++	+++	++++	++++	-	++++	++++	NA
$Cr(GTI)_2$	++++	-	++++	++++	+++	+++	-	++++	++++	NA
$Mn(GTI)_2$	++++	-	++++	++++	++++	++++	-	++++	NA	NA
$Fe(GTI)_2$	++++	-	++++	++++	++++	++++	-	++++	++++	NA
$Co(GTI)_2$	++++	-	+++	+++	++++	++++	-	++++	++++	NA
$Ni(GTI)_2$	++++	-	++++	++++	+++	++++	-	++++	++++	NA
$Cu(GTI)_2$	++++	-	++++	++++	++++	+++	-	++++	++++	NA
$Zn(GTI)_2$	++++	-	++++	++++	++	++++	-	++++	++++	NA
$Cd(GTI)_2$	++++	-	+++	+++	+++	+++	-	++++	++++	NA

Abréviations: NA - aucune activité; *S. aureus - Staphylococcus aureus; C. hoffmannii - Corynebacterium hoffmannii, B. Subtilis - Bacillus subtilis; E. Faecalis – Enterecoccus faecalis; P. mirabilis - Proteus mirabilis; E. coli - Escherichia coli; P. aeugrinosa – Pseudomonas aeruginosa, S. enteriditis - Salmonella enteriditi ; Klebsiella pneumoniae - K. pneumoniae ; C. albicans - Candida albicans; A. niger - Aspergillus niger; A. flavus - Aspergillus flavus; S. cereisiae - Saccharomyces cerevisiae*

La théorie de la chélation peut expliquer l'augmentation de l'activité contre les microorganismes. Les ions métalliques partagent partiellement la charge positive avec les groupes donneurs de ligands, ce qui diminue la polarité des ions. L'orbite du ligand et l'orbitale du cation se chevauchent. La délocalisation des π-électrons dans le cycle chélate se produit, donc la lipophilie de la complexité augmente, ce qui facilite le passage du complexe FQs-Me à travers la membrane lipidique de la cellule et la pénétration cellulaire [14, 80, 81].

L'activité antifongique des FQ a également été testée. Dans la plupart des cas, les FQ n'ont aucun effet sur les champignons, à l'exception des complexes $[Ni/Co(LOME)(H_2O)_4]Cl_2 \cdot H_2O$ (Tableau 1.5), qui ont augmenté le pouvoir inhibiteur de *C. albicans.* Les résultats ont été comparés à un antibiotique antifongique, l'amphotéricine B et le complexe LOME-Me s'étant révélés moins actifs [82]. Les complexes GTI-Me (sauf les complexes Mn^{2+} et Mg^{2+}) ont également montré une activité accrue contre *C. albicans* (Tableau 1.5) et *Fusarium solani* (données non présentées) [79]. D'un point de vue médical, ils sont des antibiotiques potentiels contre les champignons, par exemple *C. albicans, ce* qui provoque la candidose - l'une des infections les plus communes dans les hôpitaux [83]. Les complexes FQs-Me peuvent être moins toxiques pour l'être humain que d'autres composés antifongiques, tels que l'amphotéricine B. Cependant, du point de vue effet sur l'environnement, les FQ et leurs complexes métalliques peuvent perturber les communautés fongiques, qui peuvent être essentielles pour leur écosystème. Par exemple, certains champignons vivent en symbiose avec les plantes (mycorhizes) [84]. Par conséquent, la présence de composés ayant un effet toxique sur eux affecterait également la croissance de ces plantes. De plus, l'effet toxique sur les champignons peut avoir un effet négatif sur la qualité du sol, car les champignons saprophytes jouent un rôle important dans la rétention d'éléments nutritifs dans le sol [85, 86].

1.5.2. Résistance aux antibiotiques

L'exposition de l'environnement à long terme aux FQs induit la sélection de bactéries résistantes aux antibiotiques, qui sont devenues plus courantes ces dernières années. La résistance des FQs peut apparaître en raison de la mutation dans des régions spécifiques de sous-unités enzymatiques - gryA et gryB dans l'ADN gyrase et parC pour la topoisomérase IV [25]. L'autre mécanisme de résistance est la régulation à la hausse de l'efflux ou la réduction de la perméabilité de la membrane cellulaire en modifiant les porines de la membrane [87]. Une résistance à médiation par le plasmide a également été observée [88]. Les protéines, codées sur les plasmides, peuvent protéger la topoisomérase de l'attaque des quinolones.

Girardi et al. (2011) ont mené l'étude sur les gènes de résistance à la CIP présents dans les sols [62]. Les gènes n'ont pas été détectés dans les souches de bactéries testées. Cependant, les gènes de résistance sont apparus après plus de 14 jours d'incubation avec l'antibiotique.

Il a été prouvé que la présence d'ions de métaux lourds dans l'environnement est en corrélation positive avec l'abondance de certains gènes résistants aux antibiotiques [89-91]. Les métaux seuls possèdent des propriétés antibactériennes [92]. Ils peuvent entraîner un dysfonctionnement des protéines et désactiver les enzymes par échange de métal structural/catalytique (Pb (II), Ni (II)) ou par oxydation de Cys dans le site de liaison du Fe. La production d'espèces réactives de l'oxygène par Fe (III) ou Cu (II) peut, par exemple, endommager l'ADN. Ils peuvent également désactiver la fonction membranaire (Ag (I), Cu

(II), Cd (II)) ou nuire à l'absorption de nutriments (Fe (III)). Les métaux présentent également une génotoxicité (par exemple, Mn (II), Cr (VI), Cd (II), Co (II)) [92]. Par conséquent, les bactéries ont développé des mécanismes de résistance aux métaux. De plus, les gènes de résistance aux antibiotiques et aux métaux lourds peuvent être liés au même plasmide [89, 91]. Par conséquent, les métaux peuvent influencer la sélection des souches résistantes aux antibiotiques en raison d'une pression sélective à long terme vis à vis des bactéries - métaux ne subissant pas de dégradation, comme les antibiotiques et d'autres composés chimiques. Le mécanisme exact et l'influence sur les souches résistantes aux antibiotiques et aux métaux lourds nécessite encore des études plus approfondies.

Des modifications de composés connus peuvent être testées pour surmonter les bactéries et les complexes FQ-métal résistants aux FQs qui sont prometteurs pour atteindre cet objectif. Les données suggèrent que les complexes d'antibiotiques libres et FQs-Me sont transportés par deux voies d'absorption différentes. Les FQs entrent dans la cellule par des canaux non spécifiques, c'est-à-dire les porines OmpF ou OmpC, par diffusion passive et par interaction au sein des canaux [87, 93, 94]. Cependant, les bactéries ont développé une résistance à la réduction de la consommation d'antibiotiques par des modifications de la perméabilité des porines ou des mécanismes d'efflux d'antibiotiques. Cependant, les complexes FQ-Me probablement entrent dans la cellule bactérienne de différentes manières [95, 96]. L'interaction entre les lipides présents dans la membrane et le complexe antibiotique est plus forte qu'avec FQ libre (comme CIP) en raison des interactions électrostatiques entre les groupes cationiques des complexes FQ-Me et les lipides chargés négativement. Par conséquence, les métallo-antibiotiques pénètrent dans la cellule dépendamment des changements d'hydrophobie [96, 97]. D'autre part, en raison de la co-contamination des ions métalliques et des antibiotiques dans l'environnement, il serait possible pour les FQ d'obtenir également une résistance contre les métalloantibiotiques, par des modifications de la composition membranaire.

Le phénomène concerné est le développement d'une de défense bactérienne via formation de biofilms [98]. En présence d'antibiotiques, ils utilisent les propriétés de barrière de perméabilité extracellulaire du biofilm pour interférer avec l'absorption de composés toxiques. Cependant, ce processus est très coûteux sur le plan énergétique et peut donc être inefficace. La présence de cations est cruciale pour cette interaction. Le pont métallique est formé en liant le tryptophane déprotoné, présent dans les matrices de biofilms, à l'ion métallique, qui est connecté au groupe carboxyle/carbonyle des FQ. La formation d'un pont métallique entre les ions divalents, les biofilms et le CIP a été spécifiquement régulée. Sans pontage de métal, la cellule présente une perméabilité plus élevée, l'absorption de FQ, d'où la chimiotaxie défectueuse [98]. Le procédé s'avère efficace sur le plan énergétique pour les bactéries. La formation de ponts métalliques dans les matrices de biofilms est considérée comme un facteur crucial dans la résistance des bactéries aux antibiotiques.

1.5.3. Bioaccumulation

Les FQs, y compris CIP, ont été détectés dans les poussins d'aigle doré et vautours à des concentrations comprises entre 20 et 150 μg/L [99, 100]. Avec un facteur de bioaccumulation de 3262 L/kg, la CIP a montré une accumulation potentielle chez la carpe de crucian, présente dans la rivière Haihe, en Chine [101]. Les systèmes végétaux de sol ont également été étudiés [102, 103]. On a découvert que la CIP a été présent dans les racines des : chou chinois, radis, tomates, et à haricot long, et peut - être diffusé aux parties aériennes [102]. Ces données sont extrêmement alarmantes - ces légumes sont couramment utilisés dans de nombreux ménages à travers le monde. La présence du CIP peut avoir des effets néfastes sur l'homéostasie humaine, tout comme sur la flore bactérienne intestinale. Néanmoins, les connaissances sur la bioaccumulation des FQ sont encore insuffisantes, les connaissances sur l'impact des complexes FQ – métaux sont encore plus inconnues.

1.6. Mobilité des complexes de métaux fluoroquinolones dans divers compartiments

Les valeurs $logK_{OW}$ de différentes FQs (Tableau 1.1) indiquent qu'elles ont une forte affinité pour l'eau. Néanmoins, les études ont révélé que les FQs ont tendance à s'adsorber sur le sol, les sédiments et les boues [61, 104-107]. Van Doorslaer (2014) a indiqué que les valeurs rapportées dans la littérature de $logK_{OW}$ incluent des données obtenues par modélisation et à travers des expériences à l'échelle laboratoire, les valeurs expérimentales sont supérieures d'au moins 1 unité de log aux données obtenues via des outils de modélisation [108]. En outre, les données expérimentales ont montré qu'il existait une variabilité entre les valeurs $logK_{OW}$, probablement en raison de la différence au niveau de la température de la solution et de l'effet de partition du pH [108]. La nature amphotère des FQs joue également un rôle important dans ce cas en raison de leurs diverses occurrences de spéciation.

Dans les différents compartiments de l'environnement, la substance abondante susceptible d'affecter la mobilité des produits pharmaceutiques est la matière organique [75, 109, 110]. Aristilde et Sposito (2010) ont effectué des simulations moléculaires de l'interaction entre la CIP et l'acide humique, le représentant de la matière organique [111]. Dans un environnement acide, lorsque les substances humiques sont protonées, la CIP présente une plus grande affinité à leur égard. Toutefois, à pH neutre et en présence de cations divalents, deux scénarios peuvent se présenter. Le premier est la formation d'un complexe ternaire entre CIP et les substances humiques avec des ions métalliques, jouant le rôle de médiateur. Dans le second scénario, les ions divalents entravent la formation du complexe CIP-substance humique [111]. Ils ont conclu que l'amélioration de la formation du complexe dépend inversement du rayon ionique du cation – Mg^{2+} et Fe^{2+} facilitant la liaison entre la CIP et les substances humiques par rapport au Ca^{2+}.

L'échange de cations, la formation de ponts et la complexation de surface sont les mécanismes d'interaction entre les FQs et les sols [107, 112, 113]. En conditions tropicales, leur coefficient de

distribution K_d peut atteindre plus de 544,2 L/g, alors que les sulfamides dans les mêmes conditions allaient de 0,7 à 70,1 L/kg [107]. Le sol contient différentes particules, y compris des composants minéraux, tels que des oxydes hydratés. Les oxydes hydratés d'aluminium et de fer sont les minéraux les plus importants en raison de leurs surfaces hautement réactives, [114]. Ils peuvent former des complexes avec des ions métalliques ou des composés organiques. En général, ils sont amphotères. Ainsi, la sorption des FQs, tels que la CIP sur des oxydes hydratés, est un processus fortement dépendant du pH [114]. Avec l'augmentation du pH, la sorption de la CIP a été observée également augmenter, jusqu'à atteindre un pH proche de la neutralité (pH 7,8 pour les oxydes hydratés d'aluminium et de 6,5 pour les oxydes hydratés de fer). Au-delà de cette valeur de pH, l'affinité pour absorber la CIP sur les oxydes hydratés a diminué [114].

L'influence des ions divalents (Cu^{2+} et Ca^{2+} sur le transport de CIP dans du sable saturé a été étudiée [115]. Lorsque les oxydes Al/Fe étaient présents et appliqués sur le sable natif, le transport par CIP était entravé. Al/Fe avait tendance à former des complexes forts avec la CIP, ce qui entraînait l'immobilisation du CIP dans le sable et la diminution de sa concentration dans une solution aquatique. Dans ce cas, seul le Cu^{2+} pourrait légèrement favoriser le transport en mode CIP. Lorsque la CIP était pré-adsorbé sur le sable, les deux ions divalents étaient incapables de soutenir la mobilisation de l'antibiotique. La pré-sorption de Cu^{2+}/Ca^{2+} sur du sable de quartz a augmenté l'adsorption de CIP en raison de la complexation des métaux [116]. Toutefois, dans le sable propre, où les oxydes hydratés de Fe/Al ont été éliminés, le rapport de Cu^{2+}/Ca^{2+} présent en solution a permis d'améliorer la mobilité de la CIP. Bien que, l'effet promoteur du Cu^{2+} a été plus fort que celui de Ca^{2+} [115, 116]. Ces résultats indiquent que la présence d'ions métalliques peut influencer l'efficacité de sorption du CIP en fonction du type d'ions et s'ils sont présents dans la phase solide ou liquide.

Tan et al. (2015) ont mené une étude sur l'adsorption du CIP sur la goethite [117]. La présence d'ions métalliques divalents augmentait la rétention de CIP à la surface du sol, probablement via un pontage de cations. L'ordre d'affinité du CIP pour les métaux était: $Cu^{2+} > Pb^{2+} > Cd^{2+} > Ca^{2+,}$ ce qui correspondait aux valeurs des constantes de complexation obtenues. Le processus ne dépend pas du pH, on s'attend à une interaction CIP-Cu qui présente une dépendance significative au pH en raison d'une forte complexation CIP-Cu (la constante de complexation la plus élevée dans ce groupe d'ions métalliques). Le rapport de concentration de CIP et d'ions métalliques affecte l'adsorption des antibiotiques - l'adsorption la plus élevée ne s'est pas produite lorsque la concentration en ions métalliques était excessive. Cela est probablement dû à la contribution partielle des ions métalliques dans le processus de sorption du CIP. De plus, il a été prouvé que les ions métalliques peuvent concurrencer le CIP pour les sites de sorption dans le sol, comme le montre la Figure 1.3 B [115, 116]. De plus, la présence de Cu^{2+} et d'acide fluvique augmentait la sorption de CIP du le sol, bien que la concurrence entre eux et la diminution de la sorption de CIP soient attendues [117].

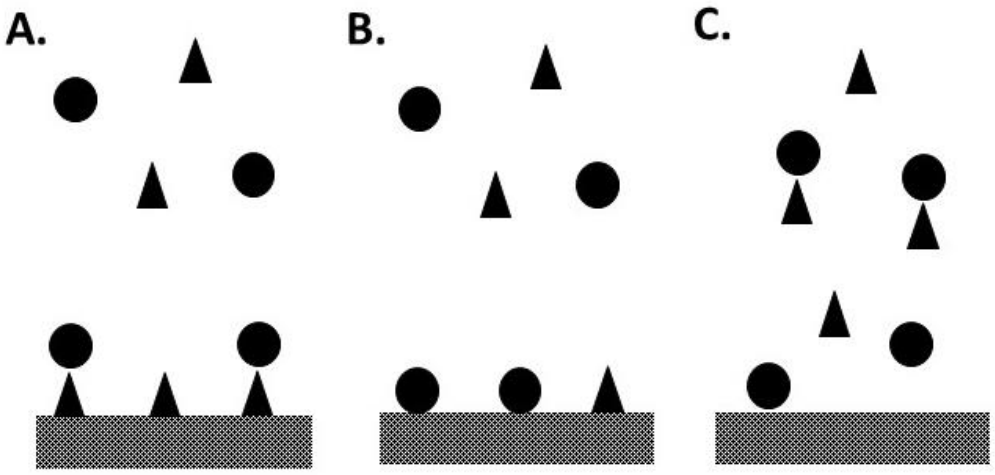

Figure 1. 3 Interactions clés entre le sol, les métaux et les fluoroquinolones, où le cercle est constitué de fluoroquinolone et le triangle d'ions métalliques; A. l'ion métallique agit comme un pont entre l'antibiotique et le sol;B L'ion métallique et la fluoroquinolone sont en compétition pour les sites de liaison dans le sol C. formation de fluoroquinolone et de complexes métalliques, qui inhibent la sorption sur le sol

La co-adsorption de la CIP et du Cu^{2+} a été étudiée également sur la montmorillonite et la kaolinite, la montmorillonite a une plus grande capacité d'échange de cations que la kaolinite [118]. Le processus de sorption a été testé dans une large gamme de pH. À pH acide (<5,0), $[Cu(CIP^{\pm})]^{2+}$, CIP^{+} et Cu^{2+} étaient présents en solution. Le $[Cu(CIP^{\pm})]^{2+}$ prévalait entre 6,0 et 7,0, et lorsque le pH atteignait 8,0, $[Cu(CIP^{-}_{2})]$ commençait à précipiter. Entre pH 4,0 et 7,0, la CIP a montré une forte capacité de sorption sur la montmorillonite par échange de cations, probablement entre le site de charge permanent sur l'argile et l'atome d'azote sur le noyau hétérocyclique de $CIP^{+}/CIP^{\pm}$ [118]. La présence d'ions de cuivre (II) n'a montré aucun effet sur la sorption de la CIP sur la montmorillonite en dessous de pH 6,0. Il est possible que la montmorillonite ait fourni une capacité de sorption suffisante et qu'elle puisse absorber complètement CIP^{+}. Cependant, au-dessus de pH 6,0, la valeur de la sorption de la CIP a augmenté lorsque le Cu (II) était présent. Le surface de montmorillonite chargée négativement a contribué à la forte adsorption de la charge positive $[Cu(CIP^{\pm})]^{2+}/[Cu(CIP^{\pm})_2]^{2+}$, plutôt que $CIP^{\pm}/CIP^{-}$. Un autre mécanisme possible pourrait intervenir: le Cu (II) s'adsorbe d'abord sur l'argile, puis le CIP forme un complexe avec l'ion métallique adsorbé [118].

La kaolinite présentait une sorption de la CIP plus forte que celle de la montmorillonite à pH plus élevé (9,5), probablement en raison de l'interaction entre la charge variable de l'argile et le groupement carboxyle de la CIP [118]. La présence de Cu (II) a diminué la sorption CIP sur la kaolinite pour des pH en dessous 6,0. La CIP^{+} était plus favorablement adsorbé sur l'argile que le complexe CIP-Cu, en raison de l'interaction interférente entre la surface chargée positivement de la kaolinite et le groupement carboxyle du CIP. À pH plus élevé, en raison de la formation de ponts cationiques, le $[Cu(CIP^{\pm})]^{2+}/[Cu(CIP^{\pm})_2]^{2+}$ avait une plus grande affinité pour absorber la kaolinite [118].

Les différences dans la composition des compartiments environnementaux sont les principaux facteurs qui influencent la mobilité des FQs et de leurs complexes métalliques. D'autres paramètres, tels que le pH, la température ambiante et le climat peuvent également avoir une influence. Cependant, les données sont encore rares, c'est la raison pour laquelle qu'il faut entreprendre des travaux plus avancés pour étudier l'effet des ions métalliques influence sur le transport des FQs.

1.7. Perspectives futures étendues à différents compartiments environnementaux

La présence des FQs dans les sols peut affecter leur fertilité. Il a été déjà démontré que la forte concentration de CIP dans le sol affecte négativement la croissance de radis [102]. En outre, les complexes FQ-métal, qui peuvent être persistants dans l'environnement, peuvent également affecter les plantes et la communauté microbienne nécessaires à la bonne fertilité du sol. La perturbation de cette dépendance peut entraîner une réduction des rendements et/ou une malformation des plantes. De plus, si la plante peut accumuler des complexes FQ-métal, ils peuvent affecter les organismes vivants, y compris l'homme lorsque la plante est consommée. Cela peut entraîner une accumulation de métaux lourds encore plus toxique en présence des antibiotiques. Jusqu'à date, l'effet exact des complexes FQs-Me sur les organismes vivants, à l'exception des bactéries, des champignons et de certains protozoaires, est toujours inconnu.

Une situation analogue se produit dans les compartiments aquatiques. Les complexes FQs-Me peuvent demeurer stable et affecter par conséquence la faune et la flore aquatiques, telles que les bactéries, les cyanobactéries, les algues vertes, les plantes aquatiques et les poissons. De plus, les rivières et les bassins hydrographiques sont souvent la source d'eau potable; par conséquent, les complexes antibiotiques-métaux peuvent être présents, ce qui pose les mêmes menaces que précédemment. En plus, en raison de la nouvelle adaptation technologique des FQs-Me, leur application pourrait s'étendre, mais leur impact éventuel sur l'environnement et leur élimination sans danger doivent être prise en compte.

De nos jours, on ignore toujours les effets nocifs des FQs et de leurs complexes métalliques. Des études approfondies devraient être effectuées pour avoir une idée sur l'influence exacte des complexes sur l'écosystème. En outre, les stations d'épuration devraient être améliorées pour la bonne détection et élimination des FQs qui peuvent être présent dans l'eau. Le traitement des boues et des sols doit également être étudié, afin d'éviter la formation de FQs-Me. Il faut sensibiliser le grand public afin que la société soit consciente de la nécessité d'éliminer les médicaments de manière à prévenir les interactions et réactions intempestives antibiotiques-métaux.

Références

1. Sharma, P.C., A. Jain, and S. Jain, Fluoroquinolone antibacterials: a review on chemistry, microbiology and therapeutic prospects. Acta Pol Pharm, 2009. **66**(6): p. 587-604.

2. He, K., et al., Detection of a wide variety of human and veterinary fluoroquinolone antibiotics in municipal wastewater and wastewater-impacted surface water. J Pharm Biomed Anal, 2015. **106**: p. 136-43.

3. Vieno, N.M., T. Tuhkanen, and L. Kronberg, Analysis of neutral and basic pharmaceuticals in sewage treatment plants and in recipient rivers using solid phase extraction and liquid chromatography–tandem mass spectrometry detection. J Chromatogr A, 2006. **1134**(1): p. 101-111.

4. Östman, M., et al., Screening of biocides, metals and antibiotics in Swedish sewage sludge and wastewater. Water Research, 2017. **115**: p. 318-328.

5. Miao, X.S., et al., Occurrence of antimicrobials in the final effluents of wastewater treatment plants in Canada. Environ Sci Technol, 2004. **38**(13): p. 3533-41.

6. Lee, H.B., T.E. Peart, and M.L. Svoboda, Determination of ofloxacin, norfloxacin, and ciprofloxacin in sewage by selective solid-phase extraction, liquid chromatography with fluorescence detection, and liquid chromatography--tandem mass spectrometry. J Chromatogr A, 2007. **1139**(1): p. 45-52.

7. Gibs, J., et al., Occurrence and partitioning of antibiotic compounds found in the water column and bottom sediments from a stream receiving two wastewater treatment plant effluents in Northern New Jersey, 2008. Sci Total Environ, 2013. **458**: p. 107-116.

8. Zhou, L.J., et al., Trends in the occurrence of human and veterinary antibiotics in the sediments of the Yellow River, Hai River and Liao River in northern China. Environ Pollut, 2011. **159**(7): p. 1877-85.

9. Lopez-Gresa, M.P., et al., Interactions of metal ions with two quinolone antimicrobial agents (cinoxacin and ciprofloxacin). Spectroscopic and X-ray structural characterization. Antibacterial studies. J Inorg Biochem, 2002. **92**(1): p. 65-74.

10. Zhang, Y., et al., Insights into aquatic toxicities of the antibiotics oxytetracycline and ciprofloxacin in the presence of metal: complexation versus mixture. Environ Pollut, 2012. **166**: p. 48-56.

11. Mohler, J.S., et al., Enhancement of antibiotic-activity through complexation with metal ions - Combined ITC, NMR, enzymatic and biological studies. J Inorg Biochem, 2017. **167**: p. 134-141.

12. Breda, S.A., et al., Solubility behavior and biopharmaceutical classification of novel high-solubility ciprofloxacin and norfloxacin pharmaceutical derivatives. Int J Pharm, 2009. **371**(1-2): p. 106-13.

13. Hoffken, G., et al., Reduced enteral absorption of ciprofloxacin in the presence of antacids. Eur J Clin Microbiol, 1985. **4**(3): p. 345.

14. Mohamed, G.G. and M.H. Soliman, Synthesis, spectroscopic and thermal characterization of sulpiride complexes of iron, manganese, copper, cobalt, nickel, and zinc salts. Antibacterial and antifungal activity. Spectrochim Acta A Mol Biomol Spectrosc, 2010. **76**(3-4): p. 341-7.

15. Park, H.-R., et al., Ionization and divalent cation complexation of quinolone antibiotics in aqueous solution. Bull Korean Chem Soc, 2000. **21**(9): p. 849-854.

16. Psomas, G. and D.P. Kessissoglou, Quinolones and non-steroidal anti-inflammatory drugs interacting with copper(II), nickel(II), cobalt(II) and zinc(II): structural features, biological evaluation and perspectives. Dalton Trans, 2013. **42**(18): p. 6252-76.

17. Pulicharla, R., et al., Toxicity of chlortetracycline and its metal complexes to model microorganisms in wastewater sludge. Sci Total Environ, 2015. **532**: p. 669-75.

18. Wang, Y.J., et al., Adsorption and cosorption of tetracycline and copper(II) on montmorillonite as affected by solution pH. Environ Sci Technol, 2008. **42**(9): p. 3254-9.

19. Zhao, Y., et al., Adsorption of tetracycline onto goethite in the presence of metal cations and humic substances. J Colloid Interface Sci, 2011. **361**(1): p. 247-51.

20. Graouer-Bacart, M., S. Sayen, and E. Guillon, Adsorption of enrofloxacin in presence of Zn(II) on a calcareous soil. Ecotoxicol Environ Saf, 2015. **122**: p. 470-6.

21. Chen, W.R. and C.H. Huang, Transformation of tetracyclines mediated by Mn(II) and Cu(II) ions in the presence of oxygen. Environ Sci Technol, 2009. **43**(2): p. 401-7.

22. Cuquerella, M.C., et al., Effects of bio-compatible metal ions on rufloxacin photochemistry, photophysics and photosensitization: copper(II). J Photochem Photobiol B, 2010. **101**(3): p. 295-303.

23. Villegas-Guzman, P., et al., Evaluation of water matrix effects, experimental parameters, and the degradation pathway during the TiO2 photocatalytical treatment of the antibiotic dicloxacillin. J Environ Sci Health A Tox Hazard Subst Environ Eng, 2015. **50**(1): p. 40-8.

24. Ribeiro, C., S.C. Lopes, and P. Gameiro, New insights into the translocation route of enrofloxacin and its metalloantibiotics. J Membr Biol, 2011. **241**(3): p. 117-25.

25. Mitscher, L.A., Bacterial topoisomerase inhibitors: quinolone and pyridone antibacterial agents. Chem Rev, 2005. **105**(2): p. 559-92.

26. Kim, S., et al., PubChem Substance and Compound databases. Nucleic Acids Res, 2016. **44**(D1): p. D1202-13.

27. Wishart, D.S., et al., DrugBank: a comprehensive resource for in silico drug discovery and exploration. Nucleic Acids Res, 2006. **34**(Database issue): p. D668-72.

28. Blondeau, J.M., Expanded activity and utility of the new fluoroquinolones: a review. Clin Ther, 1999. **21**(1): p. 3-40; discussion 1-2.

29. Wohlkonig, A., et al., Structural basis of quinolone inhibition of type IIA topoisomerases and target-mediated resistance. Nat Struct Mol Biol, 2010. **17**(9): p. 1152-3.

30. Drakopoulos, A.I. and P.C. Ioannou, Spectrofluorimetric study of the acid–base equilibria and complexation behavior of the fluoroquinolone antibiotics ofloxacin, norfloxacin, ciprofloxacin and pefloxacin in aqueous solution. Anal Chim Acta, 1997. **354**(1–3): p. 197-204.

31. Takacs-Novak, K., et al., Protonation equilibria of quinolone antibacterials. J Pharm Sci, 1990. **79**(11): p. 1023-8.

32. Uivarosi, V., Metal complexes of quinolone antibiotics and their applications: an update. Molecules, 2013. **18**(9): p. 11153-97.

33. Drlica, K. and X. Zhao, DNA gyrase, topoisomerase IV, and the 4-quinolones. Microbiol Mol Biol Rev, 1997. **61**(3): p. 377-92.

34. Tornaletti, S. and A.M. Pedrini, Studies on the interaction of 4-quinolones with DNA by DNA unwinding experiments. Biochim Biophys Acta, 1988. **949**(3): p. 279-87.

35. Palù, G., et al., Quinolone binding to DNA is mediated by magnesium ions. Proc Natl Acad Sci U S A, 1992. **89**(20): p. 9671-9675.

36. Turel, I., et al., Compounds of Antibacterial Agent Ciprofloxacin and Magnesium – Crystal Structures and Molecular Modeling Calculations. Eur J Inorg Chem, 2008. **2008**(23): p. 3718-3727.

37. Xiao, D.R., et al., Rationally designed, polymeric, extended metal-ciprofloxacin complexes. Chemistry, 2005. **11**(22): p. 6673-86.

38. Chen, Z.-F., et al., X-Ray crystal structures of Mg2+ and Ca2+ dimers of the antibacterial drug norfloxacin. Journal of the Chemical Society, Dalton Transactions, 2000(22): p. 4013-4014.

39. Drevensek, P., et al., X-Ray crystallographic, NMR and antimicrobial activity studies of magnesium complexes of fluoroquinolones - racemic ofloxacin and its S-form, levofloxacin. J Inorg Biochem, 2006. **100**(11): p. 1755-63.

40. Drevensek, P., I. Turel, and N. Poklar Ulrih, Influence of copper(II) and magnesium(II) ions on the ciprofloxacin binding to DNA. J Inorg Biochem, 2003. **96**(2-3): p. 407-15.

41. Blower, T.R., et al., Crystal structure and stability of gyrase-fluoroquinolone cleaved complexes from Mycobacterium tuberculosis. Proc Natl Acad Sci U S A, 2016. **113**(7): p. 1706-13.

42. Yuan, X.-y., J. Qin, and L.-l. Lu, Influence of metal ions on the interaction between gatifloxacin and calf thymus DNA. Spectrochimica Acta Part A: Molecular and Biomolecular Spectroscopy, 2010. **75**(2): p. 520-524.

43. Ragheb, M.A., M.A. Eldesouki, and M.S. Mohamed, DNA binding, photo-induced DNA cleavage and cytotoxicity studies of lomefloxacin and its transition metal complexes. Spectrochim Acta A Mol Biomol Spectrosc, 2015. **138**: p. 585-95.

44. Turel, I., The interactions of metal ions with quinolone antibacterial agents. Coord Chem Rev, 2002. **232**(1–2): p. 27-47.

45. Serafin, A. and A. Stańczak, The complexes of metal ions with fluoroquinolones. Russian Journal of Coordination Chemistry, 2009. **35**(2): p. 81-95.

46. Refat, M.S., Synthesis and characterization of norfloxacin-transition metal complexes (group 11, IB): spectroscopic, thermal, kinetic measurements and biological activity. Spectrochim Acta A Mol Biomol Spectrosc, 2007. **68**(5): p. 1393-405.

47. Lecomte, S., et al., Effect of magnesium complexation by fluoroquinolones on their antibacterial properties. Antimicrob Agents Chemother, 1994. **38**(12): p. 2810-6.

48. Gao, F., et al., Synthesis, characterization and antibacterial activity of novel Fe(III), Co(II), and Zn(II) complexes with norfloxacin. J Inorg Biochem, 1995. **60**(1): p. 61-7.

49. Vieira, L.M.M., et al., Platinum(II) complexes with fluoroquinolones: Synthesis and characterization of unusual metal–piperazine chelates. Inorg Chim Acta, 2009. **362**(6): p. 2060-2064.

50. Sadeek, S.A., Synthesis, thermogravimetric analysis, infrared, electronic and mass spectra of Mn(II), Co(II) and Fe(III) norfloxacin complexes. J Mol Struct, 2005. **753**(1–3): p. 1-12.

51. Refat, M.S. and G.G. Mohamed, Ti(IV), Cr(III), Mn(II), and Ni(II) Complexes of the Norfloxacin Antibiotic Drug: Spectroscopic and Thermal Characterizations. J Chem Eng Data, 2010. **55**(9): p. 3239-3246.

52. Refat, M.S., et al., Spectroscopic, thermal and kinetic studies of coordination compounds of Zn(II), Cd(II) and Hg(II) with norfloxacin. Journal of Thermal Analysis and Calorimetry, 2010. **102**(1): p. 225-232.

53. Coats, A.W. and J.P. Redfern, Kinetic Parameters from Thermogravimetric Data. Nature, 1964. **201**(4914): p. 68-69.

54. Turel, I., N. Bukovec, and E. Farkas, Complex formation between some metals and a quinolone family member (ciprofloxacin). Polyhedron, 1996. **15**(2): p. 269-275.

55. Sakai, M., et al., Comparison of the complexation of fluoroquinolone antimicrobials with metal ions by nuclear magnetic resonance spectroscopy. J Pharm Biomed Anal, 1999. **18**(6): p. 1057-67.

56. Urbaniak, B. and Z.J. Kokot, Analysis of the factors that significantly influence the stability of fluoroquinolone-metal complexes. Anal Chim Acta, 2009. **647**(1): p. 54-9.

57. Creager, S., 3 - Solvents and Supporting Electrolytes A2 - Zoski, Cynthia G, in Handbook of Electrochemistry. 2007, Elsevier: Amsterdam. p. 57-72.

58. Ross, D.L. and C.M. Riley, Physicochemical properties of the fluoroquinolone antimicrobials. II. Acid ionization constants and their relationship to structure. Int J Pharm, 1992. **83**(1): p. 267-272.

59. Zhao, Z., et al., Nutrients, heavy metals and microbial communities co-driven distribution of antibiotic resistance genes in adjacent environment of mariculture. Environ Pollut, 2017. **220**(Pt B): p. 909-918.

60. Li, B. and T. Zhang, Biodegradation and adsorption of antibiotics in the activated sludge process. Environ Sci Technol, 2010. **44**(9): p. 3468-73.

61. Jia, A., et al., Occurrence and fate of quinolone and fluoroquinolone antibiotics in a municipal sewage treatment plant. Water Res, 2012. **46**(2): p. 387-94.

62. Girardi, C., et al., Biodegradation of ciprofloxacin in water and soil and its effects on the microbial communities. J Hazard Mater, 2011. **198**: p. 22-30.

63. Do, M.T. and D.C. Stuckey, Fate and removal of Ciprofloxacin in an anaerobic membrane bioreactor (AnMBR). Bioresource Technology, 2019. **289**: p. 121683.

64. Liao, X., et al., Biodegradation of antibiotic ciprofloxacin: pathways, influential factors, and bacterial community structure. Environ Sci Pollut Res Int, 2016. **23**(8): p. 7911-8.

65. Gad-Allah, T.A., M.E. Ali, and M.I. Badawy, Photocatalytic oxidation of ciprofloxacin under simulated sunlight. J Hazard Mater, 2011. **186**(1): p. 751-5.

66. An, T., et al., Mechanistic Considerations for the Advanced Oxidation Treatment of Fluoroquinolone Pharmaceutical Compounds using TiO2 Heterogeneous Catalysis. J Phys Chem A, 2010. **114**(7): p. 2569-2575.

67. Bojer, C., et al., Clinical wastewater treatment: Photochemical removal of an anionic antibiotic (ciprofloxacin) by mesostructured high aspect ratio ZnO nanotubes. Applied Catalysis B: Environmental, 2017. **204**: p. 561-565.

68. Diao, Z.-H., et al., Enhanced catalytic degradation of ciprofloxacin with FeS2/SiO2 microspheres as heterogeneous Fenton catalyst: Kinetics, reaction pathways and mechanism. J Hazard Mater, 2017. **327**: p. 108-115.

69. Matzek, L.W. and K.E. Carter, Sustained persulfate activation using solid iron: Kinetics and application to ciprofloxacin degradation. Chemical Engineering Journal, 2017. **307**: p. 650-660.

70. Feng, M., et al., Metal-mediated oxidation of fluoroquinolone antibiotics in water: A review on kinetics, transformation products, and toxicity assessment. Journal of Hazardous Materials, 2018. **344**: p. 1136-1154.

71. Li, M.-f., et al., Cu(II)-influenced adsorption of ciprofloxacin from aqueous solutions by magnetic graphene oxide/nitrilotriacetic acid nanocomposite: Competition and enhancement mechanisms. Chemical Engineering Journal, 2017. **319**: p. 219-228.

72. Ma, J., et al., Coadsorption behavior and mechanism of ciprofloxacin and Cu(II) on graphene hydrogel wetted surface. Chemical Engineering Journal, 2020. **380**: p. 122387.

73. Liu, X., M. Liu, and L. Zhang, Co-adsorption and sequential adsorption of the co-existence four heavy metal ions and three fluoroquinolones on the functionalized ferromagnetic 3D NiFe2O4 porous hollow microsphere. Journal of Colloid and Interface Science, 2018. **511**: p. 135-144.

74. Maul, J.D., et al., Effects of the antibiotic ciprofloxacin on stream microbial communities and detritivorous macroinvertebrates. Environ Toxicol Chem, 2006. **25**(6): p. 1598-606.

75. Cuprys, A., et al., Ciprofloxacin-metal complexes -stability and toxicity tests in the presence of humic substances. Chemosphere, 2018. **202**: p. 549-559.

76. Levina, A., D.C. Crans, and P.A. Lay, Speciation of metal drugs, supplements and toxins in media and bodily fluids controls in vitro activities. Coord Chem Rev, 2017.

77. Shaikh, A.R., R. Giridhar, and M.R. Yadav, Bismuth-norfloxacin complex: synthesis, physicochemical and antimicrobial evaluation. Int J Pharm, 2007. **332**(1-2): p. 24-30.

78. Abd el-Halim, H.F., et al., Ligational behaviour of lomefloxacin drug towards Cr(III), Mn(II), Fe(III), Co(II), Ni(II), Cu(II), Zn(II), Th(IV) and UO(2)(VI) ions: synthesis, structural characterization and biological activity studies. Spectrochim Acta A Mol Biomol Spectrosc, 2011. **82**(1): p. 8-19.

79. Sultana, N., et al., Synthesis, characterization, antibacterial, antifungal and immunomodulating activities of gatifloxacin–metal complexes. J Mol Struct, 2010. **969**(1–3): p. 17-24.

80. Tümer, M., et al., Antimicrobial activity studies of the binuclear metal complexes derived from tridentate Schiff base ligands. Transit Metal Chem, 1999. **24**(4): p. 414-420.

81. Panchal, P.K., et al., Bactericidal activity of different oxovanadium(IV) complexes with Schiff bases and application of chelation theory. J Enzyme Inhib Med Chem, 2006. **21**(2): p. 203-9.

82. Sultana, N., et al., Synthesis, spectroscopic, and biological evaluation of some levofloxacin metal complexes. Med Chem Res, 2013. **22**(3): p. 1371-1377.

83. Mora Carpio, A. and A. Climaco, Candidiasis, Fungemia, in StatPearls. 2017, StatPearls Publishing

StatPearls Publishing LLC.: Treasure Island (FL).

84. Parniske, M., Arbuscular mycorrhiza: the mother of plant root endosymbioses. Nat Rev Microbiol, 2008. **6**(10): p. 763-75.

85. Robinson, C.H., et al., Nutrient and carbon dioxide release by interacting species of straw-decomposing fungi. Plant and Soil, 1993. **151**(1): p. 139.

86. Setala, H. and M.A. McLean, Decomposition rate of organic substrates in relation to the species diversity of soil saprophytic fungi. Oecologia, 2004. **139**(1): p. 98-107.

87. Pages, J.M., C.E. James, and M. Winterhalter, The porin and the permeating antibiotic: a selective diffusion barrier in Gram-negative bacteria. Nat Rev Microbiol, 2008. **6**(12): p. 893-903.

88. Zhao, X., et al., Characterization of Integrons and Resistance Genes in Salmonella Isolates from Farm Animals in Shandong Province, China. Front Microbiol, 2017. **8**: p. 1300.

89. Gao, P., et al., Impacts of coexisting antibiotics, antibacterial residues, and heavy metals on the occurrence of erythromycin resistance genes in urban wastewater. Appl Microbiol Biotechnol, 2015. **99**(9): p. 3971-80.

90. Mao, D., et al., Prevalence and proliferation of antibiotic resistance genes in two municipal wastewater treatment plants. Water Res, 2015. **85**: p. 458-66.

91. Ji, X., et al., Antibiotic resistance gene abundances associated with antibiotics and heavy metals in animal manures and agricultural soils adjacent to feedlots in Shanghai; China. J Hazard Mater, 2012. **235-236**: p. 178-85.

92. Lemire, J.A., J.J. Harrison, and R.J. Turner, Antimicrobial activity of metals: mechanisms, molecular targets and applications. Nat Rev Microbiol, 2013. **11**(6): p. 371-84.

93. Mahendran, K.R., et al., Permeation of antibiotics through Escherichia coli OmpF and OmpC porins: screening for influx on a single-molecule level. J Biomol Screen, 2010. **15**(3): p. 302-7.

94. Mach, T., et al., Facilitated permeation of antibiotics across membrane channels--interaction of the quinolone moxifloxacin with the OmpF channel. J Am Chem Soc, 2008. **130**(40): p. 13301-9.

95. Feio, M.J., et al., Fluoroquinolone-metal complexes: a route to counteract bacterial resistance? J Inorg Biochem, 2014. **138**: p. 129-43.

96. Ferreira, M. and P. Gameiro, Ciprofloxacin metalloantibiotic: an effective antibiotic with an influx route strongly dependent on lipid interaction? J Membr Biol, 2015. **248**(1): p. 125-36.

97. Ribeiro, C., S.C. Lopes, and P. Gameiro, New Insights into the Translocation Route of Enrofloxacin and Its Metalloantibiotics. J Membr Biol, 2011. **241**(3): p. 117-125.

98. Kang, F., et al., Alkali-earth metal bridges formed in biofilm matrices regulate the uptake of fluoroquinolone antibiotics and protect against bacterial apoptosis. Environ Pollut, 2017. **220**(Pt A): p. 112-123.

99. Blanco, G., et al., Wildlife contamination with fluoroquinolones from livestock: Widespread occurrence of enrofloxacin and marbofloxacin in vultures. Chemosphere, 2016. **144**: p. 1536-43.

100. Blanco, G., A. Junza, and D. Barron, Food safety in scavenger conservation: Diet-associated exposure to livestock pharmaceuticals and opportunist mycoses in threatened Cinereous and Egyptian vultures. Ecotoxicol Environ Saf, 2017. **135**: p. 292-301.

101. Gao, L., et al., Occurrence, distribution and bioaccumulation of antibiotics in the Haihe River in China. J Environ Monit, 2012. **14**(4): p. 1248-55.

102. Xiao, Q.M., J.W. Wang, and Y.L. Tang, [Degradation and bioaccumulation characteristics of ciprofloxacin in soil-vegetable system]. Ying Yong Sheng Tai Xue Bao, 2012. **23**(10): p. 2708-14.

103. Wang, J., et al., Variations in the fate and biological effects of sulfamethoxazole, norfloxacin and doxycycline in different vegetable-soil systems following manure application. J Hazard Mater, 2016. **304**: p. 49-57.

104. Chen, G., et al., Risk assessment of three fluoroquinolone antibiotics in the groundwater recharge system. Ecotoxicol Environ Saf, 2016. **133**: p. 18-24.

105. Peruchi, L.M., A.H. Fostier, and S. Rath, Sorption of norfloxacin in soils: analytical method, kinetics and Freundlich isotherms. Chemosphere, 2015. **119**: p. 310-7.

106. Peng, F.J., et al., Antibacterial activity of the soil-bound antimicrobials oxytetracycline and ofloxacin. Environ Toxicol Chem, 2014. **33**(4): p. 776-83.

107. Leal, R.M., et al., Sorption of fluoroquinolones and sulfonamides in 13 Brazilian soils. Chemosphere, 2013. **92**(8): p. 979-85.

108. Van Doorslaer, X., et al., Fluoroquinolone antibiotics: an emerging class of environmental micropollutants. Sci Total Environ, 2014. **500-501**: p. 250-69.

109. Kulshrestha, P., R.F. Giese, Jr., and D.S. Aga, Investigating the molecular interactions of oxytetracycline in clay and organic matter: insights on factors affecting its mobility in soil. Environ Sci Technol, 2004. **38**(15): p. 4097-105.

110. Fu, Q.L., et al., Sorption of roxarsone onto soils with different physicochemical properties. Chemosphere, 2016. **159**: p. 103-12.

111. Aristilde, L. and G. Sposito, Binding of ciprofloxacin by humic substances: a molecular dynamics study. Environ Toxicol Chem, 2010. **29**(1): p. 90-8.

112. Vasudevan, D., et al., pH-dependent ciprofloxacin sorption to soils: Interaction mechanisms and soil factors influencing sorption. Geoderma, 2009. **151**(3–4): p. 68-76.

113. Wu, Q., et al., Adsorption and intercalation of ciprofloxacin on montmorillonite. Appl Clay Sci, 2010. **50**(2): p. 204-211.

114. Gu, C. and K.G. Karthikeyan, Sorption of the antimicrobial ciprofloxacin to aluminum and iron hydrous oxides. Environ Sci Technol, 2005. **39**(23): p. 9166-73.

115. Chen, H., et al., Influence of Cu and Ca cations on ciprofloxacin transport in saturated porous media. J Hazard Mater, 2013. **262**: p. 805-11.

116. Chen, H., et al., Effects of Cu and Ca cations and Fe/Al coating on ciprofloxacin sorption onto sand media. J Hazard Mater, 2013. **252-253**: p. 375-81.

117. Tan, Y., et al., Effects of metal cations and fulvic acid on the adsorption of ciprofloxacin onto goethite. Environ Sci Pollut Res Int, 2015. **22**(1): p. 609-17.

118. Pei, Z., et al., Coadsorption of ciprofloxacin and Cu(II) on montmorillonite and kaolinite as affected by solution pH. Environ Sci Technol, 2010. **44**(3): p. 915-20.

2. PROBLÉMATIQUE

Dans le chapitre précédent sur la revue de la littérature, les problèmes suivants ont été soulevés:

3.1 La tendance à la hausse de l'apparition de souches résistantes aux FQ

Depuis son approbation à la fin des années 1980, la CIP a été largement utilisée pour traiter de nombreuses infections bactériennes. Cependant, **jusqu'à 65% des CIP non modifiées peuvent être excrétées dans l'environnement via l'urine et/ou les selles**. Il en résulte une concentration de CIP élevée dans l'eau et le sol, où elle exerce une pression sélective sur la communauté microbienne actuelle. Cela a conduit à la sélection et à la diffusion de la résistance aux FQ (CIP). Au Canada, la tendance à la hausse des isolats de *N. gonorrhea* résistants à la CIP a été observée entre 2004 (5%) et 2014 (34%). Le pourcentage de *Staphylococcus aureus* méticilline-résistant (SARM), résistant également à CIP, se situait entre 81,4 à 89,1% cependant, des isolats testés (2008-2014), entre 2015-2017. La tendance est passée de 81,7% à 76,3%. La proportion d'isolats d'*E. coli* résistants à la CIP est passée de 20% (2007) à 29,2% (2011). Selon le dernier rapport publié par l'Organisation mondiale de la santé (OMS), *Salmonella* spp. ont été classées comme hautement prioritaires pour la recherche et le développement de nouvelles alternatives de traitement en raison de la sensibilité réduite des souches.

De plus, la présence d'ions métalliques dans l'eau et les sols présentait une corrélation positive avec l'abondance de certains ARG; les antibiotiques et les gènes de résistance aux métaux lourds peuvent être liés au même plasmide. En outre, il est suggéré que les complexes FQs-Me pénètrent dans la cellule bactérienne par une voie différente de celle d'un antibiotique libre, solution prometteuse pour la résistance aux FQs. Toutefois, sur la base de l'hypothèse Red Queen, la bactérie pourrait également développer une résistance aux métalloantibiotiques. **L'OMS a classé les FQs comme un agent antibactérien extrêmement important pour la médecine humaine en raison de sa résistance accrue aux bactéries.**

3.2 Bioaccumulation

La CIP a été détectée dans les légumes (chou chinois, radis, tomates), **ainsi que chez les animaux** (carassin, invertébrés d'eau douce, oisillons aigle doré, et vautours).

3.3 L'influence des complexes CIP-Me sur le TEU

Le taux d'élimination de la CIP dans les eaux usée varie de 30 à 86%. **Environ 30 à 40% du CIP peuvent être adsorbées sur les boues,** ce qui réduit considérablement leur efficacité d'élimination. Cependant, la présence d'ions de métaux alcalino-terreux a pu réduire le taux de sorption des boues.

L'effet d'autres ions n'est pas connu. De plus, la biodégradation du CIP est rare en raison de son temps de rétention réduit et de son taux d'absorption élevé. **L'activité antimicrobienne modifiée des complexes CIP-Me peut également avoir une influence négative sur la communauté bactérienne présente pendant le traitement biologique.**

3.4 La mobilité du CIP dans l'eau et le sol

La CIP en tant que composé amphotère présente une spéciation différente en fonction du pH de l'environnement. En ce qui concerne les conditions acides, neutres ou alcalines, le CIP peut exercer une affinité de sorption différente avec les substances humiques, le sol ou les sédiments. **La présence d'ions métalliques influence considérablement l'efficacité de la sorption.** En général, trois scénarios ont lieu. La présence d'ions métalliques (MI) peut faciliter la sorption CIP via un pontage des métaux. D'autre part, la formation de complexes CIP-Me peut entraver la sorption sur l'HS ou les sols, ainsi le complexe restera dans l'eau. Le dernier scénario comprend la compétition entre MI et CIP; dans ce cas, le CIP est en concurrence avec le MI pour les sites de liaison du SH, etc. De plus, **l'affinité pour le CIP dépend également de la composition du compartiment environnemental**.

4 HYPOTHÈSE

La présente recherche repose sur les hypothèses suivantes :

4.1 Les composés les plus abondants dans l'eau et les sols sont le HS et le MI. Selon la littérature, la CIP est capable de former des complexes avec le MI, ce qui influence les caractéristiques physicochimiques de l'antibiotique ainsi que l'activité antimicrobienne. De plus, la CIP peut également être adsorbée sur le HS. Par conséquent, **la présence de HS peut affecter la stabilité des complexes CIP-Me**. De plus, **si les complexes CIP-Me et/ou CIP-Me + HS sont stables, ils peuvent affecter la communauté microbienne actuelle.**

4.2 La forte concentration d'antibiotiques, chlorotétracycline (CTC) et CIP peut entraîner la dissémination des ARG et des ARB. De plus, le CIP et le CTC peuvent avoir un pouvoir antimicrobien synergique ou antagoniste.

4.3 D'après les caractéristiques physicochimiques, la CIP devrait avoir une plus grande affinité pour la phase aquatique pendant le TEU. Cependant, les études ont montré qu'il peut être détecté dans les boues d'épuration des eaux usées et les eaux usées. **L'examen de la séparation de la CIP et de la corrélation de la concentration en métal peut faciliter la compréhension du devenir du CIP pendant le TEU**.

4.4 Les méthodes d'oxydation conventionnelles sont insuffisantes pour éliminer les antibiotiques pendant le traitement, ce qui se traduit par une concentration élevée dans l'eau et les sols. Les méthodes d'oxydation hybrides sont des techniques prometteuses pour augmenter le taux d'élimination des composés organiques. Par conséquent, **le développement de méthodes d'élimination hybrides peut entraîner une efficacité accrue du traitement**.

4.5 L'enzyme la plus couramment utilisée pour la dégradation enzymatique est la laccase, oxydase liant le cuivre. Cependant, le coût de l'enzyme pure est encore plus élevé. **L'application d'extrait de laccase brut pourrait permettre de transformer efficacement la CIP et de réduire les coûts du traitement enzymatique.**

4.6 Le biochar s'est avéré être une alternative au charbon actif pour éliminer les polluants organiques des eaux usées. Cependant, **la fonctionnalisation du biochar peut augmenter sa capacité d'absorption et sa sensibilité à la CIP**.

5 OBJECTIFS

L'objectif global de cette recherche est d'étudier le devenir de la CIP dans les stations d'épuration des eaux usées et l'environnement, l'influence de l'IM sur la WWT et d'essayer des méthodes de traitement chimiques, physiques et biologiques.

Le présent projet comprend les objectifs spécifiques suivants:

5.1 Étudier la stabilité et toxicité des complexes CIP-métal en présence de substances humiques
5.2 Estimer la concentration en métaux et de leur spéciation dans les boues et son influence possible sur la distribution de CIP dans TEU
5.3 Détecter les bactéries résistantes au CIP/CTC dans des échantillons d'eau de la région de Québec
5.4 Combiner la toxicité du CIP et du CTC vis-à-vis des représentants des bactéries à Gram négatif et à Gram positif
5.5 Étudier le potentiel d'extrait de laccase brut produit à partir de déchets agro-industriels pour éliminer le CIP
5.6 Comparer le couplage, électro-oxydation et oxydation enzymatique, pour éliminer le CIP des eaux usées
5.7 Tester la fonctionnalisation du biochar pour éliminer simultanément les ions de métaux lourds et la CIP

6 ORIGINALITÉ

Parmi les hypothèses précédentes, l'originalité de ce projet de recherche est la suivante:

6.1 L'influence de la présence de HS sur la stabilité et la toxicité des complexes CIP-Me nous aidera à comprendre le devenir de la CIP dans les milieux aquatiques.

6.2 La détection de l'ARB, résistant à la CIP et au CTC aidera à répondre au besoin émergent d'amélioration du TEU.

6.3 La répartition de la CIP en corrélation avec la concentration en ions métalliques aidera à connaître le sort de la CIP au cours de la STEP.

6.4 L'utilisation d'extraits enzymatiques bruts pour éliminer les polluants réduira les coûts liés à l'oxydation enzymatique à l'échelle industrielle.

6.5 L'électrooxydation séquentielle et l'oxydation enzymatique constituent une nouvelle approche pour l'élimination de la CIP.

6.6 Le biochar fonctionnalisé constituera un adsorbant économique pouvant être utilisé pendant le TEU. De plus, en raison de la complexation de CIP-Me, il sera possible d'éliminer simultanément les deux contaminants.

Globalement, l'originalité du projet de doctorat proposé est l'influence des ions métalliques sur le devenir et l'élimination de la ciprofloxacine dans l'environnement, en prenant comme exemple les eaux usées et les boues d'épuration.

7. Méthodologie

Générale

Spectroscopie infrarouge à transformée de Fourier

Tous les échantillons ont été analysés sous forme solide par spectroscopie infrarouge à transformée de Fourier en utilisant le spectromètre Cary 670 FTIR. Les spectres ont été obtenus avec une résolution de 4 cm^{-1}, dans la gamme de 4000-400 cm^{-1}.

Analyses statistiques

L'analyse a été réalisée à l'aide du logiciel SigmaPlot 13.0. L'ANOVA unidirectionnelle a été utilisée pour déterminer s'il existe une différence statistiquement significative (valeurs de p <0,05). Les données ont été présentées comme une moyenne de triple ± écart-type.

Test d'activité antimicrobienne - concentration minimale inhibitrice (CMI)

La CMI a été définie comme la concentration minimale d'antibiotique capable d'inhiber la croissance bactérienne. La CMI des complexes CIP, CIP-Me et CIP-Me en présence de HS contre les représentants Gram négatifs et / ou Gram positifs a été mesurée par la méthode de dilution sur gélose. Il a été réalisé conformément aux spécifications du Comité européen pour les tests de sensibilité aux antimicrobiens de la Société européenne de microbiologie clinique et des maladies infectieuses.

Activité antimicrobienne des produits de transformation

Pour évaluer l'activité antimicrobienne des produits de transformation, *Escherichia coli* (NRRL-3707) a été utilisé comme micro-organisme modèle. La souche d'*E. coli* a été relancée dans du bouillon Tryptone-Levure Extrait-Glucose (tryptone 5 g/L, extrait de levure 5 g/L, K_2HPO_4 1 g/L, glucose 1 g/L) suggéré par le Service de recherche agricole (NRRL) Collection Culture. Les bactéries ont été incubées pendant 24 h, 28 ° C, 150 tr/min. Par la suite, *E. coli* a été striée sur des plaques de gélose Luria (LA) (tryptone 10 g/L, extrait de levure 5 g/L, NaCl 10 g/L, gélose 1,5% p/v) et incubée pendant 24 h à 37°C. Les plaques ont été maintenues à 4°C pour une utilisation ultérieure.

Les échantillons de dégradation CIP par électro-oxydation et/ou oxydation enzymatique ont été collectés. La technique de diffusion sur puits d'agar a été utilisée pour tester l'efficacité antimicrobienne des produits de transformation. La culture *d'E. coli* a été inoculée sur des plaques LA, puis les puits ont été perforés de manière aseptique (6-8 mm) avec des pointes stériles. Ensuite, 100 µL de solutions testées (contrôles, électrooxydation et oxydation enzymatique individuellement et traitement combiné) ont été ajoutés dans les puits et incubés pendant 24h à 37°C. Après le temps d'incubation, les zones d'inhibition ont été mesurées.

Détection CTC et CIP

La concentration de CIP et de CTC a été analysée par chromatographie liquide-électrospray-ionisation-spectrométrie de masse en tandem (LC-ESI-MS / MS). Le système comprenait une pompe LC pour sondeur Finnigan reliée au spectromètre de masse triple quadruple TSQ Quantum access (Thermo Scientific, Mississauga, ON, Canada) et une interface d'ionisation par électrospray. Une aliquote de 15 µL des échantillons traités a été injectée dans la colonne BetaBasic-18 (100 mm x 2,1 mm x 3 µm). Le four à colonne a été réglé à 40 ° C et le débit a été maintenu à 0,3 mL/min. La ciprofloxacine-d8 (CIP-d8) et la sulfaméthazine ont été utilisées comme étalons internes pour la détection de la ciprofloxacine et de la chlortétracycline, respectivement. Ils ont été ajoutés à chaque échantillon avant les analyses pour donner la concentration finale de 50 µg/L et 5 µg/L pour la ciprofloxacine-d_8 et la sulfaméthazine, respectivement. Les échantillons ont été élués avec une phase mobile qui comprenait 0,1% d'acide formique (phase mobile A) et de l'acétonitrile combinés avec 0,1% d'acide formique (phase mobile B). L'élution du gradient a commencé avec 90% de la phase mobile A et 10% de la phase mobile B. Elle a été constante jusqu'à 0,5 min, puis la phase mobile A a commencé à diminuer progressivement (30%) jusqu'à 3 min. Par la suite, le gradient a été maintenu constant jusqu'à 8 min, puis il est revenu à la configuration initiale. Le spectromètre de masse a été utilisé en mode positif SRM. La tension de pulvérisation a été réglée à 4000 V et l'écumoire décalée à 20 V. La pression du gaz de collision était de 1,5 mTorr. La température capillaire était à 350 ° C. L'énergie de collision pour le CIP, le CTC, la sulfaméthazine et le CIP-d8 a été fixée à 17, 18, 17 et 19 V respectivement. Les ions précurseurs et produits (m / z) ont été sélectionnés comme suit: 332,3 et 245,3 pour CIP, 479,1 et 444 pour CTC, 340,3 et 249,3 pour CIP-d8, 285 et 185 pour sulfaméthazine.

ICP

Des étalons ont été préparés dans 10% de HNO_3 et 30% de HCl. À tous les standards et échantillons, Y 5 mg / L + CsCl 10 g / L dans 1% HNO_3 a été ajouté comme standard interne. Des échantillons choisis au hasard ont été enrichis d'une concentration connue d'éléments; la récupération de tous les éléments testés était de 100 ± 2%.

Spécifique

Interactions de la ciprofloxacine avec les métaux et les substances humiques

Préparation de la solution CIP-Me

La poudre de CIP a été dissoute dans de l'eau désionisée pour obtenir une solution mère à 100 mg / L. La même procédure a été appliquée pour une solution mère d'ions métalliques pour obtenir une concentration similaire. Avant dilution, les solutions ont été filtrées à l'aide d'un filtre (Chromafil® Xtra 0,45 µm). Plus tard, les solutions mères ont été diluées dans du tampon Tris-HCl (50 mM; pH 6,5) dans des tubes Falcon de 15 mL, où la concentration CIP était constante (10 mg/L) et la concentration en

métaux variait entre 0 et 5 mg/L. Le volume final de la composition était de 5 mL. Les solutions ont été préparées en trois exemplaires.

Constante de stabilité des complexes CIP-Me

La stabilité des complexes CIP-Me a été établie par des mesures d'intensité de fluorescence, puis leur constante de stabilité a été calculée. Les solutions obtenues ont été incubées jusqu'à ce qu'elles atteignent l'équilibre de complexation. Le sel de sodium humique (10 g/L) a été dissous dans de l'eau désionisée puis filtré sur du papier filtre en fibre de verre Whatman pour éliminer l'humine insoluble. Les solutions de CIP et de métaux ont été préparées comme décrit précédemment, avec l'ajout de sel de sodium humique, en tant que représentant de substances humiques. Les concentrations finales étaient de 10 mg/L de substances humiques, 10 mg/L de CIP et 0-5 mg/L d'ions métalliques. Les contrôles sans substances humiques ont également été préparés. Les solutions CIP-Me ont été incubées à deux températures: 18 ± 2˚C et 4 ± 1˚C; ils n'étaient ni remués ni agités. Par la suite, l'intensité de fluorescence ($\lambda_{Ex/Em}$ = 276/415 nm) a été mesurée dans des cuvettes de quartz par le spectrophotomètre à fluorescence Varian Cary Eclipse (Mississauga, Ontario) avec le système de contrôle de la température Single Cell Peltier. Le volume des échantillons mesurés était de 3 mL.

Pour utiliser la spectrofluorimétrie comme outil pour étudier les changements d'intensité de fluorescence du CIP, la validation de la méthode a été effectuée. La raison principale en était d'exclure la possibilité de résultats faussement positifs ou faux négatifs en raison de la fluorescence potentielle des ions métalliques. L'intensité de fluorescence du CIP, du CIP-Me ([Me] = 5 mg/L) et des ions métalliques à leur concentration la plus élevée ([Me] = 5 mg/L]) a été mesurée. Les résultats sont présentés sur la Figure 1.4. Comme on peut le voir, la fluorescence des ions métalliques seuls était négligeable, par conséquent, cette méthode convenait à l'étude de la stabilité des complexes CIP-Me.

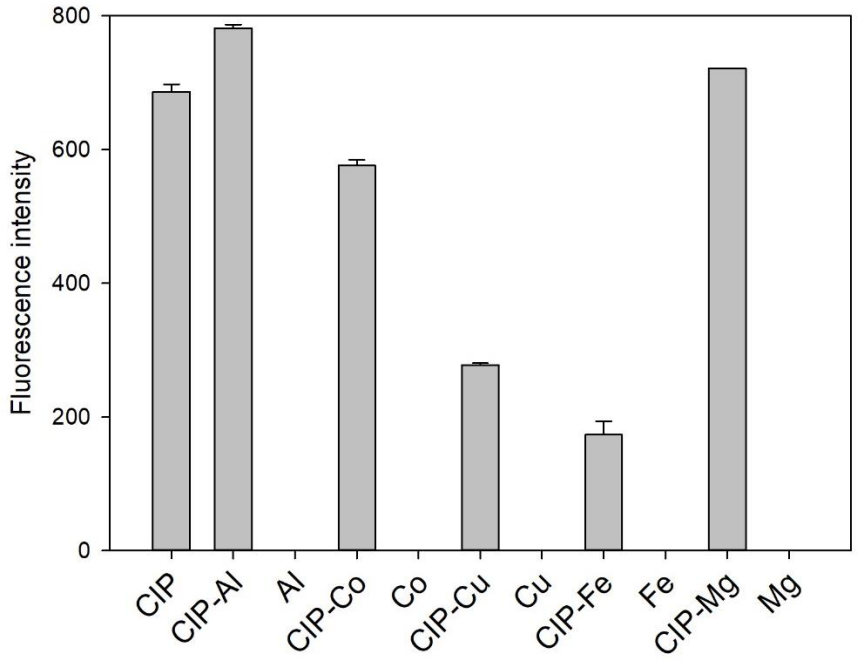

Figure 1. 4 Intensité de fluorescence des solutions testées

Spéciation des métaux dans les boues d'épuration et son influence sur la distribution d'antibiotiques

Préparation des échantillons pour l'analyse des éléments et la digestion partielle

La fraction liquide a été séparée des boues par centrifugation (7650 x g, 25 min, 4°C). Les échantillons de surnageant et de WW (affluent, effluent, unité de granulation et unité de criblage) ont ensuite été transférés pour digestion acide. Environ 0,5 g de boue séchée (ou fraction liquide) a été placé dans des tubes de 50 mL (SCP Science 10-500-262). Du HNO_3 (1 mL) a été ajouté et laissé pendant une nuit. Ensuite, 3 mL de HCl 1 M ont été ajoutés et placés dans le bloc chauffant (2 h, 95 ° C). Ensuite, les mélanges ont été refroidis et de l'eau Milli-Q a été ajoutée pour obtenir un volume de 50 mL. Les échantillons préparés ont été analysés par spectroscopie d'émission atomique à plasma à couplage inductif (ICP-AES) en double.

Spéciation chimique dans les boues

Les échantillons des sections suivantes ont été centrifugés (30 240 x g, 30 min) après chaque étape d'extraction et la partie solide a été séparée du surnageant. Par la suite, le culot a été utilisé pour l'étape d'extraction suivante, lorsque le surnageant a été filtré et analysé par ICP-AES. La récupération des métaux de cette méthode variait entre 74 et 120%. La procédure a été réalisée en duplicata.

Pour évaluer l'influence de la digestion séquentielle des boues sur les antibiotiques, les contrôles dans l'eau Milli-Q ont été effectués. La concentration de CIP n'a pas changé tout au long de la procédure; la

différence entre les fractions était inférieure à 10%. Dans le cas du CTC, la variation de sa concentration a été observée (<70% de récupération) en raison de l'isomérisation du composé.

Fraction échangeable

Les échantillons de boues (2 g) ont été extraits à température ambiante pendant 1 h avec 16 mL de solution de chlorure de magnésium (1 M $MgCl_2$, pH 7,0) dans un bain-marie. Une agitation continue a été maintenue. L'extraction dans cette fraction est principalement basée sur le processus d'adsorption-désorption.

Liés aux carbonates

Au résidu de la section précédente, 16 ml de NaOAc 1 M ont été ajoutés et le pH a été ajusté à 5,0 avec de l'acide acétique. Les échantillons ont subi 5 heures d'agitation continue à température ambiante pour co-précipiter des métaux avec des carbonates.

Oxydes liés à Fe – Mn (liés aux oxydes)

Le résidu de la section précédente a été traité à l'aide de 20 mL de 0,04 M NH^2OH – HCl dans 25% (v/v) HAc pour extraire les métaux. Les expériences ont été réalisées à 96 ° C avec une agitation occasionnelle pendant 6 heures. Dans ces conditions réductrices, Fe (III) et Mn (IV) libèrent des métaux adsorbés.

Bound-to-organiques

Du HNO_3 (4 mL) a été ajouté aux échantillons de boue (0,1 g) et laissé toute une nuit. Par la suite, 1,6 ml de HClO4 ont été ajoutés et chauffés pendant 2 h à 100°C. Ensuite, 2 mL d'HF ont été ajoutés et chauffés jusqu'à 150°C. Ensuite, 0,4 mL de HNO_3 et de l'eau jusqu'à 15 mL ont été ajoutés et incubés à température ambiante pendant 2 semaines avant les analyses ICP-AES.

Préparation des échantillons pour l'analyse CIP et CTC

Préparation d'échantillons d'eaux usées

Les échantillons d'eaux usées ont été centrifugés à 7650 x g pendant 30 min et le surnageant a été filtré à travers des filtres en fibres de verre de 2 µm (cercles de filtre G6 de marque Fisher, Fisher Scientific, Ontario, Canada). Le pH de chaque filtrat a été ajusté à pH 4,0 ± 0,1 avec HCl 0,1 M pour une extraction acide. Du Na_2EDTA a été ajouté à chaque échantillon à la concentration finale de 2 mM.

Les échantillons WWS (boues primaires, secondaires, mélangées et épaissies) ont été centrifugés à 7650 x g pendant 35 min, 4°C. La fraction solide a ensuite été séparée et congelée à -20 ° C pendant toute une nuit avant lyophilisation (Dura Frezz Dryer, Kinetics). Le surnageant a été filtré à travers des filtres en fibres de verre de 2 µm et le pH a été ajusté à pH 4,0±0,1. Du Na_2EDTA a été ajouté à chaque échantillon à la concentration finale de 2 mM.

Extraction de WWS

USE a été réalisée dans un bain d'eau à ultrasons (Fisher, FB 15069, Mississauga, Ontario) à une fréquence de 37 kHz.. Un échantillon de boue lyophilisée (0,5 g) a été transféré dans un tube Falcon de 50 mL (Fisher Scientific, Canada), suivi par l'ajout de 5 ml de tampon McIlwaine pH 3,0 et vortexé. La sonication a été effectuée pendant 20 min, puis les échantillons ont été centrifugés (12 000 x g, 15 min), le surnageant a été recueilli. Le processus d'extraction a été répété deux fois pour chaque échantillon. Les surnageant ont été combinés et pré-concentrés par extraction en phase solide.

Nettoyage et pré-concentration

La technique d'extraction en phase solide (SPE) a été utilisée pour le nettoyage et la pré-concentration des échantillons traités. Les cartouches SPE (Sep-Pak Plus C¬18) ont été installées dans le collecteur à vide (Welch, USA) connecté à une pompe à vide (Welch Rietschle Thomas, USA). Les cartouches ont été préconditionnées avec 7 mL de méthanol, puis 6 mL d'eau désionisée et 6 mL d'eau acidifiée (pH 3,0) à un débit d'environ 1,5 mL/min. De plus, l'échantillon a été chargé sur les cartouches; après pré-concentration, les échantillons ont été séchés par un système à vide (~ 15 psi). L'élution parallèle de CIP et CTC avec 2x4 mL de méthanol: acide trichloroacétique (9:1) a été utilisée pour obtenir la récupération la plus élevée possible. Chaque extrait a ensuite été évaporé sous un léger courant d'azote à sec. De plus, il a été reconstitué dans 1 ml d'acétonitrile: H_2O (1:9).

Apparition de bactéries résistantes à la ciprofloxacine/chlorotétracycline dans les eaux de la ville de Québec au Canada

Méthode Time-kill

La méthode Time-kill a été utilisée pour déterminer le taux de destruction des bactéries par les agents antimicrobiens. La procédure a été effectuée par la technique de microdilution en bouillon, comme décrit dans les directives du Comité national des normes de laboratoire clinique. *Enterobacter aerogenes* a été examiné contre le CTC, le CIP seul et dans leurs combinaisons (1/4MIC et 2MIC).

Extraction d'ADN

Les tubes contenant les colonies ont été centrifugés pendant 2 minutes à 10 000 x g. Le culot a été remis en suspension dans du tampon STE (tampon STE; Tris-HCl 10 mM pH 8,0, EDTA 1 mM, NaCl 100 mM) suivi d'une extraction. 10% (v/ v) de SDS à 10% ont été ajoutés goutte à goutte, puis les tubes ont été placés dans un bain d'eau bouillante pendant 1,5 à 2 min. Les débris cellulaires ont été agglomérés par centrifugation (10 min, 10 000 x g) à 10-15°C. Le liquide a été transféré dans un tube propre et stérile pour l'isolement de l'ADN par extraction au phénol/chloroforme suivi d'une précipitation à l'isopropanol. L'ADN a été aggloméré par centrifugation (25 min, 4°C, 14 000 x g), lavé avec de l'éthanol à 70% glacé et laissé à l'air sec. Le culot final a été remis en suspension dans du tampon TE (Tris 10 mM, pH 8,0, EDTA 1 mM) et maintenu à -20 ± 1°C.

Amplification par PCR

L'ADN isolé de la section précédente a été utilisé pour l'amplification par PCR. Les gènes ciblés étaient l'antigène plasmidique d'invasion H de *Shigella sp*. (IpaH), antigène plasmidique d'invasion B de *Salomnella sp*. (IpaB) et la séquence oligonucléotidique spécifique de *C. jejuni* (Cj). Les amorces ont été synthétisées par Invitrogen Life Sciences, Canada. Le mélange réactionnel de 10 µL de volume final comprenait 1 tampon de PCR (10 mM de chlorhydrate de Tris pH 8,3, 50 mM de KCl et 1,5 mM de $MgCl_2$), 0,2 mM de chaque dNTP, 0,11 mM d'IpaB ou Cj ou 0,1 mM d'IpaH de la PCR amorces, 1,25 U Taq polymérase (Qiagen) et 2,5 µL d'ADN. Les mélanges de réaction de contrôle négatif contenaient de l'eau désionisée stérile à la place de l'ADN matrice. Les produits de PCR obtenus ont été analysés par électrophorèse sur gel dans 1% d'agarose pour IpaH et IpaB et 3% d'agarose pour Cj (Fisher Scientific) contenant 1 µg/mL de bromure d'éthidium dans du tampon TAE (40 mM Tris-HCl, 20 mM acide acétique, 1 mM EDTA, pH 8). Transilluminateurs UV de table UVP: 3UV ont été utilisés pour visualiser les bandes d'ADN. Pour confirmer la présence de la protéine IpaB, le contrôle positif *Salmonella bongori* ATCC 43975 a été utilisé.

L'élimination de la ciprofloxacine par électrooxydation séquentielle et oxydation enzymatique

Processus d'électrooxydation

De la CIP a été ajoutée à une solution de Na_2SO_4 (1 g/L) pour donner une concentration finale de 1 mg/L. Le volume du réacteur était de 550 ml. Pour l'expérience d'électrooxydation, deux anodes ont été testées, BDD et MMO; la cathode était en titane (Ti). L'expérience a été menée à 17,7 A / cm2 pendant 60 min, où les échantillons ont été prélevés à certains intervalles de temps. Plus tard, trois densités de courant ont été testées pour atteindre l'efficacité d'élimination la plus élevée (4,42, 17,7, 35,4 A/cm^2) L'efficacité de l'électrooxydation a été testée avec l'ajout d'acide humique (10 mg/L) comme composé modèle de la matière organique naturelle. Les substances humiques peuvent accepter ou donner des électrons dans diverses réactions redox, d'où leur effet inhibiteur potentiel sur l'électrooxydation CIP a été évalué.

Dégradation enzymatique

La dégradation enzymatique a été réalisée avec de la laccase purifiée dans des tubes Falcon de 50 mL dans des conditions en absence de lumière pour éviter la photo-oxydation de la CIP. Pour imiter le pH réel des eaux usées, la réaction a été effectuée à pH 6,5 dans du tampon phosphate 100 mM. En bref, la concentration de laccase était de 0,2 mg / ml et le syringaldéhyde était de 0,8 mM. Le volume final de la réaction était de 25 mL. L'élimination de la CIP a été effectuée pendant 24 heures, à 25°C, 200 tr/min en trois exemplaires. Des échantillons ont été prélevés à différents moments pour établir la cinétique d'élimination (0, 1, 2, 3, 4, 6, 7, 8, 24 h). Avant d'analyser la concentration résiduelle de CIP, chaque échantillon a été déprotéiné par incubation dans un bain-marie à 100°C pendant 5 min. Par la suite, il a été centrifugé (2 min, 9659 x g) et le surnageant a été analysé par chromatographie liquide.

Système de retrait combiné

L'oxydation électro- et enzymatique couplée a été réalisée dans des conditions optimisées selon les résultats des sections précédentes. La première série d'expériences a consisté à tester successivement des processus électrochimiques et enzymatiques. Les eaux usées synthétiques ont été préparées dans un réservoir en verre de 550 mL contenant une solution tampon de phosphate 100 mM (pH 6,5) dans laquelle 1 mg/L de CIP et 1 g/L de Na_2SO_4 ont été ajoutés. Un volume de travail de 550 mL a été utilisé. Le mélange a ensuite été soumis à une électro-oxydation. Après 10 et 15 min, 25 mL de l'échantillon ont été collectés dans un tube Falcon de 50 ml en triple. À chaque échantillon, une laccase et un médiateur ont été ajoutés pour donner la concentration finale de 2 mg/mL et 0,8 mM, respectivement. Après chaque étape d'élimination, 1 mL d'échantillon a été prélevé pour l'analyser par chromatographie liquide.

La deuxième série d'expériences consistait à tester des processus enzymatiques suivis du processus électrochimique. On a préparé 550 ml d'une solution tampon de phosphate (100 mM, pH 6,5) contenant 1 mg/L de CIP, 1 g/L de Na_2SO_4, 2 mg/mL de laccase et 0,8 mM du médiateur. L'oxydation enzymatique a été réalisée pendant 6 heures, à 25°C, 200 tr/min. Par la suite, le mélange a été soumis au processus d'électrooxydation. Après chaque étape d'élimination, 1 mL d'échantillon a été prélevé pour l'analyser par chromatographie liquide.

Potentiel de la laccase produite par l'industrie agro-industrielle pour éliminer la ciprofloxacine

Préparation de l'inoculum

La souche lyophilisée de *Trametes versicolor* (ATCC 20869) a été inoculée dans un milieu liquide de bouillon de dextrose de pomme de terre (PDB) et incubée dans un agitateur orbital à 30±1°C et 150 tr/min pendant 7 jours. Par la suite, 100 µL d'inoculum ont été striés sur les plaques de gélose de dextrose de pomme de terre (PDA), qui ont été conservées dans un incubateur statique à 30±1°C pendant 9 jours.

Fermentation à l'état solide

Pour produire la laccase par *T. versicolor*, le marc de pomme (avec 70% en poids d'humidité et pH 4,5) a été utilisé comme substrat solide rentable. Le marc de pomme, un résidu de l'industrie du jus, a été offert par Vergers Paul Jodoin, Inc., Québec, Canada. Environ 20 g de marc de pomme ont été ajoutés à une fiole de 500 mL avec 0,5% (v/p) de Tween 80 comme inducteur, mélangés soigneusement et passés à l'autoclave à 121 ± 1°C pendant 30 min. Par la suite, le milieu solide a été inoculé avec la teneur en biomasse d'une plaque de Petri obtenue à l'étape précédente. Ensuite, il a été conservé dans un incubateur statique à 30±1°C pendant 13 jours.

Extraction et dosage d'enzymes

L'échantillon (1 g) obtenu en raison de la fermentation préparée à l'étape précédente, a été ajouté à 20 ml de tampon phosphate 50 mM pH 6,5, mélangé soigneusement pendant 1 h à 35 ± 1°C et centrifugé à 7000 x g pendant 30 min. Plus tard, le surnageant a été collecté et lyophilisé (Dura Frezz Dryer, Kinetics). L'activité relative de la laccase a été analysée en surveillant l'oxydation de l'ABTS à 420 nm (ε_{420} = 36 000 $M^{-1}cm^{-1}$) à pH = 4,5 et 45 ± 1 ° C à l'aide d'un spectrophotomètre Varian Cary-50 UV-Vis. L'unité d'activité enzymatique de la laccase a été définie comme la quantité d'enzyme nécessaire pour oxyder 1 µmole d'ABTS en 1 min dans des conditions de dosage. Les mesures ont été effectuées en triplicata.

Optimisation de la dégradation enzymatique

La dégradation de la CIP par médiation par une laccase brute a été réalisée dans des tubes Falcon de 50 ml, contenant 100 mM de tampon phosphate, pH 6,5 pour imiter les conditions réelles des eaux usées. La concentration de poudre lyophilisée de laccase brute a été optimisée (0,08 mg/mL - 4 mg/mL), ainsi que la présence de médiateurs, c'est-à-dire ABTS et SA à une concentration de 0,4 à 2,0 mM. D'environ 1 mg de laccase brute lyophilisée dissoute dans 1 ml d'eau désionisée a donné une activité de 0,1 U/mL. Toutes les expériences ont été menées pendant 6 heures à 25 ° C, 100 tr / min en trois exemplaires.

Un test de comparaison avec la laccase purifiée de *T. versicolor* a été réalisé (Sigma Aldrich, Oakville, Canada). L'activité de la poudre achetée était de 0,5 U/mg. Le test a été réalisé dans des tubes Falcon de 50 ml dans du tampon phosphate 100 mM pH 6,5 et 1 mg/L de CIP. La concentration optimisée du médiateur a été ajoutée. L'activité finale de la laccase pure et brute était de 1 U/mL. L'expérience a été menée pendant 24 heures à 25°C, 100 tr/min en trois exemplaires.

Avant d'analyser la concentration résiduelle de CIP, tous les échantillons ont été déprotéinés par incubation à 100°C pendant 5 min. Par la suite, ils ont été centrifugés (2 min, 9659 x g) et le surnageant a été analysé par LC-MS/MS.

Adsorbant fonctionnalisé pour l'élimination simultanée des métaux lourds et de la ciprofloxacine

Billes de chitosane-biochar

En bref, 1,67 mg/L de chitosane a été dissous pendant une nuit dans de l'acide acétique à 2%. Du biochar a été ajouté (biochar 1:1:chitosane) et le mélange a été agité pendant 2 heures. La suspension préparée a ensuite été ajoutée goutte à goutte à 0,6 M de NaOH et laissée pendant toute une nuit. Les billes de chitosane-biochar (CH-BB) générées ont ensuite été séparées et lavées à plusieurs reprises pour éliminer l'excès de NaOH. Par la suite, les perles ont été séchées et maintenues à température ambiante pour une utilisation ultérieure.

Caractérisation CH-BH

La morphologie du CH-BH a été obtenue par microscopie électronique à balayage (SEM) (CarlZeissEVO®50). Des micrographies MEB ont été capturées à une tension d'accélération de 10 kV. Les échantillons n'étaient pas recouverts d'or. Le potentiel zêta a été déterminé par la particule Malvern Zetasizer Nano-ZS analysée. Les spectres de spectroscopie infrarouge à transformée de Fourier (FT-IR) de l'adsorbant avant et après l'adsorption ont été obtenus via FT-IR (système Nicolet FT-IR, Thermofisher Scientific). La surface a été étudiée en utilisant des isothermes d'adsorption de N_2 et en utilisant la méthode de Brauner-Emmett-Teller (BET) pour évaluer la surface couverte par le mésopore. Le test de lixiviation des métaux de CH-BB a été effectué. Environ 0,1 g de billes ont été ajoutés à 100 mL d'eau désionisée et la solution a été laissée à température ambiante pendant 48 h. La concentration en métal a ensuite été analysée par spectrométrie de masse à plasma à couplage inductif (ICP-MS) (Agilent Technologies 8800 ICP-MS Triple Quad).

Expériences d'adsorption

La capacité d'adsorption initiale des biochars générés a été testée dans des expériences de sorption par batch. Toutes les expériences ont été menées à 20±1˚C, pH 6,0, 150 tr/min dans un agitateur orbital (Agitateur orbital multifonctionnel PSU-20i, Biosan), sauf indication contraire. Des expériences à blanc ont été incluses. Environ 0,05 g de biochar a été ajouté à un récipient de 100 ml et mélangé à 50 ml de solution de chaque contaminant (10 mg/L pour CIP, As et Cd ou 1 mg/L pour Pb). Une concentration plus faible d'ions Pb a été maintenue pour éviter la précipitation du sel en raison du pH circumneutre. Le biochar avec la capacité d'adsorption la plus élevée a ensuite été utilisé pour générer du CH-HB. Pour les études cinétiques, des expériences d'adsorption ont été réalisées individuellement (1 mg/L de métal ou CIP) et en mélange (1 mg/L chacun de métaux et CIP). L'influence du pH (5,0-9,0) sur la capacité d'adsorption a été testée pour chaque contaminant, où la concentration initiale était de 10 mg/L pour CIP, As, Cd et 1 mg/L de Pb. Pour obtenir des isothermes de sorption, le CH-HB a été agité avec des contaminants individuellement et dans le mélange, dans une plage de 2 à 100 mg / L (CIP, As, Cd) ou de 0,5 à 2 mg/L (Pb). Tous les échantillons ont été filtrés à travers des filtres à seringue PFTE de 0,22 μm (VWR) et le filtrat a été dilué en conséquence avant la mesure. Les concentrations de métaux ont été estimées via ICP-MS (Agilent Technologies 8800 ICP-MS Triple Quad). La concentration CIP a été mesurée par spectrophotométrie UV-Vis (UV-T500Pro) à une longueur d'onde de 278 nm. L'absorbance CIP est influencée par la présence d'ions métalliques dans la matrice. Les métaux présents dans le biochar et les billes peuvent se lixivier en solution (tableau S1). Par conséquent, pour éviter les résultats faussement négatifs et / ou faux positifs, tous les échantillons avec CIP ont été dilués avec HCl 0,1 M (1:1) pour protoner le CIP (CIP^+) et le libérer de la complexation des métaux.

8 SOMMAIRE DES DIFFÉRENTS VOLETS DE RECHERCHE EFFECTUÉS DANS CETTE ÉTUDE

8.1 Interactions de la ciprofloxacine avec les métaux et les substances humiques

8.1.1 Complexes ciprofloxacine-métal - Essais de stabilité et de toxicité en présence de substances humiques

La co-contamination de la ciprofloxacine (CIP) avec des ions métalliques entraîne une altération de la mobilité, de l'activité antimicrobienne et de la distribution / développement des gènes de résistance aux antibiotiques. Dans cette étude, la stabilité de cinq complexes CIP-Me [Me = Al (III), Co (II), Cu (II), Fe (III), Mg] a été étudiée en présence de substances humiques (HS) à deux températures 18 ± 2 °C et 4 ± 1 °C pendant sept jours. Les complexes les plus stables étaient CIP-Al, CIP-Cu et CIP-Co, avec les constantes de stabilité (*K*) à 18 °C, 35,5 ± 1,4, 11,5 ± 1,5 et 11,7 ± 1,5, respectivement. À plus basse température (4 °C), les constantes de stabilité ont diminué: 1 fois pour le CIP-Al, 14 fois pour le CIP-Co et 2 fois pour le CIP-Cu. La présence de substances humiques diminuait la stabilité des complexes. Les réactions chimiques de Fe^{3+} dans l'eau à un pH neutre ont entraîné une altération de la stabilité. La formation de complexes CIP-Mg à des températures plus basses et en présence de HS était limitée. Dans l'eau ultrapure, les complexes CIP-Me présentent une toxicité plus élevée vis-à-vis d'*Enterobacter aeruginosa* à Gram négatif (compris entre 0,125 et 0,5 µg / ml). Cependant, la présence de HS réduisait l'activité antimicrobienne des complexes CIP-Me d'au moins 2 fois. *Bacillus subtilis*, à Gram positifs, n'a pas été affecté par la présence d'ions métalliques et/ou de HS. La toxicité envers B. subtilis pour les complexes était égale à la toxicité de la CIP seule (CMI = 0,25 µg / ml). Ceci suggère la sensibilité différente à la CIP et à ses complexes.

8.2 Élimination insuffisante de la ciprofloxacine par le traitement des eaux usées et sa contribution à la dissémination de la résistance aux antibiotiques

8.2.1 Spéciation des métaux dans les boues d'épuration et son influence sur la distribution d'antibiotiques

La ciprofloxacine (CIP) et la chlorotétracycline (CTC) sont les antibiotiques à large spectre appartenant respectivement aux familles des fluoroquinolones et des tétracyclines. Les deux sont des composés hydrophiles, ayant la capacité de former des complexes avec des ions. La complexation de l'antibiotique avec des ions métalliques peut affecter leur distribution dans les stations de traitement des eaux usées, ce qui n'est généralement pas pris en compte. L'étude analytique a été menée pour évaluer la concentration de CIP, CTC et d'autres ions choisis dans la station d'épuration. Plus de 70% des CTC ont été récupérés lors du traitement des eaux usées. La concentration de CIP mesurée était légèrement plus élevée dans l'effluent que dans les échantillons d'eaux usées. De plus, des concentrations élevées de CIP et de CTC, de 3,9 mg/kg et de 11 mg/kg, respectivement, ont été détectées dans les fractions solides de

boues. Cette concentration élevée pourrait être due à des interactions avec des ions métalliques dans les boues (soit 39-53 g/kg d'Al, 64-89 g/kg de Ca, 52-109 g/kg de Fe ou 10-13 g/kg de Mg). Par conséquent, la spéciation des ions dans les boues a été effectuée pour les localiser plus précisément. La concentration correspondante d'antibiotiques dans chaque fraction de boues a également été évaluée.

8.2.2 Apparition de bactéries résistantes à la ciprofloxacine/chlorotétracycline dans les eaux de la ville de Québec au Canada

La plupart des agents pathogènes fécaux d'origine hydrique appartiennent à la famille des bactéries à Gram négatif. Ainsi, on a estimé les concentrations inhibitrices minimales de la chlorotétracycline et de la ciprofloxacine envers *Enterobacter aerogenes*, représentant de Gram négatif, qui étaient respectivement de 7 µg/ml et 0,125 µg/ml. L'effet antimicrobien combiné de la chlorotétracycline et de la ciprofloxacine contre *E. aerogenes* a également été étudié pour établir leur interaction potentielle avec les agents pathogènes présents dans l'eau. Finalement, des échantillons d'eau provenant de diverses STEP de la municipalité de Québec ont été testés pour détecter l'apparition de souches résistantes à la chlorotétracycline, à la ciprofloxacine et à la chlorotétracycline/ciprofloxacine.

8.3 Nouveaux procédés d'élimination de la ciprofloxacine

8.3.1 Nouvelle approche pour l'élimination de la ciprofloxacine par électrooxydation séquentielle et oxydation enzymatique

La contamination des compartiments de l'environnement par des antibiotiques est devenue un problème immense en raison de leur potentiel de sélection et de dissémination de la résistance aux antimicrobiens. La combinaison entre l'électro-oxydation et l'oxydation enzymatique a été testée pour évaluer la capacité du système à éliminer la ciprofloxacine (CIP), un antibiotique fluoroquinolone, de l'eau. Pour la partie électrochimique, deux anodes ont été étudiées, le diamant dopé au bore (BDD) et les oxydes de métaux mixtes (MMO), ainsi que trois densités de courant (4,42, 17,7and 35,4 A/cm^2). L'anode BDD à 35.4 A/cm^2 a montré l'efficacité d'extraction la plus élevée dans les temps les plus brefs (élimination> 90% en 6 min); ces paramètres ont donc été choisis pour des expériences ultérieures. Pour l'oxydation enzymatique, la laccase obtenue à partir de *Trametes versicolor* a été choisie. La Laccase seule n'a pas été en mesure de supprimer la CIP; par conséquent, l'influence des médiateurs redox a été étudiée. L'ajout de syringaldéhyde (SA) et d'acide 2,2'-azino-bis (3-éthylbenzothiazoline-6-sulfonique) (ABTS) a entraîné une transformation accrue de la CIP. Il restait environ 48,9 ± 4,0% des CIP après 4 heures de traitement lorsque la laccase à médiation SA était appliquée et 87,8 ± 6,6% dans le cas de la laccase à médiation ABTS. Ainsi, le système à médiation SA a été choisi pour des expériences ultérieures. Le couplage de l'oxydation enzymatique suivi de l'électro-oxydation a permis d'éliminer 73% de l'antibiotique. De plus, l'activité antimicrobienne a augmenté jusqu'à son efficacité initiale après le traitement. La combinaison d'une électro-oxydation suivie d'une oxydation enzymatique a conduit à une

élimination de 97 à 99% de la CIP. De plus, il n'y avait pas d'activité antimicrobienne de la solution après le traitement. Les tests avec des eaux usées réelles ont confirmé la capacité du système à éliminer le CIP de la matrice complexe.

8.3.2 Potentiel de la laccase produite par l'industrie agro-industrielle pour éliminer la ciprofloxacine

La ciprofloxacine (CIP), un antibiotique largement utilisé, est fréquemment détectée dans l'environnement en raison d'un traitement insuffisant des eaux usées et de l'eau. Par conséquent, des technologies nouvelles, vertes et rentables sont nécessaires pour améliorer l'élimination de ces polluants. La puissance des enzymes brutes, en particulier des laccases, produites par les champignons de la pourriture blanche a été testée afin d'évaluer leur pouvoir de dégradation du CIP de l'eau. La laccase brute n'est pas capable d'éliminer la CIP seule. L'addition de syringaldéhyde, un médiateur rédox, a entraîné une diminution de la concentration en antibiotiques jusqu'à 68,09 ± 0,12% en 24 h, ce qui représente l'efficacité d'élimination la plus élevée obtenue à 0,8 mM de syringaldéhyde et à 2 mg/ml de laccase brute (0,1 U/ml). Ce qui est intéressant, l'oxydation de la CIP par la laccase était inhibée après 6 heures de traitement. A titre de comparaison, une enzyme pure ayant la même activité que la protéine brute a éliminé 86% de la CIP en 24 h. Aucun effet inhibiteur pendant le traitement n'a été observé. L'estimation de l'efficacité antimicrobienne a révélé que, en 6 heures de traitement, la toxicité envers Escherichia coli diminuait de 30%. On a estimé que le traitement des eaux usées par un système à médiation par la laccase brute réduisait considérablement le coût du traitement enzymatique.

7.3.3. Adsorbant fonctionnalisé pour l'élimination simultanée des métaux lourds et de la ciprofloxacine

Le biochar est considéré comme un adsorbant écologique et rentable pour la purification de l'eau. Cependant, le biochar brut présente généralement un faible capacité d'absorption vers la plupart des contaminants dissous, ce qui peut être amélioré par sa fonctionnalisation. Les billes de chitosan-biochar (CH-BB) ont été produites et testées pour leur efficacité d'élimination de la ciprofloxacine (antibiotique) et de trois métaux lourds (As, Cd, Pb). La modification du biochar de lisier de porc brut a entraîné une augmentation de sa capacité d'absorption dans presque tous les cas, l'augmentation la plus élevée étant celle de l'As (presque 6 fois) et la plus faible celle du Cd (1,02 fois). L'adsorbant a pu éliminer simultanément tous les contaminants ciblés, individuellement et en mélange, à la suite d'une réaction de pseudo-deuxième ordre. L'affinité des contaminants envers CH-BB suivait l'ordre suivant: Pb> Cd >> As> CIP. Lorsque Pb et As étaient présents dans le même mélange, leur efficacité d'élimination augmentait en raison de leur co-précipitation. Les études de co-adsorption ont montré que le mécanisme d'absorption des polluants inorganiques était différent de celui de l'antibiotique.

9 CONCLUSIONS ET RECOMMANDATIONS POUR L'AVENIR

Conclusion

Les points suivants ont été conclus des travaux de recherche présentés:

9.1. Les complexes les plus stables à 4°C et à 18°C étaient CIP-Al, CIP-Cu et CIP-Co. Leur stabilité n'a pas changé de façon significative au cours de la période de sept jours; par conséquent, ils pourraient constituer la plus grande menace pour la communauté bactérienne présente dans l'environnement. La conversion de Fe^{3+} en $Fe(OH)_3$ a entraîné une altération majeure de la stabilité du CIP-Fe. De plus, la présence de HS déstabilise de manière cruciale la complexation CIP-Fe. La complexation CIP-Mg ne dépend pas de la concentration en Mg^{2+} à basse température (4°C). A la même température mais avec l'ajout de HS, il n'y a pas de formation de complexe entre CIP et $Mg^{2+.}$

9.2. L'activité antimicrobienne de CIP vis-à-vis de *B. subtilis* à Gram positif n'était généralement pas affectée par les ions métalliques et / ou les substances humiques. Cependant, les bactéries à Gram négatif pourraient être plus sensibles aux changements environnementaux. La CIP et ses complexes métalliques ont exercé une activité antimicrobienne plus élevée vis-à-vis d'*E. aerogenes* dans l'eau ultrapure par rapport aux substances humiques. La CIP s'adsorbe sur le HS, la grosse molécule formée ne peut pas pénétrer dans la membrane externe des bactéries à Gram négatif. La toxicité de la CIP et de ses complexes serait donc moindre.

9.3. Environ 71% des CTC ont été éliminés lors du traitement des eaux usées, alors que la CIP avait tendance à s'accumuler pendant le traitement. La principale méthode d'élimination des deux antibiotiques était l'adsorption des boues. Un mécanisme d'échange d'ions peut expliquer la concentration la plus élevée de CTC. Cependant, le mécanisme d'adsorption CIP peut probablement différer quant aux métaux qui tendent à former des complexes avec CIP n'étaient pas facilement accessibles. Ainsi, son adsorption pourrait être due à des interactions avec des groupes fonctionnels de matière organique.

9.4. Une concentration élevée de métaux lourds est alarmante, car leur complexation avec le CTC et/ou le CIP entraîne une accumulation d'antibiotiques dans les boues. Cela pourrait conduire à la co-sélection et à la co-diffusion de gènes de résistance aux antibiotiques et de gènes de résistance aux métaux lourds, avec des conséquences graves pour la santé.

9.5. La présence de CIP et de CTC dans l'eau pourrait avoir contribué à l'apparition et à la dissémination de souches résistantes à la CIP et aux CIP + dans les milieux aquatiques de la région de Québec.

9.6. L'oxydation électro-enzymatique séquentielle a efficacement éliminé la CIP de l'eau. La combinaison d'une électrooxydation de 10/15 min via une anode BBD à 35,4 mA/cm², suivie de 6 h d'oxydation de laccase à médiation par SA a conduit à une élimination de CIP de 95%. L'activité antimicrobienne de la solution testée a diminué considérablement avec le temps. De plus, l'efficacité du système a été confirmée par des tests avec de vrais effluents d'eaux usées. Le scénario inverse,

c’est-à-dire une électro-oxydation enzymatique, donnait de moins bonnes performances en raison de la présence d’une enzyme et d’un médiateur au cours de l’électrooxydation (27% d’élimination). De plus, l'activité antimicrobienne des échantillons testés présentait une toxicité envers *E. coli* similaire à celle de la solution mère d'origine.

9.7. L'extrait de laccase brut a pu éliminer 32% de la CIP en 6 heures. Une oxydation enzymatique supplémentaire n'a pas entraîné de diminution de la concentration en CIP. Cela suggère que, avec l'extrait brut, la CIP pourrait être transformée via une cascade enzymatique et que les produits de transformation générés pourraient être des facteurs limitants. L'activité antimicrobienne vis-à-vis de *E. coli* de la solution testée diminuait jusqu'à ce que la réaction enzymatique soit entravée. Après ce moment, la solution traitée présentait toujours une activité antimicrobienne, mais restait constante.

9.8. Le coût de production de la laccase brute (0,05 USD/U) était moins élevé que celui de la laccase commerciale (0,21 USD/U).

9.9. La capacité d’absorption dépendait beaucoup du type de biochar et du polluant. PM-BC a montré l'efficacité d'élimination la plus élevée pour CIP et Pb, PW-BC pour Pb et As et AS-BC pour Cd.

9.10. Le CH-BB fabriqué a pu éliminer simultanément tous les contaminants ciblés. L'adsorption de tous les contaminants ciblés a suivi un pseudo-deuxième ordre; ainsi, le mécanisme principal de leur absorption a été la chimisorption. Les études d'adsorption avec un mélange de métaux ont révélé que l'efficacité d'élimination de Cd diminuait en raison de la concurrence avec d'autres polluants par rapport aux sites actifs de l'adsorbant. Cependant, la co-contamination de As et de Pb a conduit à leur élimination accrue en raison de leur co-précipitation. La capacité d'adsorption vers le CIP n'était pas affectée par la présence d'ions métalliques. Ceci suggère que les polluants inorganiques présentent des mécanismes d'adsorption différents. Ainsi, l’antibiotique et les métaux ne seront pas en concurrence sur les sites d’adsorption et leur élimination ne sera pas entravée l’un par l’autre.

Recommandations

À partir des résultats obtenus dans l'étude du devenir et des différentes méthodes d'élimination de la CIP dans l'usine de traitement, les recommandations suivantes peuvent être formulées:

9.1. Pour mieux comprendre les interactions qui influent sur les propriétés physicochimiques et antimicrobiennes de la CIP, les tests avec les autres polluants présents doivent être effectués, en particulier avec d'autres antibiotiques. De plus, la corrélation entre la concentration en antibiotiques et la dissémination de gènes de résistance aux antimicrobiens devrait être évaluée.

9.2. Pour développer des méthodes précises d'élimination de la CIP, il convient d'étudier la relation entre l'antibiotique et les composés présents dans l'environnement ciblé. L'approche plus spécifique au site doit être réalisée. Par exemple, les propriétés de la matière organique naturelle (NOM) diffèrent d'un site à l'autre. Par conséquent, les représentants des NOM doivent être extraits du site ciblé (par exemple, l'acide humique des boues) et les études d'interaction CIP-NOM doivent être évaluées.

9.3. Les résultats obtenus par analyse PCR suggèrent que dans l'eau de Charlesbourg, Salmonella sp. peuvent être présents. Cependant, les résultats pourraient avoir été faussement positifs en raison d'une réaction non spécifique. Par conséquent, une enquête plus approfondie sur la communauté microbienne dans la région de Québec devrait être effectuée pour confirmer ces résultats. L'isolement des bactéries et le séquençage de leur ADN doivent être effectués dans la méthode de validation des résultats de la PCR.

9.4. Pour une spéciation précise lors du traitement des eaux usées, la distribution exacte et les temps de rétention des antibiotiques ciblés doivent être évalués.

9.5. Les méthodes d'élimination proposées doivent être étudiées plus en profondeur. L'accent devrait être mis sur l'influence d'autres contaminants, inorganiques et organiques, sur la production de produits de transformation et sur leur évaluation écotoxicologique.

CHAPTER II: INTERACTIONS BETWEEN CIPROFLOXACIN WITH METALS AND HUMIC SUBSTANCES

Ciprofloxacin-metal complexes –stability and antimicrobial activity tests in the presence of humic substances

Agnieszka Cuprys[a], Rama Pulicharla[a], Joanna Lecka[a], Satinder Kaur Brar[a,*], Patrick Drogui[a], R.Y. Surampalli[b]

[a] INRS-ETE, Université du Québec, 490, Rue de la Couronne, Québec, Canada G1K 9A9

[*] Corresponding author: INRS-ETE, Université du Québec, 490, Rue de la Couronne, Québec, Canada G1K 9A9. E-mail: satinder.brar@ete.inrs.ca; Telephone: + 418 654 3116; Fax: + 418 654 2600.

[b] Global Institute for Energy, Environment and Sustainability, P.O. Box 14354, Lenexa, KS 66285, USA

Chemosphere 202, 549-559 (2018)

Résumé

La co-contamination de la ciprofloxacine (CIP) avec des ions métalliques entraîne une altération de la mobilité, de l'activité antimicrobienne et de la distribution / développement des gènes de résistance aux antibiotiques. Dans cette étude, la stabilité de cinq complexes CIP-Me [Me = Al (III), Co (II), Cu (II), Fe (III), Mg] a été étudiée en présence de substances humiques (HS) à deux températures 18 ± 2 ° C et 4 ± 1 ° C pendant sept jours. Les complexes les plus stables étaient CIP-Al, CIP-Cu et CIP-Co, avec les constantes de stabilité (*K*) à 18 ° C, 35,5 ± 1,4, 11,5 ± 1,5 et 11,7 ± 1,5, respectivement. À plus basse température (4 °C), les constantes de stabilité ont diminué: 1 fois pour le CIP-Al, 14 fois pour le CIP-Co et 2 fois pour le CIP-Cu. La présence de substances humiques diminuait la stabilité des complexes. Les réactions chimiques de Fe3+ dans l'eau à un pH neutre ont entraîné une altération de la stabilité. La formation de complexes CIP-Mg à des températures plus basses et en présence de HS était limitée. Dans l'eau ultrapure, les complexes CIP-Me présentent une toxicité plus élevée vis-à-vis *d'Enterobacter aeruginosa* à Gram négatif (compris entre 0,125 et 0,5 µg/ml). Cependant, la présence de HS réduisait l'activité antimicrobienne des complexes CIP-Me d'au moins 2 fois. Bacillus subtilis, à Gram positifs, n'a pas été affecté par la présence d'ions métalliques et / ou de HS. La toxicité envers B. subtilis pour les complexes était égale à la toxicité de la CIP seule (CMI = 0,25 µg/ml). Ceci suggère la sensibilité différente à la CIP et à ses complexes.

Mots-clés: ciprofloxacine, ion métallique, stabilité, toxicité, eau, complexation

Abstract

The co-contamination of ciprofloxacin (CIP) with metal ions results in alteration of CIP mobility, antimicrobial activity and selection/dissemination of the antibiotic-resistance genes. In this study, the stability of five CIP-Me complexes [Me=Al(III), Co(II), Cu(II), Fe(III), Mg] was investigated in the presence of humic substances (HS) at two temperatures 18±2˚C and 4±1˚C for seven days period. The most stable complexes were CIP-Al, CIP-Cu, and CIP-Co with the stability constants (*K*) of 35.5±1.4 11.5±1.5 and 11.7±1.5 respectively, at 18˚C. At lower temperature (4˚C), the stability constants decreased: 1-fold for CIP-Al, 14-fold for CIP-Co and 2-fold for CIP-Cu. The presence of humic substances also decreased the stability of complexes. The chemical reactions of Fe^{3+} in water at circumneutral pH resulted in stability alteration. The formation of CIP-Mg complexes at lower temperatures and in the presence of HS was limited. In ultrapure water, CIP-Me complexes exhibit higher antimicrobial activity against Gram-negative *Enterobacter aeruginosa* (ranged between 0.125-0.5 μg/ml). However, the presence of HS reduced the antimicrobial activity of CIP-Me complexes by at least 2-fold. *Bacillus subtilis,* a Gram-positive bacteria, was not affected by the presence of metal ions and/or HS. The antimicrobial activity toward *B. subtilis* for the complexes was equal to antimicrobial activity of CIP alone (MIC=0.25 μg/ml). This suggested the different susceptibility to CIP and its complexes.

Keywords: ciprofloxacin, metal ion**,** stability, antimicrobial activity, water, complexation

Introduction

Fluoroquinolones (FQ) are the third most commonly used antibiotics in Canada, after β-lactams and cephalosporins [1]. In 2014, ciprofloxacin (CIP) was the most frequently prescribed antibiotic among the FQs in Canada. It was ranked as the third pharmaceutical with the largest proportion of all antibiotics dispensed by community pharmacies (8%), following amoxicillin (26%) and azithromycin (9%) in the years 2007-2014 [1]. It is a broad spectrum antimicrobial compound, effective against Gram-negative and Gram-positive bacteria [2]. Its frequent usage, inappropriate pharmaceutical disposal or incomplete metabolism lead to the presence of CIP in various environmental compartments [3].

The antibiotics present in the aquatic environment are subsequently introduced to the water treatment. However, the water treatment plants are not specifically designed to remove trace level contaminants, thus they do not entirely remove the antibiotics [3]. Presence of CIP in water and soil is highly alarming due to its contribution to the dissemination of drug-resistant bacterial [4]. For instance, Miao et al. (2004) detected CIP in final effluents of wastewater treatment plants from British Columbia, Alberta, and Ontario, with the average concentration of 118 ng/L and it was the highest concentration amongst the detected FQs (ranged between 50-94 ng/L) in Canada [5]. It was also the fourth highest concentration, after sulfamethazine (363 ng/L), sulfamethoxazole (243 ng/L) and tetracycline (151 ng/L), amongst the detected antibiotics [5]. Lee et al. (2007) investigated sewage treatment plant in Ontario and detected CIP at a concentration of 42-712 ng/L, which is a higher concentration than in the previous study [6]. Throughout the world, a high concentration of CIP ranging between 5 µg/L – 4.8 mg/L has been observed [7].

CIP is a hydrophilic compound with two ionizable functional groups: carboxylic group at C-3 (pKa_1 6.09) and piperazinyl group at C-7 (pKa_2 8.74). CIP, like other FQs, has a capacity to form stable complexes with metal ions [2]. Usually, they act in a bidentate manner via oxygen of carboxylic and carbonyl groups or unidentate manner through terminal nitrogen of piperazinyl group.

The generation of CIP-Me complexes occurs in all environmental compartments, due to the prevalence of metals in water and soil. [2]. This metal complexation property not only alters the physico-chemical properties of CIP but also change its antimicrobial activity. Some of the metal complexes, i.e. CIP-Cu, CIP-Co or CIP-Zn, exhibit higher antimicrobial activity towards bacteria than the CIP itself. They also contribute to the prevalence of antibiotic-resistance genes [8]. FQs-metal complexation may also influence FQs mobility and stability in water/soil [9]. They also increase the solubility of CIP [10]. This may be due to the generation of the hydrated ionic complexeswhich are more hydrophilic. The only exception is magnesium ions which coordinate water molecules and form [Mg $(H_2O)^{2+}$] cation rather than bonding directly with FQs. Hence, in the aquatic environment, Mg^{2+} generates this adduct and reduces the number of available water molecules that can dissolve CIP [10]. However, the most prevalent substances in the environment are humic substances (HS). Their concentration in natural

waters varies from 0.03 mg/L (groundwater) to 40 mg/L (lakes) [11]. The data concerning the interactions between antibiotics, metal ions and HS are still scarce. Hence, there is a need to further investigate the FQs-metal complexation as well as the effect of the presence of HS. Many questions are still unanswered, such as how metal ions and complex matrices (HS) affect the stability and degradation of CIP and these can help to design specific degradation techniques for them.

The objective of this study was to investigate the stability of CIP-Me complexes (Me = Co^{2+}, Cu^{2+}, Mg^{2+}, Al^{3+}, Fe^{3+}) for seven days at two temperatures (4˚C and 18˚C) in ultrapure water pH 6.5±0.1 to simulate the pH of wastewater. The influence of the presence of humic substances on Me-complex stability was also investigated at the above-mentioned temperatures. Further, the antimicrobial activity of CIP-Me complexes and CIP-Me complexes in the presence of HS was studied against two bacterial strains – Gram-positive, *Bacillus subtilis* and Gram-negative, *Enterobacter aerogenes.*

Materials and methods

Materials

Ciprofloxacin (98% purity) was purchased from Acros Organics (USA). The humic sodium salt (99 % assay) was purchased from Sigma-Aldrich Canada Ltd. (Oakville, ON, Canada). As metal salts, $AlCl_3$ anhydrous (98% purity), $CuSO_4$ anhydrous (98% purity), $CoSO_4 \cdot 7H_2O$ (98% purity), $Fe_2(SO_4)_3$ anhydrous (98% purity) and $MgCl_2$ anhydrous (99% purity) were used. Tris-base (≥99.8 %) was purchased from Fisher Scientific (Ontario, Canada). Tryptic soy broth was bought from EMD Chemicals Inc. (Germany).

Preparation of the CIP-Me solution

CIP powder was dissolved in deionized water to obtain a 100 mg/L stock solution. Metal ions stock solutions were prepared similarly to obtain the same concentrations. All stock solutions were filtered using a syrigne filter (Chromafil® Xtra 0.45 μm). Later, the stock solutions were diluted in Tris-HCl buffer (50 mM; pH 6.5) in 15 ml falcon tubes, where CIP concentration was constant (10 mg/L) and metals concentration ranged between 0 to 5 mg/L. The final make-up volume was made up to 5 ml. The solutions were prepared in triplicates.

Stability constant of CIP-Me complexes

The stability of the CIP-Me complexes was established by fluorescence intensity measurements following which their stability constant was calculated. The obtained solutions were incubated till they reached the equilibrium of complexation. The CIP-Me solutions were incubated at two temperatures: 18±2˚C and 4±1˚C without strirring. Subsequently, the fluorescence intensity ($\lambda_{Ex/Em}$=276/415 nm) was measured in quartz cuvettes by Varian Cary Eclipse Fluorescence Spectrophotometer (Mississauga, Ontario) with temperature controlling system Single Cell Peltier [12]. The volume of measured samples was 3 ml.

Fourier-Transform Infrared Spectroscopy of CIP-Me-HS systems

The CIP-Me complexes (Me= Al, Fe (III), Mg, Cu (II), Co (II)) were prepared as follows. The CIP was dissolved in deionized water with the addition of metal salt where the final concentrations were 0.2 mM and 0.02 mM, respectively. The solutions were left overnight to attain the equilibrium. Subsequently, it was frozen at -20˚C for 24 hours to perform the lyophilization by the freeze-drying system (Dura Frezz Dryer, Kinetics).

The solutions with the HS were prepared similarly as described above. The mixture of CIP, metal salt, and HS, with the final concentrations of 0.15 mM (48 mg/L), 0.015 mM and 48 mg/L respectively, were left for 48 hours to attain equilibrium. The sample with CIP and HS only was also prepared. Then, they were frozen at -20˚C for 24 hours to perform lyophilization by the freeze-drying system (Dura Frezz Dryer, Kinetics).

The lyophilized complexes were analyzed by Fourier-Transform Infrared Spectroscopy using Cary 670 FTIR Spectrometer. The spectra were obtained at a resolution of 4 cm^{-1}, in the range of 4000-400 cm^{-1}.

Stability test of CIP-Me complexes in the presence of humic substances

The humic sodium salt (10 g/L) was dissolved in deionized water and then filtered via Whatman glass-fiber filter paper to remove the insoluble humin. The solutions of CIP and metals were prepared as described earlier, with the addition of humic sodium salt, as a representative of humic substances. The final concentrations were of 10 mg/L of humic substances, 10 mg/L of CIP and 0-5 mg/L of metal ions. The controls without humic substances were also prepared. Later, the fluorescence intensity was measured as described earlier. The measurements were conducted for 7 days in triplicates at 18±2˚C and 4±1˚C without strirring.

Statistical analysis

The analysis was performed using SigmaPlot 13.0 software. One-way ANOVA was used to determine if there was a statistically significant difference (p-values < 0.05). The data were presented as a mean of triplicate ± standard deviation.

Antimicrobial activity test – minimal inhibitory concentration (MIC)

Two bacterial strains – Gram-negative, *E. aerogenes* (NRRL B-407) and Gram-Positive *B. subtilis* (B-59994) were used for testing the antimicrobial activity of CIP-Me complexes. For bacterial growth, the liquid media was used (Tryptic Soy Broth 3.0% w/v + yeast extract 0.3% w/v). *E. aerogenes* was incubated for 36h, at 30˚C, 150 rpm and *B. subtilis* for 18h, 37˚C, 150 rpm. Both strains were streaked onto agar plates (3.0% w/v Tryptic Soy Broth + 1.5% w/v Bacto-Agar (Quelab, Montreal, Canada)) and incubated 36h at 30˚C for *E. aerogenes* and 18h at 37˚C for *B. subtilis*. The plates were maintained at 4˚C, till further use.

MIC was defined as the minimal concentration of antibiotic, which inhibits of bacterial growth. MIC of CIP-Me complexes and CIP-Me complexes in the presence of HS against Gram-negative, *E. aerogenes* and Gram-positive, *B. subtilis* were measured by agar dilution method. It was performed as specified by European Committee for Antimicrobial Susceptibility Testing of the European Society of Clinical Microbiology and Infectious Diseases (Annex B) [13]. The MIC of CIP was compared with CIP-Me complexes. Bacteria-free, metal ions and humic substance controls were included.

Results and discussion

The calculations of CIP-Me complexes stability constant

The stability constant (*K*) is defined as an equilibrium constant for the generation of a CIP-Me complex in aquatic conditions, where the reaction can be written as:

$$CIP + MI \rightleftharpoons CIP\text{-}Me \qquad \text{Eq. 4}$$

From the definition, the *K* can be given by the equation (5):

$$K = \frac{[CIP-Me]}{[CIP][MI]} \qquad \text{Eq. 5}$$

where *[CIP-Me]*, *[CIP]* and *[MI]* are concentrations of formed CIP-metal complex, CIP, and a metal ion, respectively.

Measurements of kinetic changes in fluorescence intensity of complexes allowed calculating CIP-Me stability constant using two equations (6) and (7). For metal ions, which induced quenching effect on CIP fluorescence intensity, the stability constant and the complex ratio (*n*) were calculated, based on the Lineweaver-Burk Equation (6) [12]:

$$log\frac{(F_0-F)}{F} = logK + nlog[MI] \qquad \text{Eq. 6}$$

where F_0 is the fluorescence intensity of CIP, *F* is fluorescence intensity of mixture, *[MI]* is the metal ion concentration. For the metallic ions, which induced enhancement of fluorescence intensity, the calculations were performed based on the equation (7) [14]:

$$\frac{1}{F_{CM}-F_C} = \frac{1}{K\cdot K_i Q_{CM}[CIP]_0[MI]_0} + \frac{1}{K_i Q_{CM}[CIP]_0} \qquad \text{Eq. 7}$$

where F_{CM}-F_C is a change in fluorescence intensity of CIP-Me complexes and CIP, K_i is an instrument constant, Q_{CM} is a quantum yield of CIP-Me complex, $[CIP]_0$ is an initial concentration of CIP and $[MI]_0$ is the initial concentration of metal ion. By constructing the curve $1/(F_{CM}\text{-}F_C)$ versus $1/[MI]_0$, the stability constant was calculated according to the double reciprocal equation. Table 2.1.1 presents the values of obtained stability constants. The obtained data fitted linear regression model (R^2 >0.9). Almost all the MI complexation with CIP induced quenching of the fluorescence intensity, except for aluminum ions. Moreover, Al^{3+} exhibited the highest stability constant, which is consistent with previous data [15]. CIP-Co/Cu complexes exhibited a similar value of *K* at 18˚C. However, at 4˚C, the stability constant of

CIP-Cu is over 6-fold greater than for CIP-Co. This indicated that CIP-Cu is more stable at a lower temperature than CIP-Co. The magnesium and iron complexes were not included in the Table, which is discussed in later section.

Table 2.1. 1 Stability constant *K* and ratio *n* of CIP-Me complexes

Complex CIP-Me	**Temperature**			
	4˚C		18˚C	
	n	*K*	*n*	*K*
CIP-Al*	1:1	33±1.3	1:1	35.5±1.4
CIP-Co**	0.6	0.83±0.2	1	11.5±1.5
CIP-Cu**	0.4	5.4±0.2	0.9	11.7±1.5

*n based on eq. 7
**n based on Eq. 6

Identification of the complexation sites

The obtained spectra for CIP-Me and CIP-Me+HS complexes are presented in Figure 2.1.1. The CIP spectra are characterized by a peak at 3043 cm^{-1} which can be assigned to the amino group of piperazine system (ν(N-H)). Two peaks at 1617 and 1589 cm^{-1} are from stretching vibration of the carboxylic group (ν(OCO)) and of pyridine group (ν(CO)), respectively. The peak at 1372 cm^{-1} might be assigned to vibrations associated with nitrogen protonation of the piperazinyl group [16]. All the spectra for CIP-Me complexes (Fig. 2.1.1A) showed two peaks between 3000-3300 cm^{-1} which indicate the stretching vibrations from amino group of piperazine system and hydroxyl group (ν(O-H)). The peak at 1400±10 cm^{-1} could be assigned as symmetric CO_2 stretching from the carboxylic acid group and/or the protonation of N-4 in piperazinyl group [16]. The spectra for CIP-Al exhibited the slight shift from 1617 cm^{-1} to 1633 cm^{-1}, which correspond to stretching vibration of carboxylic group. There is also a decrease in peak intensity at 1598 cm^{-1}, the stretching vibration of pyridine group. This suggests that the Al^{3+} bound with CIP via carboxylic and carbonyl oxygen atoms. The CIP-Co/Cu/Mg complexes showed similar features as CIP-Al. The double peaks of ν(OCO) and ν(CO) shifted significantly to 1708 and 1625 cm^{-1}, respectively. The CIP-Fe spectra also suggested the CIP-metal interaction between oxygen atoms of the pyridine ring due to the peak at 1631 cm^{-1}, which can be assigned as ν(CO) stretching vibrations or ν(OCO).

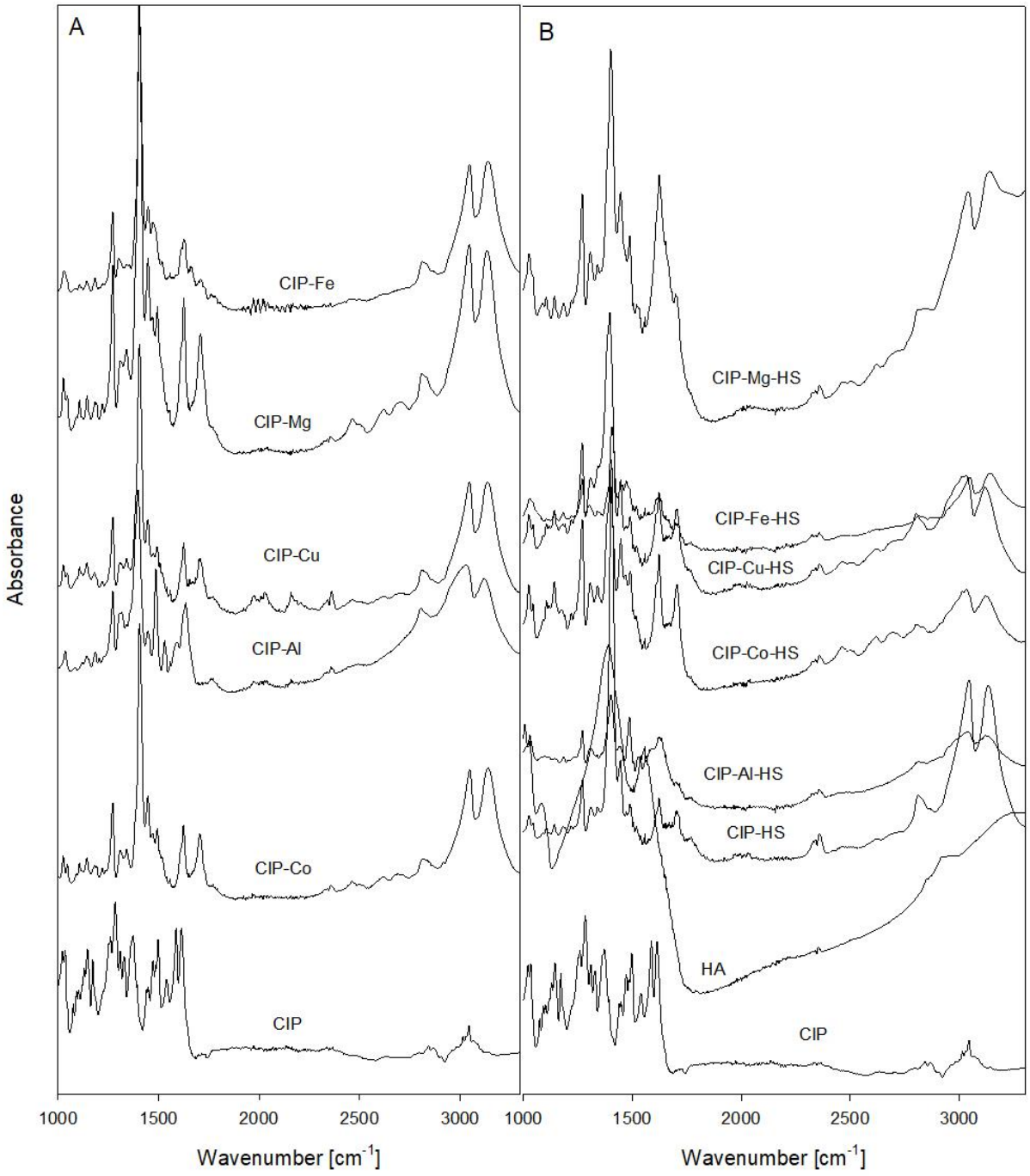

Figure 2.1. 1 The FTIR spectra of: A). CIP-Me complexes (Me=Al, Co(II), Cu(II), Fe(III), Mg) and; B.) CIP-Me complexes in the presence of humic substances (HS)

Table 2.1.2 presents the separation between the asymmetric and symmetric stretching of ν(O-C-O), Δ= $\nu(CO_2)_{asym}$- $\nu(CO_2)_{sym}$ [17, 18]. The Δ ranged between 224-300, which suggests unidentate mode of coordination. The similar complexation site between CIP and metal ions via oxygen atoms of carbonyl and the carboxylic group was also obtained in other studies [12, 18, 19].

In the spectra of HS (Fig. 2.1.1B), the main four peaks can be assigned as stretching vibrations of phenolic *ν*(O-H) between 3000-3600 cm^{-1}, asymmetric CO_2 stretching from carboxylic group and/or

aromatic *ν*(C=C) at 1554 cm^{-1}, symmetric CO_2 stretching from carboxylic group and/or aliphatic bending of *ν*(-CH) at 1394 cm^{-1} and stretching of aliphatic hydroxyl group at 1088 cm^{-1}, which is consistent with the literature [20]. In the presence of CIP, HS spectra lose the wide *ν*(O-H) peak between 3000-3600 cm^{-1}, it became a double split (3135 cm^{-1}) of carboxylic *ν*(O-H) and 3046 cm^{-1} of *ν*(N-H), as it was observed for CIP-Me spectra. It suggested that CIP was adsorbed onto HS by interaction with its -OH groups, probably due to the hydrogen bonding. The peaks at 1623 and 1695 cm^{-1} could be assigned as shifted stretching vibration of the carbonyl group *ν*(CO) and *ν*(OCO). Moreover, the disappearance or shift of the CIP peak at 1372 cm^{-1} suggested the cation exchange between negatively charged groups of HS and a positively charged amino group of CIP. This result is consistent with the data obtained from the studies on adsorption of norfloxacin and ciprofloxacin onto humic substances [16, 21]. The addition of the metal salts to HS solution resulted in changing the HS spectra as well (fig. S2, Annex B). They suggest that the complexation of HS with metal ions is due to their interaction between -OH and/or -C=O functional groups.

Table 2.1. 2 Characteristic absorption bands of FTIR spectra of CIP-metal complexes

Compound	$\nu(CO_2)_{asym}$ [cm^{-1}]	$\nu(CO_2)_{sym}$ [cm^{-1}]	$\Delta = \nu(CO_2)_{asym} - \nu(CO_2)_{sym}$ [cm^{-1}]
CIP	1617	1617	-
CIP-Al	1633	1398	235
CIP-Co	1707	1409	298
CIP-Cu	1707	1409	298
CIP-Fe	1631	1407	224
CIP-Mg	1707	1407	300

The addition of metal ions slightly changed the CIP-HS spectra. The peak at 1695 cm^{-1} which is present on CIP-HS spectra disappeared in the presence of Al^{3+} and Fe^{3+}. The spectra of CIP-Cu/Co-HS exhibit the same features, i.e. a slight shift of *ν*(O-H) and *ν*(N-H) to 3122 and 3033 cm^{-1} respectively. CIP-Mg-HS presented the similar peaks as for the CIP-Mg spectra. The only difference was an additional wide peak at 3386 cm^{-1} which may suggest the formation of an amide bond. It is possible that due to the presence of metal ions, there is a cation bridge formation between CIP oxygens of carboxylic and carbonyl groups and hydroxyl groups of HS [21]. The possible interactions between CIP-Me and CIP-Me-HS are summarized in Figure 2.1.2.

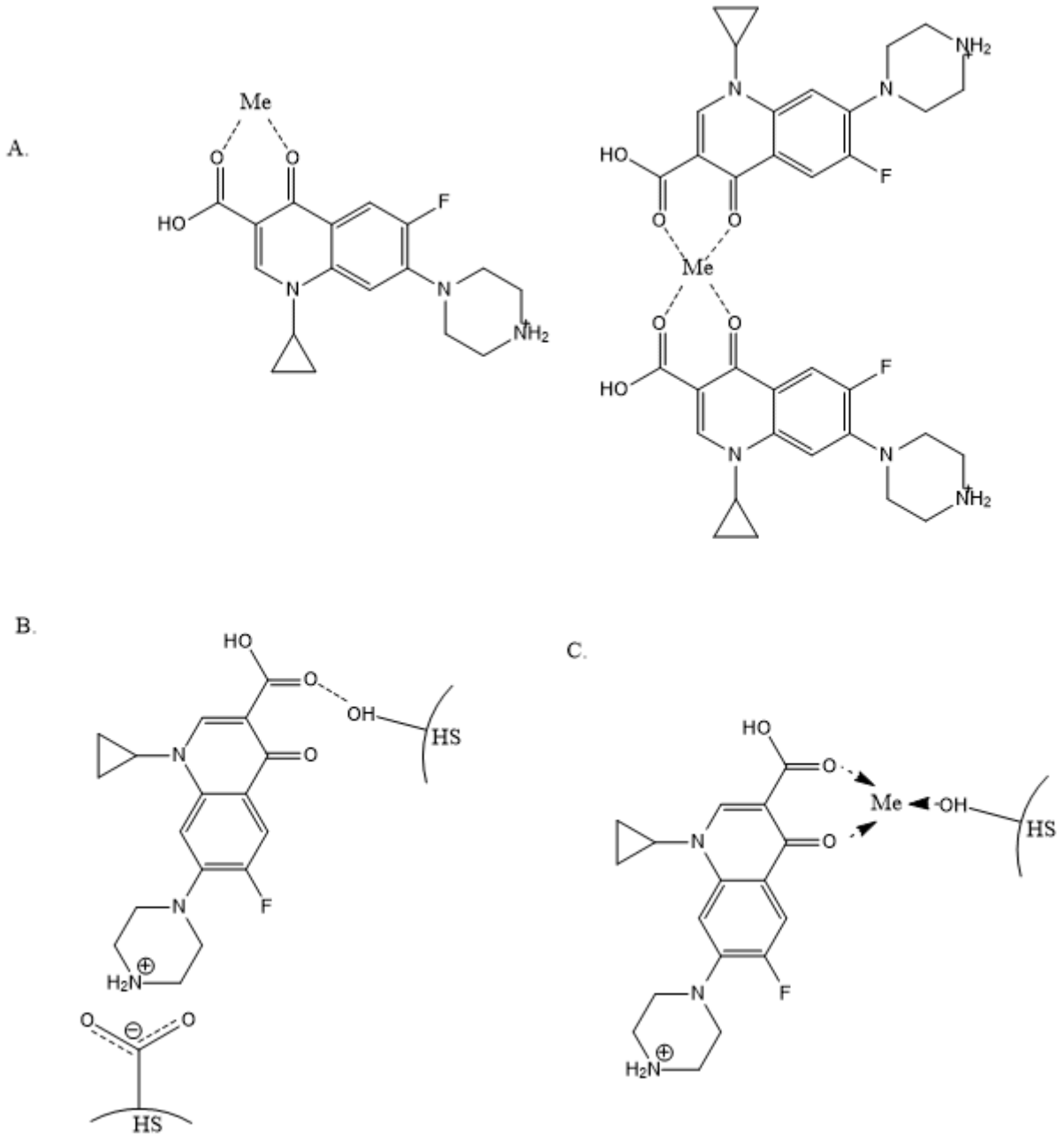

Figure 2.1. 2 The hypothetical interactions between CIP, metal ions and humic substances: A.) CIP and metal ions (Me= Al, Co(II), Cu(II), Fe(III), Mg), where the binding may be in 1:1 ratio (left) or 2:1 CIP:Me (right); B.) CIP and humic substances (HS), where they can interact via hydrogen bonding between the oxygens of carbonyl or carboxylic group of CIP and hydroxyl group of HS or by interaction between positively charged nitrogen at piperazinyl group and negatively charged HS groups; and C.) the cation bridge formed between oxygens of carbonyl or carboxylic group of CIP and hydroxyl group of HS

Stability test of CIP-Me complexes

The Figures 2.1.3-7 shows the changes of fluorescence intensity of CIP-Me complexes. They are presented as the difference between fluorescence intensity of free CIP (F_{CIP}) and complexes ($F_{CIP\text{-}Me}$) for quenching metal ions. Difference between $F_{CIP\text{-}Me}$ and F_{CIP} was displayed for fluorescence enhancing metal ions.

CIP-Al complexes

Figure 2.1.3 presents the change of fluorescence versus time for the CIP-Al complexes. In ultrapure water at 18˚C, the compound remained stable for 7 days (p>0.05). In the presence of HS, at the same temperature, the complex formation was slower. Between the first and fourth day, the fluorescence intensity increased (p<0.05) and it became stable from sixth day onwards (p>0.05). Moreover, at higher concentration of Al^{3+}, the higher deviation of fluorescence intensity can be observed. The study of Zhou et al. (2015) showed that complexation between trivalent metal ions and humic acid is 7.5 times faster than between divalent ions [20]. Thus, the delay in obtaining the equilibrium by CIP-Al complex could be due to the competition between CIP and HS over Al^{3+} as seen in the change of fluorescence intensity differences (fig. 2.1.2). The other reason could be the attaining of the equilibrium of CIP, HS and Al^{3+} system which can be observed in FTIR spectra (fig. 2.1.1).

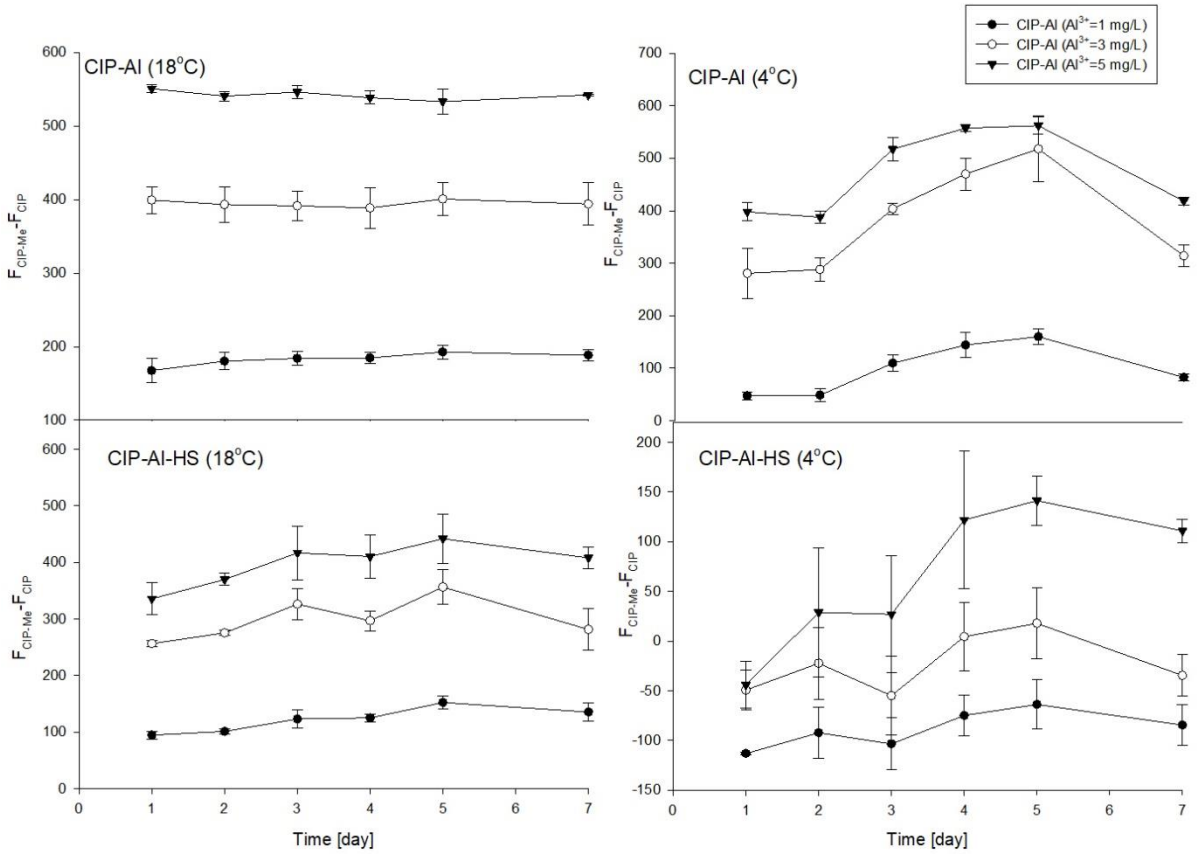

Figure 2.1. 3 Changes of fluorescence (ΔF=F_{CIP-Al}-F_{CIP}) of CIP-Al complexes in time at 18±2˚C and 4±1˚C

At 4˚C in ultrapure water, the fluorescence intensity of CIP-Al complex changed during seven-day incubation. The fluorescence intensity increased till fourth day (p<0.05) which suggested complex formation. However, after the fifth day, a decrease was noticed. On the seventh day, there is no significant difference of fluorescence intensity when compared to the first day (p>0.05), hence the complex could have disintegrated. In case of the solutions containing HS, the change in CIP concentration occurred. The spectrophotometric measurements showed that with the increase of Al^{3+} concentration, the fluorescence intensity value of the mixture increased as well, which is consistent with

the data obtained for higher temperature. However, the increase of the fluorescence intensity was below the fluorescence intensity value for CIP itself ($\Delta F<0$). At low temperature, in all CIP-Al+HS solutions with a different concentration of Al^{3+}, the brown precipitate occurred due to the decrease in the solubility of CIP complexes. The color of the precipitate suggested that it contained HS. CIP was found to adsorb onto HS, especially at acidic pH [22]. The positively charged CIP can interact with negatively charged HS. However, in this study, the pH is 6.5, where CIP is mostly present as $CIP^{\pm}$. Thus, the complexation is limited, but it cannot be excluded (fig. 2.1.1). Furthermore, Yu et al. (1994) established that CIP alone presented a 2-fold decrease in solubility when the temperature decreased from 25˚C to 6˚C [23]. With the low concentration of Al^{3+} (1-3 mg/L), the fluorescence intensity value of complexes is lower or similar to CIP alone. However, with the higher concentration, the increase of fluorescence intensity can be seen. It can be associated with the increased concentration of metal ions, which enhanced CIP solubility due to the formation of more ionic and hydrophilic compounds [10].

CIP-Co complexes

The changes in the stability of CIP-Co complexes versus time are shown in Figure 2.1.4. At 18˚C, the complex was stable for seven days in ultrapure water and with HS presence ($p>0.05$). The measurements at 4˚C showed that CIP-Co complexes were rather stable for 7 days in ultrapure water ($p>0.05$). It can be observed that the increase of Co^{2+} concentration, induced a slight decrease in fluorescence intensity value. Hence, more of CIP-Co complex is formed, however, it is to a lower extent than in the case of higher temperature ($[F_{CIP}-F_{CIP-Co}]_{T=4}<[F_{CIP}-F_{CIP-Co}]_{T=18}$).

In the presence of HS, with the low concentration of Co^{2+} (1 mg/L), the complexes were stable for 7 days ($p>0.05$). However, with the increase of ions concentration, the complex formation attained its equilibrium on the second day of incubation ($p<0.05$). Cobalt ions are able to form complexes with HS (fig. S2, Annex B) [24]. Thus, there is a possibility that with the higher concentration of Co^{2+}, there is a competition for ions between HS and CIP.

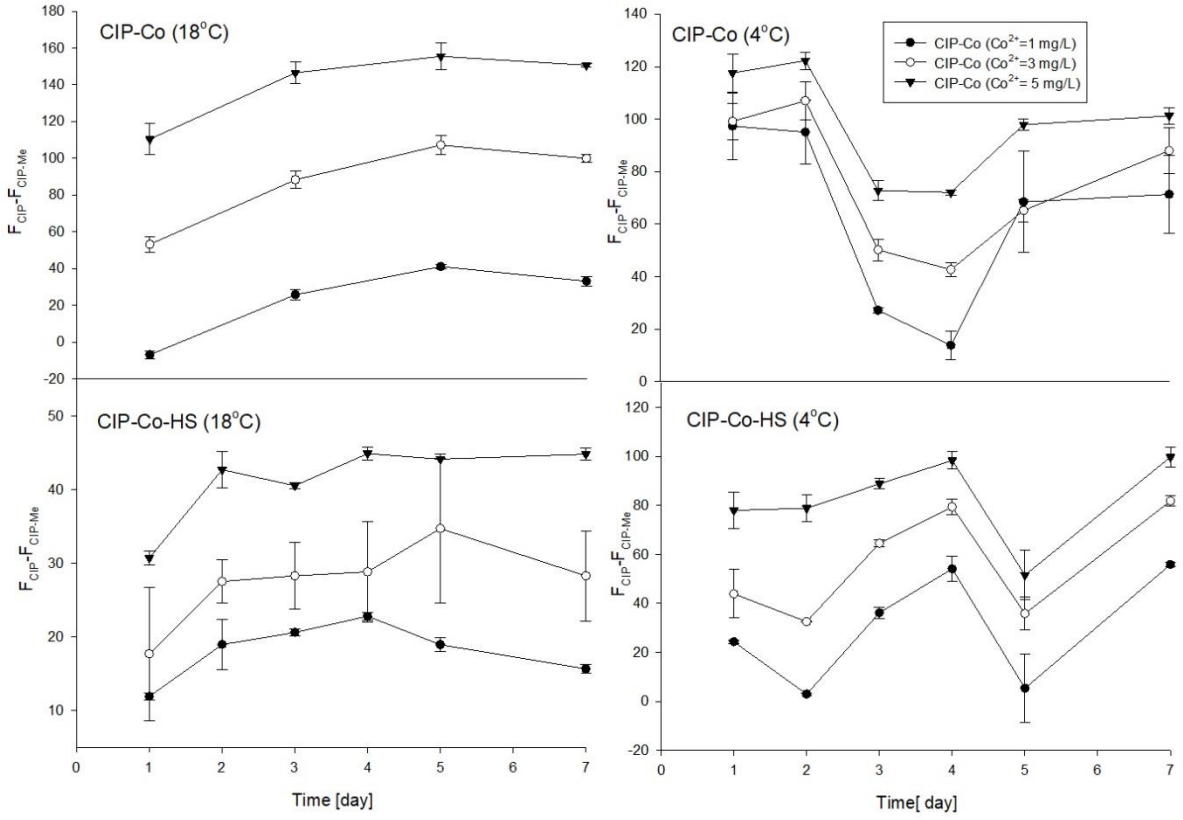

Figure 2.1. 4 Changes of fluorescence ($\Delta F=F_{CIP}-F_{CIP\text{-}Co}$) of CIP-Co complexes in time at 18±2˚C and 4±1˚C

CIP-Cu complexes

Figure 2.1.5 presents the changes of fluorescence of CIP-Cu complexes in time. In ultrapure water at 18˚C, the fluorescence intensity remained approximately the same (p>0.05), hence the complex was stable at the tested time. In the HS present, no significant changes were observed, thus the complexes also remained stable (p>0.05).

At 4˚C, in ultrapure water, the stability of complex remained unchanged for 7 days; except for the lowest concentration of Cu^{2+}. With the concentration 1-3 mg/L, the fluorescence intensity value changed. The fluorescence intensity increased and then decreased. This suggested the increase of the complex concentration till the fourth day and then it decreased, probably to attain the most stable state. In the presence of HS, the fluorescence intensity changes over seven-day incubation can be observed. This suggested the interaction between HS, CIP, and Cu^{2+}. According to Pandey et al. (2000), the stability constant between humic acid and Cu^{2+} had the highest value for the tested cations [25]. Hence, the competitive interaction between HS and CIP could have occurred.

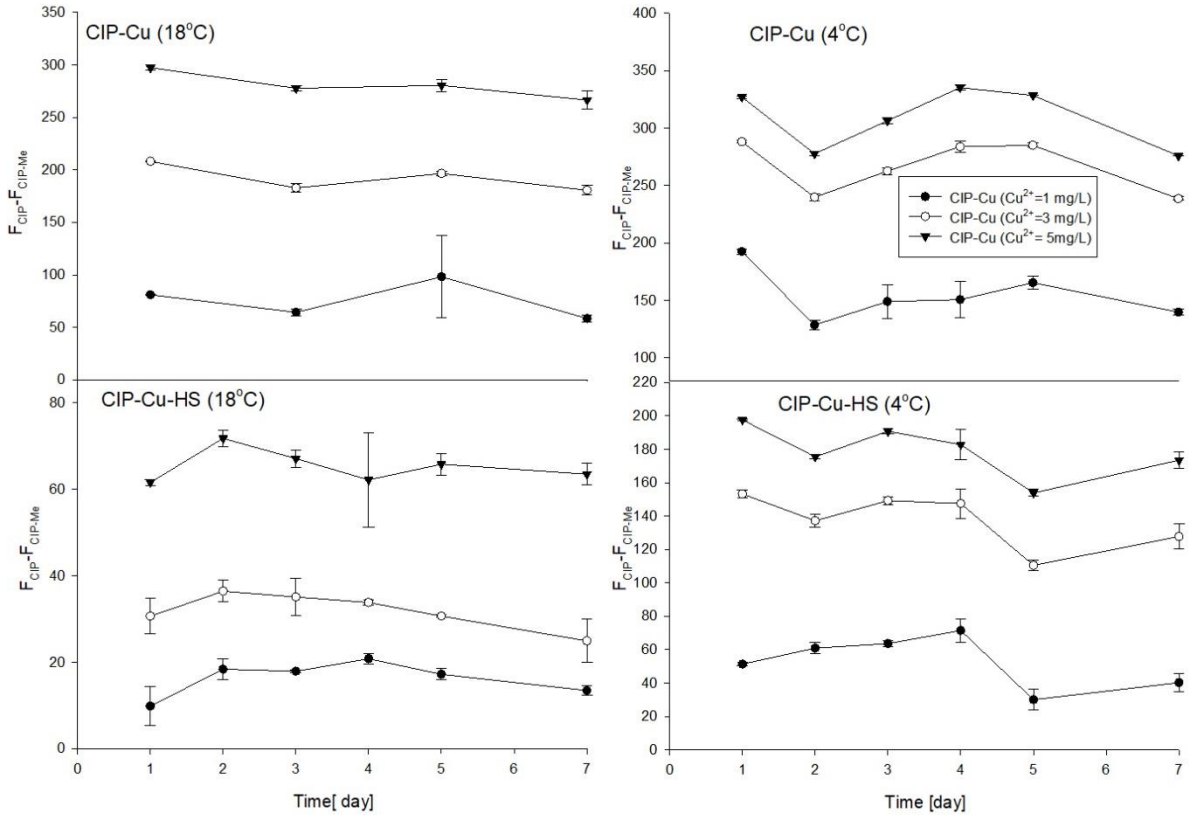

Figure 2.1. 5 Changes of fluorescence ($\Delta F=F_{CIP}-F_{CIP-Cu}$) of CIP-Cu complexes in time at 18±2˚C 4±1˚C*CIP-Fe complexes*

The changes of stability versus time for CIP-Fe complexes are presented in Figure 2.1.6. At 18˚C, in ultrapure water, the fluorescence intensity of CIP-Fe did not present a statistically significant difference (p>0.05). However, it exhibited high standard deviation. The presence of HS crucially altered CIP-Fe complexation. The fluorescence intensity of metal complexes is comparable with that of CIP alone. The standard deviation, in this case, was also higher than for the rest of the metal complexes. This suggested that Fe^{3+} underwent chemical reactions that altered the complex formation. They may be summarized in following reactions (Eq. 8-10):

$$Fe^{3+} \xrightarrow{H_2O} Fe(OH)_3 \downarrow \quad \text{Eq. 8}$$

$$Fe^{3+} \xrightarrow{HS} Fe^{2+} \quad \text{Eq. 9}$$

$$Fe^{2+} \xrightarrow{O_2} Fe^{3+} \quad \text{Eq. 10}$$

In general, the complexes with trivalent ions (Al^{3+} and Fe^{3+}) and FQs are known to be the most stable, including CIP [15]. However, in this study due to the alteration of Fe^{3+} complexes, it was impossible to calculate stability constant. In natural waters, as well as in this study, the pH is circumneutral. Under these conditions, Fe(III) is present as ferric hydroxide (Eq. 8), which is insoluble, precipitates and forms colloids [26]. Even though the concentrations of CIP and Fe^{3+} were relatively low and no turbidity was

observed, it cannot be excluded that this process did not occur during the experiment [27]. Hence, this indicated that the changes in the fluorescence intensity were as a result of sorption of CIP onto $Fe(OH)_3$ [28].

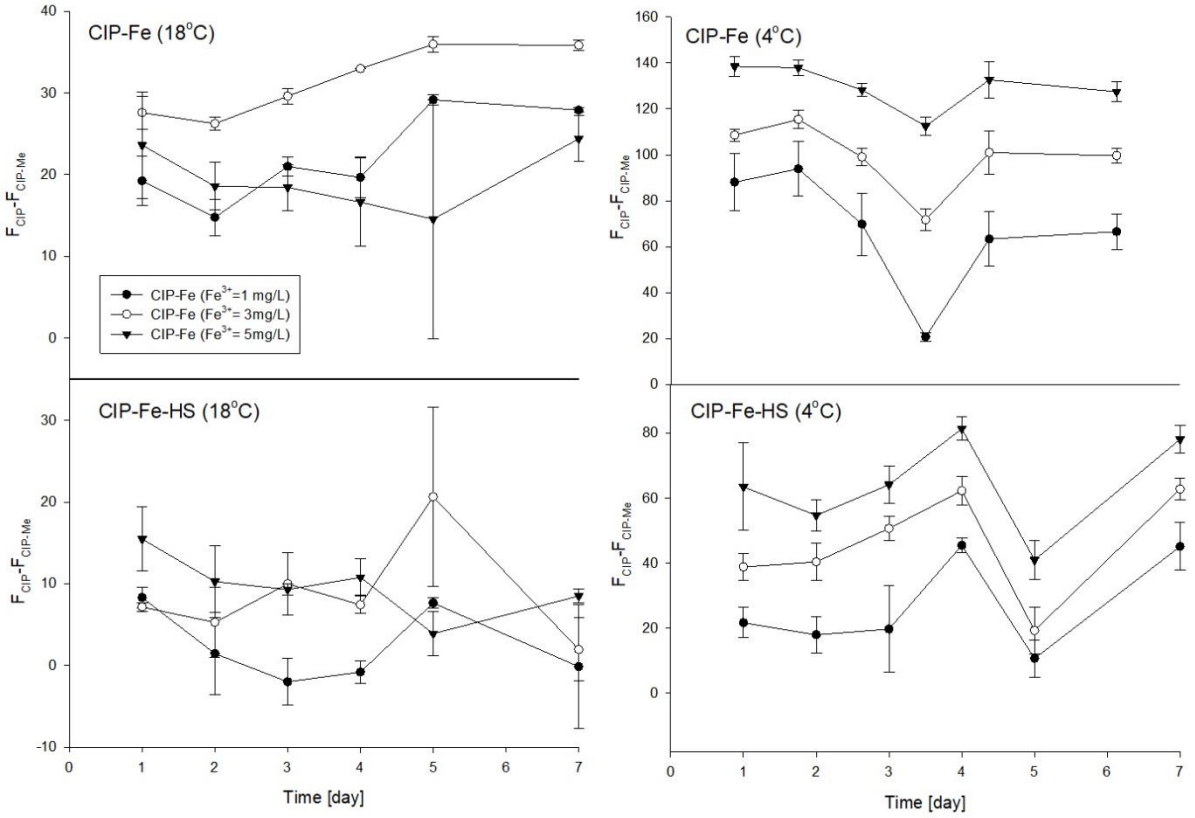

Figure 2.1. 6 Changes of fluorescence ($\Delta F=F_{CIP}-F_{CIP\text{-}Fe}$) of CIP-Fe complexes in time at18±2˚C and 4±1˚C

Fe^{3+} ions may also exhibit higher affinity of iron (III) ions towards HS than CIP. The other possibility is CIP-Fe-HS complex formation (fig. 2.1.1) [29]. Another explanation of CIP-Fe-HS complex formation is due to sorption affinity of ferric hydroxide toward CIP and HS [28, 30]. A further possibility is the reduction of Fe^{3+} to Fe^{2+} due to organic radicals and phenolic groups of HS (Eq. 9) [31]. However, this reaction is strongly inhibited at pH>3.5. Even if the redox reaction happened, due to the air access, the oxidation of Fe^{2+} to Fe^{3+} by oxygen might have occurred (Eq. 10)) [26]. In all the described cases, the linearity of Eq. 6 may be altered due to these interactions.

At lower temperature, the fluorescence intensity of CIP-Fe complexes changed during seven-day incubation (p<0.05). It may be associated with the possibilities of interactions which are slower at a lower temperature. In the presence of HS, the complex attained stability on the fourth day. In general, CIP-Fe complexes at 4˚C exhibited less dynamic changes.. which can be explained by the collision theory [32]. The theory assumes that when the two or more molecules collide with each other, only part of them lead to a chemical reaction. In most of the cases, the reaction rate depends on the temperature (an increase of temperature results in higher reaction rate) and this is observed in CIP-Fe complexation at different temperatures.

CIP-Mg complexes

The Mg^{2+} titration did not exhibit linearity throughout the whole experiment even after decreasing Mg^{2+} concentration, hence the stability constant could not be calculated. However, from the literature, it is known that CIP-Mg complexes are the least stable of the tested compounds [15]. Figure 2.1.7 presents the stability of CIP-Mg complexes in time. During seven-day incubation, in ultrapure water at 18˚C, there was no significant difference in fluorescence intensity value. Moreover, the changes of the fluorescence intensity value between CIP and increasing concentration of Mg^{2+} is minor. In the presence of HS, the complex formation attained the equilibrium on the second day (p<0.05). Moreover, the complex formation does not depend on the Mg^{2+} concentration (p>0.05). The same situation was observed for CIP-Mg in ultrapure water at 4˚C. The fluorescence intensity, in this case, varied between 300-400 during seven-day incubation (data not shown). At 4˚C, in the presence of HS, there is no statistically significant difference between fluorescence intensity of CIP and CIP-Mg. Hence, there was no complex formation.

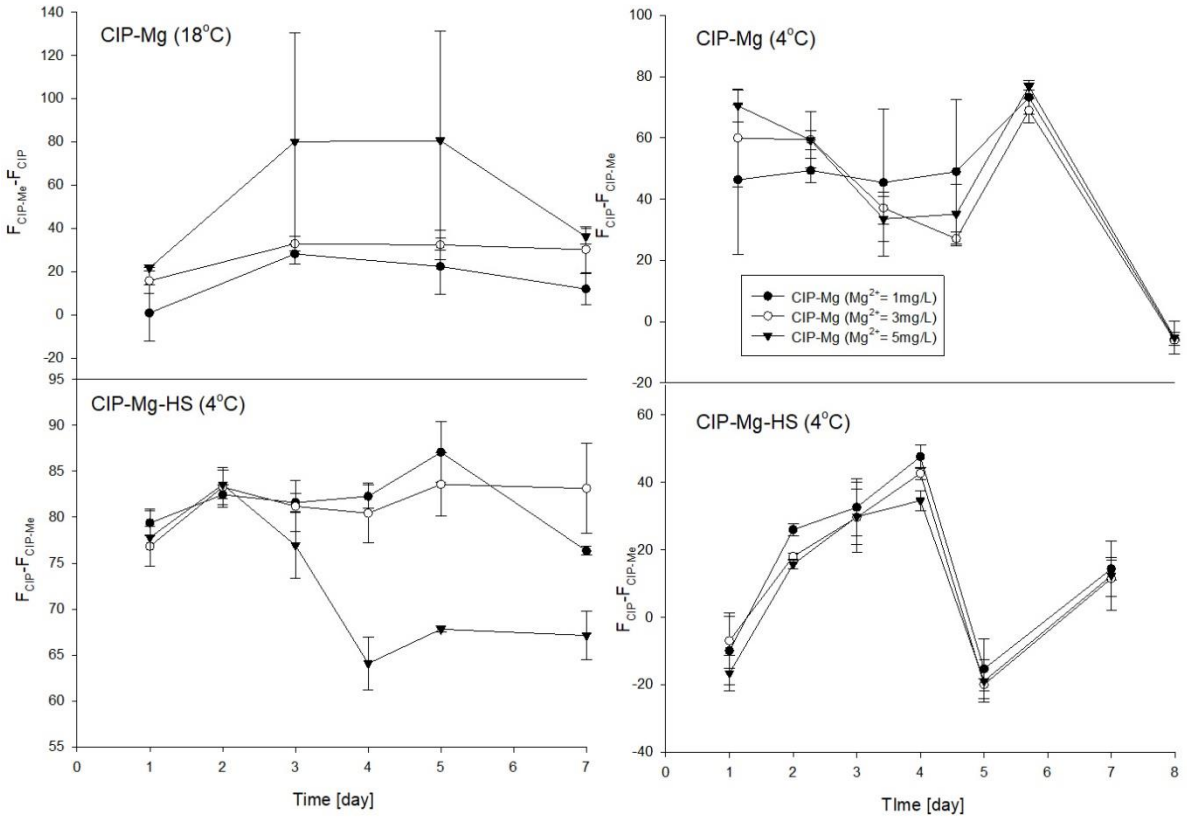

Figure 2.1. 7. Changes of fluorescence (ΔF) of CIP-Mg complexes in time at18±2˚C and 4±1˚C

Furthermore, in the presence of HS as well as at lower temperature (4˚C), the magnesium ions resulted in fluorescence quenching, and not in the enhancement, as it happened with CIP-Mg in ultrapure water (18˚C). It may be connected to the formation of different complexes which depends on the Mg^{2+} concentration [33]. Moreover, in the presence of HS, the competition between CIP and Mg^{2+} to bind to

HS might have occurred [21]. There is also a possibility of complex formation of CIP-Mg-HS (fig. 2.1.1) [29].

In general, the most stable complexes were CIP-Al, CIP-Cu, and CIP-Co and they followed the order: CIP-Al>CIP-Cu/CIP-Co at 18˚C and CIP-Al>CIP-Cu>CIP-Co at 4˚C. The complexes of CIP-Fe exhibited significant fluorescence changes, probably due to precipitation of Fe^{3+} to $Fe(OH)_3$. The CIP-Mg was found to be the least stable complexes. The presence of HS resulted in probable CIP-Me-HS formation.

Antimicrobial activity test – MIC

The MIC of CIP-Me complexes is presented in Table 2.1.3. The complexes in ultrapure water exhibited similar antimicrobial activity towards *B. subtilis*, except for CIP-Mg which exhibited 2-folds lower MIC value. Magnesium is an essential divalent metal for many enzymatic and structural functions [34]. The metal mixture (CIP+Al+Co+Cu+Fe+Mg) exhibited the same potency of bacterial growth as CIP alone. This indicated the competition of the CIP-Me complexes or the dissociation of the formed complex so that only free CIP entered the bacterial cell [18]. CIP and its complexes showed higher antimicrobial activity towards *E. aeruginosa*, as compared to *B. subtilis* (Table 2.1.3.). The highest antimicrobial potency was exhibited by CIP and its Co/Cu complexes (MIC=0.125 μg/ml), followed by trivalent ion complexes (MIC=0.25 μg/ml). The solution that contained all the five metal ions (=Al^{3+}, Co^{2+}, Cu^{2+}, Fe^{3+}, Mg^{2+}) and CIP, as well as CIP-Mg alone, had the lowest inhibition activity (0.5 μg/ml) towards *E. aeruginosa* amongst the tested mixtures (Table 2.1.3.). For both bacteria, the controls with metal solutions did not exhibit any antimicrobial activity in the tested concentrations (0.025-0.2 μg/ml).

Table 2.1. 3 MIC for CIP-MI complexes [μg/ml]

CIP-Me	CIP	CIP-Al	CIP-Co	CIP-Cu	CIP-Fe	CIP-Mg	CIP+Al+Co+Cu+Fe+Mg
				Ultrapure water			
Ea	0.125	0.25	0.125	0.125	0.25	0.5	0.5
Bs	0.25	0.25	0.25	0.25	0.25	0.125	0.25
				Water with humic substances			
Ea	0.5	0.25	0.5	0.5	0.5	0.5	0.5
Bs	0.25	0.25	0.125	0.25	0.125	0.25	0.25

Ea: Enterobacter aeruginosa; Bs: Bacillus subtilis

The presence of HS lowered the antimicrobial activity of tested complexes towards *E. aeruginosa*. This suggested that the presence of HS may hinder the CIP-Me/CIP uptake. It is consistent with other studies, where metal ions, especially trivalent ions, formed complexes with HS [20, 30]. This indicated that the HS adsorption on the bacterial outer membrane may hinder the antibiotic diffusion. For *E. aeruginosa,* the same MIC value was observed for all the complexes (0.5 μg/ml), expect for CIP-Al which was 2-fold lower. CIP-Me+HS solutions exhibited almost the same antimicrobial activity towards *B. subtilis*

as they did in ultrapure water, except for CIP-Co/Fe/Mg complexes. The antimicrobial activity of CIP-Mg complex decreased, which may be the result of complexation between magnesium ions and HS [21]. However, CIP-Co/Fe complexes displayed a 2-fold decrease of MIC value. Both complexes had lower stability in the presence of HS (fig 2.1.2 and 2.1.4), thus the elevated concentration of free ions might occur. Studies conducted by Winner (1984) and Campbell et al. (2000) presents that the presence of HS may result in enhancement of antimicrobial activity of metal ions [35, 36]. Thus, in this study, in the presence of HS, CIP and Co^{2+}/Fe^{3+} (or $Fe(OH)_3$ in case of iron) may have an additive mode of action against *B. subtilis.* The controls containing the HS and metals did not exhibit any antimicrobial activity towards bacteria in tested concentrations. The interesting part is that even though the HS was added, for the mixture of all five metal ions and antibiotics, the MIC remained the same as before HS addition.

The general trend might be observed. *E. aeruginosa,* a Gram-negative bacteria was more susceptible to environmental changes due to higher toxicity in ultrapure water and its decreased antimicrobial effect in the presence of HS. The basic difference between Gram-negative and Gram-positive bacteria is the presence of lipid outer membrane in Gram-negative bacteria, which acts as an additional protective layer. The permeability of this barrier as well as presence of porins across the cell membrane are the two entry routes for FQs antibiotics [18]. Moreover, the study of Tikhonov et al. (2013) showed that HS exhibited lower sorption onto cells of Gram-negative bacteria, probably due to the size exclusion [37]. If the CIP sorbed onto HS, the large molecule formed cannot penetrate the outer membrane, thus the antimicrobial activity of CIP and its complexes would be lower. On the other hand, no significant difference between MIC values for Gram-positive bacteria was observed, regarding CIP complexation or HS presence. Based on the study of Tikhonov et al. (2013), these bacteria are more potent to absorb HS [37]. Thus, in this case, the formed complexes could enter the bacterial cell and exert the antimicrobial activity towards bacteria. The complexes might have dissociated due to the comparable antimicrobial activity of free CIP and its complexes.

Stability of CIP-Me complexes, their antimicrobial activity and environmental impact

Antibiotic-contaminated water can play a key role in the spreading of antimicrobial resistance [38]. The presence of antimicrobials at subtherapeutic doses may induce the spontaneous mutation which results in the occurrence of resistance. Study of Girardi et al. showed that the resistance genes were not detected in the tested bacteria, however due to their incubation with CIP, the strains attained the resistance after 14 days [4]. Moreover, the antibiotics do interact with other compounds present in waters. CIP introduced to aquatic compartments can thus form stable complexes with MI and/or HS (fig 2.1.1.). As a result, CIP uptake by bacteria may be hindered due to CIP-HS interaction, as it happens with different antibiotics [39]. However, this applies to Gram-negative bacteria, whereas the Gram-positive seemed less affected by it (Table 2.1.3). In fact, the phylogenetic differences between bacteria and bacterial strains may result in varied toxic effects [18]. More studies should be performed to fully understand this relationship.

This study showed that in the presence of five cations and HS, the CIP was present for at least seven days, even at lower temperatures. Thus, long-term exposure may induce the selective pressure towards bacteria, as mentioned earlier. The most toxic cations are the ones that form the most stable complexes with CIP, i.e. trivalent ions and transition divalent ions. It is highly alarming due to the presence of antibiotic and heavy metals resistance genes linked to the same plasmid [40]. Antibiotics eventually undergo degradation, while metal ions do not, hence metal ions may lead to dissemination of metal-resistant genes as well as antibiotic-resistant genes, if they are linked.

Apart from the toxic effect of the CIP complexes, the efficiency of the CIP degradation may also be affected. The presence of HS during wastewater treatment is known to hinder the removal of other organic compounds [22, 41]. The ability of formation of CIP complexes may result in the high affinity of the compound to the sludge, rich in the HS and metal ions [9, 28, 30, 36]. CIP due to complexation may be accumulated in the sludge. Nowadays, there are no regulations regarding the acceptable concentration of organic compounds in sludge. Subsequently, the treated sludge with CIP and metal ions present may be disposed to the soil. This would result in the introduction of CIP and its possible complexes into the soils which could influence the local microbial community due to their long-term stability.

Conclusion

All the CIP-Me complexes remained in the solutions during the seven days period at 18˚C. The most stable complexes were CIP-Al, CIP-Co, and CIP-Co at 4˚C and 18˚C. The presence of HS usually resulted in slower chemical equilibrium obtainment. The low temperature also contributed to decreasing the stability. In the presence of Mg^{2+} and HS, the complexation rate did not depend on the magnesium ions concentration at 18 ˚C. At 4 ˚C, the complex between CIP-Mg-HS was not formed. The conversion of Fe^{3+} to $Fe(OH)_3$ primarily affected the stability of the CIP-Fe complex. The antimicrobial activity tests against *B. subtilis* suggested that the CIP-Me complexes maintained its antimicrobial effect, even in the presence of the humic substances, which are widely prevalent in the environment. The efficiency of CIP and its complexes against *E. aeruginosa,* was affected by HS presence, resulting in slighty decreased MIC value. Hence, depending on the bacteria type (Gram-negative or Gram-positive), the mechanism of CIP uptake was different. Moreover, the solutions with tested metal ions (Al^{3+}, Co^{2+}, Cu^{2+}, Fe^{3+}, Mg^{2+}) and CIP exhibited the same antimicrobial effect with and without HS. Thus, the complexes with heavy metal ions (iron, copper) or even the complexes with metal ions that are essential for bacteria (magnesium) in the aquatic compartments pose a threat toward the bacterial community. Even though the antimicrobial activity of mixture was lower than the CIP itself and its complexes, still the HS presence did not alter the efficacy of the antibiotic but affected the stability.

Acknowledgements

The authors are sincerely thankful to the Natural Sciences and Engineering Research Council of Canada (Discovery Grant 355254 and NSERC Strategic Grant) and Ministère des Relations Internationales du Québec (coopération Québec-Catalanya 2012-2014- project 07.302). Our sincere thanks to INRS Emeritus Professor, Prof. P.G.C. Campbell whose discussion and thoughts made us understand the direction of this work.

References

1. Canada, P.H.A.o., Canadian Antimicrobial Resistance Surveillance System Report 2016. 2016.

2. Uivarosi, V., Metal complexes of quinolone antibiotics and their applications: an update. Molecules, 2013. **18**(9): p. 11153-97.

3. Berkner, S., S. Konradi, and J. Schönfeld, Antibiotic resistance and the environment—there and back again. EMBO Reports, 2014. **15**(7): p. 740-744.

4. Girardi, C., et al., Biodegradation of ciprofloxacin in water and soil and its effects on the microbial communities. J Hazard Mater, 2011. **198**: p. 22-30.

5. Miao, X.S., et al., Occurrence of antimicrobials in the final effluents of wastewater treatment plants in Canada. Environ Sci Technol, 2004. **38**(13): p. 3533-41.

6. Lee, H.B., T.E. Peart, and M.L. Svoboda, Determination of ofloxacin, norfloxacin, and ciprofloxacin in sewage by selective solid-phase extraction, liquid chromatography with fluorescence detection, and liquid chromatography--tandem mass spectrometry. J Chromatogr A, 2007. **1139**(1): p. 45-52.

7. Van Doorslaer, X., et al., Fluoroquinolone antibiotics: an emerging class of environmental micropollutants. Sci Total Environ, 2014. **500-501**: p. 250-69.

8. Ji, X., et al., Antibiotic resistance gene abundances associated with antibiotics and heavy metals in animal manures and agricultural soils adjacent to feedlots in Shanghai; China. J Hazard Mater, 2012. **235-236**: p. 178-85.

9. Chen, H., et al., Effects of Cu and Ca cations and Fe/Al coating on ciprofloxacin sorption onto sand media. J Hazard Mater, 2013. **252-253**: p. 375-81.

10. Eboka C J, O.H.A., Aqueous solubility of ciprofloxacin in the presence of metal cations. Tropical Journal of Pharmaceutical Research, 2005. **4**(1): p. 349-354.

11. Frimmel, F.H., Aquatic Humic Substances, in Biopolymers Online. 2005, Wiley-VCH Verlag GmbH & Co. KGaA.

12. Zhang, Y., et al., Insights into aquatic toxicities of the antibiotics oxytetracycline and ciprofloxacin in the presence of metal: complexation versus mixture. Environ Pollut, 2012. **166**: p. 48-56.

13. Diseases, E.S.o.C.M.a.I., EUCAST Definitive Document E.DEF 3.1, June 2000: Determination of minimum inhibitory concentrations (MICs) of antibacterial agents by agar dilution, in Clin Microbiol Infect. 2000, European Society of Clinical Microbiology and Infectious Diseases p. 509-15.

14. Yuan, X.Y., J. Qin, and L.L. Lu, Influence of metal ions on the interaction between gatifloxacin and calf thymus DNA. Spectrochim Acta A Mol Biomol Spectrosc, 2010. **75**(2): p. 520-4.

15. Urbaniak, B. and Z.J. Kokot, Analysis of the factors that significantly influence the stability of fluoroquinolone-metal complexes. Anal Chim Acta, 2009. **647**(1): p. 54-9.

16. Zhang, Q., et al., Sorption of norfloxacin onto humic acid extracted from weathered coal. J Environ Manage, 2012. **102**: p. 165-72.

17. Deacon, G.B. and R.J. Phillips, Relationships between the carbon-oxygen stretching frequencies of carboxylato complexes and the type of carboxylate coordination. Coordination Chemistry Reviews, 1980. **33**(3): p. 227-250.

18. Feio, M.J., et al., Fluoroquinolone-metal complexes: a route to counteract bacterial resistance? J Inorg Biochem, 2014. **138**: p. 129-43.

19. Lopez-Gresa, M.P., et al., Interactions of metal ions with two quinolone antimicrobial agents (cinoxacin and ciprofloxacin). Spectroscopic and X-ray structural characterization. Antibacterial studies. J Inorg Biochem, 2002. **92**(1): p. 65-74.

20. Zhou, S., et al., Influence of Humic Acid Complexation with Metal Ions on Extracellular Electron Transfer Activity. Sci Rep, 2015. **5**: p. 17067.

21. Aristilde, L. and G. Sposito, Complexes of the antimicrobial ciprofloxacin with soil, peat, and aquatic humic substances. Environ Toxicol Chem, 2013. **32**(7): p. 1467-78.

22. Wang, W., et al., Effect of humic acid on ciprofloxacin removal by magnetic multifunctional resins. Sci Rep, 2016. **6**: p. 30331.

23. Yu, X., G.L. Zipp, and G.W. Davidson, 3rd, The effect of temperature and pH on the solubility of quinolone compounds: estimation of heat of fusion. Pharm Res, 1994. **11**(4): p. 522-7.

24. Baek, K. and J.-W. Yang, Sorption and desorption characteristics of cobalt in clay: Effect of humic acids. Korean Journal of Chemical Engineering, 2004. **21**(5): p. 989-993.

25. Pandey, A.K., S.D. Pandey, and V. Misra, Stability constants of metal-humic acid complexes and its role in environmental detoxification. Ecotoxicol Environ Saf, 2000. **47**(2): p. 195-200.

26. Geological, S., Chemistry of iron in natural water. 1962: Washington : U.S. Govt. Print. Off., 1962.

27. Frade, V.M.F., et al., Batch and Fed-Batch Degradation of Enrofloxacin by the Fenton Process. Chemical Engineering & Technology, 2017. **40**(4): p. 663-669.

28. Gu, C. and K.G. Karthikeyan, Sorption of the antimicrobial ciprofloxacin to aluminum and iron hydrous oxides. Environ Sci Technol, 2005. **39**(23): p. 9166-73.

29. Aristilde, L. and G. Sposito, Binding of ciprofloxacin by humic substances: a molecular dynamics study. Environ Toxicol Chem, 2010. **29**(1): p. 90-8.

30. Tipping, E., The adsorption of aquatic humic substances by iron oxides. Geochimica et Cosmochimica Acta, 1981. **45**(2): p. 191-199.

31. Deiana, S., et al., Iron(III) reduction by natural humic acids: a potentiometric and spectroscopic study. European Journal of Soil Science, 1995. **46**(1): p. 103-108.

32. Atkins, P.W., The Elements of Physical Chemistry. 3rd ed. 1993: Oxford University Press.

33. Drevensek, P., I. Turel, and N. Poklar Ulrih, Influence of copper(II) and magnesium(II) ions on the ciprofloxacin binding to DNA. J Inorg Biochem, 2003. **96**(2-3): p. 407-15.

34. Wakeman, C.A., et al., Assessment of the Requirements for Magnesium Transporters in Bacillus subtilis. Journal of Bacteriology, 2014. **196**(6): p. 1206-1214.

35. Campbell, C.D., et al., The effect of EDTA and fulvic acid on Cd, Zn, and Cu toxicity to a bioluminescent construct (pUCD607) of Escherichia coli. Chemosphere, 2000. **40**(3): p. 319-25.

36. Winner, R.W., The toxicity and bioaccumulation of cadmium and copper as affected by humic acid. Aquatic Toxicology, 1984. **5**(3): p. 267-274.

37. Tikhonov, V.V., et al., [Sorption of humic acids by bacteria]. Mikrobiologiia, 2013. **82**(6): p. 691-7.

38. Frade, V.M.F., et al., Environmental contamination by fluoroquinolones. Brazilian Journal of Pharmaceutical Sciences, 2014. **50**: p. 41-54.

39. Chen, Z., et al., Influence of Dissolved Organic Matter on Tetracycline Bioavailability to an Antibiotic-Resistant Bacterium. Environmental Science & Technology, 2015. **49**(18): p. 10903-10910.

40. Gao, P., et al., Impacts of coexisting antibiotics, antibacterial residues, and heavy metals on the occurrence of erythromycin resistance genes in urban wastewater. Appl Microbiol Biotechnol, 2015. **99**(9): p. 3971-80.

41. Lipczynska-Kochany, E. and J. Kochany, Effect of humic substances on the Fenton treatment of wastewater at acidic and neutral pH. Chemosphere, 2008. **73**(5): p. 745-750.

CHAPTER III: INSUFFICIENT REMOVAL OF CIPROFLOXACIN DURING WASTEWATER TREATMENT AND ITS CONTRIBUTION TO ANTIBIOTIC RESISTANCE DISSEMINATION

PART 1

Speciation of ions and its influence on antibiotics distribution in wastewater sludge

Agnieszka Cuprys[a], Joanna Lecka[a], Satinder Kaur Brar[a,b*], Tarek Rouissi[a], Patrick Drogui[a]

[a] INRS-ETE, Université du Québec, 490, Rue de la Couronne, Québec, Canada G1K 9A9

[b] Department of Civil Engineering, Lassonde School of Engineering, York University, North York, Toronto, Ontario Canada M3J 1P3

* Corresponding author: E-mail: satinder.brar@ete.inrs.ca; Satinder.Brar@lassonde.yorku.ca

Draft (to be submittedto *Journal of Environmental Sciences*)

Résumé

La ciprofloxacine (CIP) et la chlorotétracycline (CTC) sont les antibiotiques à large spectre appartenant respectivement aux familles des fluoroquinolones et des tétracyclines. Les deux sont des composés hydrophiles, ayant la capacité de former des complexes avec des ions. La complexation de l'antibiotique avec des ions métalliques peut affecter leur distribution dans les stations de traitement des eaux usées, ce qui n'est généralement pas pris en compte. L'étude analytique a été menée pour évaluer la concentration de CIP, CTC et d'autres ions choisis dans la station d'épuration. Plus de 70% des CTC ont été récupérés lors du traitement des eaux usées. La concentration de CIP mesurée était légèrement plus élevée dans l'effluent que dans les échantillons d'eaux usées d'influent. De plus, des concentrations élevées de CIP et de CTC, de 3,9 mg/kg et de 11 mg/kg, respectivement, ont été détectées dans les fractions solides de boues. Cette concentration élevée pourrait être due à des interactions avec des ions métalliques dans les boues (soit 39-53 g / kg d'Al, 64-89 g / kg de Ca, 52-109 g / kg de Fe ou 10-13 g / kg de Mg). Par conséquent, la spéciation des ions dans les boues a été effectuée pour les localiser plus précisément. La concentration correspondante d'antibiotiques dans chaque fraction de boues a également été évaluée.

Mots-clés: ciprofloxacine, chlorotétracycline, détection, eaux usées, boues, ions métalliques

Abstract

An analytical study was conducted to evaluate the concentration of ciprofloxacin (CIP), chlortetracycline (CTC) and chosen metals in the wastewater treatment plant (WWTP). The concentration of CIP was slightly higher in the effluent (0.703 ± 0.045 μg/L) than the influent (0.467 ± 0.049 μg/L) in wastewater samples. More than 70% of CTC was recovered during wastewater treatment; its concentration in wastewater effluent was at 6.13 ± 0.863 μg/L). Additionally, a high concentration of CIP and CTC, 3.9 mg/kg and 11 mg/kg respectively, were detected in the solid fractions of sludge. This elevated concentration might have been due to interactions with metals in sludge (i.e. 39-53 g/kg of Al, 64-89 g/kg of Ca, 52-109 g/kg of Fe and 10-13 g/kg of Mg) as both antibiotics have the capacity to form metal complexes. Chemical speciation of all sludge types was carried out to further investigate the distribution of targeted metals and antibiotics and to establish if there is any interdependence. The positive correlation between CTC/CIP concentration and Mg and As concentration in primary sludge was observed. This suggests that metal-antibiotic interaction may contribute to primary wastewater treatment.

Keywords: ciprofloxacin, chlortetracycline, detection, wastewater, sludge, metal ions

Introduction

Introduction

The discovery of penicillin by Alexander Fleming in 1920s revolutionized the field of medicine. Presently, antibiotics are used not only to treat human and animal infections but also, they have been used in animal farming as food additives to promote the growth and prevent the microbial contagions. However, their frequent usage, insufficient wastewater treatment (WWT) and their excess from farmlands have led to increase in amount of antimicrobials in the environment. It creates a new hazardous condition for human health as other of the antibiotics such as penicillin are degraded easily in the environment, whereas some like fluoroquinolones and tetracyclines were found to be more persistent [1].

Ciprofloxacin (CIP) is a widely used broad-spectrum antibiotic, representative of the fluoroquinolone group. It is known to treat various human infections, i.e. urinary and respiratory tract infections, anthrax or sexually transmitted diseases [2]. Other broad-spectrum antibiotics, such as chlortetracycline (CTC), belonging to tetracycline group, are commonly used as food additive in animal farming [3, 4]. The widespread utilization of CIP and CTC has led to their prevalence in various aquatic compartments at low concentrations (ng-µg/L) [4-7]. Consequently, this phenomenon has contributed to the occurrence and dissemination of antibiotic-resistant bacteria. [3].

As mentioned earlier, the presence of CTC and CIP presence in water and soils is usually associated with insufficient wastewater treatment on account of fact that wastewater treatment plants (WWTP) are not designed to remove the contaminants at that low concentration. Interestingly, even though the concentration of described antibiotics is at low parts-per-trillion (ppt)/-billion (ppb) range in wastewater, their concentration was found to be much higher in wastewater sludge. CTC and CIP can be found at concentration of mg/kg in sludge, hence at least 1000-fold higher than in liquid fraction of wastewater. This relationship may be attributed to ability of CTC and CIP to form stable complexes with metals [2, 8].

The wastewater influent and wastewater sludge (WWS) contain a high concentration of metals, as they are persistent, and are not easily removable [9]. Moreover, metals tend to accumulate in sediments, sludge, soils and in animal tissues, which may cause serious health-related adverse effects [9-11]. Moreover, the formation of stable antibiotic-metal complexes may not only significantly influences the distribution of organic pollutants, their removal and mobility in the environment but also may even promote antimicrobials resistance [2, 8], becoming an insurmountable hurdle for the health care providers.

Hence, it is crucial to know the interactions between contaminants in such an environment, as during wastewater treatment. A better understanding of the nature of targeted contaminants can surely help to develop more efficient methods of their removal. The main objective of this study was to estimate the

concentration of CIP, CTC, the representatives of fluoroquinolones and tetracyclines respectively, and metals in WWTP in Québec City, Canada. Subsequently, the chemical fraction of metals in sludge was estimated along with corresponding antibiotics concentration to evaluate a potential correlation between them.

Materials and Methods

Materials

CIP (98% purity) was obtained from Acros Organics (USA). CTC was purchased from Toronto Research Chemicals (Ontario, Canada). Cirpofloxacin-d_8 was bought from CDN Isotopes Inc. (Québec, Canada). HPLC-grade methanol (purity > 99.8%), HPLC-grade acetic acid (purity > 99.7%), trichloroacetic acid (TCA**,** 99%) and diatomaceous earth were purchased from Fisher Scientific (Ontario, Canada). Disodium ethylenediaminetetraacetate (Na_2H_2EDTA, 99%) was obtained from E-bay (Tokyo, Japan). Sep-pack® C_{18} Plus Short Cartridges (360 mg Sorbent; 37–55 mm Particle Size per Cartridge) for solid-phase extraction (SPE) were purchased from Waters (Milford, MA, USA). Deionized water was prepared in the laboratory using a Milli-Q/Milli-Ro Millipore system (Milford, MA, USA).

Wastewater samples

The wastewater samples were obtained from the Québec Urban Community wastewater treatment plant (Beauport, Québec City, Québec, Canada). The WWTP treats the wastewater, originating from industries, domestic zones, institutions, and commercial enterprises before discharging the treated water into the Saint Lawrence River. It receives approximately 215,000 $m^3 \cdot day^{-1}$ of wastewater for its treatment capacity of 400,000 $m^3 \cdot day^{-1}$. The hydraulic retention time is 45 minutes for the complete treatment. The plant comprises biofiltration wastewater treatment, consisting of 4 mechanical rake-cleaned bar screens, 5 aerated grit chambers, 7 laminar clarifiers, 30 biofilters and 5 disinfecting channels with 8480 ultraviolet lamps (working from June 1 to September 30 only). The grab samples were collected in July 2018. All samples were collected into the pre-washed containers from eight points of WWTP: influent, screening, grit, primary sludge, secondary sludge, mixed sludge (60% primary sludge and 40% secondary sludge), thickened sludge and effluent before UV treatment. Then, they were transported to the laboratory and kept in dark at 4±1˚C until further use (a week after sampling) or -20±1˚C (a month after sampling). Previous studies conducted in our laboratory for the last decade have demonstrated that when the wastewater and wastewater sludge samples are collected over different seasons and timeline, there was a ±15-20% standard error in the measurements of the different pharmaceutical compounds [data unreported]. Wastewater control parameters, i.e. pH, alkalinity, total solids (TS), volatile solids (VS), suspended solids (SS), phosphate, total organic carbon (TOC) were analyzed as described in Standard Methods (APHA, 2005) [12].

Sample preparation for elements analysis and partial digestion

The analysis of elements in wastewater (WW) and wastewater sludge (WWS) was conducted based on the work of Ashraf et al. and Dong et al. [13, 14]. The liquid fraction was separated from sludge by centrifugation (7650 x g, 25 min, 4 ˚C). Supernatant and WW samples (influent, effluent, grit unit and screening unit) were then transferred for acid digestion. About 0.5 g of dried sludge (or liquid fraction) was placed in 50 mL tubes (SCP Science 10-500-262). HNO_3 (1 mL) was added and left overnight. Subsequently, 3 mL of 1 M HCl was added and put in the heating block (2h, 95°C). Then, the mixtures were cooled down and Milli-Q water was added to obtain a volume of 50 mL Prepared samples were analyzed by Inductively Coupled Plasma Atomic Emission Spectroscopy (ICP-AES) in duplicates. The details of the measurements are given in Annex C.

Chemical speciation in sludge

The sequential extraction procedure was performed based on Dong et al. 2013 and Ashraf et al. (2012) with some modifications [13, 14]. The schematic version of the protocol is included in Figure S1 (Annex C). Samples from following sections were centrifuged (30 240 x g, 30 min) after each extraction step and the solid part was separated from the supernatant. Subsequently, the pellet was used for the next extraction step, when supernatant was filtered and analyzed by ICP-AES. The metals recovery from this method was ranged between 74-120%. The procedure was performed in duplicates.

To evaluate the influence of sludge sequential digestion on antibiotics, the controls in Milli-Q water were set up. The concentration of CIP did not change throughout the procedure; the difference between the fractions was less than 10%. In the case of CTC, a variation in its concentration was observed (<70% recovery) which could be attributed compound isomerization [15]. Figure S2 (Annex C) shows that two most common CTC isomers, iso-CTC, and epi-iso-CTC, were present in all fractions. However, to simplify the potential scenarios, only CTC form was taken under consideration in further discussion.

Exchangeable Fraction

Sludge samples (2 g) were extracted at room temperature for 1 h with 16 mL 1 M $MgCl_2$, (pH 7.0) in a water bath. Continuous agitation was maintained. Extraction in this fraction is mainly based on the adsorption-desorption process [13, 14].

Bound-to-carbonates

To the residue from the previous section, 16 mL of 1 M NaOAc was added and pH was adjusted to 5.0 with acetic acid [13, 14]. The samples underwent 5 hours of continuous agitation at room temperature to coprecipitate metals with carbonates.

Bound to Fe–Mn Oxides (Bound-to-oxides)

The residue from previous section. was treated using 20 mL of 0.04 M NH_2OH–HCl in 25% (v/v) HAc to extract metals. The experiments were performed at 96 °C with occasional agitation for 6 hours. Under these reducing conditions, Fe (III) and Mn (IV) release adsorbed metals [13, 14].

Bound-to-organics

HNO_3 (4 mL) was added to the sludge samples (0.1 g) and left overnight. Subsequently, 1.6 mL of $HClO_4$ was added and heated for 2 h at 100 °C. Then, 2 mL of HF was added and heated up to 150 °C. After, 0.4 mL of HNO_3 and water up to 15 mL was added and incubated at room temperature for 2 weeks before ICP-AES analyses.

Sample preparation for CIP and CTC analysis

Wastewater samples preparation

Wastewater samples were centrifuged at 7650 x g for 30 min and the supernatant was filtered through 2 µm glass fibers filters (Fisher brand G6 filter circles, Fisher Scientific, Ontario, Canada). The pH of each filtrate was adjusted to pH 4.0±0.1 with 0.1 M HCl for acidic extraction. Na_2EDTA was added to each sample at the final concentration of 2 mM.

WWS samples (primary, secondary, mixed and thickened sludge) were centrifuged at 7650 x g for 35 min, 4˚C. The solid fraction was then separated and frozen at -20˚C overnight before freeze-drying (Dura Frezz Dryer, Kinetics). The supernatant was filtered through 2 µm glass fibers filters and the pH was adjusted to pH 4.0±0.1. Na_2EDTA was added to each sample at the final concentration of 2 mM.

WWS extraction

The efficacy of pressurized hot water extraction (PHWE) and ultrasonic extraction (USE) to extract CIP and CTC simultaneously from WWS was compared. The detailed description of the procedure and method validation is presented in Annex C.

Clean-up and preconcentration

Solid Phase Extraction (SPE) technique was used for clean-up and preconcentration of the processed samples. The SPE cartridges (Sep-Pak Plus C_{18}) were fitted into the vacuum manifold (Welch, USA) connected to a vacuum pump (Welch Rietschle Thomas, USA). The procedure used was as described by Archana et al. (2016) with some modifications [16]. Cartridges were preconditioned with 7 mL of methanol, followed by 6 mL of deionized water and 6 mL of acidified water (pH 3-4) at the flow of approximately 1.5 mL/min. Further, the sample was loaded onto the cartridges; after pre-concentration, the samples were dried by a vacuum system (~15 psi). The parallel elution of CIP and CTC with 2 x 4 mL of methanol was optimized to achieve the highest possible recovery. The different pH values of the loaded samples (pH 3-4) and the presence of acidic additives (acetic acid and trichloracetic acid) were

taken under consideration to increase the extraction efficiency. The recoveries are presented in Annex C. Each extract was then evaporated under a gentle stream of nitrogen. Subsequently, it was reconstituted in 1 mL acetonitrile: H_2O (1:9).

CTC and CIP detection

The concentration of CIP and CTC was analyzed by liquid chromatography- electrospray- ionization-tandem mass spectrometry (LC-ESI-MS/MS). The system included a Finnigan surveyor LC pump linked to TSQ Quantum access triple quadruple mass spectrometer (Thermo Scientific, Mississauga, ON, Canada) and electrospray ionization interface. A 15 µL aliquot of the processed samples was injected into BetaBasic-18 column (100 mm x 2.1 mm x 3 µm). The column oven was set at 40˚C and the flow rate was kept at 0.3 mL/min. Ciprofloxacin-d_8 (CIP-d_8) and sulfamethazine were used as the internal standards for ciprofloxacin and chlortetracycline detection, respectively. They were added to each sample before the analyses to give the final concentration of 50 µg/L and 5 µg/L for ciprofloxacin-d_8 and sulfamethazine, respectively. The samples were eluted with a mobile phase which included 0.1% formic acid (mobile phase A) and acetonitrile combined with 0.1 % formic acid (mobile phase B). The gradient elution started with 90% of mobile phase A and 10% of mobile phase B. It was constant till 0.5 min and then mobile phase A was gradually decrease (30%) up to 3 min. Subsequently, the gradient was kept constant until 8 min and then it came back to the initial set up. The mass spectrometer was operated in SRM positive mode. Spray voltage was set at 4000 V and skimmer off-set at 20 V. Collision gas pressure was 1.5 mTorr. The capillary temperature was at 350˚C. The collision energy for CIP, CTC, sulfamethazine, and CIP-d_8 was set at 17, 18, 17 and 19 V respectively. The precursor and product ions (m/z) were selected as follows: 332.3 and 245.3 for CIP, 479.1 and 444 for CTC, 340.3 and 249.3 for CIP-d_8, 285 and 185 for sulfamethazine.

Data and statistical analysis

Recovery studies were performed in duplicates and calculations were based on eq. (11).

$$Recovery(\%) = \frac{C_f - C_0}{C_s} * 100 \qquad \text{Eq. 11,}$$

Where C_f stands for a final concentration of CTC/CIP in the spiked matrix, C_0 is the initial concentration of CTC/CIP in the matrix and C_s is spiked CTC/CIP concentration in matrix.

Statistical analysis of the obtained results was conducted via SigmaPlot 12.3 software. The Pearson correlation was applied to determine the dependence of metals chemical fraction in sludge and corresponding antibiotic concentration.

Results and Discussion

CTC/CIP distribution in WWTP

The characterization of wastewater and WWS collected from WWTP in Québec is summarized in Table 3.1.1. The average streamflow for WW (influent, screen and grit removal unit, effluent) was 7800 m^3/h. The streamflow for WWS was as follows: primary sludge, 80 m^3/h; secondary sludge, 70 m^3/h; mixed sludge, 255 m^3/h; and thickened sludge, 67 m^3/h. The average mass flow of the antibiotics was calculated with Eq. (12):

$$m = Q \times S \qquad \text{Eq. 12,}$$

Where *m* stands for mass flow (mg/h), *Q* is streamflow (m^3/h) and *S* stands for CTC/CIP concentration (μg/L or μg/kg).

Table 3.1. 1 Wastewater and wastewater sludge characterization (n=3)

Sample	Total solids [g/L]	Volatile solids [g/L]	Suspended solids [g/L]	pH	Total organic carbon [mg/L]	Alkanility [mg $CaCO_3$/L]	Phosphorous [ppm]
Influent	0.04 ± 0.45	<0.0001	0.14 ± 0.10	7.1±0.1	12.2	37.44	5.48±0.28
Screen unit	0.26 ± 0.48	<0.0001	0.20 ± 0.007	7.2±0.1	16.3	79.70	4.06±0.13
Grit removal unit	0.56 ±0.055	0.095 ± 0.015	0.23 ± 0.04	7.1±0.1	34.5	44.92	3.46±0.033
Effluent	0.46 ± 0.014	<0.0001	<0.0001	7.4±0.1	8.7	46.80	0.99±0.03
Primary sludge	3.14 ± 0.09	2.16 ± 0.056	1.03 ± 0.07	6.6±0.1	41.4	81.68	4.77±0.52
Secondary sludge	2.96 ± 0.32	2.15 ± 0.27	1.13 ± 0.01	6.7±0.1	41.6	78.62	24.58±0.49
Mixed sludge	1.41 ± 0.05	0.86 ± 0.046	0.45 ± 0.10	6.8±0.1	41.1	80.72	12.96±0.15
Thickened sludge	84.4 ± 3.0	60.05 ± 2.25	84.9 ± 4.90	5.5±0.1	35.3	-	15.42±0.65

Table 3.1.2 presents the distribution of CIP and CTC in wastewater and wastewater sludge and Figure 3.1.1 shows the mass balance of WWTP. CIP concentration is reported to be much lower than CTC but not negligible in sewage, pointing also to overall meager usage of CIP in Québec [17]. The results are consistent with the CIP concentration range of 0.042-0.712 μg/L in Ontario, Canada [18]. Relatively a higher concentration was detected also in the USA, wherein raw wastewater CIP was found to be around 1.9 μg/L [19]. CIP is mainly removed via adsorption onto sludge [20, 21]. It is consistent with much higher concentration of this fluoroquinolone detected in sludge than in wastewater (Table 3.1.2).

However, the CIP concentration in the effluent was not significantly higher than influent, suggesting negligible CIP removal as compared to the 40% CIP removal during sewage treatment in Ontario, Canada [18]. A study conducted in three WWTPs in Maryland, USA had revealed that CIP concentration was reduced up to 74%, indicating CIP accumulation during wastewater treatment via sludge adsorption [19]. Hence, in case of WWTP in Québec, it is possible that CIP undergoes adsorption onto sludge and then desorbs into the wastewater stream, leading to its elevated concentration in the effluent [22]. Detailed studies of distribution and retention time of the compound should be performed to confirm the accumulation of CIP in WWTP and its slow release into the environment.

Table 3.1. 2 Distribution of CIP and CTC in wastewater and wastewater sludge (n=3)

	Influent	**Screen unit**	**Grit removal unit**	**Primary sludge (liquid fraction)**	**Primary sludge (solid fraction)**	**Secondary sludge (liquid fraction)**
C_{CIP} [ppb]	0.467 ± 0.049	0.623 ± 0.036	0.439 ± 0.026	0.479 ± 0.113	2003 ± 6.9	0.349 ± 0.081
C_{CTC} [ppb]	21.7 ± 4.69	18.7 ± 3.46	18.2 ± 2.84	7.52 ± 0.163	6687 ± 226	7.10 ± 0.237
	Secondary sludge (solid fraction)	**Mixed sludge (liquid fraction)**	**Mixed sludge (solid fraction)**	**Thickened sludge (liquid fraction)**	**Thickened sludge (solid fraction)**	**Effluent**
C_{CIP} [ppb]	1978 ± 131	0.516 ± 0.116	3948 ± 157	0.516 ± 0.116	2388 ± 117	0.703 ± 0.045
C_{CTC} [ppb]	3849 ± 313	0.89 ± 0.191	11019	5.06 ± 3.46	5752 ± 1255	6.13 ± 0.863

CTC – chlortetracycline; CIP – ciprofloxacin

While the CIP level for Québec municipality waterworks was not reported before, the influent concentration of CTC is 3-fold lower than in the previous reports for Québec. The concentration reported by Pulicharla et al. (2014) in influent and effluent was 61.5 µg/L and 7.3 µg/L respectively [9]. The differences may correspond to seasonal variation. This study was conducted in summer while Pulicharla and colleagues had conducted the study in autumn [9]. The augmented runoff during spring and summer might have diluted CTC concentration in the wastewater [23, 24]. Furthermore, this difference might also reflect the usage of alternative to antibiotics in animal farming, which seems to be more probable as more alternatives are being tried every day [25]. Hence, lower concentration recorded in these studies may suggest overall decreased usage of CTC in agricultural and animal farming practices. Moreover, WWTP in Québec was able to remove up to 71% CTC mostly due to its adsorption on sludge in spite of the fact that removal efficiency obtained is lower than previously presented efficiency of 90% [9].

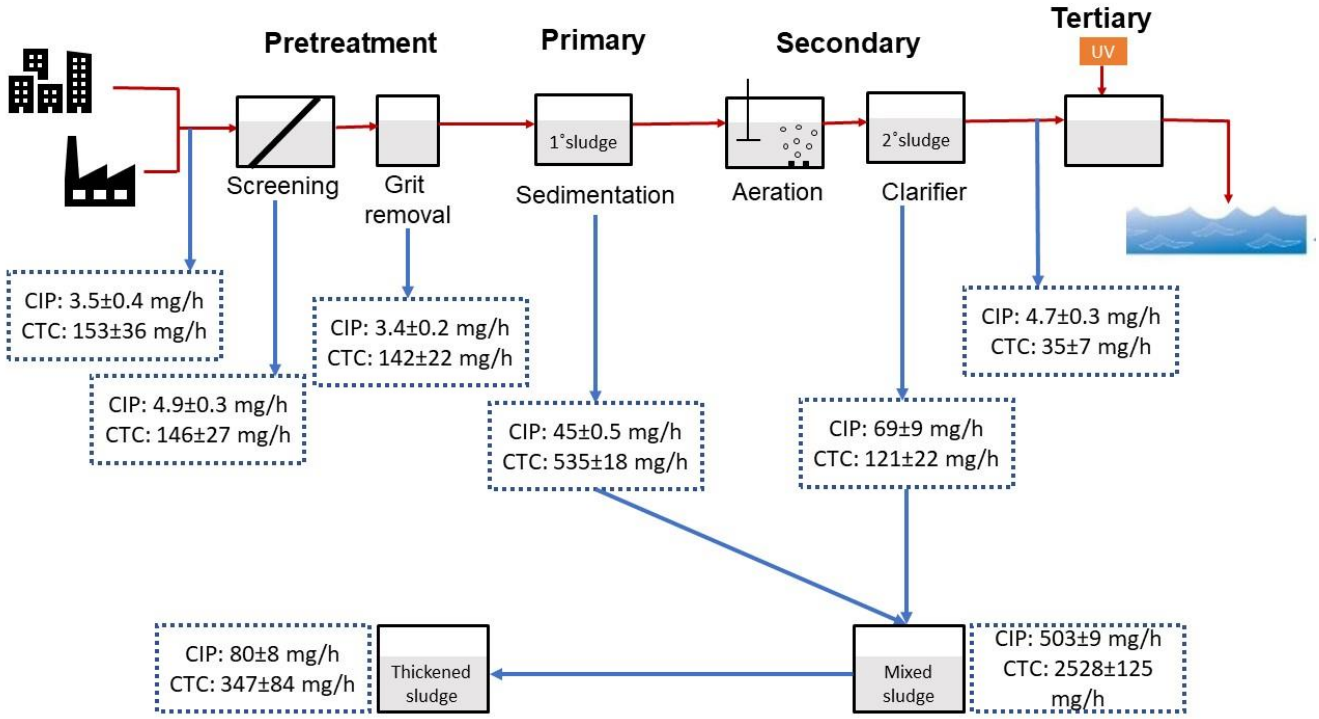

Figure 3.1. 1.Mass distribution of ciprofloxacin (CIP) and CTC (chlortetracycline) in the wastewater treatment plant in Quebec, Canada

Metals distribution in WWTP

The concentration of elements found in WWTP is presented in Table 3.1.3. Alkali earth metals were the most abundant metals in wastewater and sludge. For instance, Mg ranged between 4.9 – 51.3 mg/L in wastewater and 9692 – 12881 mg/kg in sludge, when Na varied from 1376 to 4216 mg/kg in sludge and between 44.0 – 76.3 mg/L in wastewater. Furthermore, most detected metals preferably bound to solid parts of the sludge. Mn, Mo, Sc, Se, Ti, and Zr were below limit of detection in wastewater. Cu, Cr, and Fe were present in the influent, however in further WWTP compartments, they were not detected. Their high concentration in sludge (Cu 649-1607 mg/kg, Cr 204-1292 mg/kg, Fe 52209-109604 mg/kg) suggests that they were completely removed from the wastewater via adsorption onto sludge. The concentrations of most of the heavy metal ions in sludge were below the recommended standards for Québec province and their level in both primary and secondary sludge did not vary except for Cr, Cu, Co and Zn ions [26].

Table 3.1. 3 Metals concentration (after partial digestion) in wastewater and wastewater sludge; ND – not detected

Element	Concentration in samples (mg/kg or mg/L)											
	Primary sludge (solid)	Secondary sludge (solid)	Mixed sludge (solid)	Thickened sludge (solid)	Influent	Effluent	Grit unit	Screen unit	Primary sludge (liquid)	Secondar sludge (liquid)	Mixed sludge (liquid)	Thickened sludge (liquid)
As	7.53±5.13	21.28±2.32	3.60±2.70	3.44±1.40	0.64±0.19	0.20±0.02	0.35±0.12	0.29±0.21	0.28±0.057	0.16±0.002	0.33±0.13	0.29±0.02
Ba	1329.28±5.77	1560.65±3.2	311.31±0.26	850.68±1.33	0.05±0.002	0.11±0.014	0.002±0.005	0.01±0.0007	ND	ND	ND	0.08±0.01
Ca	77177.80±30394	78922.70±1622	63678.40±10414	89191.90±3697	47.82±2.21	44.50±0.91	45.12±2.25	51.21±1.33	39.80±0.66	54.19±2.00	40.18±1.24	452.75±1.64
Cd	7.014±2.35	8.11±2.17	4.67±1.09	6.07±1.27	0.06±0.006	0.06±0.004	0.07±0.011	0.06±0.0008	0.07±0.007	0.06±0.002	0.06±0.002	0.07±0.007
Co	ND	17.31±3.41	8.27±9.04	16.60±7.04	0.40±0.007	0.22±0.04	0.22±0.03	0.23±0.01	0.22±0.03	0.26±0.04	0.32±0.04	0.20±0.03
Cr	674.97±1.90	811.13±9.05	204.41±3.44	1292.13±3.89	0.34±0.12	ND	ND	ND	ND	ND	ND	ND

Element	Concentration in samples (mg/kg or mg/L)											
	Primary sludge (solid)	Secondary sludge (solid)	Mixed sludge (solid)	Thickened sludge (solid)	Influent	Effluent	Grit unit	Screen unit	Primary sludge (liquid)	Secondar sludge (liquid)	Mixed sludge (liquid)	Thickened sludge (liquid)
Cu	888.40±0.46	1607.33±4.03	649.84±1.56	1058.26±3.37	0.26±0.02	ND	ND	ND	ND	ND	ND	ND
Fe	96091.40±130	109604.00±331	52209±16.33	66264.70±331	0.57±0.06	ND	ND	ND	12.22±1.52	16.42±0.55	ND	342.57±3.86
K	13055.60±15.25	8393.00±109	5476.73±53.96	6006.70±91.39	15.96±0.02	14.97±0.3	15.72±0.06	15.49±0.3	24.38±0.16	32.70±0.41	23.05±0.16	107.99±0.04
Mg	12881.00±158	11731.70±53.01	9692.99±83.59	9991.22±87.53	5.60±0.15	5.17±0.08	5.22±0.14	5.63±0.008	4.90±0.08	8.07±0.3	6.50±0.2	51.27±0.23
Mn	966.34±6.61	940.90±7.13	600.77±8.94	695.81±4.43	ND	ND	ND	ND	ND	ND	ND	3.92±0.004
Mo	26.24±3.52	20.15±1.67	11.08±1.40	10.88±1.60	ND	ND	ND	ND±0.1	0.05±0.03	ND	0.09±0.06	ND

Element	Concentration in samples (mg/kg or mg/L)											
	Primary sludge (solid)	Secondary sludge (solid)	Mixed sludge (solid)	Thickened sludge (solid)	Influent	Effluent	Grit unit	Screen unit	Primary sludge (liquid)	Secondar sludge (liquid)	Mixed sludge (liquid)	Thickened sludge (liquid)
Na	4216.34±113.69	4111.38±75.38	1376.56±10.34	2523.13±27.64	75.03±0.4	76.34±0.63	73.76±0.2	73.40±0.02	44.01±0.2	79.14±1	72.60±1.3	70.87±0.08
P	88196.00±355	99244.40±600	44079.40±133.45	50431.80±496	5.48±0.3	1.00±0.03	3.45±0.03	4.06±0.12	4.77±0.5	24.58±0.5	12.96±0.14	15.42±0.7
Pb	111.60±77.06	106.83±69.46	113.94±43.77	158.34±42.86	0.35±0.02	ND	0.21±0.2	0.15±0.03	ND	ND3.44±0.11	ND	0.39±0.01
S	10924.80±28.2	5855.96±169.83	5834.03±80.64	6941.54±109.99	17.94±0.7	17.54±0.09	16.01±0.07	18.60±0.04	1.46±0.2	0.81±0.04	3.38±0.7	10.43±0.005
Sb	18.28±8.59	14.00±1.45	5.46±0.98	11.97±7.12	1.00±0.08	0.91±0.04	0.91±0.18	0.90±0.05	0.93±0.06	ND	0.90±0.006	1.04±0.15
Sc	11.80±0.099	10.28±0.33	11.45±1.62	14.12±0.28	ND	ND	ND	ND	ND	ND	ND	ND
Se	18.66±3.86	23.04±3.01	7.81±0.51	51.70±17.62	ND	ND	0.24±0.006	ND	ND	2.75±0.4	0.94±0.2	ND

Element	Concentration in samples (mg/kg or mg/L)											
	Primary sludge (solid)	Secondary sludge (solid)	Mixed sludge (solid)	Thickened sludge (solid)	Influent	Effluent	Grit unit	Screen unit	Primary sludge (liquid)	Secondar sludge (liquid)	Mixed sludge (liquid)	Thickened sludge (liquid)
Si	1990.98±10.26	1106.56±10.01	1007.75±0.23	1355.79±5.68	2.70±0.24	2.02±0.26	1.42±0.12	2.52±0.13	0.80±0.3	ND	1.36±0.2	23.17±1.04
Sr	757.74±13.90	915.01±23.31	512.49±10.33	672.97±5.20	0.54±0.002	0.52±0.01	0.51±0.007	0.55±0.003	0.40±0.01	0.58±0.03	ND	ND
Ti	562.47±11.41	391.23±6.64	622.12±0..0025	593.50±0.47	ND	ND	ND	ND	ND	ND	0.50±0.08	3.19
Tl	2.39	7.06±6.37	1.35±0.55	3.72±3.07	0.72±0.4	ND	ND	0.52±0.3	1.04±0.7	ND	ND	ND
Zn	2067.00±25.56	1949.18±33.97	1613.99±14.75	1852.96±26.33	0.36±0.1	0.23±0.05	0.3±0.0090	0.30±0.007	0.48±0.2	0.20±0.1	0.28±0.03	0.35±0.07
Zr	0.55±0.65	3.51±1.35	3.98±0.52	1.32±0.37	ND	ND	ND	ND	ND	ND	ND	ND

The high concentration of Mg and Ca in solid parts of sludge is responsible for the higher concentration of CTC in sludge as both metals have the highest chelating affinity towards CTC compared with other metals [27]. The presence of Al and Fe in sludge (solid part) lead to CIP binding to the same environment, as CIP forms the most stable complexes with trivalent metals, even when both are in the forms of oxides [28, 29]. Moreover, CTC and CIP exhibit high affinity towards the transition metals [8, 28]. Hence, to further investigate the potential co-dependence between metals and antibiotics concentration in sludge via chemical speciation, the certain metals, i.e. Al, Ca, Co, Cr, Cu, Fe, Mg, Pb, Zn and one metalloid, As, were selected based on their potential toxicity and potency to form a complex with targeted antibiotics.

Chemical speciation of targeted metals and antibiotics

Figure 3.1.2 presents distribution of the selected metals in four types of sludge in WWTP, showing speciation between the four fractions. In an exchangeable fraction, the cation can be weakly adsorbed and released by an ion-exchange process [13, 14, 30]. In primary and secondary sludge there isthe highest abundance of this fraction. As and Mg were present at >68% and >97% respectively. Moreover, the high level of Co (44-46%) and Pb (38-50%) was also weakly bound to both types of sludge. The small percentage of Ca (7-11%) and Zn (1-4%) was also weakly adsorbed to onto both types of sludges.

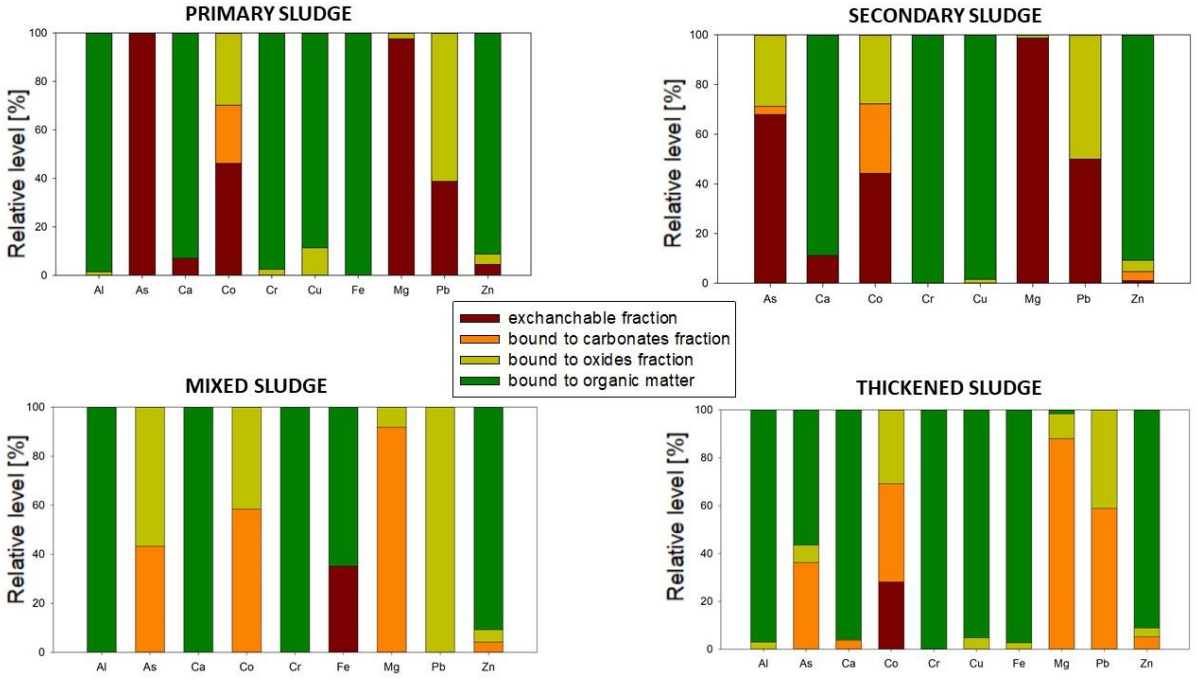

Figure 3.1. 2 Metals distribution in wastewater sludges

In bound-to-carbonates fraction, metals that are bound to organic matter, mineral particles or living organisms are released due to the oxidation and degradation of these substances [13, 14, 30], whereas in the fraction called bond-to-oxides, iron (III) and manganese (IV) oxides are capable of binding to various metals [13, 14, 30]. On the other hand, the reducing conditions during digestion resulted in releasing these metals from oxides [13, 14, 30]. Ae high concentration of Pb was found in bound-to-

oxides fraction in all sludges (primary 61.2%, secondary 50%, mixed 100%, thickened 41.2%). Only in thickened sludge, Pb level inbound-to-carbonate fraction (58.8%) was higher than to the oxides. Around 91.8% and 88.0% of Mg was detected to bound-to-carbonates fraction in mixed and thickened sludge respectively. Zn level in secondary, mixed and thickened sludge remained constant; around 5% and 4% of Zn was bound-to-carbonates and oxides respectively.

In bound-to-organics fraction, the metals complexed by the organic matter are released due to strong oxidative conditions [30]. Al, Fe, Ca, Cr, Cu, and Zn was mostly accumulated in this fraction (>88%). Thus, they were not easily accessible and probably did not affect CTC and CIP mobility during WWTP [31].

Overall, in agreement with previous studies, in primary and secondary sludge, the highest fractions of exchangeable and bound-to-carbonates are observed [32]. However, it can be observed that in thickened sludge most of the detected metals were present in bound to the organic fraction. The metals concentration was proportional to the material condensation.

Metals and antibiotics correlation

Each fraction from chemical speciation was tested for presence of CTC/CIP. Figure 3.1.3 presents the concentration of targeted antibiotics in different sludge fractions. The results from bound-to-organics fraction are not included, as the treatment was too harsh for the antibiotics. In primary sludge, the highest level of antibiotics was detected in the exchangeable fraction. The relative level of antibiotics and metals in secondary sludge (Fig. 3.1.3) differed from primary sludge. CIP concentration was still the highest in exchangeable fraction, however, CTC was equally distributed in all three fractions. In mixed (Fig. 3.1.3) and thickened sludge (Fig. 3.1.3), antibiotics are distributed in a similar way as it was observed in the primary sludge.

CTC and CIP predominantly exist as a zwitterion in the range of pH of tested wastewater (Table 3.1.1), hence they were able to form metal complexes in tested matrix [2, 8]. Main metal complexation sites of CTC including β-diketone system along with enol and carboxamide may factorize into the chelating potential of targeted metals [8]. In the case of CIP, the metals are usually chelated via two oxygens in the carboxyl and carboxylic group, a negatively charged moiety [2].

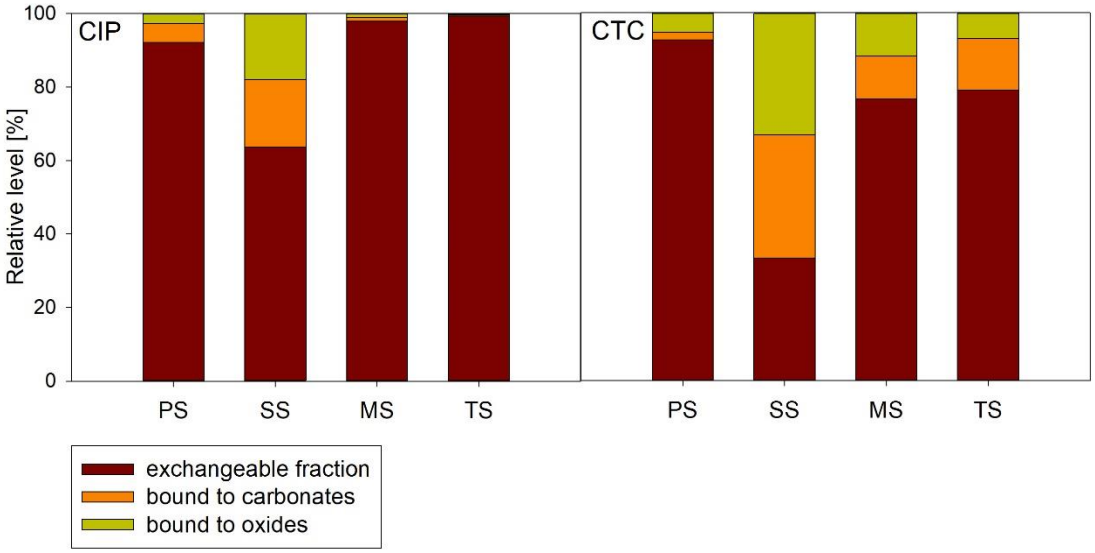

Figure 3.1. 3 Antibiotics distribution in waster sludges; PS – primary sludge; SS – secondary sludge; MS – mixed sludge; TS – thickened sludge; CTC – chlortetracycline; CIP - ciprofloxacin

To examine if there is any interdependence between metals and changes in antibiotic concentration in each chemical fraction, the Pearson correlation was applied. A positive correlation coefficient and *p*-value < 0.05 corresponds to positive correlation, i.e. when one variable increases (metal concentration), then the second variable tends to increase with it (antibiotic concentration). When the correlation coefficient is negative and *p*-value < 0.05, it corresponds to negative correlation, i.e. when one variable decreases (metal concentration), the other increases (antibiotic concentration). When *p*-value > 0.05, there is no significant correlation between the two variables.

Table 3.1.4 presents the results of statistical analysis. It can be seen that in primary sludge there is a positive correlation between both antibiotics and As, and Mg concentration. The highest concentration of these pollutants was in exchangeable fraction (fig.3.1.2-3). Thus, the metal-antibiotic complexes may be formed with metals weakly adsorbed onto sludge via cation exchange mechanism. In the secondary sludge, CIP concentration was positively correlated with Mg and Co, while CTC did not interdepend with any targeted metals. With the addition to different speciation of CTC in secondary sludge (Figure 3.1.3), one may assume that CTC is involved in other types of interactions during secondary treatment compared to the primary treatment.

There was no correlation found in mixed and thickened sludge, where metals were mostly distributed in bound-to-carbonates and oxides fraction. Hence, the accumulation of antibiotics in these fractions was probably due to the mixing of two types of sludge (primary and secondary) and not metal interaction. Alternative explanation here is the involvement of antibiotics' functional groups in the interaction with functional groups of natural organic matter, i.e. humic or fulvic acid [9, 33]. Overall, this may suggest that the key interdependence between CTC/CIP and metals bound mostly to exchangeable fraction is observed during primary wastewater treatment.

Figure 3.1. 4 Pearson correlation between targeted metals and antibiotics in each type of sludge; top value corresponds to correlation coefficient, bottom value to p-value

PRIMARY SLUDGE										
	Al	As	Ca	Co	Cu	Cr	Fe	Mg	Pb	Zn
CIP	0.520 0.652	**1.000** **0.015**	- -	0.962 0.177	0.520 0.652	0.520 0.652	- -	**0.999** **0.028**	0.129 0.918	0.504 0.663
CTC	0.474 0.686	**1.000** **0.019**	- -	0.975 0.143	0.474 0.686	0.474 0.686	- -	**1.000** **0.006**	0.182 0.883	0.550 0.629
SECONDARY SLUDGE										
	Al	As	Ca	Co	Cu	Cr	Fe	Mg	Pb	Zn
CIP	-	0.919 0.258	- -	**1.000** **0.008**	0.503 0.665	-	-	**1.000** **0.009**	0.497 0.669	0.973 0.149
CTC	-	0.218 0.860	0.182 0.884	0.197 0.874	0.942 0.217	-	-	0.170 0.891	0.761 0.450	0.407 0.733
MIXED SLUDGE										
	Al	As	Ca	Co	Cu	Cr	Fe	Mg	Pb	Zn
CIP	-	0.973 0.147	-	0.960 0.180	-	-	1.000 0.000	0.568 0.615	0.500 0.667	0.987 0.102
CTC	-	0.973 0.147	-	0.960 0.180	-	-	1.000 0.000	0.568 0.615	0.500 0.667	0.987 0.102
THICKENED SLUDGE										
	Al	As	Ca	Co	Cu	Cr	Fe	Mg	Pb	Zn
CIP	0.499 0.667	0.656 0.545	0.602 0.589	0.662 0.540	0.499 0.667	0.499 0.667	0.499 0.667	0.591 0.598	0.957 0.188	0.958 0.185
CTC	0.574 0.611	0.586 0.601	0.528 0.646	0.592 0.596	0.574 0.611	0.574 0.611	0.574 0.611	0.517 0.654	0.927 0.245	0.929 0.242

Conclusion

The concentration of CTC in each of the WWTP compartments was much higher than CIP. Nevertheless, around 71% of CTC was removed during the WW treatment, resulting in its reduced concentration of 6.13±0.86 μg/L in final effluent. On the other hand, CIP tended to accumulate during treatment; the higher concentration of CIP in effluent (0.70 ± 0.05 μg/L) compared to influent (0.47±0.05 μg/L) suggests that CIP adsorbs and desorbs from sludge. Our study represents preliminary estimation of these antibiotics in different speciation during WW treatment, and the results suggest that

more precise examinations are necessary for new purification protocols. As the main removal method for both antibiotics is through sludge adsorption, an ion-exchange mechanism may explain the highest concentration of CTC (33-92%) and CIP (63-99 %) in exchangeable fraction. The positive correlation between CTC/CIP concentration and Mg and As was found in primary sludge. In addition, a high concentration of heavy metals in sludge is alarming (Cu 650 – 1607 mg/kg, Cr 204 – 1292 mg/kg or Pb 158 – 106 mg/kg), as their complexation with CTC and/or CIP leads to antibiotic accumulation in sludge, an inadvertent source of perennial presence of antibiotics in the environment with a perfect recipe for microbes to become resistant due to selective pressure on bacteria present in the WWT. Since the sludge can be potentially used as fertilizer and soils primed with bacteria loaded with resistant genes can transmit them to other bacteria through horizontal gene transfer. Additionally, it may lead to co-selection and co-dissemination of antibiotic resistance genes and heavy metal resistance genes with grave health-related consequences.

Acknowledgments

The authors are sincerely thankful to the Natural Sciences and Engineering Research Council of Canada (Discovery Grant 355254 and NSERC Strategic Grant). We would like to also thank Mr. Stephane Moise for his technical support with Liquid Chromatography analysis. We would like to thank Dr. Manjit Singh Rana for his critical readings and comments.

References

1. Larsson, D.J., *Antibiotics in the environment.* Upsala journal of medical sciences, 2014. **119**(2): p. 108-112.

2. Cuprys, A., et al., *Fluoroquinolones metal complexation and its environmental impacts.* Coordination Chemistry Reviews, 2018. **376**: p. 46-61.

3. Sharma, C., et al., *Antimicrobial Resistance: Its Surveillance, Impact, and Alternative Management Strategies in Dairy Animals.* Front Vet Sci, 2017. **4**: p. 237.

4. Barkovskii, A.L. and C. Bridges, *Persistence and Profiles of Tetracycline Resistance Genes in Swine Farms and Impact of Operational Practices on Their Occurrence in Farms' Vicinities.* Water, Air, & Soil Pollution, 2012. **223**(1): p. 49-62.

5. Miao, X.S., et al., *Occurrence of antimicrobials in the final effluents of wastewater treatment plants in Canada.* Environ Sci Technol, 2004. **38**(13): p. 3533-41.

6. Administration, U.S.F.a.D., *2016 Summary report on Antimicrobials Sold or Distributed for Use in Food-Producing Animals*. 2017, U.S. Food and Drug Administration: Center for veterinary medicine.

7. Canada, P.H.A.o., *Canadian Antimicrobial Resistance Surveillance System 2017 Report*. 2017, Public Health Agency of Canada.

8. Pulicharla, R., et al., *Tetracyclines metal complexation: Significance and fate of mutual existence in the environment.* Environmental Pollution, 2017. **221**: p. 1-14.

9. Puicharla, R., et al., *A persistent antibiotic partitioning and co-relation with metals in wastewater treatment plant—Chlortetracycline.* Journal of Environmental Chemical Engineering, 2014. **2**(3): p. 1596-1603.

10. Wei, B. and L. Yang, *A review of heavy metal contaminations in urban soils, urban road dusts and agricultural soils from China.* Microchemical Journal, 2010. **94**(2): p. 99-107.

11. Rajaganapathy, V., et al., *Heavy metal contamination in soil, water and fodder and their presence in livestock and products: a review*. Journal of Environmental Science and Technology, 2011. **4**(3): p. 234-249.

12. Apha, A., *WEF, 2005.* Standard methods for the examination of water and wastewater, 2005. **21**: p. 258-259.

13. Dong, B., et al., *Changes of heavy metal speciation during high-solid anaerobic digestion of sewage sludge.* Bioresour Technol, 2013. **131**: p. 152-8.

14. Ashraf, M., M. Maah, and I. Yusoff, *Chemical speciation and potential mobility of heavy metals in the soil of former tin mining catchment.* The Scientific World Journal, 2012. **2012**.

15. Gaugain, M., et al., *6-Iso-chlortetracycline or keto form of chlortetracycline? Need for clarification for relevant monitoring of chlortetracycline residues in food.* Food Additives & Contaminants: Part A, 2015. **32**(7): p. 1105-1115.

16. Archana, G., R. Dhodapkar, and A. Kumar, *Offline solid-phase extraction for preconcentration of pharmaceuticals and personal care products in environmental water and their simultaneous determination using the reversed phase high-performance liquid chromatography method.* Environmental Monitoring and Assessment, 2016. **188**(9): p. 512.

17. Canada, P.H.A.o., *CANADIAN ANTIMICROBIAL RESISTANCE SURVEILLANCE SYSTEM UPDATE 2018*. 2018, Public Health Agency of Canada.

18. Lee, H.B., T.E. Peart, and M.L. Svoboda, *Determination of ofloxacin, norfloxacin, and ciprofloxacin in sewage by selective solid-phase extraction, liquid chromatography with fluorescence detection, and liquid chromatography--tandem mass spectrometry.* J Chromatogr A, 2007. **1139**(1): p. 45-52.

19. He, K., et al., *Detection of a wide variety of human and veterinary fluoroquinolone antibiotics in municipal wastewater and wastewater-impacted surface water.* J Pharm Biomed Anal, 2015. **106**: p. 136-43.

20. Jia, A., et al., *Occurrence and fate of quinolone and fluoroquinolone antibiotics in a municipal sewage treatment plant.* Water Res, 2012. **46**(2): p. 387-94.

21. Li, B. and T. Zhang, *Biodegradation and adsorption of antibiotics in the activated sludge process.* Environ Sci Technol, 2010. **44**(9): p. 3468-73.

22. Van Doorslaer, X., et al., *Fluoroquinolone antibiotics: an emerging class of environmental micropollutants.* Sci Total Environ, 2014. **500-501**: p. 250-69.

23. Amarakoon, I.D., et al., *Runoff Losses of Excreted Chlortetracycline, Sulfamethazine, and Tylosin from Surface-Applied and Soil-Incorporated Beef Cattle Feedlot Manure.* Journal of Environmental Quality, 2014. **43**(2): p. 549-557.

24. Li, N., et al., *Occurrence, seasonal variation and risk assessment of antibiotics in the reservoirs in North China.* Chemosphere, 2014. **111**: p. 327-335.

25. Suresh, G., et al., *Alternatives to antibiotics in poultry feed: molecular perspectives.* Critical Reviews in Microbiology, 2018. **44**(3): p. 318-335.

26. *A Review of the Current Canadian Legislative Framework for Wastewater Biosolids*. 2010, Canadian Council of Ministers of the Environment.

27. Pulicharla, R., et al., *Toxicity of chlortetracycline and its metal complexes to model microorganisms in wastewater sludge.* Sci Total Environ, 2015. **532**: p. 669-75.

28. Urbaniak, B. and Z.J. Kokot, *Analysis of the factors that significantly influence the stability of fluoroquinolone-metal complexes.* Anal Chim Acta, 2009. **647**(1): p. 54-9.

29. Gu, C. and K.G. Karthikeyan, *Sorption of the antimicrobial ciprofloxacin to aluminum and iron hydrous oxides.* Environ Sci Technol, 2005. **39**(23): p. 9166-73.

30. Fuentes, A., et al., *Phytotoxicity and heavy metals speciation of stabilised sewage sludges.* Journal of Hazardous Materials, 2004. **108**(3): p. 161-169.

31. Liang, X., et al., *Concentrations and speciation of heavy metals in sludge from nine textile dyeing plants.* Ecotoxicology and Environmental Safety, 2013. **98**: p. 128-134.

32. Álvarez, E.A., et al., *Heavy metal extractable forms in sludge from wastewater treatment plants.* Chemosphere, 2002. **47**(7): p. 765-775.

33. Cuprys, A., et al., *Ciprofloxacin-metal complexes -stability and toxicity tests in the presence of humic substances.* Chemosphere, 2018. **202**: p. 549-559.

PART 2

Appearance of ciprofloxacin/chlortetracycline-resistant bacteria in waters of Québec City in Canada

Agnieszka Cuprys[a], Joanna Lecka[a], François Proulx[b], Satinder K. Brar[a,c*], Patrick Drogui[a]

[a] INRS-ETE, Université du Québec, 490, Rue de la Couronne, Québec City, QC., Canada G1K 9A9

[b] Ville de Québec, Service du traitement de l'eau, 214 avenue Saint-Sacrement, Québec City, QC., Canada G1N 3X6

[c] Department of Civil Engineering, Lassonde School of Engineering , York University, North York, Toronto, Ontario Canada M3J 1P3

* Corresponding author: Satinder.Brar@lassonde.yorku.ca, satinder.brar@ete.inrs.ca

Journal of Infection and Public Health, 12, Issue 6, 897-899(2019)

Résumé

La plupart des agents pathogènes fécaux d'origine hydrique appartiennent à la famille des bactéries à Gram négatif. Ainsi, on a estimé les concentrations inhibitrices minimales de la chlorotétracycline et de la ciprofloxacine envers *Enterobacter aerogenes*, représentant de Gram négatif, qui étaient respectivement de 7 µg/mL et 0,125 µg/mL. L'effet antimicrobien combiné de la chlorotétracycline et de la ciprofloxacine contre *E. aerogenes* a également été étudié pour établir leur interaction potentielle avec les agents pathogènes présents dans l'eau. Finalement, des échantillons d'eau provenant de diverses usines de traitement de l'eau potable de la municipalité de Québec ont été testés pour détecter l'apparition de souches résistantes à la chlorotétracycline, à la ciprofloxacine et à la chlorotétracycline/ciprofloxacine.

Mots-clés: résistance aux antibiotiques, eau, ciprofloxacine, chlorotétracycline

Abstract

Most of the waterborne fecal pathogens belong to the family of Gram-negative bacteria. Hence, minimal inhibitory concentrations of chlortetracycline and ciprofloxacin antibiotics towards Gram-negative representative, *Enterobacter aerogenes* were estimated, which were 7 μg/ml and 0.125 μg/ml, respectively. The combined antimicrobial effect of chlortetracycline and ciprofloxacin against *E. aerogenes* was also investigated to establish their potential interaction towards the pathogens present in water. Eventually, the water samples obtained from various drinking water treatment plants from Québec municipality were tested for the occurrence of chlortetracycline-, ciprofloxacin- and chlortetracycline/ciprofloxacin-resistant strains.

Keywords: antibiotic resistance, water, ciprofloxacin, chlortetracycline

Introduction

Waterborne fecal pathogens usually belong to Enterobacteriaceae family that cause gastrointestinal illnesses. Between 1974-2001, *Shigella* and *Salmonella* caused around 56% drinking water outbreaks in Canada [1]. At the same time, the *Campylobacter* waterborne outbreak was ranked as a second causative agent (24 outbreaks), following *Giardia* (51 outbreaks) [1]. These bacterial infections can be treated with antibiotics. However, their frequent usage has resulted in their high concentration in various environmental compartments, which has led to selective pressure and the occurrence of antibiotic-resistant bacteria [2].

The goal of this study was to investigate the combined antimicrobial activity of two widely used antibiotics, chlortetracycline (CTC) and ciprofloxacin (CIP), towards Gram-negative representative bacteria - *Enterobacter aerogenes*. The objective of this work was to investigate the appearance of CTC-resistant, CIP-resistant and CIP-CTC-resistant strains in the water compartments from different areas of the Québec City. The presence of three pathogenic bacteria that were potential resistant-gained species, *Campylobacter* sp., *Shigella* sp. and *Salmonella* sp. was investigated.

Methodology

Minimal inhibitory concentration

Minimal inhibitory concentration (MIC) was defined as the minimal concentration of antimicrobial agent, which exerts the visible inhibition of bacterial growth.. *E. aerogenes* (NRRL B-407) growth and MIC estimation were conducted as described previously [3].

Time-kill method

Time-kill method was used to determine the killing rate of bacteria by antimicrobial agents. The procedure was carried out by broth microdilution technique, as described in the National Committee for Clinical Laboratory Standards guidelines [4]. *E. aerogenes* was examined against CTC, CIP alone and in their combinations (1/4MIC and 2MIC). The pairwise t-test ($p>0.05$) was performed via SigmaPlot 12.3 to determine significant differences in the effectiveness of different antibiotic mixtures based on triplicate measurements.

Water samples and bacteria isolation

The sampling was done in November 2017. Water samples were obtained from upstream of the Drinking Water Treatment Plant (UTE) of Québec (UTE Québec), UTE Ste-Foy, UTE Charlesbourg and Desîlets. The treated water samples (UTE's downstream) were obtained from UTE Ste-Foy, UTE Québec, and UTE Charlesbourg. All samples were collected into the ethanol-washed containers after rinsing them twice with appropriate sample water. After transporting the samples to the laboratory on the same day, they were kept in dark at 4±1˚C.

Water samples were inoculated (1% v/v) in 3% w/v Tryptic Soy Broth (TSB) in triplicates to enrich present bacterial culture (48-72 h, 42±1˚C). Subsequently, they were plated onto solid media, with (CIP, CTC, CIP+CTC) and without antibiotics. Obtained colonies were harvested, DNA was isolated and polymerase chain reaction (PCR) was performed to confirm if the bacteria belonged to *Shigella sp.*, *Salmonella sp.*, or *Campylobacter jejuni*.

DNA extraction

The tubes containing colonies were centrifuged for 2 minutes at 10,000 x g. The pellet was resuspended in STE buffer (STE buffer; 10 mM Tris-HCl pH 8.0, 1 mM EDTA, 100 mM NaCl) followed by DNA extraction as described by Czekalski et al. with some changes [5]. 10% (v/v) of 10% SDS was added dropwise and the tubes were placed in a boiling water bath for 1.5-2 min. Cellular debris was pelleted by centrifugation (10 min, 10,000 x g) at 10-15˚C. The supernatant was transferred to a clean, sterile tube for DNA isolation by phenol/chloroform extraction followed by isopropanol precipitation. DNA was pelleted by centrifugation (25 min, 4˚C, 14,000 x g), washed with ice-cold 70% ethanol and left to air dry. Final pellet was resuspended in TE buffer (10 mM Tris, pH 8.0, 1 mM EDTA) and stored at -20±1˚C.

PCR amplification

The isolated DNA from previous section was used for PCR amplification. The targeted genes were the invasion plasmid antigen H of *Shigella* sp. (*IpaH*), invasion plasmid antigen B of *Salomnella* sp. (*IpaB*) and the oligonucleotide sequence which was specific towards *C. jejuni* (*Cj*). The specific information about the oligonucleotide primers of targeted sequences were obtained from the literature [6, 7] and their thermal profiles of PCR are presented in Table 3.2.1. The primers were synthesized by Invitrogen Life Sciences, Canada. The reaction mixture of final volume 10 µL included 1 X PCR buffer (10 mM Tris hydrochloride pH 8.3, 50 mM KCl and 1.5 mM $MgCl_2$), 0.2 mM of each dNTP, 0.11 mM of IpaB or Cj or 0.1 mM of IpaH of the PCR primers, 1.25 U Taq polymerase (Qiagen) and 2.5 µL of DNA. Negative control reaction mixtures contained sterile deionized water in place of template DNA. Obtained PCR products were analyzed by gel electrophoresis in 1% agarose for IpaH and IpaB and 3% agarose for Cj (Fisher Scientific) containing 1 µg/ml ethidium bromide in TAE buffer (40 mM Tris-HCl, 20 mM acetic acid, 1 mM EDTA, pH 8). UVP Benchtop UV Transilluminators: 3UV was used to visualize DNA bands. To confirm the presence of IpaB protein *Salmonella bongori* ATCC43975 was used as the positive control.

Table 3.2. 1 The primer details and thermal profiles of PCR-amplified gene targets of three types of pathogenic bacteria

Primer	Sequence 5'-3'	Targeted gene/organism	Expected product size [bp]	Thermal profile of PCR	Ref.
Cj-F **Cj-R**	CTGAATTTGATACCTTAAGTGCAGC AGGCACGCCTAAACCTATAGCT	*Campylobacter jejuni*	86	heat denaturation at 95˚C, 10 min 40 cycles: heat denaturation 95˚C, 20 sec, primer annealing 60˚C ,1 min DNA extension 72˚C, 2 min. Incubation, 72˚C, 10 min cooling 4˚C.	[7]
IpaH-F **IpaH-R**	CCTTGACCGCCTTTCCGATA CAGCCACCCTCTGAGGTACT	Invasion plasmid antigen H-*Shigella* sp.	606	heat denaturation at 94˚C, 2 min 40 cycles: heat denaturation 94˚C, 1 min, primer annealing 62˚C, 1 min DNA extension 72˚C, 2.5 min. Incubation, 72˚C, 10 min cooling 4˚C.	[6]
IpaB-F **IpsaB-R**	GGACTTTTTAAAAGCGGCGG GCCTCTCCCAGAGCCGTCTGG	Invasion plasmid antigen B-*Salmonella* sp	314		

Results and discussion

To understand the possible repercussions of the presence of CTC/CIP in water, the combined antimicrobial activity tests were conducted. Obtained MIC values for Gram-negative representative, *E. aerogenes* were 0.125 and 7 μg/mL for CIP and CTC, respectively. Figure 3.2.1 shows the antimicrobial activity of both antibiotics alone and in combination. $1/4MIC_{CIP}$ was able to eliminate all the cells in less than 6 hours. *E. aerogenes* growth at $1/4MIC_{CTC}$ was significantly slower than the control. The addition of CIP resulted in enhanced antimicrobial efficiency of CTC compared to $1/4MIC_{CTC}$, with hindering the activity of CIP ($1/4MIC_{CIP}$). The increase of CTC concentration ($1/4MIC_{CIP}+2MIC_{CTC}$) resulted in similar killing-rate as $2MIC_{CTC}$. Hence, CIP and CTC interact in an antagonistic way.

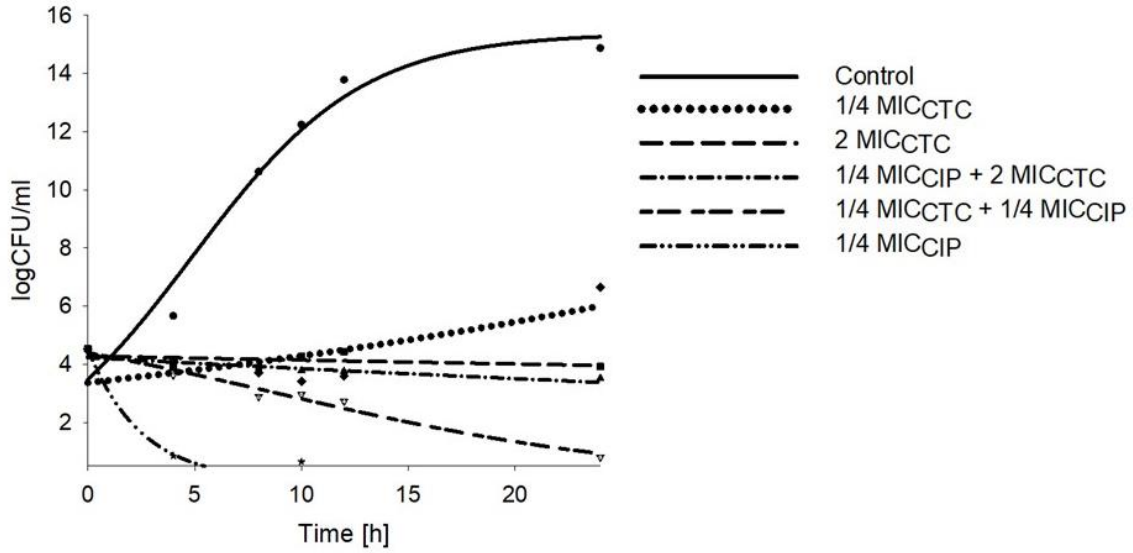

Figure 3.2. 1 Time-kill curves of ciprofloxacin (CIP) and chlortetracycline (CTC) at different concentration combinations against Gram-negative Enterobacter aerogenes. The curves representing $2MIC_{CIP}+2MIC_{CTC}$, $2MIC_{CIP}$, $2MIC_{CIP}+1/4MIC_{CTC}$ are not shown due to high killing-rate of the solutions (all bacteria killed within 4 first hours); graphs represent the trend for a mean of the triplicate experiment.; MIC -minimal inhibitory concentration

Generally, there is a suppressive antibiotic interaction between inhibitors of DNA (CIP) and protein (CTC) synthesis, which applies in our case [8]. The bacterial cells can grow, even under the DNA stress, due to the regulation of ribosomal genes. Other studies confirm this interaction [8, 9]. However, the antagonism between norfloxacin (fluoroquinolone) and tetracycline changed into synergy towards green alga at their higher concentration [10]. Thais would suggest that the antagonistic effect depends on the concentration and the targeted organism.

Qualitative detection of bacteria in water samples

Figure 3.2.2 A presents the detection of bacteria with possible resistant genes in water samples from Québec City municipality. The bacterial growth was observed in all seven sampling sites. The isolates from upstream samples of UTE Charlesbourg and Ste-Foy grew when CTC was present, suggesting the presence of potential CTC-resistant bacteria. The raw water from UTE Ste-Foy also contained bacteria that grew in the presence of CIP and CTC+CIP. This suggests the presence of CIP-resistant or even multi-resistant strains. The inherence of bacteria not affected by both antibiotics is also possible. In the Charlesbourg samples, PCR confirmed the presence band corresponding to *IpaB* gene, specific for *Salmonella* sp. (Fig.3.2.2 B). The other targeted pathogens were not detected. However, obtained results should be further validated by sequencing of extracted DNA.

A.

Media	RAW WATER				TREATED WATER		
	UTE Québec	UTE Charlesbourg	Desîlets	UTE Ste-Foy	UTE Québec	UTE Charlesbourg	UTE Ste-Foy
TSB/TBA	+	+	+	+	+	+	+
TSA+CTC	-	+	-	+	-	+	-
TSA+CIP	-	-	-	+	-	-	-
TSA+CTC+CIP	-	-	-	+	-	-	-

TSB: Tryptic soya broth; TSA: Tryptic soya agar; CTC: chlortetracycline; CIP: ciprofloxacin; UTE: drinking water treatment plant

B.

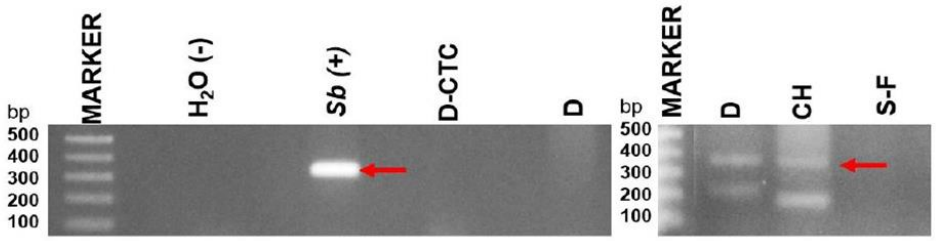

Figure 3.2. 2 A. The presence of bacteria from water samples; B. The 1% agarose gel electrophoresis of PCR products for detection of *Salmonella* sp.; Abbreviation of DNA samples: H2O (-) –negative control; Sb (+) –positive control (*Salmonella bongori*); D-CTC –colonies with potential chlortetracycline-resistance from raw water from Desilets; D – colonies from raw water from Desilets; CH –colonies from raw water from Charlesbourg Drinking Water Treatment Plant; S-F -colonies from raw water from Sainte-Foy Drinking Water Treatment Plant

According to the latest Canadian Antimicrobial Resistance Surveillance System (2017), the usage of antibiotics in Canada remained relatively stable over the last 10 years [11]. However, CIP was ranked as the most commonly purchased antibiotic for human medicine in Canada between 2010-2016. The usage of veterinary antibiotics, like CTC, follows decreasing trend in Canada due to concern regarding development of antimicrobial resistance [11]. However, pathogens may attain the antibiotic resistance from other bacteria, thus the presence of bacteria resistant to CIP/CTC was a concern [12]. The occurrence of CIP-resistant *Salmonella* strains in Canada has significantly increased from 0% (2003) to 14% (2014) [11]. *Campylobacter* sp. isolates were resistant to tetracycline (44-78%) and CIP (11%) in 2014 [11]. Moreover, CTC concentration (7-62 µg/L) is much higher than CIP (<0.7 µg/L) in Canadians waters [13, 14]. Thus, one can suspect that in the aquatic environment, the possible scenario would be the antagonistic interaction of $2MIC_{CTC}+1/4MIC_{CIP}$. This may lead to selective pressure from antimicrobials leading to bacterial mutation and antibiotic resistance. The occurrence of tetracycline-resistant genes is linked with a high concentration of tetracyclines in the environment, while fluoroquinolone resistance genes exhibited negative correlation [2]. Hence, this would explain the relatively high frequency of CTC-resistant bacteria presented in this study. Another study showed that antagonism between CTC and CIP may suppress the evolution of resistance [15].

Conclusion

Even though the pathogens were detected only in one water source, the presence of potentially resistant bacteria in the Quebec area is alarming. The time-kill studies showed the antagonistic relationship between CIP and CTC. Based on previous studies, such interaction may hinder the evolution of

antibiotic-resistant strains. In fact, during the monitoring of drinking water, sanitary quality and improvement of the water plant are important and as well, the efficiency of antimicrobials removal should be the priority.

Acknowledgments

The authors are sincerely thankful to the Natural Sciences and Engineering Research Council of Canada (Discovery Grant 355254 and NSERC Strategic Grant). Our sincere thanks to the Division de la qualité de l'Eau, Ville de Quebec for their help in processing the water samples.

References

1. Schuster, C.J., et al., *Infectious disease outbreaks related to drinking water in Canada, 1974-2001.* Can J Public Health, 2005. **96**(4): p. 254-8.

2. Xu, J., et al., *Occurrence of antibiotics and antibiotic resistance genes in a sewage treatment plant and its effluent-receiving river.* Chemosphere, 2015. **119**: p. 1379-85.

3. Cuprys, A., et al., *Ciprofloxacin-metal complexes -stability and toxicity tests in the presence of humic substances.* Chemosphere, 2018. **202**: p. 549-559.

4. Standards, N.C.f.C.L., *Methods for determining bactericidal activity of antimicrobial agents: NCCLS document M26-P*. 1987, National Committee for Clinical Laboratory Standards, Villanova, Pa.

5. Czekalski, N., et al., *Does human activity impact the natural antibiotic resistance background? Abundance of antibiotic resistance genes in 21 Swiss lakes.* Environ Int, 2015. **81**: p. 45-55.

6. Kong, R.Y., et al., *Rapid detection of six types of bacterial pathogens in marine waters by multiplex PCR.* Water Res, 2002. **36**(11): p. 2802-12.

7. Nogva, H.K., et al., *Application of the 5'-nuclease PCR assay in evaluation and development of methods for quantitative detection of Campylobacter jejuni.* Appl Environ Microbiol, 2000. **66**(9): p. 4029-36.

8. Bollenbach, T., et al., *Nonoptimal microbial response to antibiotics underlies suppressive drug interactions.* Cell, 2009. **139**(4): p. 707-18.

9. Ocampo, P.S., et al., *Antagonism between bacteriostatic and bactericidal antibiotics is prevalent.* Antimicrobial agents and chemotherapy, 2014. **58**(8): p. 4573-4582.

10. González-Pleiter, M., et al., *Toxicity of five antibiotics and their mixtures towards photosynthetic aquatic organisms: Implications for environmental risk assessment.* Water Research, 2013. **47**(6): p. 2050-2064.

11. Canada, P.H.A.o., *Canadian Antimicrobial Resistance Surveillance System 2017 Report*. 2017, Public Health Agency of Canada.

12. Munita, J.M. and C.A. Arias, *Mechanisms of Antibiotic Resistance.* Microbiology spectrum, 2016. **4**(2): p. 10.1128/microbiolspec.VMBF-0016-2015.

13. Puicharla, R., et al., *A persistent antibiotic partitioning and co-relation with metals in wastewater treatment plant—Chlortetracycline.* Journal of Environmental Chemical Engineering, 2014. **2**(3): p. 1596-1603.

14. Lee, H.B., T.E. Peart, and M.L. Svoboda, *Determination of ofloxacin, norfloxacin, and ciprofloxacin in sewage by selective solid-phase extraction, liquid chromatography with fluorescence detection, and liquid chromatography--tandem mass spectrometry.* J Chromatogr A, 2007. **1139**(1): p. 45-52.

15. Chait, R., A. Craney, and R. Kishony, *Antibiotic interactions that select against resistance.* Nature, 2007. **446**(7136): p. 668-71.

CHAPTER IV: NOVEL METHODS OF CIPROFLOXACIN REMOVAL

PART 1

Ciprofloxacin removal via sequential electrooxidation and enzymatic oxidation

Agnieszka Cuprys [a], Paisley Thompson [a], Yassine Ourda [a], Gayatri Suresh [a], Tarek Roussi [a], Satinder Kaur Brar [a,b,*], Patrick Drogui [a], Rao Y. Surampalli[c]

[a] INRS-ETE, Université du Québec, 490, Rue de la Couronne, Québec, Canada G1K 9A9

[b] Department of Civil Engineering, Lassonde School of Engineering, York University, North York, Toronto, Ontario Canada M3J 1P3

[c] Department of Civil Engineering, University of Nebraska-Lincoln, N104 SEC PO Box

886105, Lincoln, NE 68588-6105, USA

[*] Corresponding author: E-mail: satinder.brar@ete.inrs.ca; Satinder.Brar@lassonde.yorku.ca

Submitted to *Journal of Hazardous Materials* (accepted)

Résumé

La contamination des compartiments de l'environnement par des antibiotiques est devenue un problème immense en raison de leur potentiel de sélection et de dissémination de la résistance aux antimicrobiens. La combinaison d'électro-oxydation et d'oxydation enzymatique a été testée pour évaluer la capacité du système à éliminer la ciprofloxacine (CIP), un antibiotique fluoroquinolone, de l'eau. Pour la partie électrochimique, deux anodes ont été étudiées, le diamant dopé au bore (BDD) et les oxydes de métaux mixtes (MMO), ainsi que trois densités de courant (4,42, 17,7and 35,4 A/cm^2). L'anode BDD à 356.4 A/cm^2 a montré l'efficacité d'extraction la plus élevée dans les temps les plus brefs (élimination> 90% en 6 min); ces paramètres ont donc été choisis pour des expériences ultérieures. Pour l'oxydation enzymatique, la laccase obtenue à partir de *Trametes versicolor* a été choisie. La Laccase seule n'a pas été en mesure de supprimer la CIP; par conséquent, l'influence des médiateurs redox a été étudiée. L'ajout de syringaldéhyde (SA) et d'acide 2,2'-azino-bis (3-éthylbenzothiazoline-6-sulfonique) (ABTS) a entraîné une transformation accrue de la CIP. Il restait environ 48,9 ± 4,0% des CIP après 4 heures de traitement lorsque la laccase à médiation SA était appliquée et 87,8 ± 6,6% dans le cas de la laccase à médiation ABTS. Ainsi, le système à médiation SA a été choisi pour des expériences ultérieures. Le couplage de l'oxydation enzymatique suivi de l'électro-oxydation a permis d'éliminer 73% de l'antibiotique. De plus, l'activité antimicrobienne a augmenté jusqu'à son efficacité initiale après le traitement. La combinaison d'une électro-oxydation suivie d'une oxydation enzymatique a conduit à une élimination de 97 à 99% de la CIP. De plus, il n'y avait pas d'activité antimicrobienne de la solution après le traitement. Les tests avec des eaux usées réelles ont confirmé la capacité du système à éliminer le CIP de la matrice complexe.

Mots-clés: ciprofloxacine, électro-oxydation, laccase, syringaldéhyde, eaux usées

Abstract

The contamination of environmental compartments with antibiotics has become an immense problem due to their potential for selection and dissemination of antimicrobial resistance. The combination of electrooxidation and enzymatic oxidation was tested to evaluate the potency of this system to remove ciprofloxacin (CIP), a fluoroquinolone antibiotic, from water. For the electrooxidation, two anodes were investigated, boron-doped diamond (BDD) and mixed metal oxides (MMO), with three current densities (4.42, 17.7and 35.4A/cm^2). BDD anode at 35.4 A/cm^2 exhibited the highest removal efficiency in the shortest time (>90% removal in 6 min). For the enzymatic oxidation, laccase obtained from *Trametes versicolor* was chosen. Laccase alone was not able to remove CIP; hence the influence of redox mediators was investigated. Addition of syringaldehyde (SA) and 2,2'-azino-bis(3-ethylbenzothiazoline-6-sulphonic acid) (ABTS) resulted in enhanced CIP transformation. About 48.9±4.0% of CIP remained after 4 hours of treatment when SA-mediated laccase was applied and 87.8±6.6% in the case of ABTS-mediated laccase. The coupling of enzymatic oxidation followed by electrooxidation led to 73% removal of the antibiotic. Additionally, the antimicrobial activity was not decreased. The combination of electrooxidation followed by enzymatic oxidation led to 97-99 % removal of CIP. Moreover, there was no antimicrobial activity of the solution after the treatment. The tests with real wastewater confirmed the efficacy of the system to remove CIP from the complex matrix.

Keywords: ciprofloxacin, electrooxidation, laccase, syringaldehyde, wastewater

Introduction

Ciprofloxacin (CIP) is a widely used antibiotic belonging to the fluoroquinolone family, having a broad spectrum of antimicrobial activity [1]. However, the human body is not able to metabolize CIP completely, which results in the excretion of almost 65% of unmetabolized CIP into the environment via feces and/or urine [2]. Consequently, the antibiotic is introduced to the wastewater treatment plants (WWTPs). However, conventional WWTPs are not designed to remove these types of pollutants, resulting in the introduction of CIP to the aquatic environment at relatively low concentration (ng-μg/L) [3, 4]. This leads to the classification of CIP as the contaminant of the emerging concern due to the limited understanding of its further fate and nature in water and soil [5]. These type of contaminants have no regulatory guidelines, but many countries and organizations have started to consider them as potentially harmful [6-8]. However, the main threat of CIP released into the environment is induction, selection, and dissemination of antimicrobial resistance, which is currently one of the largest global problems [9, 10]. There is no safe antibiotic's concentration that would prevent the development of antimicrobial resistance. Even when there is small amount of the antibiotic present in the ecosystem, it may lead to selective pressure and kill bacteria that are susceptible to it. As the result, only antimicrobial resistant bacteria will survive and further multiply. Therefore, various novel techniques are tested to improve WWT.

In recent years, electrochemical technologies have gained major attention as the potential methods for the removal of organic pollutants [11]. Electro-oxidation is the simplest and most popular between electrochemical oxidation methods. With the electro-oxidation, either partial transformation of the organic pollutants into highly biodegradable compounds or the electrochemical mineralization of the parent compounds can be achieved. The generation of free radicals, which are the green oxidizing agents, is summarized in the following reactions (eq. 13-19):

$H_2O \rightarrow {}^{\cdot}OH + H^+ + e^-$ Eq. 13

$2Cl^- \rightarrow Cl_2 + 2e^-$ Eq. 14

$Cl_2 + H_2O \rightarrow HOCl + H^+ + Cl^-$ Eq. 15

$HOCl \rightarrow H^+ + OCl^-$ Eq. 16

${}^{\cdot}OH \rightarrow H_2O_2$ Eq. 17

$H_2O_2 \rightarrow O_2 + 2H^+ + 2e^-$ Eq. 18

$O_2 + {}^{\cdot}O \rightarrow {}^{\cdot}O_3$ Eq. 19

Hydroxyl radicals are generated on anode's surface which can lead to direct oxidation (reaction (13)). The other radicals are obtained indirectly from chlorine, hypochlorite, ozone or hydrogen peroxide (reaction 14-19). The main advantages of the process are high energy efficiency, simplicity of the

equipment required, operation under mild conditions and most importantly electron as a clean reagent. However, the high electricity cost, fouling on the electrodes and need for electrolyte addition due to low conductance of wastewater are the main drawbacks.

The various materials, such as lead, lead oxide, mixed metal oxides or graphite, are used as anodes in WWT [11]. However, the most efficient electrode was found to be a boron-doped diamond anode (BDD) [11]. It exhibits exquisite corrosion and electrochemical stability, and the highest oxygen evolution overpotential value, meaning it generates the highest amount of hydroxyl radicals. It has good current efficiency and good conductivity. However, its main disadvantage is a high cost compared to other electrodes. The alternative anode material is mixed metal oxides (MMO). The main advantages of MMO anodes are the relatively low cost and high stability under extreme conditions of electrolysis. However, MMO exhibits much lower oxygen over-potential compared to BDD [12].

The other removal method widely investigated is the enzymatic degradation of pollutants. The major advantage of this system is its environmental friendliness and specificity. Special attention has been given to a group of oxidoreductase enzymes, laccases (EC 1.10.3.2). They are widely produced with other ligninolytic enzymes, manganese peroxidase, and lignin peroxidase, by white-rot fungi, such as *Trametes versicolor* or *Pleurotus ostreatus* [13]. Laccases catalyze the oxidative coupling of compounds, i.e., promote their bond cleavage via one-electron oxidation or radicals formation [13]. Laccases can transform a wide range of compounds. To expand the substrate specificity, the application of electron mediators has been widely tested [14, 15]. However, even though the system is very promising, its main drawback is a low degradation efficiency.

To improve removal efficiency, researchers have combined electrooxidation with other oxidation techniques to degrade CIP. Rahmani et al. (2018) reported 94% of CIP removal in 90 minutes when electrooxidation was coupled with ozonation method [16]. The addition of the second technique significantly improved the water treatment; electrooxidation alone led to a decrease of CIP concentration up to 70% in 120 min. Yahya et al. (2014) reported high efficiency of CIP removal via electro-Fenton process [17]. The total mineralization was 94% after 6 hours of treatment.

Based on this, the objective of this study is to couple two techniques: electrooxidation and enzymatic oxidation to efficiently remove CIP. To the best knowledge of the authors, the combination of electro and enzymatic oxidation described in this study was the first attempt to test this system. The use of two anodes, BDD and MMO, for the electrochemical part was evaluated along with different current densities. For the enzymatic degradation, the addition of mediators, i.e. syringaldehyde (SA) and 2,2′-Azino-bis-3-ethyl-benzothiazoline-6-sulfonic acid (ABTS) was investigated. The optimized conditions were selected and coupling of the two systems was assessed. The antimicrobial activity of transformation products was also analyzed.

Materials and methods

Materials

Ciprofloxacin (98% purity) was purchased from Across Organics, USA. Sodium sulphate anhydrous (99 %) and Tween 80 were bought from Fisher Scientific (Ottawa, Canada). Potato dextrose broth was obtained from Tekniscience, Canada. ABTS and SA were provided by Sigma-Aldrich (Oakville, Canada). HPLC-grade water was produced in the laboratory using a Milli-Q/Milli-Ro system (Millipore, USA). Purified laccase from *T. versicolor* was obtained from Sigma-Aldrich (Oakville, Canada), and its activity was 0.5 U/mg.

Electrooxidation process

CIP was added to Na_2SO_4 solution (1 g/L) to give the final concentration 1 mg/L. The volume of the reactor was 550 ml. For electrooxidation experiment two anodes were tested, BDD and MMO; the cathode was made of titanium (Ti). The experiment was conducted at 17.7 A/cm^2 for 60 min, where the samples were taken at certain intervals of time. Later, three current densities were tested to achieve the highest removal efficiency (4.42, 17.7, 35.4 A/cm^2) The efficiency of electrooxidation was tested with the addition of humic acid (10 mg/L) as the model compound of natural organic matter. The humic substances may accept or donate electrons in various redox reactions, hence their potential inhibiting effect on CIP electrooxidation was evaluated [18].

Enzymatic degradation

The enzymatic degradation was conducted with purified laccase in 50-ml Falcon tubes under dark conditions to avoid photooxidation of CIP. To imitate the real wastewater pH, the reaction was carried out at pH 6.5 in 100 mM phosphate buffer. The concentration of mediators and laccase were based on literature with minor changes [19]. Briefly, the concentration of laccase was at 0.2 mg/ml and the mediators (SA or ABST) were at concentration 0.8 mM. The final volume of the reaction was 25 ml. CIP removal was carried out for 24 hours, at 25˚C, 200 rpm in triplicates. Samples were taken at different times to establish the kinetics of removal (0, 1, 2, 3, 4, 6, 7, 8, 24 h). Before analyzing residual CIP concentration, each sample was deproteinized by incubation in a water bath at 100˚C for 5 min. Subsequently, it was centrifuged (2 min, 9659 x g) and the supernatant was analyzed by liquid chromatography

Combined removal system

The coupled electro- and enzymatic oxidation was carried out under optimized conditions according to results from previous sections. The experimental procedure is presented in 4.1.1.

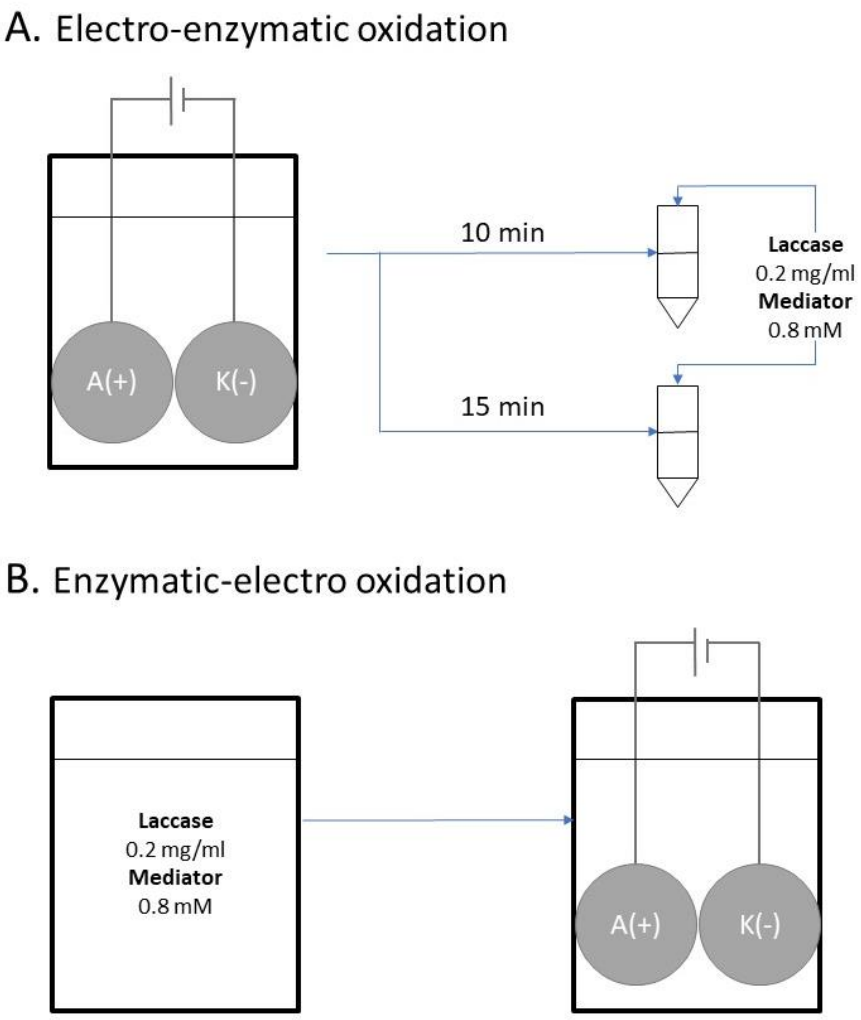

Figure 4.1. 1 Scheme of sequential removal systems

The first set of experiments consisted of successively testing electrochemical and enzymatic processes (fig. 4.1.1A). Synthetic wastewater was prepared in a 550 mL glass-tank containing 100 mM phosphate buffer solution (pH 6.5) in which 1 mg/L of CIP and 1 g/L of Na_2SO_4 was added. A working volume of 550 mL was used. The mixture was then subjected to electrooxidation. After 10 and 15 min, 25 ml of sample was collected to 50 ml Falcon tube in triplicate. To each sample, laccase and mediator was added to give the final concentration of 2 mg/mL and 0.8 mM, respectively. After each removal step, 1 mL of sample was taken to analyze it by liquid chromatography.

The second set of experiments was carried out to test enzymatic process followed by electrochemical process (fig. 4.1.1B). A 550 ml of phosphate buffer solution (100 mM, pH 6.5) containing 1 mg/L of CIP, 1 g/L Na2SO4, 2 mg/ml of laccase and 0.8 mM of mediator was prepared. The enzymatic oxidation was performed for 6 hours, at 25°C, 200 rpm. Subsequently, the mixture was subjected to electrooxidation process. After each removal step, 1 mL of sample was taken to analyze it by liquid chromatography.

Subsequently, the most efficient system was tested in spiked (1 mg/L CIP) and non-spiked wastewater effluent. The wastewater was collected in May 2019 from the Quebec Urban Community wastewater treatment plant (Beauport, Québec City, Québec, Canada). The characterization of wastewater is presented in Table S1 (Annex D). For electrooxidation part of the experiment, 1 g/L of Na_2SO_4 was added to increase wastewater conductivity.

Antimicrobial activity of transformation products

To evaluate the antimicrobial activity of transformation products, *Escherichia coli* (NRRL-3707) was used as a model microorganism. *E. coli* strain was revived in Tryptone-Yeast Extract-Glucose broth (tryptone 5 g/L, yeast extract 5 g/L, K_2HPO_4 1 g/L, glucose 1 g/L) suggested by Agricultural Research Service (NRRL) Culture Collection. Bacteria were incubated for 24 h, 28˚C, 150 rpm. Subsequently, *E. coli* was streaked onto Luria agar (LA) plates (tryptone 10 g/L, yeast extract 5 g/L, NaCl 10 g/L, agar 1.5 % w/v) and incubated for 24 h at 37˚C. The plates were maintained at 4˚C for further use.

The minimal inhibitory concentration (MIC) of CIP, defined as minimal concentration of the antibiotic that inhibits the bacterial growth, was determined against *E. coli.* It was evaluated by agar dilution method, as described by the European Committee for Antimicrobial Susceptibility Testing [20].

The samples of CIP degradation by electrooxidation, enzymatic oxidation, individually and in combination were collected. Agar well diffusion technique was used to test the antimicrobial efficiency of transformation products [21]. The overnight *E. coli* culture was inoculated onto LA plates and then, wells were punched aseptically (6-8 mm) with sterile tips. Then, 100 µl of tested solutions (controls, electrooxidation, and enzymatic oxidation individually and combined treatment) were added into the wells and incubated for 24h at 37˚C. After the incubation time, the inhibition zones were measured, and the inhibition index was calculated according to equation 20:

$$I_i = 1 - \frac{IZ_S - IZ}{IZ_S} \qquad \text{Eq. 20,}$$

Where I_i stands for inhibition index, IZ_S is the inhibition zone for untreated samples and IZ is the inhibition zone for the treated solution.

Analytical method

Samples were analyzed by liquid chromatography coupled with tandem mass spectrometry (LC-MS/MS). The system included a Finnigan surveyor LC pump linked to TSQ Quantum access triple quadruple mass spectrometer (Thermo Scientific, Mississauga, ON, Canada) and electrospray ionization interface. A 10 µL aliquot of the processed samples was injected into BetaBasic-18 column (100 mm x 2.1 mm x 3 µm). The column oven was at 40˚C and the flow rate was set at 0.3 mL/min. Ciprofloxacin-d_8 was used as the internal standard for CIP detection, and was added to each sample before the analyses to give the final concentration of 50 µg/L. Samples were eluted with a mobile phase which included

0.1% formic acid (mobile phase A) and acetonitrile combined with 0.1 % formic acid (mobile phase B). The gradient elution started with 90% of mobile phase A and 10% of mobile phase B. It was constant till 0.5 min and then mobile phase A started gradually decrease (30%) up to 3 min. Subsequently, the gradient was kept constant until 8 min and then it came back to the initial set up. The mass spectrometer was operated in SRM positive mode. Spray voltage was set at 4000 V and skimmer off-set at 20 V. Collision gas pressure was 1.5 mTorr. The capillary temperature was at 350˚C. The collision energy for CIP and CIP-d_8 was set at 17, and 19 V respectively. The precursor and product ions (m/z) were selected as follows: 332.3 and 245.3 for CIP and 340.3 and 249.3 for CIP-d_8. To minimize the matrix effect for wastewater samples, the calibration curve was made in wastewater effluent.

Statistical analysis

The statistical analysis was performed via SigmaPlot 13.0 software. One-way ANOVA was used to evaluate statistically significant difference (*p*-values < 0.05). The data were presented as a mean of replicates (n= 2-4) ± standard deviation.

Economic aspects

The economic study contained the consideration of chemicals and energy consumption to study cost efficacy of the proposed system. The electric cost was estimated to be around 0.05 $US kWh. The energy consumption (EC, kWh) was calculated using equation 21*:*

$$E_c = \frac{U_c \cdot I_e \cdot t}{1000} \qquad \text{Eq. 21}$$

Where I_e stands for applied current, t is treatment time, U_e stands for cell voltage. The cost of materials (industrial grade) is presented in Table S2 (Annex D). The total cost was presented in terms of $US/$m^3$ of treated solution.

Results and discussion

Electrooxidation process

Selection of anode

Generally, the type of anode significantly affects the electrooxidation process which can be attributed to the variation in its crystalline nature [22]. The electrooxidation efficiency of two anodes, BDD and MMO, was tested by evaluating the change of the CIP concentration against time. Figure 4.1.2 A presents their comparison via decrease of CIP concentration, when the current density was 17.7A/cm^2. As can be observed, at the initial stage, the BDD efficiency to remove CIP was higher when compared with MMO anode (p-value < 0.05 between 0 and 20 min). After 20 min, BDD was able to decrease CIP concentration down to 4.5±0.2% which presents a significant difference (p-value = 0.00011) compared to MMO where CIP concentration decreased to 24.0±0.1%. These results are consistent with previous

studies indicating that BDD anode performed better than MMO to degrade other contaminants, like methyl orange dye [12] or microcystin-LR [23].

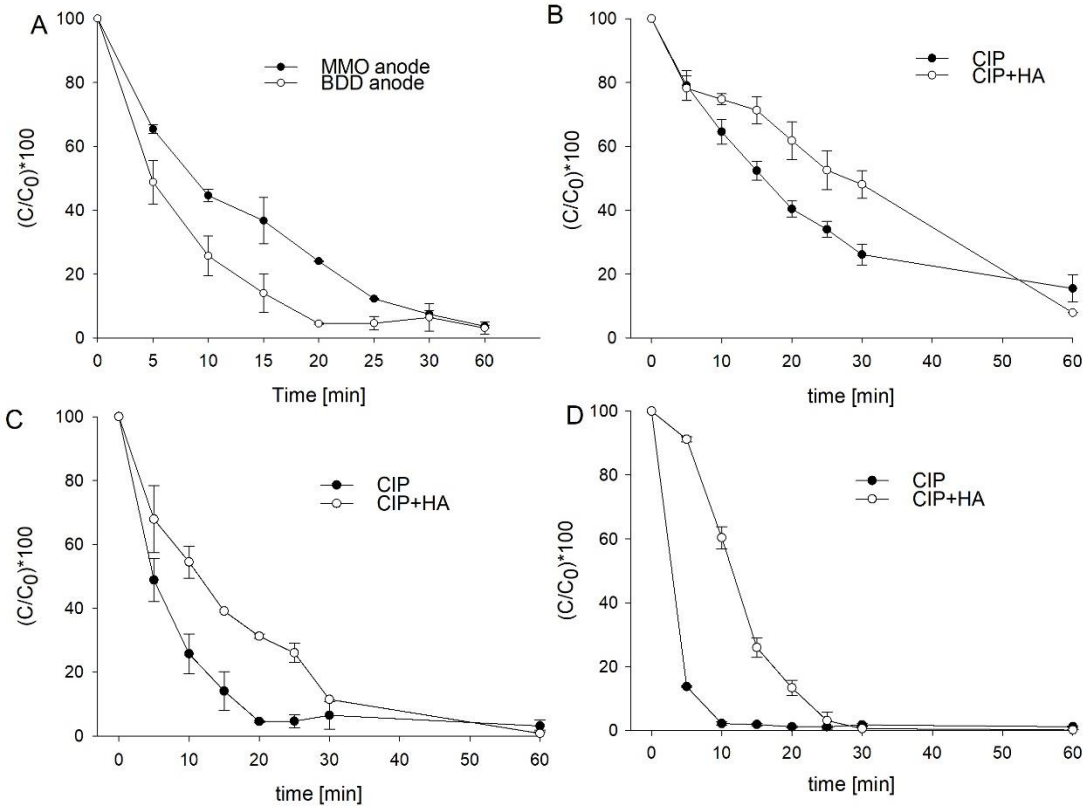

Figure 4.1. 2 Electrooxidation of CIP A. with two anodes BBD and MMO, current density 1.0 A, electrolyte: Na_2SO_4 1g/L, CIP 1 mg/L; B. in the presence of humic acid (HA), current density 0.5 A electrolyte: Na_2SO_4 1g/L, CIP 1 mg/L, BDD anode; C. in the presence of humic acid (HA), current density 1.0 A electrolyte: Na_2SO_4 1g/L, CIP 1 mg/L, BDD anode; D. in the presence of humic acid (HA), current density 2.0 A electrolyte: Na_2SO_4 1g/L, CIP 1 mg/L, BDD anode; C – concentration of CIP in time, C_o – initial concentration of CIP

The difference in electrooxidation performance might be associated with higher hydroxyl radicals generation on BDD anode than MMO (Eq. 13) [23]. Interestingly, after 30 min of electrooxidation both anodes reached around 7% of the original concentration of CIP (BDD 6.5±3.1%; MMO 7.4±0.8%; p-value = 0.79) which can be related to the apparent rate constants presented as the function of anode material in Table 4.1.1. BDD exhibits higher value (0.1362 s^{-1}) than MMO (0.083 s^{-1}). CIP removal was well fitted to pseudo-first-order reaction, which was also found in case of electrooxidation of norfloxacin (fluoroquinolone) using BDD anode [24]. Thus, overall, the BDD anode was chosen as working anode for CIP removal in further experiments.

Table 4.1. 1 Apparent rate constants as the function of various parameters

Parameter	Reaction order	Rate constant [s^1]		R^2	
Anode material					
BBD		0.1362		0.94	
MMO		0.083		0.96	
Current density [A/cm^2]		CIP	CIP+HA	CIP	CIP+HA
4.42		0.044	0.041	0.99	0.94
17.1	Pseudo-first	0.1419	0.070	0.98	0.98
35.4		0.41	0.17	0.99	0.90
Mediator					
SA		0.18		0.96	
ABTS		0.035		0.87	

ABTS - 2,2'-azino-bis(3-ethylbenzothiazoline-6-sulphonic acid); BDD- boron-doped diamond; CIP – ciprofloxacin; HA – humic acid; MMO – mixed metal oxides; SA – syringaldehyde

Influence of current density

Figure 4.1.2 B-D presents the performance of the system while using three different current densities using BDD anode material. With the increase of current density, the residual CIP concentration decreased. Removal of more than 90% of CIP original concentration was achieved after 20 and 6 min when 17.7 A/cm^2 and 35.4A/cm^2 was applied, respectively (fig. 4.1.2 B, C). In the case of 4.42A/cm^2 application, after 60 min of electrooxidation, 15.5±3.0% of CIP was still present in the reactor (fig. 4.1.2 B). Thus, the higher the applied current density, the more effective and more rapid is the CIP oxidation. A similar trend was observed by Tran et al. (2013) while studying microcystin-LR electrooxidation [25]. After 60 min oxidation, there was a reduction of the initial concentration of microcystin, from 12 μg/L, to 7.02 μg/L and 0.16 μg/L when 2.6 mA/cm^2 and 51 mA/cm^2 were applied respectively. Table 4.1.1 presents the apparent rate constants as the function of the applied current density. Generally, value of the rate constants increases with the increase of applied current.

Effect of humic acid on electro-oxidation

Additionally, the effect of HA on CIP removal was also tested (fig. 4.1.2 B-D). The addition of HA hindered CIP oxidation in all three cases. The electrochemical oxidation occurs on the anode (BDD) due to the electrophilic attack of electrochemically generated hydroxyl radicals on electron-rich functional groups. Both CIP and HA are electron-rich compounds due to the presence of group like -C=C-, -C=O, -COOH, etc. [25, 26]. Thus, the competition over radicals, mainly hydroxyl radicals, is responsible for decreased removal efficiency CIP. The rate constants were also affected by the presence of HA; in general, the rate constants decreased with the addition of HA (Table 4.1.1). Based on the presented results, 35.4 A/cm^2 was selected for further experiments as applied current intensity.

Enzymatic degradation

The potential of laccase to remove CIP is presented in Figure 4.1.3. In the present study, laccase itself was not able to degrade CIP, which is in agreement with previously reported studies [15, 19]. This is because the chemical structure of CIP Figure (fig. S1, Annex D) does not favor laccase-mediated oxidation. The presence of strong electron-withdrawing groups, i.e. ketone, carboxylic acid, a fluorine atom, and the benzene ring, limits the electron availability, leading to reduction of compound's susceptibility towards laccase. However, to increase laccase's affinity towards various substrates, the redox mediators are used [13]. In this study, the addition of ABTS, a widely tested synthetic mediator, led to an 87.8±6.6% decrease in the antibiotic's concentration in 4 hours (fig. 4.1.3A). Longer enzymatic oxidation in the presence of this mediator did not improve the CIP removal; after 24 hours, 83.4±4.4% of CIP remained in the mixture (data not shown). Prieto et al. (2011) presented that ABTS-mediated laccase oxidation from *T. versicolor* led to an almost complete removal of CIP in 30 hours [27]. On the other hand, Parra Guardado et al. (2019) reported no degradation of the antibiotic by ABTS system [15]. The variations between studies may be related to removal conditions as well as different fungal species that were used to produce laccase.

SA-mediated system efficiently removed CIP; in four hours its concentration decreased up to 48.9±4.0% (fig. 4.1.3A). After 24 hours, only 31.1±3.4% of CIP remained (fig. 4.1.3B). A similar removal efficiency was reported by Parra Guardado et al. (2019), where 40 % of CIP was removed in 3 hours [15]. Interestingly, Ding et al. (2016) presented an opposite trend, where removal of quinolone antibiotics, including CIP, was negligible [19]. Based on the results presented in Figure 4.1.3A, the apparent rate constants were calculated, which are presented in Table 4.1.1. For ABTS-mediated reaction, it was found to be 0.035 s^{-1}, while for SA-mediated reaction was 5-fold higher (0.18 s^{-1}).

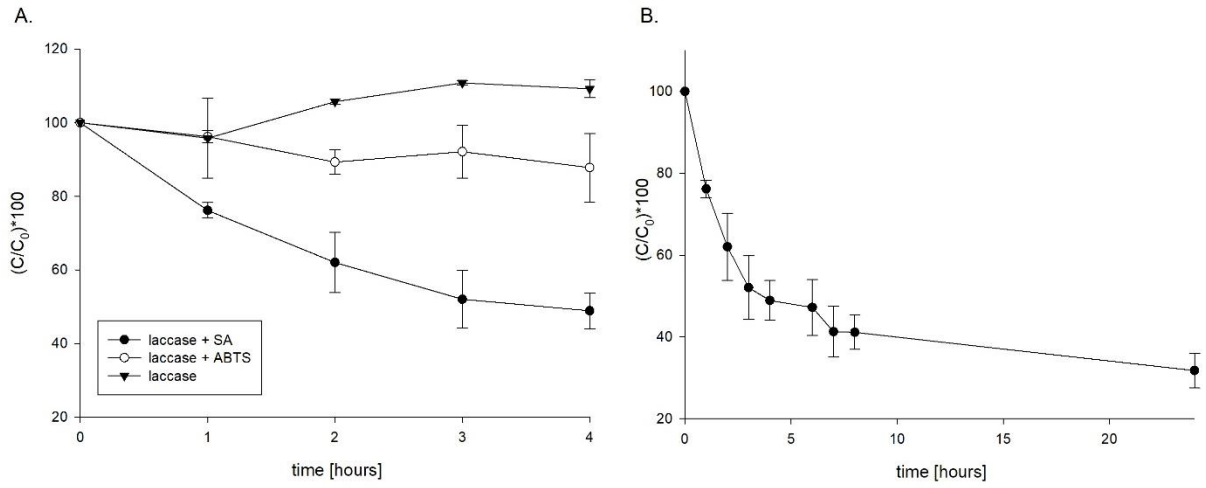

Figure 4.1. 3 Removal of CIP via laccase oxidation A. with and without the addition of mediators; B. with SA only; 1 mg/L CIP, 0.2 mg/ml laccase, phosphate buffer pH 6.5, 25°C, 200 rpm, 0.8 mM mediators; SA – syringaldehyde; ABTS - 2,2'-azino-bis(3-ethylbenzothiazoline-6-sulphonic acid); C – concentration of CIP in time; C_0 – initial concentration of CIP

Generally, the efficiency of laccase mediated removal depends on the redox potential difference between the substrate and one of the copper atoms in the active site of the enzyme [13]. The mediators are small molecules which can act as an electron shuttle between the enzyme and substrate or increase laccase's redox potential. However, different mediators have various mechanisms. The structures of used mediators are presented in Figure S1, Annex D. ABTS-mediated system follows an electron transfer route [13]. Firstly, the radical $ABTS^{\cdot+}$ is generated, which is oxidized to cationic form $ABTS^{2+}$ [14]. The potential explanation for insufficient mediation of CIP oxidation could be due to the radical instability or transformation of the radical into its dicationic form, which can no longer act as the mediator [15, 28]. In the case of SA, the phenolic group is oxidized by laccase, which gives the radical stabilized by two methoxy groups in the ortho position [14]. Hence, phenoxy radical generated is more stable, which improves the efficiency of SA-mediated CIP removal than ABTS-mediated removal. This confirms the results obtained in this study. Thus, the SA-mediated system was chosen as more suitable for the next experiments.

Combined removal system

Electro-enzymatic system

Figure 4.1.4 presents the removal of CIP via the electro-oxidation system. For the electrooxidation part, two times of treatment were chosen: 10 and 15 min, those parameters exhibited high efficiency of CIP removal with and without HA (fig. 4.1.2). Electro-oxidative treatment after 10 min, in phosphate buffer with the addition of Na2SO4, decreased CIP concentration up to 22.6±1.8%. Subsequent enzymatic treatment led to a significant reduction of antibiotic's concentration within the first hour. Further, the trend of decrease slowed down; after 6 hours only 3.3±1.2% of CIP remained in the solution. In the case of electrooxidation for 15 mins, 4.8±0.5% of CIP remained in the solution. The following enzymatic

treatment led to the almost complete removal of the compound (0.8±0.07%). Generally, in both cases, once the concentration of CIP was below 10%, a slower removal trend can be observed. It is most probably related to the low concentration of CIP, hence there was a lesser chance of laccase SA-mediated system to oxidize the compound. Moreover, transformation products generated could be competing with the remaining residue of CIP. Based on total organic carbon measurements and chromatograms, it can be proposed that CIP underwent partial oxidation (data not shown).

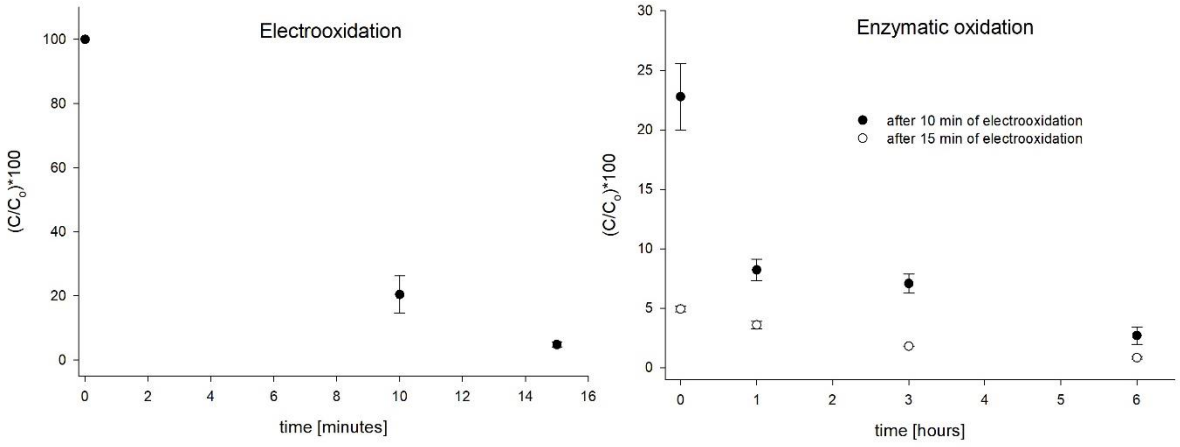

Figure 4.1. 4 Removal of CIP via electro-enzymatic system; 1 mg/L CIP, 0.2 mg/mL laccase, 1 g/L Na_2SO_4, phosphate buffer pH 6.5, 0.8 mM SA; C – concentration of CIP in time; C_0 – initial concentration of CIP

Enzymatic-electro system

The reverse system (enzymatic-electrooxidation) was also tested. For laccase oxidation, 6 hours of treatment was chosen as it is a slower removal method. CIP was partly oxidized, and its concentration reached around 50% of its original concentration, and from that point, the removal process was much slower (fig. 4.1.3). Figure 4.1.5 presents the removal of CIP in time when the system was applied. After 6 hours of laccase oxidation, 47.4±0.7% of CIP remained in the mixture. Subsequently, the solution was subjected to electrooxidation (35.4 A/cm^2, BDD). After 15 min of electrooxidation, the CIP concentration was at 26.7±0.9% of its original amount. Slower electrooxidation than in the previous system may be associated with the presence of SA and laccase. It has been reported previously that BDD anode is able to oxidize proteins [29, 30]. Hence, electro-generated radicals are attacking not only CIP or SA, but also laccase, which is a large molecule containing various electron-donating functional groups. To avoid this competition, the enzyme should be removed before applying the electrooxidation treatment. The solution would be to immobilize laccase for effective stability and long use [31].

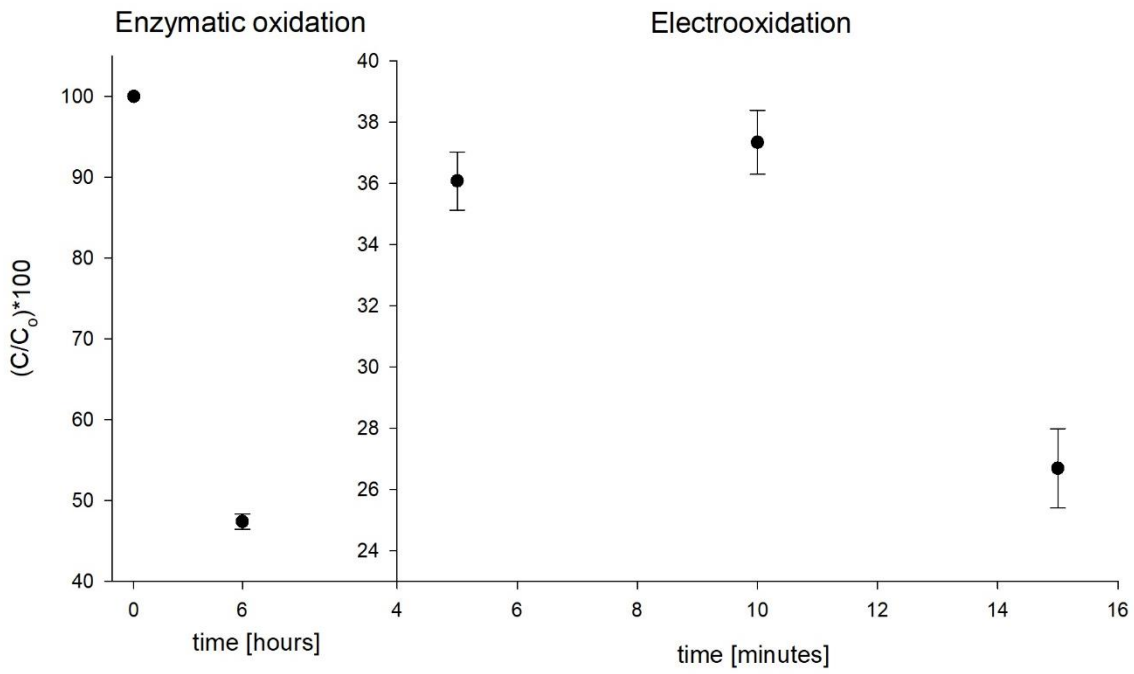

Figure 4.1. 5 Removal of CIP via enzymatic-electro system; 1 mg/L CIP, 0.2 mg/mL laccase, 1 g/L Na_2SO_4, phosphate buffer pH 6.5, 0.8 mM SA; C – concentration of CIP in time; C_0 – initial concentration of CIP

Antimicrobial activity of transformation products

Samples from both treatment systems were withdrawn and were tested for the potential antimicrobial activity of residual CIP and its transformation products. The antimicrobial activity is represented by inhibition index ($0 \leq I \leq 1$), when I=0, the treated solution exhibits no antimicrobial efficiency and when *I*=1, the transformation products mixture has the same antimicrobial potency before treatment.

Electro-enzymatic system

Figure 4.1.6 presents the changes in antimicrobial activity against *E. coli* for the enzymatic-electro system. It was observed that enzymatic treatment reduced only 10% of the antibacterial efficiency of the solution, even though the concentration of CIP decreased 2-fold. It is consistent with the finding of Cvancarová et al. (2015) [32]. They reported that even though the concentration of CIP significantly decreased due to fungal biotransformation, the transformation products contributed to the residual antimicrobial activity. The fungal biotransformation usually leads to substitution or decomposition of the piperazine ring of CIP [27, 32]. The presence of this functional group generally improves the antimicrobial potency of the compound [33]. The modification of this group, however, does not lead to loss of antibacterial activity. This explains the slight decrease of antimicrobial activity of treated mixture. As mentioned earlier, the electrooxidation resulted in a minor reduction of the antibiotic concentration. Moreover, after 10 min of the treatment, the antimicrobial activity increased up to its original potency. This may suggest the formation of transformation products that exhibit similar antimicrobial activity as CIP.

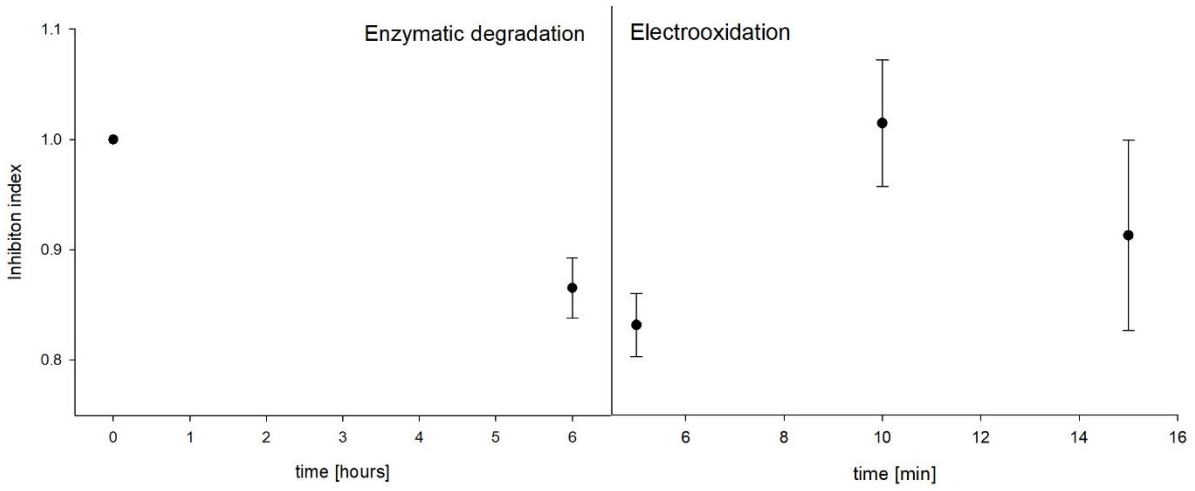

Figure 4.1. 6 Inhibition index of CIP and its transformation products during enzymatic-electro treatment *Enzymatic-electro system*

Figure 4.1.7 presents the changes in antimicrobial activity during electro-enzymatic treatment. Around 40% decrease of the antibacterial potency was achieved after 10 min of electrooxidation. Subsequent enzymatic treatment resulted in complete loss of antimicrobial activity after 6 hours (CIP concentration below 100/ µg/L). Moreover, after 15 min of electrooxidation, the solution did not exhibit any antimicrobial efficiency towards tested bacteria (CIP concentration below 100 µg/L). The subsequent enzymatic treatment did not result in the generation of reversion of toxicity (data not shown). The results, when I = 0, are in accordance with the MIC value, which was found to be 125 µg/L. Moreover, the transformation products generated did not exhibit antimicrobial activity. Hence, the system would not contribute to release of potentially new compounds that would have antimicrobial potency.

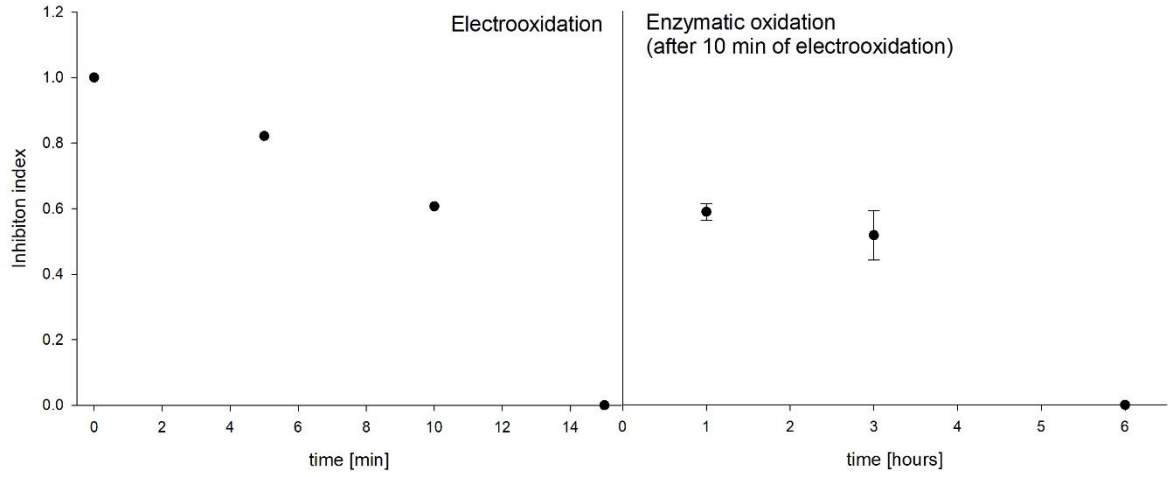

Figure 4.1. 7 Inhibition index of CIP and its transformation products during electro-enzymatic treatment

Tests with real wastewater effluent

Based on the above results, the electro-enzymatic sequence was found to be the more efficient sequence was. Its potency was tested with spiked wastewater, which is presented in 4.1.2. The electrooxidation

alone was able to remove more than 95% of CIP (10- and 15-min treatment). Even though the concentration of the antibiotic after electrooxidation was low (9-26 μg/L), laccase was still able to decrease CIP concentration. The efficiency of the system was also tested with non-spiked wastewater effluent (Table 4.1.2). It can be observed that both treatment, 10 and 15 min of electrooxidation followed by enzymatic oxidation, led to 80-84 % removal of CIP. However, there was no significant difference between the two treatments (p-value = 0.6). Hence, the system is able to efficiently remove the antibiotic in real wastewater, even if the initial concentration is high (up to 1 mg/L) or low (2 μg/L). Hence, the sequential electrooxidation and enzymatic oxidation could be potentially used in the water treatment plant.

Table 4.1. 2 CIP removal efficiency of electro-enzymatic treatment in spiked wastewater

Treatment	C_{CIP} in spiked wastewater [μg/L]	Remaining concentration [%]	C_{CIP} in non-spiked wastewater [μg/L]	Remaining concentration [%]
Electrooxidation 10 min	1002.5 ±0.5	5.5±0.2	2.85 ±0.62	20±0.2
Enzymatic oxidation		2.5±0.7		
Electrooxidation 15 min		3.0±0.2		16±0.1
Enzymatic oxidation		1.5±0.2		

CIP – ciprofloxacin; CCIP – concentration of ciprofloxacin

Economic aspect

The estimated costs, including only energy consumption and material costs, are presented in Table 4.1.3. The highest costs were associated with enzymatic oxidation due to higher cost of materials (laccase, syringaldehyde). Future work should focus on lowering these prices. The potential solution could be: 1) decrease electrooxidation time, 2) increase of laccase production[34, 35], 3) immobilization of laccase and/or mediators to improve its catalytic ability and recovery [36] 4) finding alternative enzymatic system that would be more efficient than laccase and would not need the redox mediators.

Table 4.1. 3 Estimated costs of water treatment via electro-enzymatic oxidation

Cost [USD/m^3]	Treated effluent via electro- (10 min) + enzymatic oxidation	Treated effluent via electro- (15 min) + enzymatic oxidation
Power consumption:		
Electrooxidation	0.45	0.63
+ stirring	0.36	0.52
Power consumption:		
Enzymatic oxidation (stirring only)	13.00	
Material costs		
Electrooxidation	0.30	
Enzymatic oxidation	29.72	
Total cost	43.83	44.17

Conclusion

The study showed the potential of removal of CIP from the water via sequential electro-enzymatic oxidation. For the electrooxidation, BDD anode was chosen over MMO due to better performance. The removal efficiency was found to increase with the increasing current density. At 35.4 A/cm^2, after 5 min of treatment, around 90% of antibiotic was removed. When HA was added, similar results were obtained after 20 min of electrooxidation. Hence, following electrooxidation tests were carried out at 35.4 A/cm2. As for the enzymatic removal via laccase, the SA-mediated system exhibited much better performance than ABTS-mediated system. Laccase alone was not able to degrade CIP. The electrooxidation (2A, BBD anode) followed by SA-mediated enzymatic oxidation showed more than 95% of CIP removal. The tests with real wastewater effluent confirmed the efficiency of the system. Interestingly, laccase treatment followed by electrooxidation did not give similar performance. The enzymatic treatment was able to remove more than 50% of CIP, but sequential electrooxidation led to decrease of CIP only to 26.7±0.9% of its original concentration. Moreover, the antimicrobial activity of tested samples exhibited similar toxicity towards E. coli as the original stock solution. Hence, only electro-enzymatic sequence showed the potential for efficient water treatment.

Acknowledgements

The authors are sincerely thankful to the Natural Sciences and Engineering Research Council of Canada (Discovery Grant 355254 and NSERC Strategic Grant). We also would like to thank James and Joanne

Love Chair in Environmental Engineering for support and collaboration. We would like to also thank Mr. Stephane Moise for his technical support with Liquid Chromatography analysis.

References

1. Janecko, N., et al., *Implications of fluoroquinolone contamination for the aquatic environment-A review.* Environ Toxicol Chem, 2016. **35**(11): p. 2647-2656.

2. Frade, V.M.F., et al., *Environmental contamination by fluoroquinolones.* Braz J Pharm Sci, 2014. **50**: p. 41-54.

3. Van Doorslaer, X., et al., *Fluoroquinolone antibiotics: an emerging class of environmental micropollutants.* Sci Total Environ, 2014. **500-501**: p. 250-69.

4. Jia, A., et al., *Occurrence and fate of quinolone and fluoroquinolone antibiotics in a municipal sewage treatment plant.* Water Res, 2012. **46**(2): p. 387-94.

5. Noguera-Oviedo, K. and D.S. Aga, *Lessons learned from more than two decades of research on emerging contaminants in the environment.* Journal of Hazardous Materials, 2016. **316**: p. 242-251.

6. Organization, W.H., *Antimicrobial Resistance: An Emerging Water, Sanitation and Hygiene Issue* 2014.

7. Canada, E., *Threats to Sources of Drinking Water and Aquatic Ecosystem Health in Canada.* . 2001, National Water Research Institute, Burlington, Ontario. p. 72.

8. Geissen, V., et al., *Emerging pollutants in the environment: A challenge for water resource management.* International Soil and Water Conservation Research, 2015. **3**(1): p. 57-65.

9. Ventola, C.L., *The antibiotic resistance crisis: part 1: causes and threats.* P & T : a peer-reviewed journal for formulary management, 2015. **40**(4): p. 277-283.

10. Berkner, S., S. Konradi, and J. Schönfeld, *Antibiotic resistance and the environment—there and back again.* EMBO Reports, 2014. **15**(7): p. 740-744.

11. Särkkä, H., A. Bhatnagar, and M. Sillanpää, *Recent developments of electro-oxidation in water treatment — A review.* Journal of Electroanalytical Chemistry, 2015. **754**: p. 46-56.

12. Zhou, M., H. Särkkä, and M. Sillanpää, *A comparative experimental study on methyl orange degradation by electrochemical oxidation on BDD and MMO electrodes.* Separation and Purification Technology, 2011. **78**(3): p. 290-297.

13. Yang, J., et al., *Laccases: Production, Expression Regulation, and Applications in Pharmaceutical Biodegradation.* Front Microbiol, 2017. **8**: p. 832.

14. Canas, A.I. and S. Camarero, *Laccases and their natural mediators: biotechnological tools for sustainable eco-friendly processes.* Biotechnol Adv, 2010. **28**(6): p. 694-705.

15. Parra Guardado, A.L., et al., *Effect of redox mediators in pharmaceuticals degradation by laccase: A comparative study.* Process Biochemistry, 2019. **78**: p. 123-131.

16. Rahmani, A.R., et al., *A combined advanced oxidation process: Electrooxidation-ozonation for antibiotic ciprofloxacin removal from aqueous solution.* Journal of Electroanalytical Chemistry, 2018. **808**: p. 82-89.

17. Yahya, M.S., et al., *Oxidative degradation study on antimicrobial agent ciprofloxacin by electro-fenton process: Kinetics and oxidation products.* Chemosphere, 2014. **117**: p. 447-454.

18. Page, S.E., et al., *Hydroxyl Radical Formation upon Oxidation of Reduced Humic Acids by Oxygen in the Dark.* Environmental Science & Technology, 2012. **46**(3): p. 1590-1597.

19. Ding, H., et al., *Simultaneous removal and degradation characteristics of sulfonamide, tetracycline, and quinolone antibiotics by laccase-mediated oxidation coupled with soil adsorption.* Journal of Hazardous Materials, 2016. **307**: p. 350-358.

20. Diseases, E.S.o.C.M.a.I., *EUCAST Definitive Document E.DEF 3.1, June 2000: Determination of minimum inhibitory concentrations (MICs) of antibacterial agents by agar dilution*, in *Clin Microbiol Infect*. 2000, European Society of Clinical Microbiology and Infectious Diseases p. 509-15.

21. Balouiri, M., M. Sadiki, and S.K. Ibnsouda, *Methods for in vitro evaluating antimicrobial activity: A review.* Journal of Pharmaceutical Analysis, 2016. **6**(2): p. 71-79.

22. Feng, C., et al., *Development of a high performance electrochemical wastewater treatment system.* Journal of Hazardous Materials, 2003. **103**(1): p. 65-78.

23. Zhou, S., et al., *A comparative study of microcystin-LR degradation by electrogenerated oxidants at BDD and MMO anodes.* Chemosphere, 2016. **165**: p. 381-387.

24. Coledam, D.A.C., et al., *Electrochemical mineralization of norfloxacin using distinct boron-doped diamond anodes in a filter-press reactor, with investigations of toxicity and oxidation by-products.* Electrochimica Acta, 2016. **213**: p. 856-864.

25. Tran, N. and P. Drogui, *Electrochemical removal of microcystin-LR from aqueous solution in the presence of natural organic pollutants.* Journal of environmental management, 2013. **114**: p. 253-260.

26. Stichnothe, H., et al., *Reduction of Tributyltin (TBT) and Other Organic Pollutants of Concern in Contaminated Sediments by means of an Electrochemical Oxidation.* Acta hydrochimica et hydrobiologica, 2002. **30**(2-3): p. 87-93.

27. Prieto, A., et al., *Degradation of the antibiotics norfloxacin and ciprofloxacin by a white-rot fungus and identification of degradation products.* Bioresour Technol, 2011. **102**(23): p. 10987-95.

28. Kurniawati, S. and J.A. Nicell, *Efficacy of mediators for enhancing the laccase-catalyzed oxidation of aqueous phenol.* Enzyme and Microbial Technology, 2007. **41**(3): p. 353-361.

29. Roeser, J., et al., *Boron-Doped Diamond Electrodes for the Electrochemical Oxidation and Cleavage of Peptides.* Analytical Chemistry, 2013. **85**(14): p. 6626-6632.

30. Chiku, M., et al., *Direct electrochemical oxidation of proteins at conductive diamond electrodes.* Journal of Electroanalytical Chemistry, 2008. **612**(2): p. 201-207.

31. Becker, D., et al., *Removal of Endocrine Disrupting Chemicals in Wastewater by Enzymatic Treatment with Fungal Laccases.* Organic Process Research & Development, 2017. **21**(4): p. 480-491.

32. Čvančarová, M., et al., *Biotransformation of fluoroquinolone antibiotics by ligninolytic fungi – Metabolites, enzymes and residual antibacterial activity.* Chemosphere, 2015. **136**: p. 311-320.

33. Sharma, P.C., A. Jain, and S. Jain, *Fluoroquinolone antibacterials: a review on chemistry, microbiology and therapeutic prospects.* Acta Pol Pharm, 2009. **66**(6): p. 587-604.

34. Rodgers, C.J., et al., *Designer laccases: a vogue for high-potential fungal enzymes?* Trends in Biotechnology, 2010. **28**(2): p. 63-72.

35. Hou, H., et al., *Enhancement of laccase production by Pleurotus ostreatus and its use for the decolorization of anthraquinone dye.* Process Biochemistry, 2004. **39**(11): p. 1415-1419.

36. Ba, S., et al., *Laccase immobilization and insolubilization: from fundamentals to applications for the elimination of emerging contaminants in wastewater treatment.* Critical Reviews in Biotechnology, 2013. **33**(4): p. 404-418.

PART 2

Potential of agro-industrial produced laccase to remove ciprofloxacin

Agnieszka Cuprys [a], Paisley Thompson [a], Gayatri Suresh [a], Tarek Roussi [a], Satinder Kaur Brar [a,b,*], Patrick Drogui [a]

[a] INRS-ETE, Université du Québec, 490, Rue de la Couronne, Québec, Canada G1K 9A9

[b] Department of Civil Engineering, Lassonde School of Engineering, York University, North York, Toronto, Ontario Canada M3J 1P3

[*] Corresponding author: E-mail: satinder.brar@ete.inrs.ca; Satinder.Brar@lassonde.yorku.ca

Draft (to be submitted)

Résumé

La ciprofloxacine (CIP), un antibiotique largement utilisé, est fréquemment détectée dans l'environnement en raison d'un traitement insuffisant des eaux usées et de l'eau. Par conséquent, des technologies nouvelles, vertes et rentables sont nécessaires pour améliorer l'élimination de ces polluants. La puissance des enzymes brutes, en particulier des laccases, produites par les champignons de la pourriture blanche a été testée afin d'évaluer leur pouvoir de dégradation du CIP de l'eau. La laccase brute n'est pas capable d'éliminer la CIP seule. L'addition de syringaldéhyde, un médiateur rédox, a entraîné une diminution de la concentration en antibiotiques jusqu'à 68,09 ± 0,12% en 24 h, ce qui représente l'efficacité d'élimination la plus élevée obtenue à 0,8 mM de syringaldéhyde et à 2 mg / ml de laccase brute (0,1 U/mL). Ce qui est intéressant, l'oxydation brute de la CIP par la laccase était inhibée après 6 heures de traitement. A titre de comparaison, une enzyme pure ayant la même activité que la protéine brute a éliminé 86% de la CIP en 24 h. Aucun effet inhibiteur pendant le traitement n'a été observé. L'estimation de l'efficacité antimicrobienne a révélé que, en 6 heures de traitement, la toxicité envers Escherichia coli diminuait de 30%. On a estimé que le traitement des eaux usées par un système à médiation par la laccase brute réduisait considérablement le coût du traitement enzymatique.

Mots-clés: ciprofloxacine, laccase brute, eaux usées, syringaldéhyde, calcul technoéconomique

Abstract

Ciprofloxacin (CIP), a widely used antibiotic, is frequently detected in the environment due to insufficient wastewater and water treatment. Hence, novel, green and cost-effective technologies are needed to improve the removal of these pollutants. Crude laccases produced by white-rot fungi was tested to evaluate its potency to degrade CIP from water. Crude laccase alone was not able to remove CIP. The addition of syringaldehyde, a redox mediator, resulted in a decrease in antibiotic concentration up to 68.09±0.12% in 24 h, which was the highest removal efficiency achieved at 0.8 mM syringaldehyde and 2 mg/ml of crude laccase (0.1 U/ml). Interestingly, crude laccase oxidation of CIP was inhibited after 6 hours of treatment. To compare, pure enzyme with the same activity as the crude one removed 86% of CIP in 24 h. No inhibitory effect during the treatment was noticed. The estimation of antimicrobial efficiency revealed that in 6 hours of treatment, the toxicity against *Escherichia coli* decreases by 30%. The wastewater treatment by the crude laccase-mediated system was estimated to significantly reduce the cost of enzymatic treatment.

Keywords: ciprofloxacin, crude laccase, wastewater, syringaldehyde, technoeconomic calculation

Introduction

The discharge of pharmaceuticals into the environment due to insufficient wastewater treatment (WWT) has become an emerging problem around the world. Their presence in water and/or soil may lead to adverse effects on present fauna and flora, i.e. chronic and acute toxicity, bioaccumulation in organisms' tissues [1, 2]. Especially, the introduction of antibiotics is an alarming problem due to their possibility of dissemination of antibiotic resistance [3]. Hence, novel and cost-effective techniques to improve wastewater and water treatment are needed.

Ciprofloxacin (CIP) is a widely used antibiotic, which makes it one of the most frequently detected fluoroquinolone in the environment [4, 5]. Various techniques have been tested to improve the removal of CIP from wastewater, including advanced oxidation processes [6, 7], adsorption [8, 9] and biological methods [10]. While the chemical and physical techniques present rather satisfying removal efficiency of CIP, the biological systems are more demanding. The conventional biological treatment used for WWT, like membrane bioreactors or activated sludge, are able to degrade simple compounds, such as ibuprofen, when the complex structure exhibits no degradation [11]. The alternative approach, that is being currently investigated, is the usage of white-rot fungi and the enzymes they produce. They were found to be capable of degrading various pollutants, including pharmaceuticals [12]. Their effectiveness is due to various extracellular enzymes, especially lignin peroxidases, manganese-dependent peroxidases, and laccases. The latter is of special interest in research. Laccases (EC 1.10.3.2) are copper-containing enzymes that catalyze the oxidation of phenolic and non-phenolic compounds using oxygen as electron acceptor [13]. The reaction involves the generation of free radical due to the transfer of a single electron to laccase.

The oxidation efficiency of laccases depends on the redox potential between the substrate and one of the copper molecules in laccases [13]. However, oxidation efficiency may be enhanced by the application of redox mediators. They are small molecules which can act as an electron shuttle between the substrate and enzyme or increase the redox potential of laccases. The most common mediators currently in use are synthetic compounds like 2,2′-azino-bis (3-ethylbenzothiazoline-6-sulfonate) (ABTS) and 1-hydroxybenzotriazole or natural phenolic compounds, i.e. syringaldehyde (SA) and acetosyringone [13, 14].

The enzymatic WWT requires large amounts of enzymes, hence the development of cost-effective procedure of their production is crucial. The cost of commercial laccases is high (around USD 95 /g), which is the main drawback of their use in real water treatment. The alternative to purified enzymes is the use of crude laccases, which would be a preferred format for environmental applications. Additionally, white-rot fungi are able to grow on agro-industrial wastes, which significantly decreases the cost of enzyme production [15]. Hence, the aim of this study was to grow white-rot fungi *Trametes versicolor* on apple pomace, waste from the apple juice industry, to produce laccase. Subsequently, the

extracted crude enzyme was tested to degrade CIP, with and without mediators (ABTS and SA). Later, the evaluation of transformation products' antimicrobial activity was carried out. The estimation of the material costs and power consumption of crude enzyme production and WWT was carried out.

Materials and methods

Materials

Ciprofloxacin (98% purity) was obtained from Across Organics, USA. Tween 80 was bought from Fisher Scientific (Ottawa, Canada). Potato dextrose broth was obtained from Tekniscience, Canada. ABTS and SA were purchased by Sigma-Aldrich (Oakville, Canada). HPLC-grade water was produced in the laboratory using a Milli-Q/Milli-Ro system (Millipore, USA).

Inoculum preparation

Lyophilized strain of *Trametes versicolor* (ATCC 20869) was inoculated in potato dextrose broth (PDB) liquid medium, and as incubated in an orbital shaker at 30 ± 1 °C and 150 rpm for 7 days. Subsequently, 100 µL of inoculum was streaked onto the potato dextrose agar (PDA) plates, which were kept in a static incubator at 30 ± 1 °C for 9 days.

Solid-state fermentation

To produce laccase by *T. versicolor*, apple pomace (with 70 wt % moisture and pH 4.5) was used as a cost-effective solid substrate as previously described [16]. Apple pomace, a juice industry residue, was gifted by Vergers Paul Jodoin, Inc., Quebec, Canada. About 20 g of apple pomace was added to a 500 mL flask along with 0.5% (v/w) Tween 80 as inducer, mixed thoroughly, and autoclaved at 121 ± 1 °C for 30 min. Subsequently, the solid media was inoculated with the biomass content of one Petri plate obtained in the previous step. Then, it was kept in a static incubator at 30 ± 1 °C for 13 days.

Enzyme extraction and assay

The sample (1 g) obtained from the fermentation prepared in the previous step, was added to 20 mL of 50 mM phosphate buffer pH 6.5, mixed thoroughly for 1 h at 35 ±1 °C, and centrifuged at 7000 x g for 30 min. Later, the supernatant was collected, lyophilized (Dura Frezz Dryer, Kinetics). The relative laccase activity was analyzed by monitoring the oxidation of ABTS at 420 nm (ε_{420} = 36 000 $M^{-1}cm^{-1}$) at pH = 4.5 and 45 ± 1 °C using a Varian Cary-50 UV−vis spectrophotometer. Enzyme activity unit of laccase was defined as the amount of enzyme required to oxidize 1 µmol of ABTS within 1 min under assay conditions. The measurements were performed in triplicate.

Enzymatic degradation optimization

Crude laccase-mediated degradation of CIP was performed in 50 mL Falcon tubes, containing 100 mM phosphate buffer, pH 6.5 to imitate the real wastewater conditions. The concentration of lyophilized powder of crude laccase was optimized (0.08 mg/mL – 4 mg/mL), along with the presence of mediators,

i.e. ABTS and SA at concentration 0.4-2.0 mM. About 1 mg of lyophilized crude laccase dissolved in 1 ml of deionized water, gave the activity of 0.1 U/mL. All the experiments were conducted for 6 hours at 25˚C, 100 rpm in triplicates.

A comparison test with laccase purified from *T. versicolor* was performed (Sigma Aldrich, Oakville, Canada). The activity of purchased powder was 0.5 U/mg. The test was carried out in 50-ml Falcon tubes in 100 mM phosphate buffer pH 6.5 and 1 mg/L of CIP. The optimized concentration of mediator was added. Final activity of pure and crude laccase was 1 U/ml. The experiment was conducted for 24 hours at 25˚C, 100 rpm in triplicates.

Before analyzing residual CIP concentration, all samples were deproteinized by incubation at 100˚C for 5 min. Subsequently, they were centrifuged (2 min, 9659 x g) and the supernatant was analyzed by LC-MS/MS.

Antimicrobial activity of transformation products

Escherichia coli (NRRL-3707) was used as a model microorganism to evaluate the antimicrobial activity of transformation products. Firstly, the *E. coli* strain was revived as suggested by Agricultural Research Service (NRRL) Culture Collection (tryptone 5 g/L, yeast extract 5 g/L, K_2HPO_4 1 g/L, glucose 1 g/L). Bacteria were incubated for 24 h, 28˚C, 150 rpm. Then, *E. coli* was streaked onto Luria agar (LA) plates (tryptone 10 g/L, yeast extract 5 g/L, NaCl 10 g/L, agar 1.5 % w/v) and incubated for 24 h at 37˚C. The plates were maintained at 4˚C till further use.

The samples of 1 mg/L CIP degradation by enzymatic oxidation were collected. Agar well diffusion method was used to evaluate the antimicrobial activity of transformation products [17]. The overnight *E. coli* culture was inoculated onto LA plates and subsequently, wells are punched aseptically (6-7 mm) with sterile tip. Then, 50 µl of tested solutions (controls, enzymatic oxidation) were added to the wells and incubated for 24h at 37˚C. After the incubation time, the inhibition zones were measured, and the inhibition index was calculated according to equation 20.

Determination of CIP concentration

The concentration of CIP was analyzed by liquid chromatography-electrospray ionization- tandem mass spectrometry (LC-MS/MS). The system included a Finnigan surveyor LC pump coupled with TSQ Quantum access triple quadruple mass spectrometer (Thermo Scientific, Mississauga, ON, Canada) and electrospray ionization interface. A 10 µL aliquot of the processed sample was injected into the BetaBasic-18 column (100 mm x 2.1 mm x 3 µm) with the flow rate set at 0.2 mL/min. The column oven was set at 40˚C. Ciprofloxacin-d_8 was used as the internal standard. It was added to each sample before the analyses to give the final concentration of 50 µg/L. The samples were eluted with a mobile phase which included 0.1% formic acid (mobile phase A) and acetonitrile combined with 0.1 % formic acid (mobile phase B). The gradient elution started with 90% of mobile phase A and 10% of mobile

phase B. It was constant till 0.5 min and then mobile phase A started gradually decrease (30%) up to 3 min. Subsequently, the gradient was kept constant until 8 min and then it came back to the initial set up. The mass spectrometer was operated in SRM positive mode. Spray voltage was set at 4000 V and skimmer off-set at 20 V. Collision gas pressure was 1.5 mTorr. The capillary temperature was at 350˚C. The MS/MS parameters for CIP and CIP-d_8 analysis are presented in Table 4.2.1.

Table 4.2. 1 MS/MS parameters for CIP and CIP-d_8 analysis

Compound	Precursor ion mass (Da) $[M+H]^+$ (m/z)	Product ion mass (Da) (m/z)	Collision energy (V)
Ciprofloxacin	332.3	245.3	17
Ciprofloxacin-d_8	340.3	249.3	19

Statistical analysis

The statistical analysis was performed via SigmaPlot 13.0 software. The data were presented as a mean of replicates (n= 3) ± standard deviation. One-way ANOVA was used to evaluate statistically significant difference (p-values < 0.05).

Techno-economic estimation

The economic study included the cost of chemicals and energy consumption. The electricity cost was estimated to be USD 0.15 per kWh. The energy consumption (E_C, kWh) was calculated using equation 22:

$$E_c = \frac{P \cdot t}{1000} \qquad \text{Eq. 22}$$

Where P stands for power and t is treatment time. The calculation related to the cost of laccase production was based on work of Osma et al. (2011) [18].

Results and discussion

Effect of the mediators

The potential of crude laccase to remove CIP was tested with and without redox mediators. The results are presented in Figure 4.2.1. The crude laccase itself was not able to transform CIP from media which can be connected to its chemical structure [13]. The similar results were obtained by Parra Guardado et al. (2019), when the crude laccase obtained from *Pycnoporus sanguineus*, grown on tomato media, was not able to degrade CIP [14].

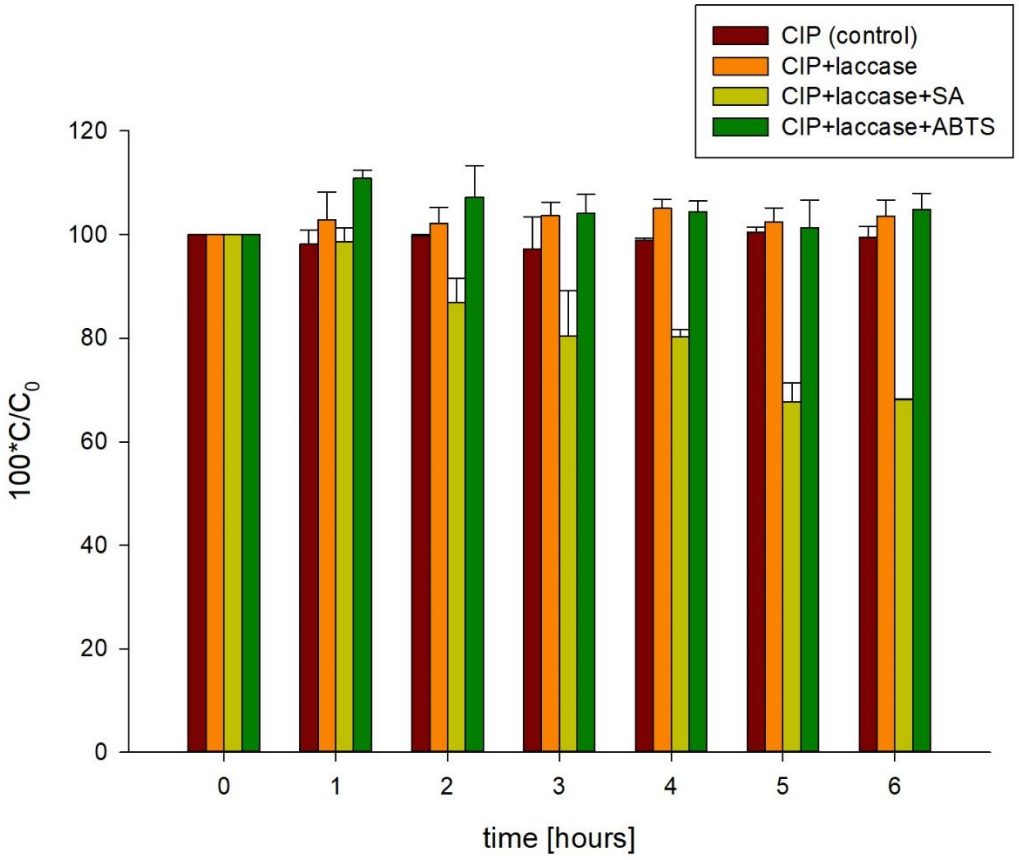

Figure 4.2. 1 Different CIP treatments via crude laccase oxidation; 1 mg/L CIP, 2 mg/ml crude laccase, phosphate buffer pH 6.5, 25˚C, 200 rpm, 0.8 mM mediators (syringaldehyde, ABTS); C – concentration of CIP in time, C_0 – initial concentration of CIP

To expand the enzyme-substrate range, the redox mediators are used to produce highly reactive radicals [13]. However, the addition of ABTS, well known synthetic laccase mediator, did not induce enzymatic oxidation. On the other hand, the addition of SA, naturally occurring mediator, led to decrease of CIP concentration up to 68.09±0.12% in 24 h (fig. 4.2.1). The ABTS and SA alone (without laccase) did not affect CIP concentration (data not shown). The results are in compliance with the study conducted by Parra Guardado et al. (2019) [14]. ABTS was not able to promote oxidation of CIP when the addition of SA resulted in 60% CIP removal in 8 h. Ding et al. (2016) reported that SA-mediated laccase oxidation was ineffective to degrade CIP [19]. Moreover, the study of Prieto et al. (2011) presents that the addition of ABTS to purified laccase led to 97.7% of CIP removal [20]. Another study reported that crude extract from *P. sanguineus* containing laccase led to 85% removal of CIP in 72 hours when ABTS was added [21]. The differences between obtained results may be due to the various oxidation conditions, different fungal strains and usage of purified laccase by most of the authors, whereas in this study the crude laccase was applied.

Optimization of enzymatic oxidation

The influence of SA concentration on crude laccase performance was also investigated. The results are presented in Figure 4.2.2A. The increase of SA concentration beyond 0.8 mM did not give significant improvement with removal efficiency (p-value = 0.38). Ding et al. (2016) presented similar results; the removal efficiency would not improve even when the SA concentration was at 2 mM [19].

The various crude laccase concentrations were also tested (Fig. 4.2.2B). The highest removal of CIP was obtained when the crude enzyme was at concentration 2 mg/ml. Interestingly, the increase in the concentration of lyophilized powder did not significantly increase removal efficiency (p-value = 0.37). Analogous interaction was observed by other researchers [16, 22]. For instance, degradation efficiency of carbamazepine increased when crude laccase activity was at 60 U/L, but decreased when activity was set at 80 U/L. It can be associated with enhancement of the collisions and interactions between enzymes of crude extract, when the laccase concentration is increased, which may lead to blockage of their active sites and decrease of enzyme's efficiency [16]. Lonappan et al. (2017) observed that increase of crude laccase activity up to 500 U/L led to almost complete diclofenac removal after 24 hours [22]. However, a further increase of enzyme activity did not enhance the compound's removal efficiency; higher activities of crude laccase led to almost complete degradation around the same time [22].

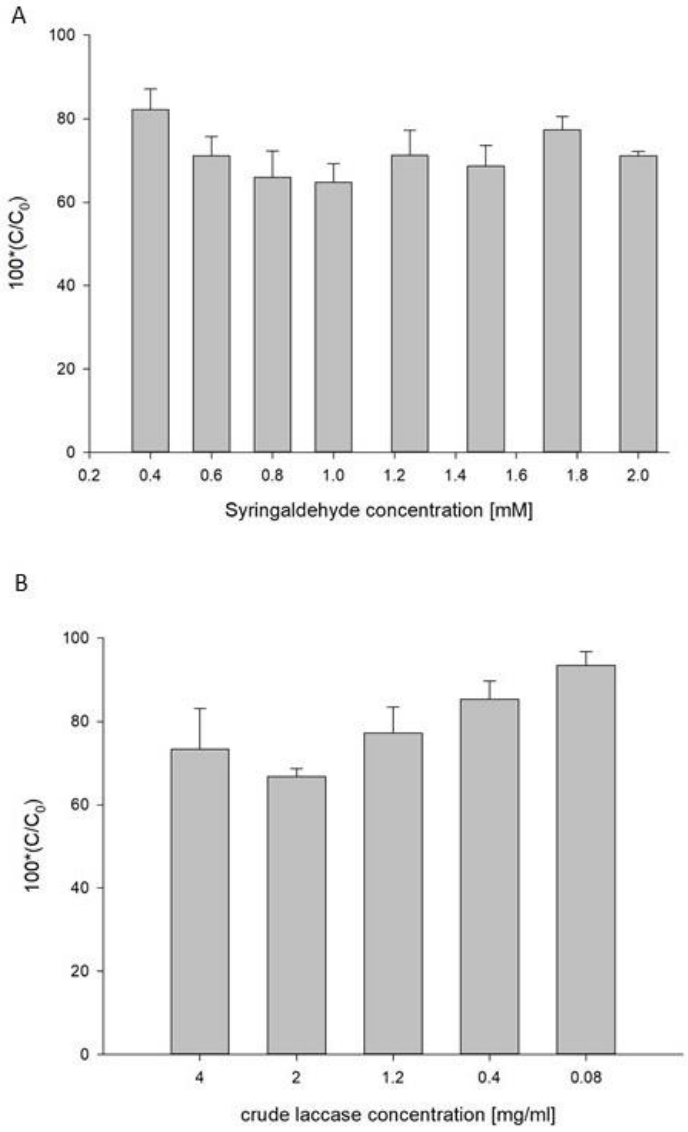

Figure 4.2. 2 Optimization of CIP removal via crude laccase (1 mg/L CIP, phosphate buffer pH 6.5, 25˚C, 200 rpm, 6 h) [A]. Different syringaldehyde concentrations (crude laccase 2 mg/ml); and [B]. crude laccase concentration (SA 0.8 mM)

Kinetics of CIP degradation

Figure 4.2.3 presents the enzymatic removal of CIP with optimized conditions. As can be seen, after 6 hours no significant difference in CIP concentration was observed (p-value >0.05). Hence, after CIP reaches around 30% of removal, the crude laccase is not able to proceed with the transformation of the compound. The activity of laccases may be inhibited by small anions, i.e. halides, halides, fluoride, cyanides or hydroxides, which bind to two copper atoms in catalytic center, resulting in disruption of electron transfer [23]. Hence, one can suspect that during enzymatic oxidation of CIP, the transformation product is formed which has an ability to inhibit the catalytic properties of crude enzyme. The crude laccase obtained from *T. versicolor* grown on apple pomace was tested before in our group for the

potential removal of other pharmaceuticals. The produced enzyme was able to efficiently remove chlortetracycline [24], carbamazepine [16] or diclofenac [22] without inhibition of laccase activity.

The comparison between the performance of crude and pure laccase was investigated. The results are presented in Figure 4.2.3. Pure laccase was able to remove around 50% of CIP in 6 hours. Moreover, the enzymatic oxidation continued, even though the oxidation was slower (fig. 4.2.3). After 24 h of treatment, the concentration of CIP decreased to around 14%. Hence, generated transformation products did not result in inhibition of pure enzyme activity. It suggests, that specifically CIP transformation products generated by crude extract can alter enzyme activity or CIP is degrading via enzymatic cascade and the products are rate limitation factor [25, 26]. *T. versicolor*, apart from laccases, produces other enzymes, that exhibit potency to transform xenobiotics, mainly lignin peroxidase and manganese peroxidase [27]. However, during solid-state fermentation, the activity of these enzymes were not detected [16]. Moreover, Gao et al (2018) reported that crude extract from *Phanerochaete chrysosporium*, containing these enzymes, was not able to remove CIP [21]. Further studies are required to understand the exact mechanism.

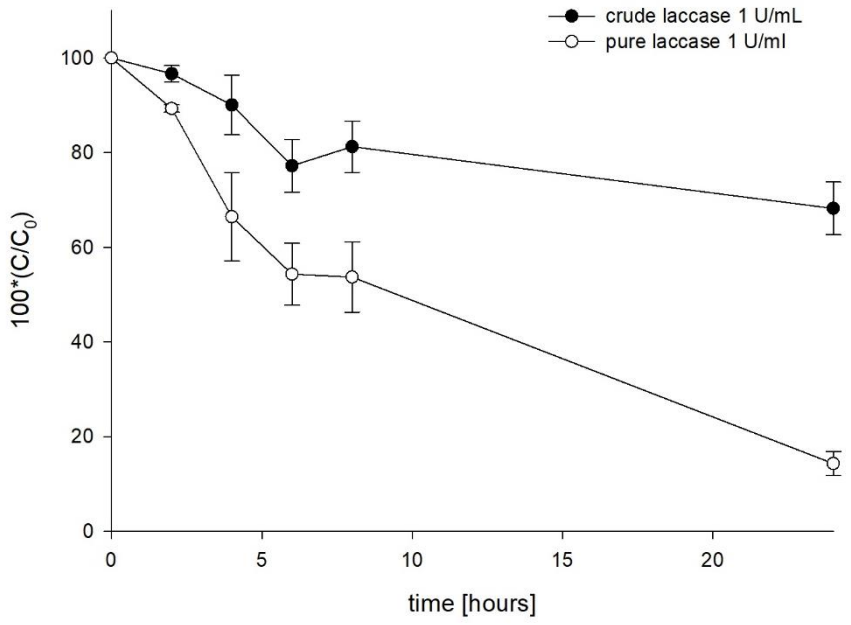

Figure 4.2. 3 Comparison of removal performance between crude and pure laccase; C – concentration of CIP in time, C_0 – initial concentration of CIP

Since the laccase-mediated removal was observed only in the first 6 hours, this period was chosen to plot logarithmic concentration versus time. The results are presented in Figure 4.2.4. As can be seen, the CIP removal followed first-order kinetics (R^2=95%). The rate constant k_1 was determined as 0.03 h^{-1}.

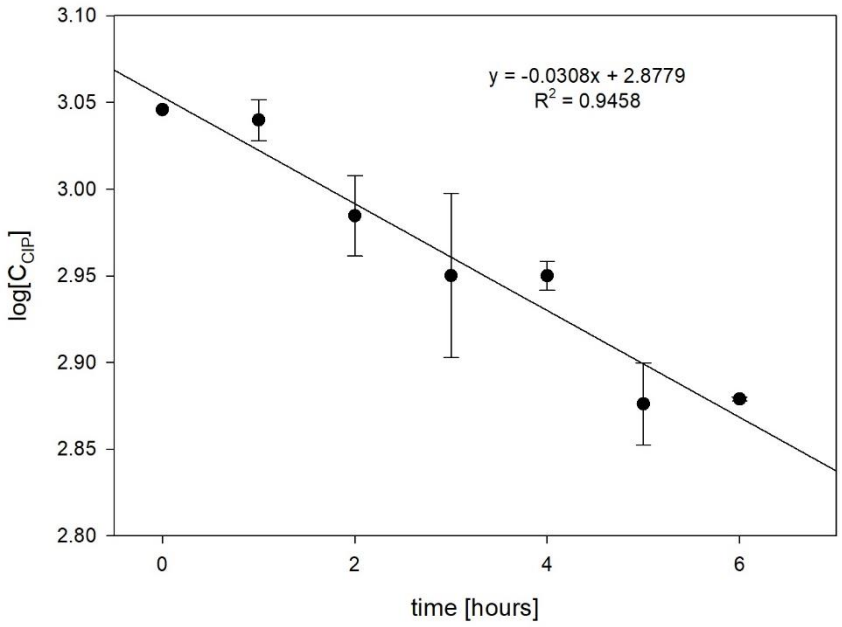

Figure 4.2. 4. A plot of logarithmic concentration versus time of CIP enzymatic oxidation (1 mg/L CIP, 0.8 mM SA, pH 6.5, 25˚C)

Antimicrobial activity of transformation products

Figure 4.2.5 presents the inhibition index of the treated solution, which contains CIP and its transformation products. The treatment of CIP with crude laccase resulted in around 25-30% decrease of antimicrobial activity in 6 hours. Then, the affinity of CIP and its transformation products remain constant throughout time. It may be attributed to remaining CIP residues (~750 mg/L). Moreover, the transformation products generated during enzymatic oxidation after 6 hours of treatment did not contribute to an increase in overall antimicrobial activity. Crude extract and mediator did not exhibit any antimicrobial potency.

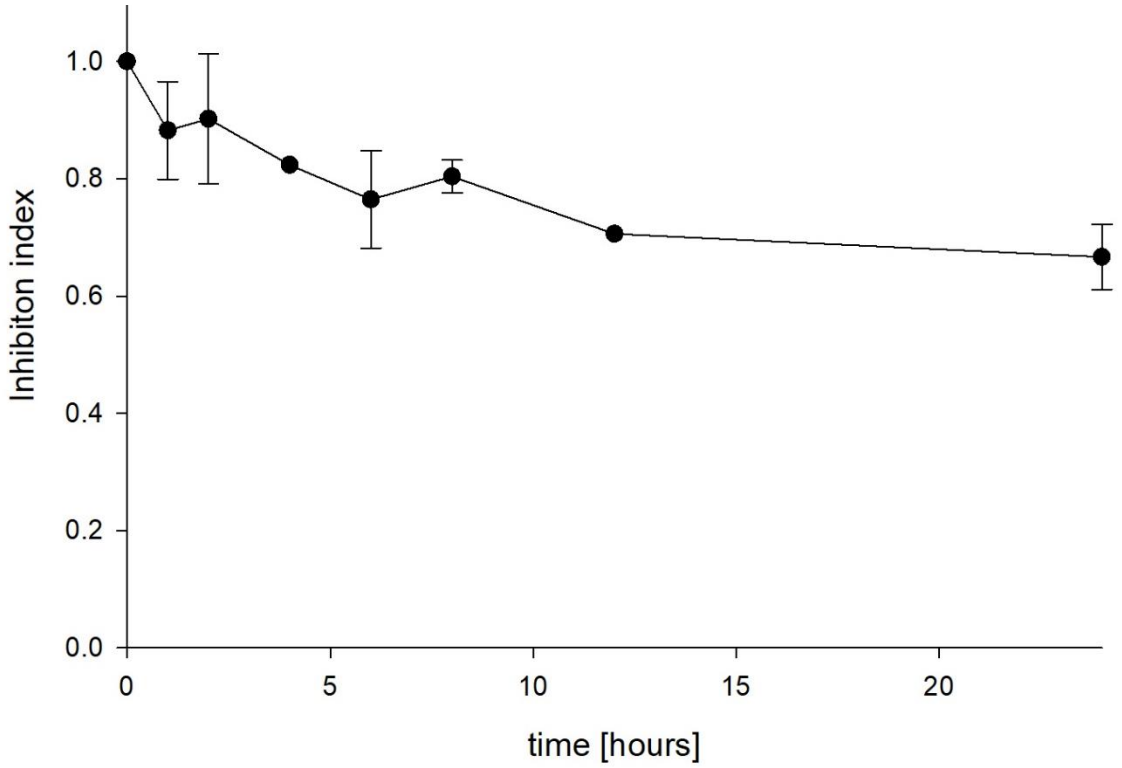

Figure 4.2. 5 Inhibition index of CIP as the function of time

Techno-economic estimation: crude laccase vs pure laccase treatment

Cost estimation of crude laccase production

Firstly, to compare crude laccase treatment with pure laccase treatment, there is a need to estimate the price of crude laccase. Three terms were taken under consideration: material cost ($Cost_M$), equipment cost ($Cost_{eq}$) and operation cost ($Cost_{op}$). The prices of materials and equipment, along with their specification are shown in Table S1 (Annex E). The material cost was calculated for one cycle (=13 days) of crude laccase production. The calculations regarding solid-state fermentation were based on previous work from our research group [16].

The $Cost_{eq}$ includes the cost of incubator P_i (solid-state fermentation), mixer P_m and centrifuge P_c (enzyme extraction). The lifetime (*LF*) and capacity (*Cap*) of the instrument was taken into the consideration. For instance, the solid-state fermentation lasts 13 days, hence in a year the incubator might be run for 28 cycles. The warranty for the equipment is 2 years, thus 56 cycles can be performed. The capacity of the incubator is around 330 Erlenmeyer flasks (500 mL capacity each). In summary, the following equation has been proposed (eq. 23) [18]:

$$Cost_{eq,incubator} = \frac{P_i}{\frac{t_{ssf}}{365} \cdot LF_{incubator} \cdot Cap_{incubator}} \quad \text{Eq. 23}$$

Where t_{ssf} stands for time of solid-state fermentation. The remaining cost of equipment might be calculated accordingly. However, it can be assumed that mixer and centrifuge capacity depend on incubator capacity. Hence, the general cost equipment may be calculated as follows (eq. 24):

$$Cost_{eq} = \frac{\frac{t}{365}}{Cap_{incubator}} \cdot \left(\frac{P_i}{LF_{incubator}} + \frac{P_m}{LF_{mixer}} + \frac{P_c}{LF_{centrifuge}} \right) \quad \text{Eq. 24}$$

The operational cost was determined as the cost of energy consumption of equipment during one cycle multiplied by electricity cost (eq. 25):

$$Cost_{op,equipment} = E_c \cdot 0.14 \quad \text{Eq. 25}$$

The total operation cost is the sum of $Cost_{op,incubator}$, $Cost_{op,mixer}$ and $Cost_{op,centrifuge}$. The total cost of laccase production ($Cost_{lacc}$) was determined as follows (eq. 26):

$$Cost_{lacc} = \frac{Cost_M + Cost_{eq} + Cost_{op}}{laccase\ activity \cdot V} \quad \text{Eq. 26}$$

Where laccase activity was defined as U/L and *V* stands for the volume of extract. Based on the described calculations, the results are presented in Table 4.2.2. As can be seen, the highest cost can be attributed to material expenses, it accounted for more than 70% of total cost. Similar results were obtained by Osma et al. (2011) [18]. In their study, the material cost ranged between 61-89% of total cost, depending on the type of fermentation. The estimated cost of crude laccase (USD/U) was almost 4-fold lower than the price for commercial laccase (Table 4.2.2). However, the calculations did not include all industrial aspects, like packaging, manpower, storage or distribution. The crude laccase production from *Phanerochaete chrysosporium* grown on apple pomace was estimated to cost around 0.02 USD/U, thus comparable with the price obtained in this study [28]. On the other hand, the calculation of Gassara F. (2012) included one additional step of enzyme formulation [28]. According to Osma et al. (2011), the production of laccases from mandarins waste was below 1 cent [18]. However, their study did not include the enzyme extraction.

Table 4.2. 2 Cost analysis of crude laccase production and comparison with commercial laccase price

Parameter	Crude laccase [this study]	Commercial laccase (supplier: Sigma Aldrich)
***Cost*$_{eq}$ [USD]**	1.09	-
***Cost*$_{op}$ [USD]**	74.45	-
***Cost*$_{M}$ [USD]**	2.93	-
Total cost [USD]	78.47	-
Price [USD/g]	-	105
Laccase activity	1800 U/L	500 U/g

***Cost*$_{lacc}$ [USD/U]**	0.05	0.21
Cost/removal efficiency ratio	439	483

The cost of both enzymes, i.e. crude laccase obtained in this study and pure laccase purchased from Sigma Aldrich (Canada), is based on lab-scale fermentation and does not account for bulk production. Hence, once the system will be scaled up, the price of laccase (USD/U) would decrease due to automatization of the process, decreased time of fermentation and continuous extraction of the enzyme [29]. For instance, the cost of pure laccase purchased in bulk can range between 10^{-7} – 10^{-5} USD/U (Xi'an Huisun bio-Tech Co., Novozymes). Hence, presented calculation should be treated as an estimate.

CIP removal from water

For the total cost of wastewater treatment, the only variable for laccase-mediated system (crude vs pure) is material cost. Hence, the comparison, between estimated costs regarding material cost to treat 1 m^3 of water and removal efficiency of crude and pure laccase used in this study, is presented in Figure 4.2.6. Expanses connected to crude laccase-mediated treatment are lower than for pure laccase-mediated system, but the treatment by pure laccase is more efficient. Overall, based on the cost/removal efficiency ratio (Table 4.2.2), crude laccase mediated system is more economically feasible than pure laccase.

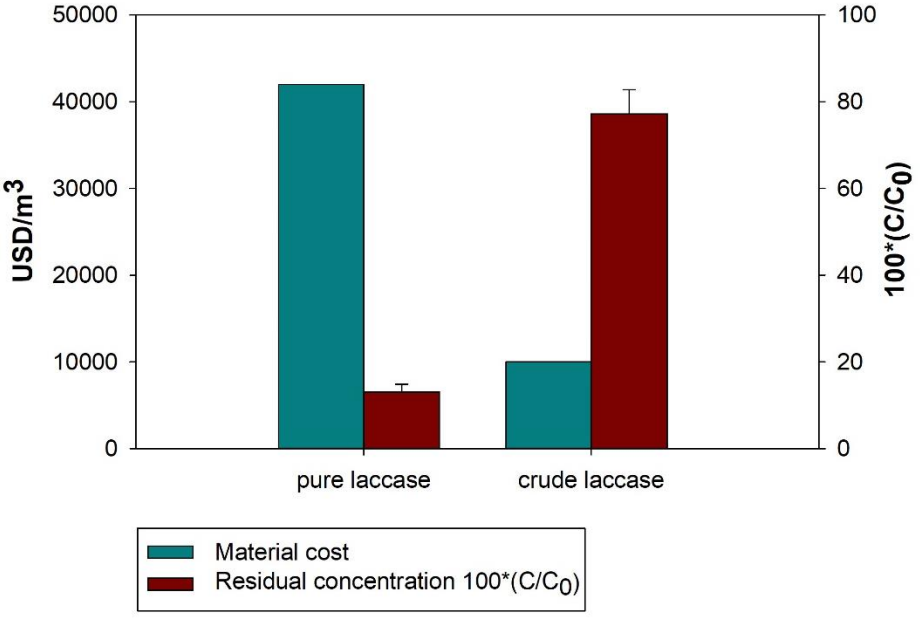

Figure 4.2. 6 Comparison between material cost to treat m^3 of solution and removal efficiency of two laccase-mediated systems

Comparison of crude laccase potency obtained from T. versicolor to remove other pollutants

The wastewater and wastewater sludge are complex matrices containing various kinds of organic and inorganic pollutants [1]. Pharmaceuticals are one of the most concerning group of contaminants present in water systems. Enzymatic oxidation was proposed as cost-effective, eco-firendly removal method.

Table 4.2.3 presents the comparison between various pharmaceuticals removal potency of crude laccase obtained from *T. versicolor* via solid fermentation from agro-industrial waste, apple pomace. Diclofenac and chlortetracycline were efficiently removed without any mediator; their removal efficiency was 100% and 87% respectively (Table 4.2.3). Crude laccase alone was able to transform only 30% of carbamazepine. However, once ABTS was added, the compound was almost completely removed (95%). As described above, CIP was not susceptible to laccase-mediated oxidation (fig. 4.2.1.). Moreover, the type of mediator also played a role; the addition of ABTS did not promote the enzymatic transformation of the antibiotic. Only the SA-mediated reaction was able to oxidize CIP.

Table 4.2. 3 Comparison of pollutants removal potency of crude laccase obtained from *T. versicolor* via solid-state fermentation from apple pomace

Compound	Crude laccase activity [U/L]	Mediator's concentration [μM]	Conditions	Removal efficiency [%]	References
Carbamazepine (anticonvulsant medication)	60	NM	35 °C, 24 h, pH 6.0, DI water	30	[16]
		18 (ABTS)	1 mg/L of pollutant	95	
Ciprofloxacin (fluoroquinolone antibiotic)	200	800 (SA)	25°C, 24 h, pH 6.5, 100 rpm phosphate buffer	32	This study
		800 (ABTS)	1 mg/L of pollutant	No removal	
Chlortetracycline (tetracycline antibiotic)	0.5	NM	21°C, 48 h, pH 7.5, 150 rpm wastewater	87	[24]
			2 mg/L of pollutant		
Diclofenac (nonsteroidal anti-inflammatory drug)	500	NM	25°C, 24 h, pH 6.5, 150 rpm, DI water	100	[22]
			1 mg/L of pollutant		

ABTS - 2,2'-azino-bis(3-ethylbenzothiazoline-6-sulphonic acid); NM – no mediator; SA - syringaldehyde

In general, the type of functional groups of substrates plays an important role in laccase-mediated oxidation [13]. The presence of electron-donating functional groups (-OH, $-NH_2$, -RO, -COR) promotes laccase-mediated oxidation, when electron-withdrawing functional groups (-C=O, -C=C-, -COOH, $-CONH_2$, halogens) may lead to steric shield formation and restrict the electron availability, hence unable the oxidation [13]. Carbamazepine and CIP contain strong electron-withdrawing groups, i.e. amide group (carbamazepine) carboxylic acid, ketone, and fluoride (CIP), hence it is not surprising that they are recalcitrant to laccase-mediated oxidation [14]. Moreover, ABTS radical instability might be a

potential explanation for insufficient ABTS-mediated laccase oxidation. $ABTS^{\cdot+}$ transforms into its $ABTS^{2+}$ and can no longer act as the mediator [14, 30]. On the other hand, SA radical is stabilized via two methoxy groups in its structure, making it more stable than $ABTS^{\cdot+}$ [31].

Structure of chlortetracycline, on the other hand, includes five electron-donating hydroxyl groups along with one tertiary amine, which makes it susceptible to laccase oxidation, despite the presence of electron-withdrawing groups. In diclofenac's structure, two chlorine atoms are found, but the compound is still more susceptible to enzymatic transformation than carbamazepine and CIP.

Taheran et al. (2017) tested the potency of immobilized crude laccase from *T. versicolor* to degrade diclofenac, carbamazepine, and chlortetracycline [32]. The removal efficiency was found to be 73%, 63% and 49% for diclofenac, chlortetracycline, and carbamazepine, respectively. More studies and optimization regarding the simultaneous removal potency of various contaminants should be performed to fully understand the potency of the crude enzymatic extract.

Conclusions

The crude laccase extract, obtained from *T. versicolor* grown on agro-industrial waste, was tested toward CIP transformation in aquatic media. The crude enzyme was able to remove 32% of the antibiotic in 6 hours. Further enzymatic oxidation did not lead to a decrease in CIP concentration. The comparison between pure and crude laccase was performed, however, oxidation via pure laccase did not exhibit any inhibitory effect. Moreover, pure laccase was able to efficiently remove 85% of CIP in 24 h. That suggests that with crude extract CIP might be transformed via enzymatic cascade and generated transformation products might be rate-limiting factors. During the oxidation of CIP via crude laccase, the antimicrobial activity towards *E. coli* was decreasing. Once the enzymatic reaction was hindered, the treated solution still exhibited antimicrobial potency, however, it remained constant. Most of the estimated costs of enzyme production were accounted for material cost. Other solutions should be investigated to decrease expenses. Even though CIP was not removed only to some extent, other studies reported the high removal efficiency of other pharmaceuticals via tested enzymatic extract. Thus, more studies are needed to evaluate the potency of crude laccase obtained from *T. versicolor* to transform the mixture of various contaminants.

Acknowledgments

We are sincerely thankful to the Natural Sciences and Engineering Research Council of Canada (Discovery Grant 355254 and NSERC Strategic Grant). We also would like to thank James and Joanne Love Chair in Environmental Engineering for support and collaboration. We would like to also thank Mr. Stephane Moise for his technical support with Liquid Chromatography analysis. We would like to thank Pratik Kumar, MTech. and Rama Pulicharla, PhD for her suggestions regarding technoeconomic assessment.

References

1. Archer, E., et al., The fate of pharmaceuticals and personal care products (PPCPs), endocrine disrupting contaminants (EDCs), metabolites and illicit drugs in a WWTW and environmental waters. Chemosphere, 2017. **174**: p. 437-446.

2. Blanco, G., A. Junza, and D. Barron, Occurrence of veterinary pharmaceuticals in golden eagle nestlings: Unnoticed scavenging on livestock carcasses and other potential exposure routes. Sci Total Environ, 2017.

3. Berkner, S., S. Konradi, and J. Schönfeld, Antibiotic resistance and the environment—there and back again. EMBO Reports, 2014. **15**(7): p. 740-744.

4. Cuprys, A., et al., Fluoroquinolones metal complexation and its environmental impacts. Coordination Chemistry Reviews, 2018. **376**: p. 46-61.

5. Van Doorslaer, X., et al., Fluoroquinolone antibiotics: an emerging class of environmental micropollutants. Sci Total Environ, 2014. **500-501**: p. 250-69.

6. An, T., et al., Kinetics and mechanism of advanced oxidation processes (AOPs) in degradation of ciprofloxacin in water. Applied Catalysis B: Environmental, 2010. **94**(3): p. 288-294.

7. Rahmani, A.R., et al., A combined advanced oxidation process: Electrooxidation-ozonation for antibiotic ciprofloxacin removal from aqueous solution. Journal of Electroanalytical Chemistry, 2018. **808**: p. 82-89.

8. Wang, F., et al., Removal of ciprofloxacin from aqueous solution by a magnetic chitosan grafted graphene oxide composite. Journal of Molecular Liquids, 2016. **222**: p. 188-194.

9. Wu, Q., et al., Adsorption and intercalation of ciprofloxacin on montmorillonite. Appl Clay Sci, 2010. **50**(2): p. 204-211.

10. Xiao, Q.M., J.W. Wang, and Y.L. Tang, [Degradation and bioaccumulation characteristics of ciprofloxacin in soil-vegeTable system]. Ying Yong Sheng Tai Xue Bao, 2012. **23**(10): p. 2708-14.

11. Kruglova, A., et al., Biodegradation of ibuprofen, diclofenac and carbamazepine in nitrifying activated sludge under 12°C temperature conditions. Science of The Total Environment, 2014. **499**: p. 394-401.

12. Naghdi, M., et al., Removal of pharmaceutical compounds in water and wastewater using fungal oxidoreductase enzymes. Environmental Pollution, 2018. **234**: p. 190-213.

13. Yang, J., et al., Laccases: Production, Expression Regulation, and Applications in Pharmaceutical Biodegradation. Front Microbiol, 2017. **8**: p. 832.

14. Parra Guardado, A.L., et al., Effect of redox mediators in pharmaceuticals degradation by laccase: A comparative study. Process Biochemistry, 2019. **78**: p. 123-131.

15. Gassara, F., et al., Screening of agro-industrial wastes to produce ligninolytic enzymes by Phanerochaete chrysosporium. Biochemical Engineering Journal, 2010. **49**(3): p. 388-394.

16. Naghdi, M., et al., Biotransformation of carbamazepine by laccase-mediator system: Kinetics, by-products and toxicity assessment. Process Biochemistry, 2018. **67**: p. 147-154.

17. Balouiri, M., M. Sadiki, and S.K. Ibnsouda, Methods for in vitro evaluating antimicrobial activity: A review. Journal of Pharmaceutical Analysis, 2016. **6**(2): p. 71-79.

18. Osma, J.F., J.L. Toca-Herrera, and S. Rodriguez-Couto, Cost analysis in laccase production. J Environ Manage, 2011. **92**(11): p. 2907-12.

19. Ding, H., et al., Simultaneous removal and degradation characteristics of sulfonamide, tetracycline, and quinolone antibiotics by laccase-mediated oxidation coupled with soil adsorption. Journal of Hazardous Materials, 2016. **307**: p. 350-358.

20. Prieto, A., et al., Degradation of the antibiotics norfloxacin and ciprofloxacin by a white-rot fungus and identification of degradation products. Bioresour Technol, 2011. **102**(23): p. 10987-95.

21. Gao, N., et al., Simultaneous removal of ciprofloxacin, norfloxacin, sulfamethoxazole by co-producing oxidative enzymes system of Phanerochaete chrysosporium and Pycnoporus sanguineus. Chemosphere, 2018. **195**: p. 146-155.

22. Lonappan, L., et al., Agro-industrial-Produced Laccase for Degradation of Diclofenac and Identification of Transformation Products. ACS Sustainable Chemistry & Engineering, 2017. **5**(7): p. 5772-5781.

23. Call, H.P. and I. Mücke, History, overview and applications of mediated lignolytic systems, especially laccase-mediator-systems (Lignozym®-process). Journal of Biotechnology, 1997. **53**(2): p. 163-202.

24. Pulicharla, R., et al., Degradation kinetics of chlortetracycline in wastewater using ultrasonication assisted laccase. Chemical Engineering Journal, 2018. **347**: p. 828-835.

25. Kuk, S.K., et al., Photoelectrochemical Reduction of Carbon Dioxide to Methanol through a Highly Efficient Enzyme Cascade. Angewandte Chemie International Edition, 2017. **56**(14): p. 3827-3832.

26. Lorenzo, M., et al., Inhibition of laccase activity from Trametes versicolor by heavy metals and organic compounds. Chemosphere, 2005. **60**(8): p. 1124-1128.

27. Asgher, M., et al., Recent developments in biodegradation of industrial pollutants by white rot fungi and their enzyme system. Biodegradation, 2008. **19**(6): p. 771.

28. Gassara, F., Production économique d'enzymes ligninolytiques par fermentation à l'état solide des déchets agroindustriels et leurs applications, in Institut national de la recherche scientifique. 2012, University of Quebec: Quebec. p. 317.

29. Nüske, J., et al., Large scale production of manganese-peroxidase using agaric white-rot fungi. Enzyme and microbial technology, 2002. **30**(4): p. 556-561.

30. Kurniawati, S. and J.A. Nicell, Efficacy of mediators for enhancing the laccase-catalyzed oxidation of aqueous phenol. Enzyme and Microbial Technology, 2007. **41**(3): p. 353-361.

31. Canas, A.I. and S. Camarero, Laccases and their natural mediators: biotechnological tools for sustainable eco-friendly processes. Biotechnol Adv, 2010. **28**(6): p. 694-705.

32. Taheran, M., et al., Covalent Immobilization of Laccase onto Nanofibrous Membrane for Degradation of Pharmaceutical Residues in Water. ACS Sustainable Chemistry & Engineering, 2017. **5**(11): p. 10430-10438.

PART 3

Functionalized adsorbent for simultaneous removal of heavy metal ions and ciprofloxacin

Agnieszka Cuprys[a], Joseph Sebastian[a], Zakhar Maletskyi[b], Tarek Rouissi[a], Harsha Ratnaweera[b], Satinder Kaur Brar[a,b*], Émile Knystautas[c], Patrick Drogui[a]

[a] INRS-ETE, Université du Québec, 490, Rue de la Couronne, Québec, Canada G1K 9A9

[b] Faculty of Science and Technology (REALTEK), Norwegian University of Life Sciences, P.O. Box 5003, 1432 Aas, Norway

[b] Department of Civil Engineering, Lassonde School of Engineering, York University, North York, Toronto, Ontario Canada M3J 1P3

[c] Department of Physics, Physical Engineering and Optics, Laval University, 1045 Avenue de la Médecine, Québec, Canada G1V 0A6

[*] Corresponding author: E-mail: satinder.brar@ete.inrs.ca; Satinder.Brar@lassonde.yorku.ca

Draft (to be submitted)

Résumé

Le biochar est considéré comme un adsorbant écologique et rentable pour la purification de l'eau. Cependant, le biochar cru présente généralement un faible capacité d'absorption vers la plupart des contaminants dissous, ce qui peut être amélioré par sa fonctionnalisation. Les billes de chitosan-biochar (CH-BB) ont été produites et testées pour leur efficacité d'élimination de la ciprofloxacine (antibiotique) et de trois métaux lourds (As, Cd, Pb). La modification du biochar de lisier de porc brut a entraîné une augmentation de sa capacité d'absorption dans presque tous les cas, l'augmentation la plus élevée étant celle de l'As (presque 6 fois) et la plus faible de la Cd (1,02 fois). L'adsorbant a pu éliminer simultanément tous les contaminants ciblés, individuellement et en mélange, à la suite d'une réaction de pseudo-deuxième ordre. L'affinité des contaminants envers CH-BB suivait l'ordre suivant: Pb> Cd >> As> CIP. Lorsque Pb et As étaient présents dans le même mélange, leur efficacité d'élimination augmentait en raison de leur co-précipitation. Les études de co-adsorption ont montré que le mécanisme d'absorption des polluants inorganiques était différent de celui de l'antibiotique.

Mots-clés: ciprofloxacine, plomb, cadmium, arsenic, adsorption, biochar, chitosan

Abstract

Biochar is considered as a green and cost-effective adsorbent for water purification. However, raw biochar generally exhibits low adsorption capacity towards most of dissolved contaminants which can be improved by its functionalization. The chitosan-biochar beads (CH-BB) were produced and tested for their removal efficiency of ciprofloxacin (antibiotic) and three heavy metals (As, Cd, Pb). Modification of raw pig manure biochar resulted in increase of its adsorption capacity in almost all cases, with the highest increment for As (almost 6-fold) and the lowest for Cd (1.02-fold). The adsorbent was able to simultaneously remove all targeted contaminants, individually and in mixture, following pseudo-second-order reaction. The affinity of contaminants towards CH-BB followed the order: Pb>Cd>>As>CIP. When Pb and As were present in the same mixture, their removal efficiency increased due to their co-precipitation. The co-adsorption studies showed that the uptake mechanism of inorganic pollutants was different from that of the antibiotic.

Keywords: ciprofloxacin, lead, cadmium, arsenic, adsorption, biochar, chitosan

Introduction

Pollution caused by pharmaceuticals, especially antibiotics, is an emerging problem with well-documented evidence of environmental risks, particularly in relation to antimicrobial resistance and human health [1]. Fluoroquinolones are a family of broad-spectrum antibiotics, which have been classified as critically important antibacterial agents for human medicine by the World Health Organization due to their increased propensity to develop resistance [2]. Ciprofloxacin (CIP) is one of the most frequently prescribed fluoroquinolone worldwide [3]. Once it enters the human body, up to 65% of CIP can be excreted unmetabolized in the urine and/or feces, and therefore can enter the environment [4].. The presence of CIP in water and soils has led to increased antimicrobial resistance throughout the years [3]. Additionally, it is persistent in nature and not easily biodegradable. In its structure, CIP consists of two ionizable groups, i.e. carboxylic and piperazinyl groups. These groups can interact with metal ions, and form stable CIP-metal complexes [5]. The complexation between antibiotics and metals present in the environment, results in alteration of mobility, solubility and antimicrobial properties of compound [4].

Contamination with metals, especially heavy metals, is considered as a serious environmental threat [6]. Arsenic, lead and cadmium are considered as one of the ten chemicals of major public health concern, listed by the WHO. All of these occur in the environment naturally at lower concentration. However, due to anthropogenic activities, their concentration has increased significantly [6]. Arsenic (As) is a carcinogenic metalloid, detected worldwide in groundwater, surface water or sediments [7]. Due to its high toxicity towards living organisms, including humans, the WHO set a guideline value of 10 μg/L, which is much lower compared to other heavy metals. Lead (Pb) is a toxic metal, found in petrol, paint or plumbing. It has a cumulative toxic effect on many body systems. New legislation was proposed to the European Parliament, that will introduce new guidelines to restrict the maximum limits of selected pollutants, including lead [8]. Cadmium (Cd), similarly to As, is considered as a cancerogenic agent, which is easily accumulated in many organisms. Its exposure to humans is mostly through consumption of contaminated food or inhalation of tobacco smoke.

Furthermore, their co-existence with antibiotics in the environment is highly alarming. The positive correlation between the presence of heavy metals and some antimicrobial-resistance genes has been reported previously [9, 10]. Studies have shown that the genes for resistance to antibiotics and heavy metals s may be linked in the same bacterial plasmid. Thus, the presence of heavy metals and/or certain antibiotics may exert selective pressure on the bacteria and disseminate both types of resistance simultaneously [9, 10]. Moreover, the metal resistance and the antibiotic resistance by microbes can be dominated by cross-resistance [11]. It happens, when two antimicrobial agents target the same microorganism. Together, they initiate the common pathway, that leads to cell apoptosis. Based on the review by Nguyen et al. (2019), metals most commonly associated with antimicrobial resistance were

Cd and Zn [11]. Pb and As also contributed to the dissemination of antimicrobial resistance, although, at lower scale. Hence, it is important to remove both antibiotics and heavy metals from the environment.

Adsorption is one of the most promising removal methods as it is simple, cost-effective, and environment friendly. Biochar is a carbon-rich material obtained by the pyrolysis of biomass, and has gained interest as a potential adsorptive materials they are microporous and have high surface area[12]. Moreover, the production of biochar is economical and less energy-consuming compared to commercially available activated carbon [12]. Biochars have been extensively tested for the removal of various types of contaminants [13-15]. However, raw biochar may exhibit relatively lower adsorption capacity. Hence, various modifications have been tested, i.e. surface activation with steam, acid or alkali, and generation of biochar-based adsorbents with clays, metal oxides, organic compounds, carbonaceous materials or biofilms [16]. Chitosan, one of the most abundant natural polymers, has been used to modify biochar surface [17, 18]. The amine group of chitosan enhances the adsorption capacity of the modified material. Moreover, chitosan, like biochar, is obtained from waste (crustacean waste), and it is considered to be cost-effective and non-toxic [19].

Till date, research has been focused mainly on removal techniques of only one kind of contaminant, i.e. organic or inorganic. Hence, the key objective of this study was to test the potency of chitosan-functionalized biochar to individually and simultaneously remove CIP and three heavy metals, i.e. lead, cadmium and arsenic individually as well as simultaneously. The influence of different pH contact time and contaminant concentration were evaluated. Adsorption studies were performed for targeted pollutants individually and in the mixture. Additionally, the removal efficiency was also measured in real wastewater.

Materials and methods

Materials

Ciprofloxacin (CIP) (98% purity) was purchased from Acros Organics (USA). HPLC-grade methanol (purity > 99.8%) and HPLC-grade acetic acid (purity > 99.7%) were obtained from Fisher Scientific (Ontario, Canada). Low molecular weight chitosan (50-160 kDa, 75-85% deacetylated) and sodium arsenate dibasic heptahydrate (purity >98%) were obtained from Sigma Aldrich (Ontario, Canada). Sodium hydroxide (pellet) and disodium ethylenediaminetetraacetate (Na_2H_2EDTA, 99%) were purchased from Merck (Germany). Cadmium sulfate (purity 98%) and lead sulfate (purity >99.9%) were obtained from VWR. Standards and internal standard for metal detection were purchased from Inorganic venture (Inorganic Ventures, Christiansburg, USA). Nitric acid (65%) was obtained from Normapur and 37% hydrochloric acid from EMSURE. Deionized 18.2MΩ type I water was used for both standards and samples. Lead stock solution was prepared by dissolving lead sulphate in a mixture of 1:1 nitric and hydrochloric acid and its final concentration was determined by ICP-MS. Cadmium stock solution was

prepared by dissolving cadmium sulphate in deionized water with nitric acid. Arsenic stock solution was prepared by dissolving sodium arsenate in deionized water.

Pinewood biochar (PW-BC) and almond shell biochar (AS-BC) were obtained from Pyrovac Inc. (Quebec, Canada). BC-PW was derived by the pyrolysis of a softwood mix of white pine wood (80% v/v), spruce and fir (20%). BC-PW was produced at 525 ± 1 °C under atmospheric pressure for 2 min in an oxygen-free environment. BC-AS was produced by the pyrolysis of almond shells at 520 ± 1 °C for4 h. Pig manure (PM-BC) was donated by Research and Development Institute for Agri-Environment (IRDA), Quebec, Canada. BC-PM was produced by the pyrolysis of the solid fraction of pig slurry at 400 ± 1 °C, 2 h at 15 °C min^{-1} in the presence of nitrogen at a flow rate of 2 L min^{-1} during heating. . The characterization of each biochar was described previously [13, 20]. All biochars were ground to make a fine powder and sieved through a uniform sieve size of 0.25 mm. The prepared biochar samples were preserved at room temperature for further analyses.

Chitosan-biochar beads

Chitosan-biochar beads (CH-BB) were prepared as described by Azfal et al. (2018) with minor modifications [17]. Briefly, 1.67 mg L^{-1} of chitosan was dissolved overnight in 2% acetic acid. Biochar was added (1:1 biochar: chitosan) and the mixture was stirred for 2 hours. The prepared suspension was then added dropwise to 0.6 M NaOH and left overnight. Generated beads were then separated and repeatedly washed to remove the excess NaOH. Subsequently, the beads were dried and kept at room temperature for further use.

CH-BH characterization

The morphology of CH-BH was obtained via scanning electron microscopy (SEM) (CarlZeissEVO®50). SEM micrographs were captured at 10 kV accelerating voltage. The samples were not gold coated. The zeta potential was determined by the Malvern Zetasizer Nano-ZS particle analyzed. Fourier-transform infrared spectroscopy (FT-IR) spectra of adsorbent before and after adsorption was obtained via FT-IR (Nicolet FT-IR system, Thermofisher Scientific). The spectra were obtained at a resolution of 4 cm^{-1}, in the range of 4000-400 cm^{-1}. The surface area was investigated using N_2 adsorption isotherms and using Brauner-Emmett-Teller (BET) method to evaluate mesopore-enclosed surface area. The metal leaching test from CH-BB was performed. Around 0.1 g of beads were added to 100 ml of deionized water, and the solution was left at room temperature for 48 h. Metal concentration was then analyzed via inductively coupled plasma mass spectrometry (ICP-MS) (Agilent Technologies 8800 ICP-MS Triple Quad).

Adsorption experiments

The initial adsorption capacity of generated biochars was tested in batch sorption experiments. All experiments were conducted at 20±1 ˚C, pH 6.0, 150 rpm in an orbital shaker (PSU-20i Multi-functional Orbital Shaker, Biosan) unless stated otherwise. Blank experiments were included. About 0.05 g of

biochar was added to a 100-ml container and mixed with 50 ml solution of each contaminant (10 mg/L for CIP, As and Cd or 1 mg/L for Pb). Lower concentration of Pb ions was kept to avoid the precipitation of the salt due to circumneutral pH. Biochar with the highest adsorption capacity was then used to generate CH-HB (Section 2.2). For kinetic studies, adsorption experiments were performed individually (1 mg/L of metal or CIP) and in a mixture (1 mg/L each of metals and CIP). The influence of pH (5.0-9.0) on adsorption capacity was tested for each contaminant, where the initial concentration was 10 mg/L for CIP, As, Cd and 1 mg/L of Pb. To obtain sorption isotherms CH-HB was shaken with contaminants individually and in mixture, in a range of of 2-100 mg/L (CIP, As, Cd) or 0.5-2 mg/L (Pb). All samples were filtered through 0.22 μm PFTE syringe filters (VWR) and the filtrate was further diluted accordingly before measurement. Metal concentrations were estimated via ICP-MS (Agilent Technologies 8800 ICP-MS Triple Quad). CIP concentration was measured via UV-Vis spectrophotometry (UV-T500Pro) at a wavelength of 278 nm. CIP absorbance is influenced by presence of metal ions in matrix [21]. The metals present in biochar and beads may leach into solution (Table S1). Hence, to avoid false negative and/or false-positive results, all samples with CIP were diluted with 0.1 M HCl (1:1) to protonate CIP (CIP^+) and release it from metal complexation.

The absorption capacity of ciprofloxacin/metals, q_e (mg/g) was calculated by using Eq. (27).

$$q_e = \frac{(C_0 - C_e)V}{m} \quad \text{Eq. 27}$$

where C_0 and C_e are the concentrations of ciprofloxacin/metals (mg/L) before and after adsorption, V is the initial solution volume (L), and m is the weight of adsorbent (g).

ICP

All analyses were performed using an Agilent Technologies 8800 Triple Quad ICP-QQQ with collision/reaction cell (CRC). Instrumental method for simultaneous measurement of As, Cd and Pb with oxygen as reaction gas was provided by Karl Andreas Jensen from Norwegian University of Life Sciences, Faculty of Environmental Sciences and Natural Resource Management. Robust instrument settings together with oxygen reaction gas were chosen due to the high concentrations used in the experiments. A quality control standard was performed every 10-12 samples for instrument drift.

Mass 118 was monitored for mathematical removal of any isobar contribution from natural isotopes of both ^{114}Cd and internal standard ^{115}In. Mo 95 -> 127 was also monitored to verify low interference levels on ^{114}Cd determination from $^{98}Mo^{16}O^+$ and $^{96}Mo^{18}O^+$. Lead was determined as the sum of the three major isotopes as variations from isotopic ratios change depending on the source of lead.

^{208}Pb = M(206->206) + M(207->207) + M(208->208) Eq. 28

^{114}Cd = M(114->114) – M(118->118)*0.0268 Eq. 29

^{115}In = M(115->115) – M(118->118)*0.0140 Eq. 30

Tests in real wastewater

The treated wastewater was taken from pilot scale wastewater treatment plant (NMBU). Samples were spiked with 1 mg/L of As, Cd, Pb and CIP, and the pH was adjusted to 6.0. Adsorption experiments were performed by adding 50 mg of CH-BB to 50 mL of prepared wastewater and shaking for 24h, 150 rpm, at 20±1˚C. To evaluate the removal efficiency of the generated adsorbent, comparison tests between CH-BB, PM-BC and commercial granulated active carbon (GAC, Filtrasorb 400) were performed. PM-BC and GAC were sieved to obtain the same particle size as CH-BB. After adsorption experiments, the samples were filtered through 0.22 μm PFTE syringe filters. The filtrates were then analyzed for heavy metals concentration via ICP-MS-MS. The residual concentration of CIP was detected via liquid chromatography coupled with tandem mass spectrometry (LC-MS/MS).

LC-MS/MS

The system included a Finnigan surveyor LC pump linked to TSQ Quantum access triple quadruple mass spectrometer (Thermo Scientific, Mississauga, ON, Canada) along with electrospray ionization interface. A 10 μL aliquot of the filtrates were injected into BetaBasic-18 column (100 mm x 2.1 mm x 3 μm). The column oven was at 40˚C and the flow rate was set to 0.3 mL/min. Ciprofloxacin-d_8 was selected as the internal standard and was added to each sample to give a final concentration of 50 μg/L before the analyses. Samples were eluted with a mobile phase of 0.1% formic acid (mobile phase A) and acetonitrile with 0.1 % formic acid (mobile phase B). Gradient elution started with 90% of mobile phase A and 10% of mobile phase B. It was constant till 0.5 min, following which, mobile phase A was gradually decreased to 30% up to 3 min. The gradient was kept constant till 8 min and after it was brought back to the initial set up. The mass spectrometer was operated in SRM positive mode. Spray voltage was set at 4000 V, skimmer off-set at 20 V. Collision gas pressure was set at 1.5 mTorr. The capillary temperature was at 350˚C. The collision energy for CIP and CIP-d_8 was set at 17, and 19 V respectively. The precursor and product ions (m/z) were selected as follows: 332.3 and 245.3 for CIP and 340.3 and 249.3 for CIP-d_8.

Statistical analysis

Statistical analysis was performed using SigmaPlot 13.0 software. One-way ANOVA was used to evaluate statistically significant difference (p-values < 0.05). The data were presented as a mean of triplicates ± standard deviation.

Results and discussion

Adsorption onto raw biochar

To generate CH-BB, suitable raw biochar had to be chosen. Depending on the feedstock used, specific biochars with different functional groups that could potentially attract the contaminants were produced

(Figure S1, Annex F) [13]. Hence, the comparison of adsorption capacity s between PW-BC, AS-BC, and PM-BC was carried out (Table 4.3.1). All tested biochars were able to adsorb CIP and heavy metals. PM-BC exhibited the highest adsorption capacity for CIP, which can be attributed to high surface area [13]. The π-π interaction between CIP and PM-BC functional groups possibly contributed to antibiotic adsorption [22]. In a previously reported study, higher removal efficiency was obtained due to adsorption onto PM-BC than PW-BC for another pharmaceutical, diclofenac [13]. On the other hand, PM-BC and PW-BC had the same adsorption capacity for Pb. Almost 100% of this metal was adsorbed onto both biochars, while only 72% of Pb was adsorbed onto AS-BC. PW-BC was also more efficient to remove As from the solution. The potency of PW-BC to adsorb As is consistent with previous reports [23]. AS-BC had the highest adsorption capacity towards Cd ions. Based on the overall results, the PM-BC was selected for the fabrication of CH-BB.

Table 4.3. 1. Adsorption capacity of the tested adsorbents; pH 6.0, 150 rpm, 48 h

Contaminant (initial concentration [mg/L])	Adsorption capacity [mg/g]			
	PM-BC	PW-BC	AS-BC	CH-BB
Ciprofloxacin (10)	1.36±0.02	1.05±0.08	1.23±0.02	1.49±0.06
As (10)	0.24±0.24	0.77±0.15	0.56±0.19	1.38±0.15
Cd (10)	4.88±0.41	1.06±0.08	6.34±0.72	6.49±0.34
Pb (1)	0.99±0.004	0.99±0.001	0.72±0.07	0.95±0.01

Abbreviations: PM-BC – pig manure biochar; PW-BC – pinewood biochar; AS-BC – almond shell biochar; CH-BB – chitosan-biochar beads

CH-BB characterization

SEM images of the fabricated CH-BB are shown in fFigure 4.3.1 A-C. Two surface morphologies can be distinguished in CH-BB: coarse (fig. 4.3.1C) and stratified (fig. 4.3.1B). The coarse area had small pores, which were unevenly distributed, while the stratified surface had many grooves, furrows, and tiny particles. The modification with chitosan changed the surface of raw biochar (comparison based on SEM images from Lonappan et al. (2018) [20]). The point of zero charged was found to be at pH 6.02 (fig. 4.3.1D). Based on the BET analysis, the specific surface area was 42.0 and 36.6 for CH-BB and PM-BC respectively. Thus, CH-BB had higher surface area than PM-BC.

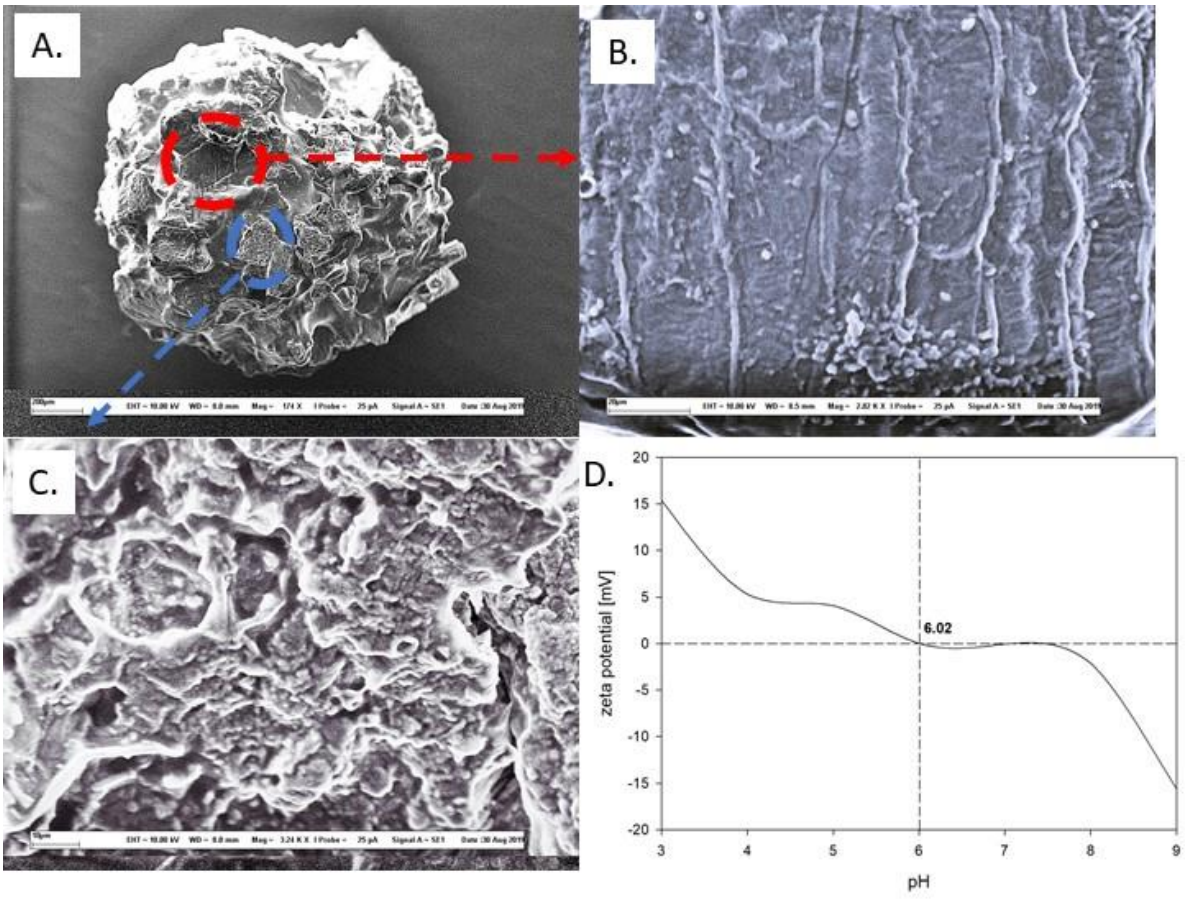

Figure 4.3. 1. SEM images of chitosan-biochar beads (A-C); D. zeta potential of chitosan-biochar beads

To detect functional groups, present in the generated adsorbent, FTIR analysis was carried out (Figure 4.3.2). The surface of CH-BB differs from raw PM-BC (Fig. S1, Annex F). The wide peak between 3000 and 3600 cm^{-1} in PM-BC belongs to O-H stretching. In CH-BB, this region changed, the peak shifted and widened, suggesting additional presence of amino group [17]. The peak at 2960 cm^{-1} corresponds to the presence of aliphatic hydrocarbons and stretching vibrations of -CH/-CH_2 groups. The band at 1660 cm^{-1} belongs to C=O vibrations. Three peaks at 1190 (C-O-C stretching), 1100 and 1030 cm^{-1} (C-O stretching) can be identified as characteristic bands for saccharide chitosan structure [17]. The adsorption of CIP and heavy metals resulted in changes in CH-BB spectra (Fig. 4.3.2). The adsorption of Cd and Pb was via hydroxyl group as evidenced by the disappearance of the peak in the region between 3000-3500 cm^{-1}. In case of As and CIP, the sharp, wide shoulder appeared at 3400 cm^{-1}. This also indicated binding of both contaminants in the region that corresponds to O-H stretching. It suggests that CIP and As may sorb via surface complexation reaction or ion exchange [24]. Moreover, in case of As spectra, the changes between 1016-1200 cm^{-1}, connected to C-O stretching of alcohol esters and -COOH groups, can be observed. It could be associated with adsorption of various As speciation via electrostatic interactions or ion exchange [25]. The assessment of metals leaching from CH-BB was also performed (Table S1, Annex F). There was lesser leaching of metals from CH-BB as

compared to raw PM-BC. This is linked to extensive washing of beads after soaking it in NaOH. Hence, most of the metals that were present in raw biochar were washed away.

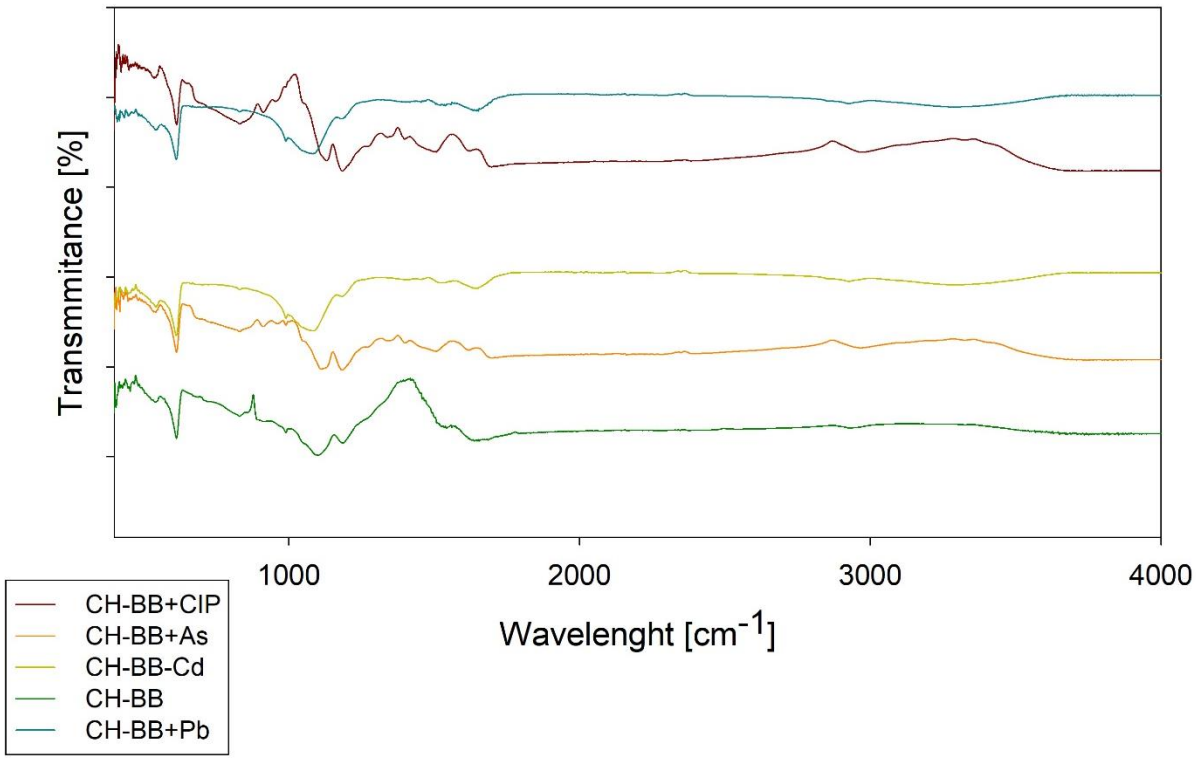

Figure 4.3. 2 FTIR of CH-BB before and after adsorption of CIP or heavy metals; CH-BB – chitosan biochar beads, CIP - ciprofloxacin

Modification of raw PM-BC resulted in an increase in its adsorption capacity in almost all cases (Table 4.3.1). The highest increment was noticed for As (almost 6-fold) and the lowest for Cd (1.02-fold). However, the adsorption capacity towards Pb was slightly decreased.

Adsorption onto CH-BB

Effect of pH

The effect of pH on adsorption of CIP and heavy metals was tested (Figure 4.3.3). The pH had no significant effect on the removal of CIP (*p*-value = 0.104) and Pb (*p*-value = 0.114). For Cd and As, the optimum pH for removal was found to be 6.0. For CIP, the results are consistent with the report of Afzal et al. (2018)[17]. CIP has two main ionizable groups, carboxylic (pK_{a1} 6.09) and piperazinyl (pK_{a2} 8.74), which makes the compound amphoteric. In the tested range of pH, CIP is present in the solution as zwitterion, hence it can adsorb onto CH-BB when its surface is protonated (pH <6) or negatively charged (pH>6) [26]. Moreover, further increase of pH would result in a decrease of CIP-adsorption potency due to the higher concentration of CIP^-, as previously suggested [17, 27].

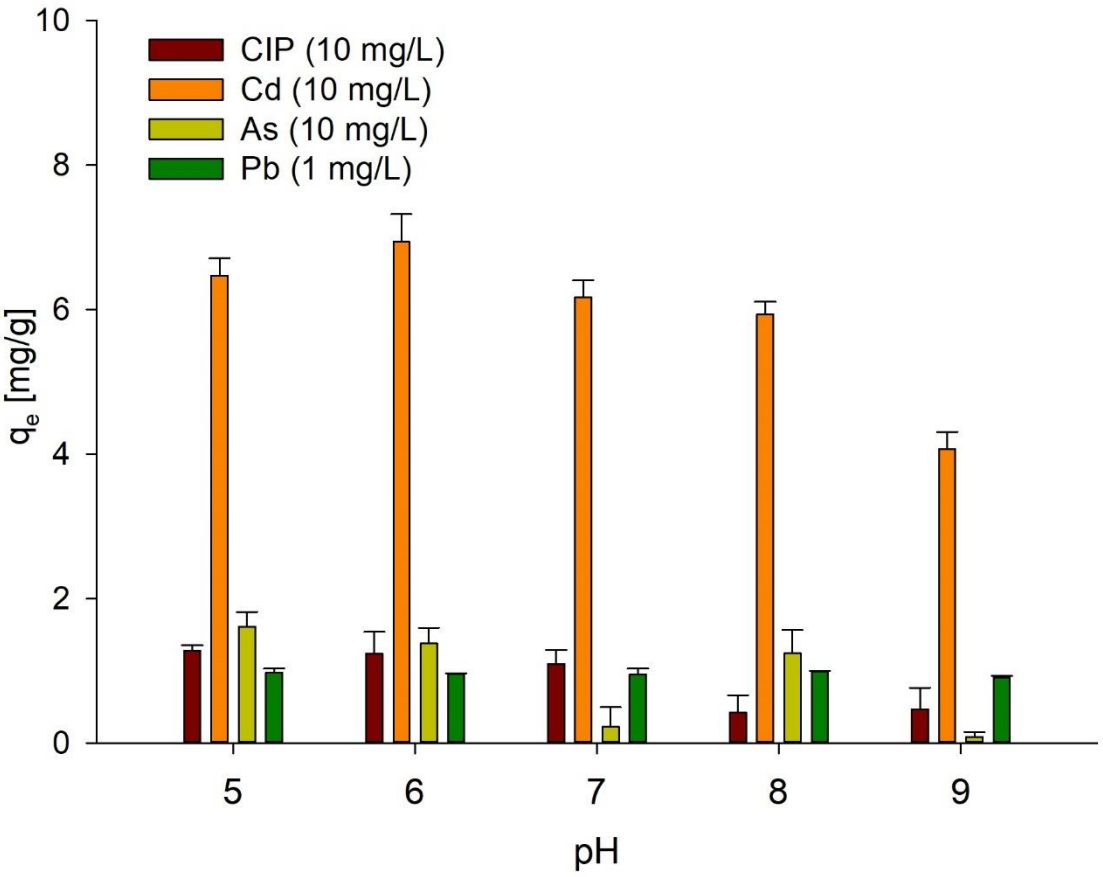

Figure 4.3. 3 Influence of pH on adsorption of ciprofloxacin (CIP) and heavy metals

At around pH 6, the functional groups of CH-BB containing oxygen are deprotonated, hence they can attract most of the metals. Moreover, the presence of amine group of chitosan (pK_a 6.5) increases the number of active sites [28-30]. The adsorption capacity towards As and Cd decreased with the increase of pH above 6. At the tested pH, As is present mostly as $H_2AsO_4^-$, however, due to its speciation, it is not certain if this main form of As was the one that was adsorbed onto CH-BB surface [7]. In the case of Cd, the adsorption capacity increased significantly from pH 5 to 6 (p-value = 0.021) and then started to decrease gradually. Generally, at higher pH, the adsorption capacity decreases due to the formation of soluble hydroxylated complexes of the metal ions [30, 31]. Based on these, pH 6 was selected for further experiments.

Adsorption kinetics

Figure 4.3.4 presents the adsorption capacity of the four pollutants against time. All contaminants exhibited a similar trend of adsorption onto CH-BB. As (Fig. 4.3.4A). CIP (Fig. 4.3.4D) reached equilibrium in first 3 hours when tested individually or in mixture. It can be attributed to the availability of active sites present on the adsorbent surface. In the case of Pb (Fig. 4.3.4C) and Cd (Fig. 4.3.4B), around 24 h was required to attain equilibrium. This may be linked to the diffusion-controlled mechanism of metal adsorption [18]. The pore network of the adsorbent could hinder the intraparticle

mass transfer of metals which could explain the delay in adsorption equilibrium time. The adsorption capacity of Cd decreased from 0.99±0.02 mg/g to 0.78±0.007 mg/g and 0.68±0.005 mg/g in metal mixture and metal mixture with CIP, respectively. Hence, Cd competed for adsorption sites with other metals and CIP, which led to significant decrease in its removal (p-value < 0.001) [32]. In the case of As, the adsorption capacity increased almost 2-fold when other metals were present. A similar trend was observed for Pb adsorption capacity. It can be associated with co-precipitation of lead and arsenate as mimetite, which follows the reaction presented in Equation (31)[33]:

$$5\ Pb^{2+} + 3\ AsO_4^{3-} + Cl^- \rightarrow Pb_5(AsO_4)_3Cl\downarrow \qquad \text{Eq. 31}$$

The addition of CIP to the metal mixture decreased the adsorption capacity of As and Pb, however, it was still slightly higher than the removal of these two metals individually. It can correspond to potency of CIP to chelate metals. To confirm if CIP can form a complex with As and Pb, antibiotic and metals were mixed in different ratios at pH 6 and then scanned via UV-Vis spectrophotometer. The absorption of CIP was quenched when As was added and enhanced in the presence of Pb (Fig. S2, Annex F), thus it suggested that CIP was able to complex with As and Pb [21]. Most probably, when CIP-As/Pb complex is formed, the reaction presented in Equation 31 is hindered due to the decrease of concentration of free ions. On the other hand, the adsorption capacity of CIP was not altered by the presence of metals.

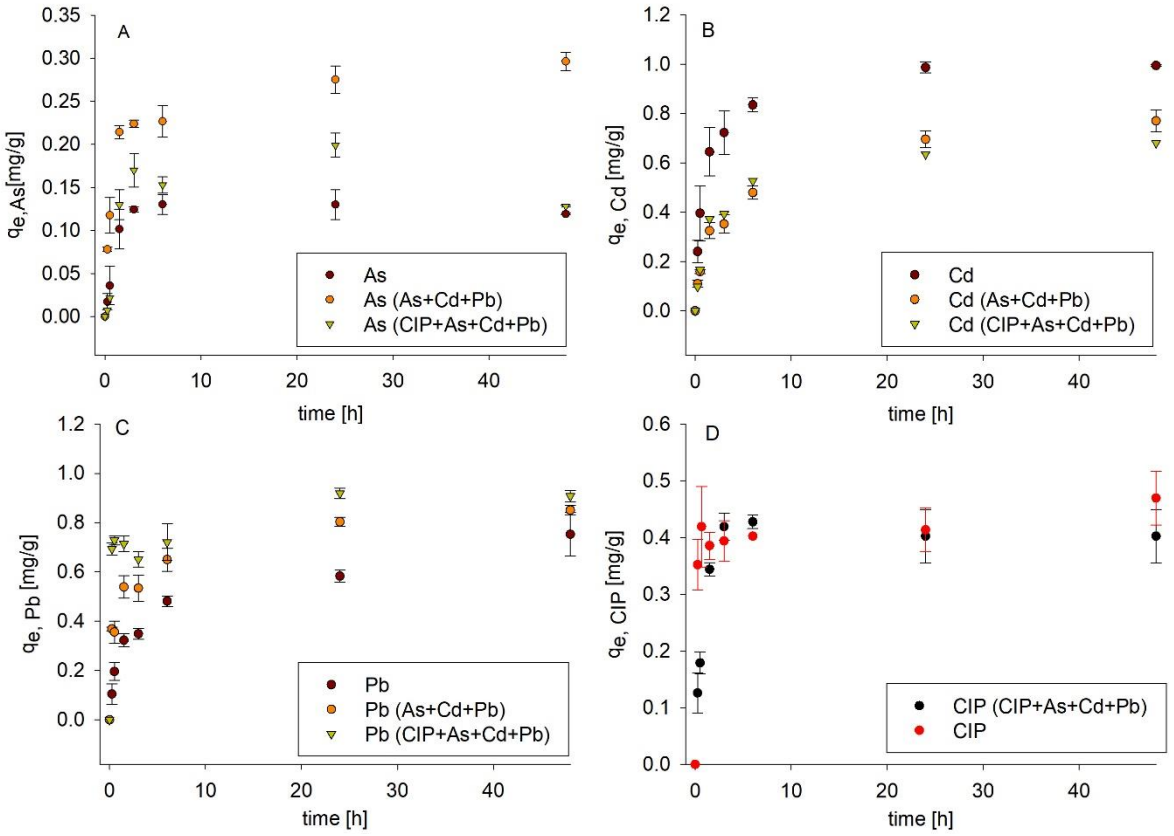

Figure 4.3. 4. Kinetics curves of A. As; B. Cd; C. Pb; D. ciprofloxacin (CIP) individually and in mixtures

To understand the kinetics of the adsorption mechanism of tested pollutants, three models, i.e. pseudo-first-order, pseudo-second-order and intraparticle diffusion model, was tested [17]. The equations and model parameters are presented in Table S2 (Annex F). The results are presented in Table 4.3.2. Generally, adsorption of all pollutants (individually and in mixtures) onto CH-BB followed pseudo-second order (R^2>0.90). It suggested that chemisorption was the main mechanism of the contaminant uptake. The higher values of k_2 for CIP and As can be correlated to reaching equilibrium state more rapid than Cd and Pb [30]. Additionally, in some cases, the correlation coefficient (R^2) was also higher for pseudo-first order (e.g. As, R^2 = 0.996), hence physical adsorption might have contributed to the overall uptake mechanism.

Table 4.3. 2. Kinetic parameters of the pollutants adsorption onto chitosan-biochar beads

Contaminant		**Pseudo-first order**		**Pseudo-second order**		**Intraparticle diffusion**	
		k_1	R^2	k_2	R^2	k_p	R^2
As	Individually	0.84	0.99	19.34	0.99	0.08	0.95
	Metal mixture	0.68	0.98	3.27	0.99	0.11	0.90
	Metal mixture + CIP	0.80	0.76	5.99	0.95	0.14	0.94
Cd	Individually	0.09	0.90	1.06	0.99	0.43	0.96
	Metal mixture	0.20	0.97	0.45	0.99	0.21	0.96
	Metal mixture + CIP	0.47	0.77	0.83	0.99	0.21	0.75
Pb	Individually	0.21	0.36	0.53	0.98	0.26	0.67
	Metal mixture	0.33	0.90	1.02	0.99	0.27	0.68
	Metal mixture + CIP	0.64	0.63	1.11	0.99	-0.02	0.28
CIP	Individually	2.77	0.75	10.44	0.99	0.88	0.72
	Metal mixture + CIP	25.96	0.90	17.44	0.95	0.03	0.48

Abbreviations: CIP – ciprofloxacin; k_1 [1/h] - the rate constant of pseudo-first-order adsorption; k_2 [g/mg h] - the rate constant of pseudo-second-order adsorption; k_p [mg/g $h^{1/2}$] the intraparticle diffusion rate constant

Adsorption isotherms

Figure 4.3.5 presents the adsorption capacity of CH-BB against the equilibrium concentration (C_e) of pollutants. Plots for Pb and CIP are L-shaped, which suggested that when the concentration of

contaminant increases, the absorption was hindered as most of adsorption sites were occupied. The isotherms for Cd and As are linear, which may indicate that both metals are distributed between the bulk solution phase and interfacial phase.

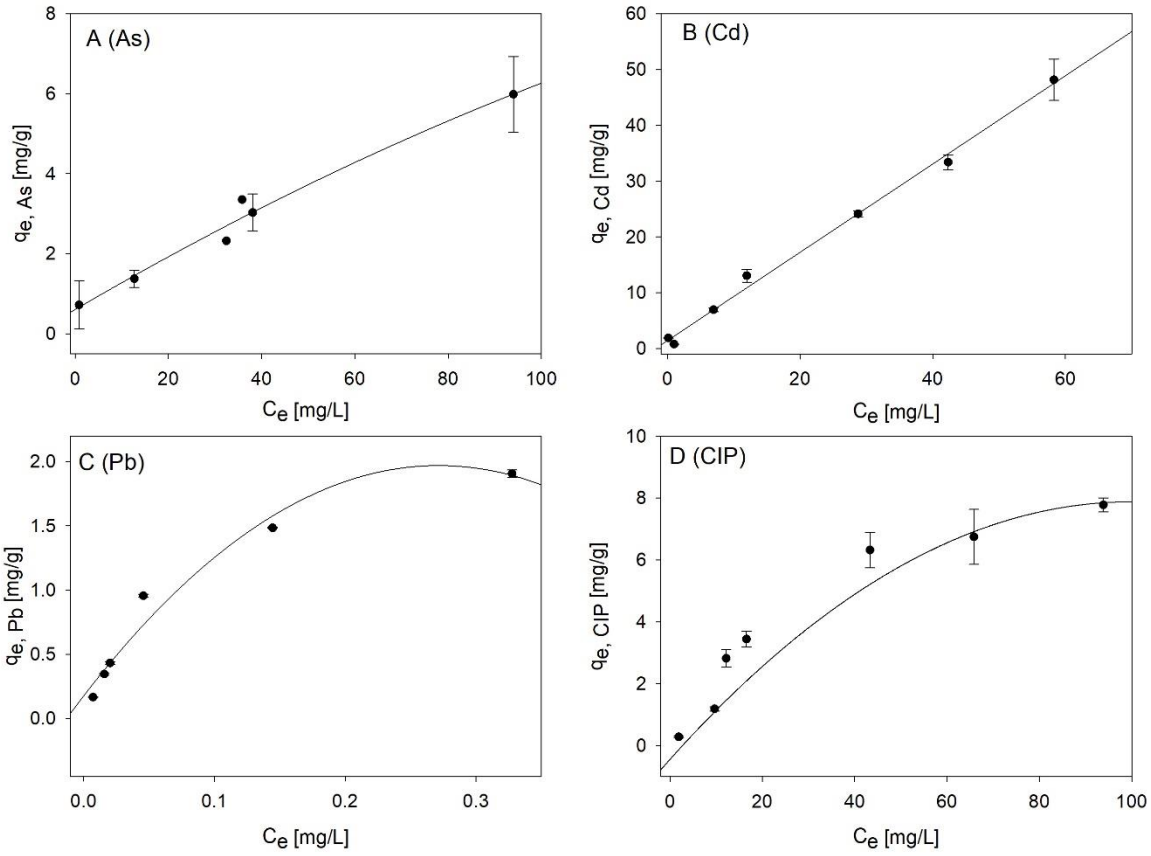

Figure 4.3. 5 Adsorption isotherms of A. As; B. Cd; C. Pb; D. ciprofloxacin (CIP)

To better understand the relationship between capacity of adsorbent and targeted pollutants, the three models, i.e. Langmuir, Freundlich, and Temkin (Table S2, Annex F), were fitted to experimental data. The results are presented in Table 4.3.3. Langmuir model fitted Pb adsorption (R^2=0.99) better than Freundlich model (R^2=0.96), indicating that it was monolayer adsorption. The data are consistent with previous reports [18, 28, 29]. It was reported that lead sorption may be influenced by coordination of chitosan amine groups, which usually is in agreement with Langmuir adsorption [18]. Liu et. al (2009) reported that as compared to this study, maximum adsorption capacity of lead onto biochars derived from hydrothermal liquefaction of biomass ranged between 2.40-4.25 mg/g [31]. On the other hand, Zhou et al. (2013) reported the maximum adsorption capacity of lead onto chitosan-modified biochar to be 14.3 mg/g [18], which is around 7-fold higher than the q_m (2.46 mg/g) in this study. It may be associated with different feedstocks used for biochar generation and pyrolysis conditions. The separation factor (R_L), known as equilibrium parameter of Langmuir model, is used to establish if the adsorption is favorable thermodynamically. When R_L is higher than 1, then the reaction is unfavorable; when the parameter ranges between 0 and 1, it means that the reaction is favorable; when R_L is equal to 0, then

the adsorption is irreversible. For lead adsorption, R_L = 0.05, hence the Pb uptake by CH-BB was thermodynamically favored.

Table 4.3. 3 Isotherm constants of ciprofloxacin (CIP) and heavy metals onto chitosan-biochar beads

Isotherm	Parameter	As	Cd	Pb	CIP
Langmuir	q_m [mg/g]	7.92	57.47	2.46	40.32
	K_l [L/mg]	0.02	0.03	10.66	0.003
	R_L	0.48	0.33	0.05	3.68
	R^2	0.62	0.61	**0.99**	0.08
Freundlich	*1/n*	0.43	0.48	0.63	0.92
	K_F [L/mg]	0.65	4.45	4.69	0.13
	R^2	**0.90**	**0.94**	0.96	**0.95**
Temkin	K_T [L/mg]	1.13	4.11	147.46	0.32
	B	0.91	5.37	0.48	2.00
	b_T [J/mol]	2666.75	453.65	5088.94	1220.36
	R^2	0.66	0.65	0.98	0.81

The rest of the pollutants followed the Freundlich model of adsorption ($R^2 \geq 0.90$) which is in accordance with previous reports [15, 34]. This suggests that adsorption of CIP, As and Cd was obtained onto heterogeneous surface of CH-BB. The value of *1/n* (<1) indicated that the adsorption of contaminants was favorable. The K_F followed order: Pb>Cd>>As>CIP, which means that CH-BB had higher affinity towards Pb and Cd than As and CIP. It corresponded to much higher adsorption capacities of these two metals onto tested adsorbent (Table 4.3.1). On the other hand, Afzal et al (2018, 2019) reported that adsorption of the antibiotic onto chitosan-biochar hydrogel beads fitted Langmuir model [17, 27]. Furthermore, removal of As and Cd via biochars and functionalized biochars generally followed Langmuir model [23, 30]. Similar to reports of Pb adsorption, the differences in reported results could be due to the various feedstocks and protocols for biochar generation.

Co-adsorption of CIP and heavy metals

To further investigate the influence of organic and inorganic contaminants on their removal via CH-BB, the co-adsorption test was performed. The metal concentration remained constant (4 mg/L), while the CIP concentration ranged between 0.5 – 20 mg/L. The results are presented in fFigure 4.3.6. The increasing CIP concentration generally did not have a significant influence on Cd (*p*-value = 0.99) and

As (p-value = 0.053) adsorption capacity. The Pb adsorption capacity was enhanced when initial concentration of CIP and Me was almost equal (5:4). After this point, Pb removal was constant (p-value > 0.05). The results suggest that the adsorption of heavy metals follows different mechanisms than the CIP uptake. It is consistent with the work presented by Liu et al (2018), where the co-adsorption of heavy metal ions and fluoroquinolones on the functionalized ferromagnetic microsphere was tested [32]. The inorganic contaminants did not alter the adsorption of antibiotics and vice versa due to different uptake mechanisms.

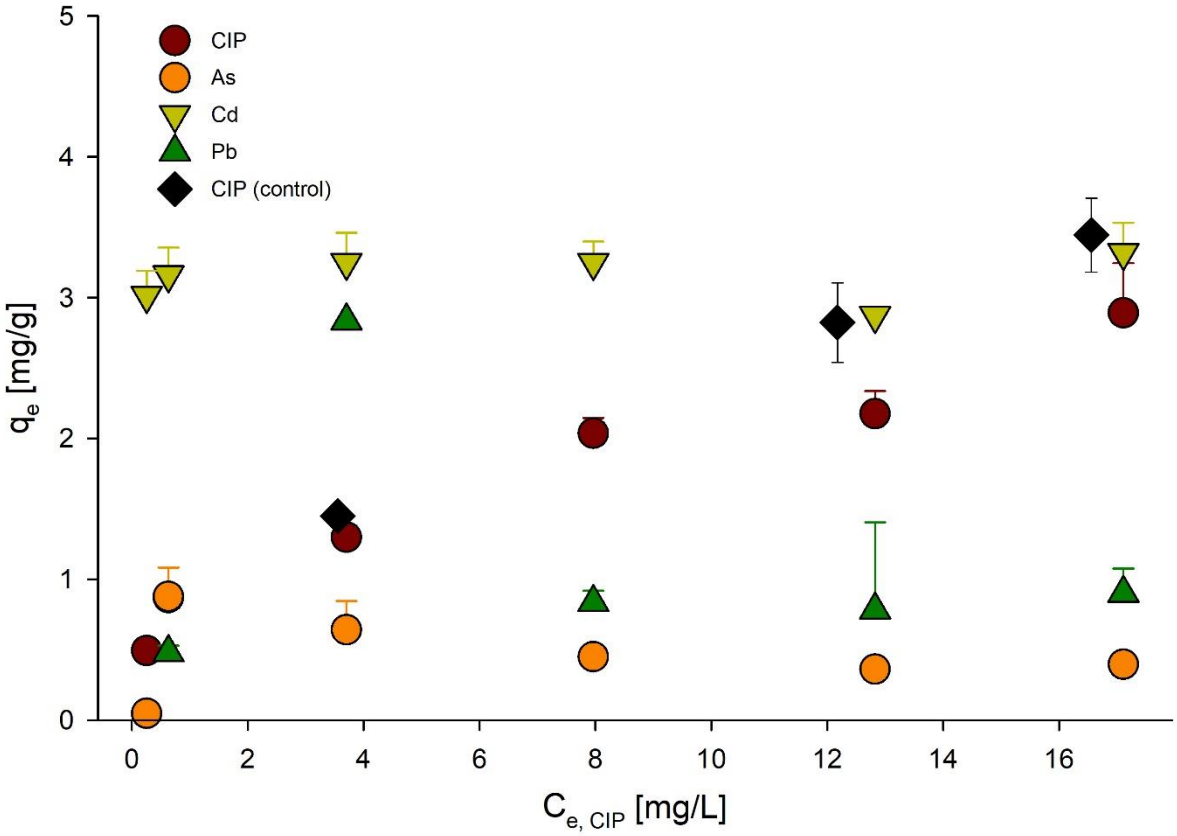

Figure 4.3. 6 Co-adsorption of ciprofloxacin (CIP) and heavy metals; CIP concentration 0.5 – 20 mg/L, heavy metals 4 mg/L)

Test with real wastewater

The results of the removal efficiency test are presented in Table 4.3.4. Pb removal was almost 100% for all tested adsorbents. In case of As and Cd, adsorbent generated in this study exhibited better removal efficiency than raw biochar and commercial GAC. Only CH-BB could remove As (4.5%). More than 90% of cadmium was removed from wastewater. Moreover, adsorption of Cd increased 2-fold and 3-fold when compared with PM-BC and GAC respectively. However, adsorption of CIP followed different order. Almost 90% of CIP was removed by GAC, when the CH-BB exhibited the lowest removal efficiency (35%). This proved that CH-BB is suitable adsorbent for heavy metals removal, however for CIP, the further improvements are needed.

Table 4.3. 4 Comparison of removal efficiency between different adsorbents

Adsorbent	As [% removed]	Cd [% removed]	Pb [% removed]	CIP [% removed]
CH-BB	4.50±0.76	92.86±0.68	99.99±0.03	34.95±4.03
PM-BC	NR	42.54±6.25	99.74±0.07	43.57±6.71
GAC	NR	31.20±0.00	99.52±0.12	87.93±6.71

Abbreviations: CH-BB chitosan-biochar beads; PM-BC pig manure biochar; GAC granulated active carbon; CIP – ciprofloxacin; NR – no removal

Conclusion

All tested raw biochars were able to remove all targeted pollutants. However, their adsorption capacity depended on the type of biochar and the pollutant. PM-BC exhibited the highest removal efficiency for CIP and Pb, PW-BC for Pb and As and AS-BC for Cd. Based on the data, the PM-BC was selected for its further modification. The fabricated CH-BB demonstrated an increased adsorption capacity towards all targeted pollutants compared to PM-BC, except for Pb, which decreased slightly. The optimal pH of adsorption studies was found to be at 6.0. Based on the kinetic studies, the adsorption of all targeted contaminants followed pseudo-second order, thus the main mechanism of their uptake was via chemisorption. The adsorption of CIP and As was rapid than for Cd and Pb. The adsorption studies with metal mixture revealed that Cd removal efficiency decreased due to the competition with other pollutants over the adsorbent active sites. However, the co-contamination of As and Pb led to their increased removal due to their co-precipitation as mimetite. The adsorption capacity towards CIP was not affected by the presence of metal ions. The increased CIP concentration mostly did not influence metals adsorption onto CH-BB. This suggests that inorganic pollutants exhibit different adsorption mechanisms. Hence, there should be no competition between CIP and heavy metals over adsorption sites. This indicates that the water treatment of these two types of pollutants will not cancel each other. The comparison of removal efficiency in real wastewater between CH-BB, PM-BC and GAC showed that CH-BB had much better performance than the rest of tested adsorbents.

Acknowledgments

The authors are sincerely thankful to the Natural Sciences and Engineering Research Council of Canada (Discovery Grant 355254 and NSERC Strategic Grant) and MITACS Globalink Internship Award for financial assistance.

References:

1. European Union Strategic Approach to Pharmaceuticals in the Environment. 2019, European Comission: Brussels.

2. Organization, W.H., Critically important antimicrobials for human medicine 5th revision. 2017, World Health Organization.

3. Conley, Z.C., et al., Wicked: The untold story of ciprofloxacin. PLoS pathogens, 2018. **14**(3): p. e1006805-e1006805.

4. Cuprys, A., et al., Fluoroquinolones metal complexation and its environmental impacts. Coordination Chemistry Reviews, 2018. **376**: p. 46-61.

5. Uivarosi, V., Metal complexes of quinolone antibiotics and their applications: an update. Molecules, 2013. **18**(9): p. 11153-97.

6. Bolisetty, S., M. Peydayesh, and R. Mezzenga, Sustainable technologies for water purification from heavy metals: review and analysis. Chemical Society Reviews, 2019. **48**(2): p. 463-487.

7. Vithanage, M., et al., Interaction of arsenic with biochar in soil and water: A critical review. Carbon, 2017. **113**: p. 219-230.

8. Procedure 2017/0332/COD. 2019, European Parliment.

9. Gao, P., et al., Impacts of coexisting antibiotics, antibacterial residues, and heavy metals on the occurrence of erythromycin resistance genes in urban wastewater. Appl Microbiol Biotechnol, 2015. **99**(9): p. 3971-80.

10. Ji, X., et al., Antibiotic resistance gene abundances associated with antibiotics and heavy metals in animal manures and agricultural soils adjacent to feedlots in Shanghai; China. J Hazard Mater, 2012. **235-236**: p. 178-85.

11. Nguyen, C.C., et al., Association between heavy metals and antibiotic-resistant human pathogens in environmental reservoirs: A review. Frontiers of Environmental Science & Engineering, 2019. **13**(3): p. 46.

12. Tan, X., et al., Application of biochar for the removal of pollutants from aqueous solutions. Chemosphere, 2015. **125**: p. 70-85.

13. Lonappan, L., et al., An insight into the adsorption of diclofenac on different biochars: Mechanisms, surface chemistry, and thermodynamics. Bioresource Technology, 2018. **249**: p. 386-394.

14. Xu, X., X. Cao, and L. Zhao, Comparison of rice husk- and dairy manure-derived biochars for simultaneously removing heavy metals from aqueous solutions: Role of mineral components in biochars. Chemosphere, 2013. **92**(8): p. 955-961.

15. Zeng, Z.-w., et al., Comprehensive Adsorption Studies of Doxycycline and Ciprofloxacin Antibiotics by Biochars Prepared at Different Temperatures. Frontiers in Chemistry, 2018. **6**(80).

16. Sizmur, T., et al., Biochar modification to enhance sorption of inorganics from water. Bioresource Technology, 2017. **246**: p. 34-47.

17. Afzal, M.Z., et al., Enhancement of ciprofloxacin sorption on chitosan/biochar hydrogel beads. Sci Total Environ, 2018. **639**: p. 560-569.

18. Zhou, Y., et al., Sorption of heavy metals on chitosan-modified biochars and its biological effects. Chemical Engineering Journal, 2013. **231**: p. 512-518.

19. Bhatnagar, A. and M. Sillanpää, Applications of chitin-and chitosan-derivatives for the detoxification of water and wastewater—a short review. Advances in colloid and Interface science, 2009. **152**(1-2): p. 26-38.

20. Lonappan, L., et al., Covalent immobilization of laccase on citric acid functionalized micro-biochars derived from different feedstock and removal of diclofenac. Chemical Engineering Journal, 2018. **351**: p. 985-994.

21. Cuprys, A., et al., Ciprofloxacin-metal complexes -stability and toxicity tests in the presence of humic substances. Chemosphere, 2018. **202**: p. 549-559.

22. Zhang, P., et al., Adsorption and catalytic hydrolysis of carbaryl and atrazine on pig manure-derived biochars: Impact of structural properties of biochars. Journal of Hazardous Materials, 2013. **244-245**: p. 217-224.

23. Wang, S., et al., Removal of arsenic by magnetic biochar prepared from pinewood and natural hematite. Bioresource Technology, 2015. **175**: p. 391-395.

24. Niazi, N.K., et al., Arsenic removal by perilla leaf biochar in aqueous solutions and groundwater: an integrated spectroscopic and microscopic examination. Environmental Pollution, 2018. **232**: p. 31-41.

25. Samsuri, A.W., F. Sadegh-Zadeh, and B.J. Seh-Bardan, Adsorption of As(III) and As(V) by Fe coated biochars and biochars produced from empty fruit bunch and rice husk. Journal of Environmental Chemical Engineering, 2013. **1**(4): p. 981-988.

26. Aristilde, L. and G. Sposito, Complexes of the antimicrobial ciprofloxacin with soil, peat, and aquatic humic substances. Environ Toxicol Chem, 2013. **32**(7): p. 1467-78.

27. Afzal, M.Z., et al., Enhanced removal of ciprofloxacin using humic acid modified hydrogel beads. Journal of Colloid and Interface Science, 2019. **543**: p. 76-83.

28. Fan, L., et al., Highly selective adsorption of lead ions by water-dispersible magnetic chitosan/graphene oxide composites. Colloids and Surfaces B: Biointerfaces, 2013. **103**: p. 523-529.

29. Wan, M.-W., et al., Adsorption of copper (II) and lead (II) ions from aqueous solution on chitosan-coated sand. Carbohydrate Polymers, 2010. **80**(3): p. 891-899.

30. Bogusz, A., P. Oleszczuk, and R. Dobrowolski, Application of laboratory prepared and commercially available biochars to adsorption of cadmium, copper and zinc ions from water. Bioresource Technology, 2015. **196**: p. 540-549.

31. Liu, Z. and F.-S. Zhang, Removal of lead from water using biochars prepared from hydrothermal liquefaction of biomass. Journal of Hazardous Materials, 2009. **167**(1): p. 933-939.

32. Liu, X., M. Liu, and L. Zhang, Co-adsorption and sequential adsorption of the co-existence four heavy metal ions and three fluoroquinolones on the functionalized ferromagnetic 3D NiFe2O4 porous hollow microsphere. J Colloid Interface Sci, 2018. **511**: p. 135-144.

33. Long, H., et al., Comparison of arsenic(V) removal with different lead-containing substances and process optimization in aqueous chloride solution. Hydrometallurgy, 2019. **183**: p. 199-206.

34. Cheng, Q., et al., Adsorption of Cd by peanut husks and peanut husk biochar from aqueous solutions. Ecological Engineering, 2016. **87**: p. 240-245.

ANNEX A

Fluoroquinolones metal complexation and its environmental impacts

Agnieszka Cuprys[a], Rama Pulicharla[a], Satinder Kaur Brar[b], Patrick Drogui[a], Mausam Verma[c], Rao Y. Surampalli[d]

[a] INRS-ETE, Université du Québec, 490, Rue de la Couronne, Québec, Canada G1K 9A9

[b] Corresponding author: INRS-ETE, Université du Québec, 490, Rue de la Couronne, Québec, Canada G1K 9A9. E-mail: satinder.brar@ete.inrs.ca; Téléphone: + 418 654 3116; Fax: + 418 654 2600.

[c] CO2 Solutions Inc., 2300, rue Jean-Perrin, Québec, Canada G2C 1T9

[d] Department of Civil Engineering, University of Nebraska-Lincoln, N104 SEC PO Box 886105, Lincoln, NE 68588-6105, USA

Coordination Chemistry Reviews, Volume 376, 2018, Pages 46-61

Abstract: Fluoroquinolones (FQs), the group of broad-spectrum antimicrobials, are frequently detected in different environmental compartments, mostly due to incomplete metabolism in the target organism, inefficient wastewater treatment, and disposal of expired FQs directly into the environment. Another group of the contaminants, widely present in water, air, and soils, are the metal ions (Me). In general, FQs can form stable complexes with metal ions and their co-existence with Me in the environment leads to metal complexation. The most stable complexes are formed between FQs and trivalent ions, whereas FQs and alkali-earth metal ions, i.e. Ca^{2+} and Mg^{2+}, are the least stable composites. This interaction between FQs and metal ions may alter antibiotic properties. Antibacterial activity of metal complexes is generally comparable with the parent compound; however, some FQs-metal complexes are found to exhibit higher antibacterial activity. Moreover, it was proved that FQs-Me complex can display antifungal potency toward *Candida albicans.* The mobility of FQs in soil and/or water strongly depends on pH, temperature, and type of metal ions, present in the environment. This review provides a brief description of FQs, their properties, and capacity to form complexes with metal ions. It summarizes influence of FQs-Me complexes on microorganisms and their mobility in different media. Further, the review provides a linkage between the presence of these metal ions in the environment and their effect on the chemistry and biology of fluoroquinolone antibiotics.

Keywords: fluoroquinolones; metals; metal complexation; environment; toxicity; transport

Chemical compounds reviewed in this article:

Ciprofloxacin (PubChem CID: 2764); enrofloxacin (PubChem CID: 71188); gatifloxacin (PubChem CID: 5379); levofloxacin (PubChem CID: 149096); lomefloxacin (PubChem CID: 3948); norfloxacin (PubChem CID: 4539); ofloxacin (PubChem CID: 4583); sparfloxacin (PubChem CID: 60464)

Table of Contents

Highlights:

1**.** Fluoroquinolones-trivalent metal ion complexes are more stable than divalent metal ions.

2. Metal ions may act as an intermediate in binding between fluoroquinolones and DNA /enzyme.

3. Correlation of antibacterial and sorption properties of fluoroquinolones was affected by metal complexation.

4. Mobility fluoroquinolones is affected by environmental factors such as pH , temperature and presence of metal ions.

Introduction

The discovery of antibiotics, as the large group of antimicrobials, has revolutionized pharmaceutical industry. Nevertheless, their widespread use in human and veterinary medicine has led to the fact that they are repeatedly detected in environmental compartments, mostly due to their inefficient removal during wastewater treatment [1-3]. Moreover, the deposition of antibiotics has an adverse impact on the ecosystem, due to their toxic concentration [4]. Their presence exerts a selective pressure on bacteria, leading to the occurrence, selection and dissemination of antibiotic resistant genes and antibiotic resistant bacteria, which can be detected in surface water [5-7], groundwater [5], wastewater [8] and sediments [9, 10]. Moreover, it has been indicated, that antibiotics may interact with surrounding substances and their transformation products can retain their pharmacological activity, due to the preserving or gaining moiety, responsible for antimicrobial potency. For instance, a by-product of enrofloxacin is ciprofloxacin and both belong to FQ family of antibiotics having a characteristic structure of 4-pyridone-3-carboxylic acid with a ring at C-5 or C-6 position, which is essential for their antibacterial activity [11]. Thereby, antibiotics and their transformation products are a potential threat to the environment.

Fluoroquinolones (FQs) are a family of broad-spectrum synthetic antibiotics, developed in the 1970s [12-14]. They belong to quinolone antibiotics, which are based on the structure of antimalarial quinine. FQs main characteristic is a fluorine atom attached to the central ring system. Most of the FQ's name ends with the "-floxacin" suffix, i.e. ciprofloxacin (CIP) [15], ofloxacin (OFL) [16], norfloxacin (NOR) [13], levofloxacin (LEVO) [17], gatifloxacin (GTI) [18] or enrofloxacin (ENR) [19]. FQs are active

against Gram positive and Gram negative strains of bacteria - their effectiveness is due to their potency to inhibit bacterial DNA gyrase and/or topoisomerase IV [20].

FQs have a higher frequency of detection in different environmental compartments. For instance, they are widely present in raw wastewater. In China, the prevailing FQs were OFL and NOR, with concentrations of 1287 ng/L and 775 ng/L, respectively [21]. In Maryland, USA, the concentration of CIP was found to be 1900 ng/L and OFL 600 ng/L in raw wastewater [22]. Moreover, the frequency of CIP detection was 100%, across all sampling sites. In Japanese wastewater influent, FQs were detected with the third and fourth highest concentration - 255 to 587 ng/L for LEVO and 155 to 486 ng/L for NOR, following clarithromycin and azithromycin [23]. In Finland, amongst all targeted pharmaceuticals (FQs, beta-blockers, antiepileptic drug) FQs, especially CIP (200-650 ng/L), were the most prevalent compounds detected in sewage influents [24]. During wastewater treatment, FQs tend to adsorb onto sludge so that high concentration of OFL and NOR, 7.29 mg/kg and 7.01 mg/kg, respectively, was found in the sludge [21]. In the WWTPs in Michigan, USA, OFL was found in secondary effluent at a concentration of 204 ng/L and in final effluent at a concentration of 100 ng/L. [25] It was calculated that daily 4.8 g of OFL was discharged into the river due to insufficient wastewater treatment. Miao et al. (2004) investigated final effluents in WWTPs in five Canadian cities (i.e. the Greater Vancouver Regional District, British Columbia; Calgary, Alberta; Burlington, Peterborough, and Windsor in Ontario) and detected CIP, NOR and OFL with the average concentrations of 118, 50 and 94 ng/L respectively [26]. Lee et al. (2007) analyzed sewage treatment plant in Ontario, Canada, and discovered that concentration of CIP in primary and final effluent ranged between 42-721 ng/L [27].

Apart from wastewater samples, the other environmental compartments were also investigated. For instance, FQs were detected in Chinese reclaimed water and groundwater [28]. NOR, OFL and ENR concentration ranged between 45-181 ng/L in reclaimed water and followed the order [NOR]> [OFL]> [ENR]. The groundwater FQs concentration was between 36.2-96.8 ng/L, in the following order [NOR]> [ENR]> [OFL]. The analysis of contamination in the Seine river, France, showed that sulfamethoxazole (sulfonamide antibiotic) and NOR were the compounds with the highest concentrations of 40 ng/L and 31 ng/L, respectively [29]. According to the study of Gibs et al. (2013), in New Jersey, USA, the concentration of CIP in Hohokus Brook waters (downstream of WWTP discharge), increased from 0.03 μg/L to 0.077 μg/L in years 2001 – 2008 [30]. Moreover, in the same sampling site, two FQs antibiotics were detected in the sediments: OFL (21 μg/kg) and CIP (10 μg/kg), which were the second and the third highest concentrations of present antibiotics, following macrolide antibiotic, azithromycin (44 μg/kg). In Chinese rivers, FQs (CIP, NOR, OFL, LOME) exhibited the highest concentration in their sediments (ranged between 1.67-156 ng/g) amongst four targeted classes of antibiotics [10]. Furthermore, FQs have been also detected in soils – for instance, ENR concentration ranged between 17.36 – 26.69 μg/kg in Brazil [31] and 20-50 μg/kg in Turkey [32].

FQs frequent detection is due to their widespread usage. According to the Report of Public Health Agency of Canada, FQs were the third most-prescribed antimicrobials to Canadians between 2010-2013 [33]. Moreover, the overall quantity of FQs, distributed for use in animals has expanded since 2010, probably due to the approval of a new indication for use [33]. According to European Medical Agency, sales of veterinary antimicrobials decreased by 7.9 % (in mg/ population correction unit) in twenty-six European countries between 2011 and 2013. However, the sale of FQs, along with 3rd- and 4th-generation of cephalosporins, remained stable (or slightly increased) during this period [34].

The presence of FQs in the environment was also due to incomplete metabolism of the pharmaceutical in the target organism. In fact, from 8% (trovafloxacin) to 83% (GTI) of antibiotic may be released via urine and feces in active form into the environment [35]. For instance, unchanged CIP is excreted in 65% via urine and 25% in feces [36]. This contributes to an increasing trend of drug-resistant bacteria occurrence. In 2014-2015, in Europe, *Escherichia coli* isolates were resistant mostly to aminopenicillins (57.2% of isolates) and FQs (22.8% of isolates) [37]. Between 2012-2015, a significant increase of FQs-resistant *Klebisiella pneumoniae* was also noticed. Moreover, multidrug resistance, including FQs-resistance, of *E. coli* and *K. pneumoniae,* was observed as an increasing trend [37]. Thus, WHO classified FQs as critically important antibacterial agent for human medicine due to the its increased bacterial resistance [38].

Nowadays, much attention has been given to antibiotics co-contamination with metal ions. Many pharmaceuticals, including FQs, possess an ability to form metal complexes, which may modify properties of FQs, i.e. altering the antimicrobial activity of antibiotic [39-41], solubility [42] or bioavailability [43]. The extensive studies have been performed for many pharmaceuticals-metal complexes, i.e. tetracyclines, quinolones or β-lactams [41, 44-47]. It was proved that metal ions presence alters antibiotic adsorption and desorption [48-50], photolysis [51-53] or uptake [47, 54].

Previous reviews were mostly related to the chemical aspect of FQ-metal complexes and its biological properties, which could be used in pharmaceuticals applications [46, 55, 56]. There are also assessments, which are concerned about FQs and their environmental impact [57, 58]. However, the goal of this review is to summarize the knowledge about FQs-metal complexation through a brief description of FQs properties (medical usage, physicochemical and biological properties), followed by FQs-Me complexes characteristics. The impact of FQs-Me complexes on wastewater treatment is presented. The next objective is to introduce the influence of FQs-Me complexes on living organisms. Later, it is shown as to how the presence of metal ions affects the mobility of FQs in water and soils. The novel technological approaches towards FQs-Me complexation are introduced. Finally, the outlook for FQs-Me complexation is presented.

Fluoroquinolones: medical usage, structure, physicochemical properties

The effectiveness of the first-generation FQs was mostly against Gram-negative bacteria [59]. However, due to the modifications in their structure, the newer-generation of FQs possess broad antimicrobial spectrum, against Gram-positive and Gram-negative strains. They are used to treat infections of the skin, urinary, gastrointestinal and respiratory tracts or sexually transmitted diseases as shown in Table 1 [60, 61]. Their structure differs from quinolones due to fluorine atom attached to the central ring at the C-6 position and piperazine ring (or another N-heterocycle) at C-7 position (Table 1). The addition of these two groups improved antibiotic activity and pharmacokinetic properties [62]. Two ionizable groups are present in the FQs structure, i.e. carboxylic group at C-3 and piperazinyl group at C-7 with the macroscopic dissociation constants, which are referred to as pK_{a1} and pK_{a2}, respectively, as shown in Figure 1. Different substituents, i.e. additional fluorine atom (lomefloxacin (LOME)) or methoxy group (GTI) at C-8, cyclopropane group (CIP, sparfloxacin) and ethyl group (NOR, LOME) at N-1 in central ring, amine group at C-5 (sparfloxacin), various N-heterocycles at C-7, modify features of the compound [11, 59]. However, groups at C-4 (carbonyl group), as well as C-2 (hydrogen atom) and C-3 (carboxyl group) remain unchanged due to their key role in antibacterial activity [59, 63]. In aquatic solutions, FQs can exist in protonated form in acidic pH (H_2FQ^+). At pH 1, this form is present in nearly 100%. Zwitterionic ($HFQ^{\pm}$) or uncharged (HFQ^0) form occurs in slightly acidic or neutral pH and anionic form in alkaline pH (FQ^-) [56, 64, 65]. In general, FQs exist as a zwitterion, in broad pH spectrum (pH may range between 3 and 11) [56].

FQs target two bacterial enzymes, which are essential in DNA replication and/or transcription [59, 66]. DNA gyrase is a bacterial enzyme, which catalyzes negative super-coiling of double-stranded DNA. A homolog of gyrase, topoisomerase IV, is responsible for partitioning of chromosomal DNA following DNA replication. FQs form stable ternary complex that includes the antibiotic, enzyme and DNA segment. FQs bind to DNA via carbonyl and carboxylate oxygen atoms by hydrogen bonds, as shown in Figure 2 A, while the fluorine atom, N-heterocycle group at C-7 and carboxylate ion are connected with the enzyme [11]. This leads to the restraining of enzyme activity and blocks the regulation of conformational changes in the bacterial chromosome during replication and transcription. It probably causes the cleavage of DNA and release of double-strand DNA ends, followed by cell death [66].

The presence of Mg^{2+} is essential due to its role as a mediator between FQs, DNA, and targeted enzymes. The importance of magnesium ions in DNA unwinding, in the presence of FQs, was observed by Tornaletti and Pedrini (1988) [67]. Later, the mediator role of Mg^{2+} was confirmed by Palu et al. (1992) [68]. Subsequently, researchers aimed to investigate FQs-Mg-DNA-enzyme interaction. Based on the crystal structure, it was proved that magnesium ions are chelated by FQs via two oxygen atoms in the carboxylic group and the carboxyl group of FQ [69-72]. Further experiments, which investigated the CIP-Me complexes, suggesting that CIP-Mg complex is bound to DNA by phosphate group of DNA [73]. Two groups of researchers succeeded in obtaining the crystal structure of the complex between FQs and topoisomerase IV mediated by magnesium ions [63, 74]. It was proved that magnesium ions

are coordinated by FQ molecule via oxygen atoms in the carboxylic group (C-3) and a carboxyl group (C-4) (fig. 2 B) [63, 74]. Later, Mg^{2+}, with coordinated water molecules, binds to one of the enzyme subunits by hydrogen bonds (fig. 2C), while groups at C-1 and C-8 FQ intercalate DNA. It was observed that the bases, which surround antibiotic, adapt FQ molecule and direct the base polar atoms Mg^{2+} and its water coordinates [63]. The N-heterocyclic group at C-7 opens the pocket between the enzyme subunit and DNA. Figure 2C presents the coordination sphere around magnesium ion, which shows the importance of Mg^{2+} in interaction with moxifloxacin, DNA and enzyme as described earlier, due to the coordinated water molecules, moxifloxacin-Mg^{2+} complex may bind with DNA bases and enzyme. However, the studies on GTI presented that Mg^{2+}, may also be a bridge in FQs – DNA interaction by binding with the phosphate group of DNA [75]. Also, different divalent ions, i.e. Cu^{2+}, Cd^{2+} and Co^{2+}, may increase GTI – DNA binding ability – transition ions bind with N-7 of purine base of DNA, which is in inside its molecule (fig. 2 D) They facilitate the FQ binding by acting as an intermediate between GTI and DNA (fig. 2 E) [75]. Mediating properties of ions in FQs-DNA interaction were also confirmed for OFL and Cu^{2+}, LOME and Cu^{2+}, Ni^{2+}, Co^{2+}, Zn^{2+} [76].

In general, magnesium ion was found to be the most potent in DNA-enzyme-FQs binding, even though its formation constant log β with FQs is relatively low as compared to other metal ions ($\log\beta_{Mg}$ may range between 10-12, $\log\beta_{Cu}$=13-29, $\log\beta_{Zn}$=11-26). Mg^{2+} has the lowest ability to bind to DNA bases amongst tested complexes, but it binds strongly with the DNA phosphate group [75]. However, there is not enough data about the exact influence of metal ions on FQs–enzyme–DNA interaction. Hence, extensive studies should be performed to understand the importance of FQs-metal complexation on a molecular level.

FQs metal complexation

The formation of FQs-metal complexes generally alters the properties of the parent compound. The first report was concerned about the malabsorption of ciprofloxacin in the presence of antacid, which contained magnesium/aluminum [43]. The decrease of absorption occurred due to the formation of CIP and ion metal chelate. Ever since the extensive studies of FQs metal complexation have been performed.

Ability of FQs to form complexes

The structure of FQs allows them to form metal complexes. Figure 1 presents FQs potential metal binding sites. A detailed description of FQs binding properties was presented by Turel (2002) [55], updated by Serafin and Stanczak (2009) [77] and most recently by Uivarosi V. (2013) [56]. Usually, they act as a bidentate ligand, through one of the oxygen atoms of a carboxylic group and a carbonyl ring oxygen atom [39, 78, 79]. They can also coordinate ions in a unidentate manner via terminal nitrogen atom in piperazinyl group [78]. Rarely, it is possible to form a FQs-metal complex by two carboxyl oxygen atoms or both piperazine nitrogen atoms [80, 81]. Hence, it can be observed that FQs

do not exhibit unitary manner of metal complexation. It makes the generation of FQs-Me complexes difficult to examine.

The investigation of thermodynamic parameters of decomposition process was performed to have more insight into complexation mechanism. The energy of activation (E^*), the entropy of activation (ΔS^*), enthalpy of activation (ΔH^*) and Gibbs free energy (ΔG^*) of NOR-Me complexes are presented in Table 2 [82-84]. They were calculated graphically by adapting Coats–Redfern equations as given in 1-3 [85]:

$$\Delta S^* = R \cdot ln(Ah/kT) \quad (1)$$

$$\Delta H^* = E^* - RT \quad (2)$$

$$\Delta G^* = \Delta H^* - T\Delta S^* \quad (3)$$

where R is the gas constant, A is the Arrhenius constant, h is the Planck constant, k is Boltzmann constant, T is the peak temperature of the decomposition. The values of activation energy of decomposition are relatively high, and they show the thermal stability of the complex. All complexes exhibit negative values of ΔS^*, which increased the overall value of ΔG^*. This indicates that the process of decomposition is non-spontaneous, and the reaction is disfavored. The positive values of ΔH^* indicates, that the process is endothermic – the system requires energy for the reaction to move onwards. Overall, the data presented in Table 2 proves that FQs form stable complexes with metal ions.

Equilibrium of FQs-metal complexes

FQs bind with divalent ions in 1:1 or 1:2 ratio (metal:ligand) and with trivalent ions, in 1:1 or 1:3 ratio, rarely 1:2 [39, 56]. Apart from the concentration of metal ion and ligand, the preferences of complex molar ratio may be pH dependent. For instance, during CIP-Cu complexation, 1:1 ratio is favored in more acidic regions, but at higher pH, 1:2 complex is formed [86]. Furthermore, it was discovered that FQs forms more stable complexes with trivalent cations than with divalent. The least stable FQs complexes are with magnesium (II) and calcium (II) [87, 88], The factor that affects the stability of the complex is also dielectric constant of solvent [89]. The dielectric constant ε (relative permittivity) is an ability of media to isolate charges. It is also related with the chemical polarity of media. In solutions, when the dielectric constant is high (e.g. water, ε = 78), there is no ion association due to the high polarization of media, metal ions and FQs in ionic form would exist as free ions. However, when ε is lower (e.g. MeOH, ε = 32.6), the complex can be formed via ion-pairing [89]. Hence, the lower dielectric constant, the more stable compound due to stronger ion association occurrence. However, the formation of metal complexes is a favored reaction and created compound exhibits high stability, which results in complex formation even in water (high dielectric constant). Complex formation is also pH-dependent, due to ionization of compound [90]. FQs are zwitterionic, due to the presence of carboxylic acid group and basic piperazinyl group. When pH is low (acidic), the basic group will be stronger ionized. With

increasing pH, ionization of basic group weakens, but ionization of acidic group increases. Hence, FQs affinity to bind ions differs, depending on ionization form of antibiotic. The affinity of LOME for two divalent ions (Mg^{2+}, Ca^{2+}) decreases in the order anion>zwitterion>>cation [56].

Extensive studies have been performed to establish stability constants (logβ) of FQs metal complexes. However, the values of the logβ may differ from each other, due to various methods and experimental conditions that were used, especially pH. Table 3 presents overall stability constants of representative FQs-metal complexes, obtained by Urbaniak et al. (2009) [88]. The potentiometric titration experiments were performed at pH 2-11 range and ionic strength I= 0.1 M NaCl, so that all logβ values were determined in the same conditions. Later, obtained data were analyzed by Hyperquad program. The highest values of the logβ are found for complexes with trivalent ions, ranging between 15.8 and 51.6, which confirms that they are the most stable in tested conditions. The lowest logβ values can be observed for complexes with Mg(II) and Ca(II) – the values varied from 9.39 to 11.88. Hence, they are the least stable FQs complexes [87, 88].

Park et al. (2000) investigated the divalent cation complexation with OFL and NOR [45]. The complex formation constants values for cations, which belong to the beryllium group, decrease in the manner Mg^{2+}>Ca^{2+}>Ba^{2+}, owing to increase of cationic radii. If the constant values for transition ion metals are compared, they are lower for Mn^{2+} and Zn^{2+} than for Ni^{2+} and Co^{2+}. The lowered constants are due to the occupation of the electrons in d-orbital. For instance, Zn^{2+} d orbital is fully filled, hence the interaction between the metal ion and FQs orbitals is weak and the constant value is mainly determined by ion-dipole interaction. The cations, Ni^{2+} or Co^{2+} form more stable complexes than Mn^{2+} and Zn^{2+}, due to additional electron-electron interactions between metal ion and ligands. In conclusion, the complex formation value increases with the increase of nuclear charge of metal ions. Thus, generally alkali-earth metal ions, commonly present in water and soils, form less stable complexes. However, metal ions that are considered as heavy metal ions, have higher nuclear charge, forms complexes which are more persistent and pose a greater threat to the environment [40, 91].

Impact of FQs complexation on wastewater treatment

In recent years, the scientific community has focused on the investigation of FQs fate in WWTPs. However, the data concerned about FQs metal complexation influence on the WWTPs is still scarce. Generally, FQs are mostly removed by adsorption on the sludge, with 80-90% of removal efficiency [21, 92]. It was observed that presence of Mg^{2+} and Ca^{2+} inhibited sorption of NOR, OFL, and CIP in saline sewage [92]. As mentioned earlier, Mg^{2+} and Ca^{2+} generate the least stable complexes, hence it is possible that metal ions, like Cu^{2+} or trivalent ions, may exhibit the different effect. Formed complexes may enhance FQs affinity to the sludge or make them more resistant to further degradation, which may be anaerobic/aerobic digestion by bacteria. Studies showed that generally biodegradation of FQs is negligible, mostly due to the low hydraulic retention time of FQs in the system or/and predominance of

adsorption as a removal method [21, 92]. Moreover, the persistence of OFL and its toxicity towards *Pseudomonas putida* in activated sludge was observed [93]. As presented in next section (5.1.), FQs-Me complexes may exhibit toxicity towards bacteria. This may result in a reduction of bacterial community, present in activated sludge. Thus, biological wastewater treatment would be less efficient. Furthermore, CIP was found to be difficult to degrade in aqueous systems, yet in soils, the mineralization was observed [94]. However, if CIP generates stable metal complexes, it is possible that mineralization will be slower, thus environmental exposure of antibiotic is longer. Hence, apart from FQs presence itself, other variables should be taken into consideration during wastewater treatment, such as the presence of other compounds, that may react with them, including metal ions.

Numerous studies were performed to determine the efficiency of FQs degradation during physicochemical treatment. The most promising methods are advanced oxidation processes. For instance, it was proved that CIP can be effectively removed from via oxidation using titanium dioxide [95, 96]. The solar photocatalytic ozonation, using TiO_2, exhibited high mineralization rate (around 85%) of OFL, along with other pharmaceuticals and additionally this system decreased ecotoxicity of the compounds [97]. Over 90% of ENR was degraded during oxidation, using H_2O_2, facilitated by copper oxide and titanium carbide nanoparticles [98]. The effectiveness of Fenton process was also tested. Diao et al. (2017) developed a system, where FeS_2/SiO_2 microspheres were used as a Fenton catalyst [99]. As a result, almost 100% of CIP was degraded within 60 minutes. Even though presented methods are promising to degrade FQs, yet there is no information available on the possible degradation of FQs-metal complexes. They may facilitate the breakdown of such compounds or disturb the lysis due to relatively high stability constant of complexes.

Impact of the FQs complexation on the microorganisms in the water and soil

Antimicrobial activity of FQs-Me complexes

The presence of FQs and its persistence in environmental compartments may induce a toxic effect on microorganisms living in soil and water [94, 100]. It was proved that CIP maintained its antimicrobial activity in both systems, with the inhibition potency stronger in water than in soils. The FQs metal complexes may have the same antimicrobial efficiency as the parent compound, however, they may be more toxic. Factors that influence the complex efficiency against microorganisms are: (1) the nature of the metal ion; (2) the nature of the ligands; (3) the chelate effect, i.e. complexes with bidentate chelating ligands (FQs) and N, N′-donor ligands, exhibit increased antimicrobial potency; (4) the overall charge of complex – usually the antimicrobial activity follows the order: cationic> zwitterionic> anionic complex; (5) the nature and existence of the ion neutralizing the ionic complex; (6) the number of central metal atoms joined in the coordination compound (nucleus) - in general, dinuclear complexes are more potent than the mononuclear ones [46].

Table 4 presents antimicrobial activity expressed by minimal inhibition concentration (MIC) [μg/ml] – the lowest concentration of compound that prevents the visible growth of bacteria [39, 72, 101-105]In Table 5, the results obtained via diffusion method, qualitative antimicrobial susceptibility test, are introduced [106-108]. In some cases, the efficiency to inhibit microorganisms is lower than the ligand itself. However, in general, FQs metal complexes exhibit similar or enhanced antimicrobial activity, comparing with free ligands. In fact, the composition of the media that was used and the experimental condition may affect the outcome of the toxicity assays [109]. The interaction between the antibiotic-metal complex and media components may lead to complex alteration, i.e. hydrolysis. Thus, the active compound that exhibits toxic effect towards the microorganism, may not be necessarily tested substance.

Chelation theory can explain the increase in the activity against microorganisms. Metal ions partially share positive charge with the donor groups of ligands, thus the polarity of ions is decreased. The orbital of ligand and orbital of the cation are overlapping. The delocalization of π-electrons in the chelate ring occurs, thus the lipophilicity of the complex increases, which facilitates the passage of FQs-Me complex through the cell lipid membrane and cell penetration [44, 110, 111].

The antifungal activity of FQs was also tested. In most cases, FQs have no effect on fungi, except for $[Ni/Co(LOME)(H_2O)_4]Cl_2 \cdot H_2O$ complexes (Table 5), which increased inhibition potency against *C. albicans* [106]. The results were compared with a standard antifungal antibiotic, Amphotericin B and LOME-Me complex proved to be less active. GTI-Me complexes (except for Mn^{2+} and Mg^{2+} complexes) also exhibited enhanced activity against *C. albicans* (Table 5) and *Fusarium solani* (data not shown) [108]. From a medical point of view, they are potential antibiotics against fungi, e.g. *C. albicans*, which causes candidiasis - one of the most common hospital infection [112]. FQs-Me complexes may be less toxic for humans than other antifungal compounds, such as amphotericin B. However, on the environmental point of view, FQs and their metal complexes may disturb fungal communities, which can be essential for their ecosystem. For instance, some of the fungi live in the symbiosis with plants (mycorrhiza) [113]. Hence, the presence of compounds that have a toxic effect on them, would also affect the growth of these plants. Moreover, the toxic effect on fungi may have an adverse effect on soil quality, since saprophytic fungi are important for retaining nutrients in the soil [114, 115].

Antibiotic resistance

Long-term exposure to FQs in the environment induces the selection of antibiotic-resistance bacteria, which has become more prevalent in recent years. Girardi et al. (2011) conducted the study concerned about CIP resistance genes present in soils [94]. The genes were not detected in tested bacteria strains, however, resistance genes occurred after >14 days of incubation with the antibiotic.

The resistance of FQs may appear due to the mutation in specific regions of enzyme subunits – gryA and gryB in DNA gyrase and parC for topoisomerase IV [59]. The other resistance mechanism is

upregulation of efflux or reduction of the cell membrane permeability by altering membrane porins [116]. The plasmid-mediated resistance has been also observed [117]. Proteins, encoded on plasmids, can protect topoisomerase from the attack of quinolones.

It was proved that presence of heavy metal ions in environment exhibits positive correlation with the abundance of some antibiotic-resistant genes [118-120]. Metals alone possess antibacterial properties [121]. They may lead to protein dysfunction and deactivate enzymes by exchange of structural/catalytic metal (Pb(II), Ni(II)) or oxidation of Cys in Fe-binding site. Production of reactive oxygen species by Fe(III) or Cu(II) may cause, for example, DNA damage. They may also disable membrane function (Ag(I), Cu(II), Cd(II)) or interfere with nutrient uptake (Fe(III)), Metals also exhibit genotoxicity (e.g. Mn(II), Cr(VI), Cd(II), Co(II)) [121]. Hence, bacteria have developed resistance mechanisms toward metals. Furthermore, the antibiotic and heavy metal resistance genes may be linked in the same plasmid [118, 120]. Hence, metals may influence selection for antibiotic-resistant strains due to a long-term selective pressure to bacteria – metal does not undergo degradation, like antibiotics and other chemical compounds. The exact mechanism and influence on antibiotic-resistant strains of heavy metals is yet to be further investigated.

Modifications of known compounds can be tested to overcome the FQs-resistant bacteria and FQs-metal complexes which is promising in achieving this objective. The data suggested, that free antibiotic and FQs-Me complexes are transported via two different intake routes. FQs enter the cell through non-specific channels, i.e. OmpF or OmpC porins, via passive diffusion and interaction within channels [116, 122, 123]. However, bacteria have developed resistance to reduce antibiotic intake by changes in the permeability of porins or antibiotic efflux mechanisms. In fact, FQs-Me complexes probably enter the bacterial cell in a different manner [124, 125]. The interaction between lipids present in the membrane and antibiotic complex were found to be much stronger, than with free FQ, due to the electrostatic interaction between cationic FQ-Me complex and negatively charged groups of lipids. As a result, metalloantibiotic enter the cell based on hydrophobicity changes [125, 126]. On the other hand, due to the co-contamination of metal ions and antibiotics in the environment, it would be possible for FQs to obtain resistance against metalloantibiotics as well, by changes in membrane composition.

The concerning phenomenon is the development of bacterial defense method via formation of biofilms [127]. In the presence of antibiotics, they use the extracellular biofilm permeability barrier to interfere with the uptake of toxic compounds. However, this process is energetically very costly, hence it may be ineffective. The presence of cations is crucial for this interaction. The metal bridge is formed by binding deprotonated tryptophan, present in biofilm matrices, to the metal ion, which is connected to carboxyl/carbonyl of FQs. Without metal bridging, the cell exhibits higher permeability, FQs uptake, hence the defective chemotaxis occurs [127]. The process is found to be cost-effective energetically for bacteria. Metal bridging forming in biofilm matrices is considered as a crucial factor in antibiotic resistance of bacteria.

Bioaccumulation

FQs were found in golden eagle nestlings and vultures in a concentration range between 20-150 μg/L [128, 129]. With bioaccumulation factor value of 3262 L/kg, CIP exhibited potential accumulation in crucian carp, present in the Haihe River, China [130]. The vegetable-soil systems were also investigated [131, 132]. It was discovered that CIP was absorbed by roots of Chinese cabbage, radish, tomato and long bean and then may be distributed to aboveground parts [131]. NOR was found to accumulate in radish and pakchoi [132]. This data is highly alarming – these vegetables are commonly used in many households throughout the world. Their presence may have an adverse effect on human homeostasis, like affecting gut bacterial flora. Nevertheless, the knowledge about FQs bioaccumulation is still insufficient and more so of the impact of FQs-metal complexation.

Mobility of FC-metal complexes in different environments (water & soil)

The $\log K_{O/W}$ values of different FQs (Table 1) indicate that they have a high affinity for water. Nevertheless, the studies revealed that FQs tend to adsorb to soil, sediments, and sludge [21, 28, 133-135]. Van Doorslaer (2014) indicated that the reported literature values of $\log K_{O/W}$ include modeled and experimental data, where experimental values are at least 1 log unit higher than data obtained via modeling tools [57]. Furthermore, the experimental data showed that there is variability between $\log K_{O/W}$ values, probably due to different temperature of solution and pH depending partitioning [57]. The amphoteric nature of FQs also played a significant role in this case due to their various speciation occurrence.

In the environmental compartments, the abundant substance, that may affect pharmaceuticals mobility is the organic matter [136, 137]. Aristilde and Sposito (2010) conducted the molecular simulations of the interaction between CIP and humic acid, the representative of the organic matter [138]. In an acidic environment, when the humic substances are protonated, CIP exhibits higher affinity towards them. However, at neutral pH and in the presence of divalent cations, two scenarios may take place. The first one is the formation of a ternary complex between CIP and humic substances with metal ions, acting as the mediator. In the second scenario, divalent ions impede the formation of the CIP-humic substance complex [138]. They concluded that the enhancement of the complex formation inversely depends on the ionic radius of the cation – Mg^{2+} and Fe^{2+} facilitating the bonding between CIP and humic substances when compared with Ca^{2+}.

Cation exchange, bridging, or surface complexation are the interaction mechanisms between FQs and soils [135, 139, 140]. In tropical conditions, their distribution coefficient K_d value can reach over 544.2 L/g, while for sulfonamides under the same conditions, it ranged between 0.7-70.1 L/kg [135]. The soil contains different environmental particles, including mineral components, like hydrous oxides. One of the most important minerals, due to their highly reactive surfaces, are hydrous oxides of aluminum and iron [141]. They can form complexes with metal ions or organic compounds. In general, they are

amphoteric. Thus, sorption of the FQs, such as CIP, onto hydrous oxides is a highly pH-dependent process [141]. With the increased pH, the sorption of CIP increased as well, until it reached near neutral pH (pH 7.8 for hydrous oxides of aluminum, and 6.5 for hydrous oxides of iron). Beyond this pH value, the affinity to sorb CIP onto hydrous oxides decreased [141].

The influence of divalent ions (Cu^{2+} and Ca^{2+}) on CIP transport in saturated sand media was investigated [142]. When Al/Fe oxides were present, coated onto the native sand, CIP transport was hindered. Al/Fe tended to form strong complexes with CIP, which resulted in CIP immobilization onto sand and decrease of its concentration in aquatic solution. In this case, only Cu^{2+} could slightly promote CIP transport. When CIP was pre-sorbed onto the sand, both divalent ions were unable to support the mobilization of antibiotic. The pre-sorption of Cu^{2+}/Ca^{2+} onto quartz sand increased CIP adsorption due to metal complexation [143]. However, in clean sand, where Fe/Al hydrous oxides were removed, Cu^{2+}/Ca^{2+}, present in solution, enhanced the mobility of CIP. Though, the effect of Cu^{2+} promotion was stronger than the effect of Ca^{2+} [142, 143]. These results indicate that the presence of metal ion may enhance or reduce CIP sorption efficiency, depending on the metal ion type and if they are present in solid or liquid phase.

FQs adsorption onto diverse types of soils in the presence of divalent ions have been performed. The presence of Zn^{2+} influenced the retention of the ERN on a calcareous soil, leading to an increase of the adsorbed ENR amounts, as presented in Figure 3 A [50]. The distribution coefficient K_d value for ENR adsorption was K_d=0.66 L/g, but for ENR in the presence of zinc (ENR-Zn complex, ratio 1:2), K_d was higher at 1.04 L/g [50]. The influence of Cu^{2+} on ENR has also been investigated– and the ion presence significantly enhanced ENR amount, which adsorbed onto the soil [144]. The data shows that ENR and Cu^{2+} create ternary surface complex, where Cu^{2+} binds in a bidentate fashion to the surface in an inner-sphere mode and it forms a bridge between ENR and soil surface.

The similar dependence was observed with CIP adsorption on goethite [145]. The presence of divalent metal ions increased CIP retention on the soil surface, probably via cation bridging. The order of metal binding affinity of CIP was Cu^{2+}>Pb^{2+}>Cd^{2+}>Ca^{2+}, which corresponded with the obtained complexation constants values. The process did not depend on pH, except for CIP-Cu interaction, which exhibited significant pH dependency due to strong CIP-Cu complexation (the highest complexation constant value in this group of metal ions). The concentration ratio of CIP and metal ions affected antibiotic adsorption – the highest antibiotic adsorption did not occur when the metal ion concentration was in excess. It probably happened due to the partial contribution of metal ions in the CIP sorption process. Moreover, it was proved that metal ions can compete with CIP for the sorption site in the soil as shown in Figure 3 B [142, 143]. Furthermore, the presence of Cu^{2+} and fluvic acid enhanced the sorption of CIP on soil, though the competition between them and decrease of CIP sorption was expected [145].

The co-adsorption of CIP and Cu^{2+} was also investigated on montmorillonite and kaolinite, where montmorillonite have greater cation exchange capacity than kaolinite [146]. The sorption process was tested in wide pH range. In acidic pH (<5.0), $[Cu(CIP^{\pm})]^{2+}$, CIP^{+} and Cu^{2+} were present in solution. $[Cu(CIP^{\pm})]^{2+}$ was prevalent between pH 6.0-7.0, and when pH reached 8.0, $[Cu(CIP^{-}{}_{2})]$ started to precipitate. Between pH 4.0 – 7.0 CIP exhibited strong sorption ability on montmorillonite by cation exchange, probably between permanent charge site on the clay and nitrogen atom on heterocyclic ring of $CIP^{+}/CIP^{\pm}$ [146]. The presence of copper (II) ions showed no effect on CIP sorption on montmorillonite below pH 6.0. It is possible, that montmorillonite provided sufficient sorption capacity and it could sorb CIP^{+} completely. However, above pH 6.0, the value of the CIP sorption increased, when Cu(II) was present. The negatively charged surface of montmorillonite affected the high adsorption of positively charged $[Cu(CIP^{\pm})]^{2+}/[Cu(CIP^{\pm})_2]^{2+}$, rather than $CIP^{\pm}/CIP^{-}$. Another possible mechanism could be that first Cu(II) adsorbs onto clay and then CIP forms a complex with the adsorbed metal ion [146].

Kaolinite exhibited stronger sorption of CIP at higher pH (9.5) than montmorillonite, probably due to the interaction between the variable charge of the clay and carboxyl group of CIP [146]. Cu(II) presence decreased CIP sorption onto kaolinite below pH 6.0. CIP^{+} was more favorably adsorbed onto clay than CIP-Cu complex, because of the interfering interaction between the positively charged surface of kaolinite and carboxyl group of CIP. At higher pH, due to the cation bridge formation, $[Cu(CIP^{\pm})]^{2+}/[Cu(CIP^{\pm})_2]^{2+}$ had a stronger affinity to sorb onto kaolinite [146].

Studies investigating the influence of Ca^{2+} on adsorption of LEVO on goethite demonstrated another relationship between the metal ion and the antibiotic [147]. LEVO is a protonated form (H_2LEVO^{+}) at pH<5.0, which deprotonated ($LEVO^{-}$) above pH 8.5 and it was neutral/zwitterionic ($LEVO^{0}/LEVO^{\pm}$) at pH range between its pK_a values. The highest LEVO adsorption onto goethite is at pH 6.0 and it decreased above or below this pH value. The presence of Ca^{2+} inhibits adsorption which is pH independent. LEVO forms complexes with Ca^{2+} (fig. 3C), which are more positively charged than LEVO itself. Below pH 8.0, CaH_2LEVO^{3+}, $CaHLEVO^{2+}$ or $CaLEVO^{+}$ may be detected, which contributed to lowering of the concentration of absorbed LEVO. Probably, Ca^{2+} competed with the positively charged surface of goethite to form complexes with the carboxyl group of LEVO.

Another research, conducted on three types of soils (Paddy H, Paddy G, and Red J), revealed that NOR adsorption capacity decreases, as the concentration of metal ions increases [148]. However, another study showed that in general, with increasing Cu^{2+} concentration, the K_d value and sorption amount of NOR in black soil, flavor-aquic soil and red soil increase, but then the sorption amount is reduced, regardless NOR concentration. Nevertheless, the inhibition effect of divalent ions on NOR adsorption follows the order $Cu^{2+}>Mg^{2+}>Ca^{2+}>Zn^{2+}$ for paddy soils and $Cu^{2+}>Zn^{2+}>Ca^{2+}>Mg^{2+}$ for red soil. The different ion inhibition order depends on soil properties, like containing additional clay mineral – smectite by paddy soils or higher cation exchange capacity of paddy soils than red soils [148]. Moreover,

the formation of the antibiotic-metal complex may affect sorption affinity of NOR onto soils, by affecting antibiotic properties. The other factor may be metal ions, which entered solution from tested soils. This may have changed the overall concentration of presentions and caused predominance of one metal ion over another.

The differences in environmental compartment composition are the main factors that influence the mobility of FQs and their metal complexes. Other parameters, such as pH, ambient temperature, and climate may also have influence. However, the data is still scarce, hence further evaluation of metal ions influence on FQs transportation should be performed.

Novel approaches towards FCs-metal complexation

FQs-metal complexes are not only tested as antibacterial compounds but also, they have other applications. For instance, [$CoCl_2$[149]($H_2O)_2$] and [$CoCl_2$(SPR)($H_2O)_2$] exhibit activity against the intracellular form of *Trypanosoma cruzi*, a parasite which causes Chagas disease. This potentially life-threatening illness is mostly found in Latin America countries and during acute phase usually manifests as a skin lesion or a purplish swelling of the lids of one eye, but the chronic phase affects the heart or digestive system. SPR and NOR alone have a weak effect on the parasite, though. Moreover, FQs-Me complexes with phenanthroline (phen), [$CuCl_2$(phen)] with [$CuCl_2$(phen)(SPR)], present the significant efficacy against two bloodstream trypomastigotes and intracellular forms of *T. cruzi* [150]. Similar effectiveness has been displayed by LEVO-Cu complexes [151].

The ability of FQs to inhibit type II topoisomerases makes them an interesting potential anti-tumor drug, due to the same cellular target [152, 153]. Moreover, the combination of antimicrobial activity and cytotoxicity against tumor cells display the positive effect on patient survival. To enhance the potency of FQs, the studies, including metal-complexation influence, has been performed. The studies on FQs complexes with Zn (II) revealed that Zn-NOR complexes (1:2) displayed an efficiency to significantly decrease the viability of MDA (human breast adenocarcinoma), Caco-2 (human colon adenocarcinoma) and HeLa (human cervix carcinoma) cell lines [105]. The activity of complexes was higher than their ligand. However, the most promising application as an antitumor drug FQs-Me complexes are organoruthenium (II). The research group from the University of Ljubljana, Slovenia, have investigated complexes between Ru(II) and representatives of FQs (nalidixic acid, cinoxacin, OFL, LEVO, oxolinic acid) [154-157]. For instance, OFL-Ru complexes exhibited cytotoxicity against human tumor cell lines - colon adenocarcinoma and ovarian carcinoma [155]. The thiolated derivative of nalidixic acid and ruthenium complex exhibited higher inhibition potency of the two enzymes, involved in cancer progression and other human diseases – cathepsin B and S [156]. Furthermore, one of the complexes presented the activity against three different human tumor cell lines (small cell lung carcinoma, colon adenocarcinoma, and ovarian carcinoma) [156]. The novel nalidixic acid and Ru(II) complex exhibited cytotoxicity against HeLa cell line and weakly inhibited cathepsin enzymes [157].

The Mannich base is a CIP derivate, which was found to have more antitumor efficiency against human hepatoma cell lines (HCT-116 and HepG2) than its parent compound [158]. Moreover, the Mannich base complex with Cu^{2+} presented significant activity, however, its IC_{50} was lower than Mannich base itself. The cytotoxicity mechanism of the copper compound involved the stabilization of the intermediate of cleavage DNA-topoisomerase II complex and interference with the mitochondrial respiration chain. On the other hand, the Mannich base itself exhibited different mechanism: it caused cell cycle arrest, disrupted ATP production and inhibited topoisomerase II activity through regulation of a pro-apoptotic gene [158].

Komarnicka et al. (2016) presented cytotoxic effectiveness of complexes of Cu(I) and phosphine derived from SPR against mouse colon carcinoma CT26 and human lung adenocarcinoma A549 cell lines [159, 160]. All compounds tended to accumulate in tumor cells and they induced their apoptosis. The stronger activity was exhibited by complexation with halogen ligands. The mechanism of cytotoxicity probably involves their interactions with DNA. Moreover, the presence of free radicals indicates that they may influence the antitumor activity of complexes as well [160].

FQs-metal complexes are also used as a detection method. FQs complexes with Tb^{3+} and Eu^{3+} exhibit luminescence and chemiluminescence properties, which may be useful for analytical applications [161, 162]. The detection method based on these interactions have been tested for presence of ENR [163, 164], trovafloxacin [165], CIP [166], OFL [167], LEVO [168] or GTI [169]. FQs metal complexes may also be used to detect other compounds. For instance, the sensitive spectrofluorometric method has been developed to detect ATP due to its interaction with Al-GTI [170]. The fluorescence response of the complex has been enhanced by the increasing concentration of ATP. Moreover, the method is simple and cost-effective [170]. A similar method may be applied for DNA determination via Tb-prulifloxacin complex [171]. The enhancement of fluorescence intensity of the FQ-Me complex occurs after addition of DNA. The method is very sensitive and environmentally friendly.

Future outlook as extended to different environmental compartments

Long FQs exposure in soils may affect soil fertility. It has been already proved that high concentration of CIP in soil significantly decreased radish growth [131]. Furthermore, FQs-metal complexes, which may be persistent in the environment, may also affect plants and microbial community, which is necessary for proper soil fertility. Disturbance of this dependence may cause reduction of yields or malformation of plants. Moreover, if the plant can accumulate FQs-metal complexes, they may affect living organisms, including human, when the plant is edible. This may lead to accumulation of heavy metals, which exhibit toxicity when alone, but also the presence of antibiotic may have adverse effects. However, the exact effect of FQs-Me complexes on living organisms, except for bacteria, fungi, and some protozoa, is still unknown.

The analogous situation takes place in aquatic compartments. FQs-Me may remain stable in solutions, hence they may affect aquatic fauna and flora, i.e. bacteria, cyanobacteria, green algae, aquatic plants or fish. Furthermore, rivers or water basins are often drinking water source, thus antibiotic-metal complexes may be present in households, which pose the same threats as mentioned earlier. Furthermore, due to the novel technological adaptation of FQs-Me, their application may expand, however, their possible environmental impact and safe disposal must be considered.

Nowadays, there is still unawareness of harmful effects that are posed by FQs and its metal complexes. Extensive studies should be performed to know exact influence of the complexes on the ecosystem. Furthermore, the WWTPs should be improved to detect and eliminate FQs presence in water. Treatment of sludge and soils should also be investigated, to avoid the formation of FQs-Me occurrence. Awareness must be raised so that society will be sensible towards proper drug disposal preventing inadvertent antibiotic-metal interactions and reactions.

Conclusion

The FQs ability to form metal complexes has been widely studied, as well as their potential medical use. They form complexes with divalent and trivalent ions, however interaction between trivalent metal ions and FQs is stronger due to higher formation constant. Formation of FQs-Me complexes and their influence on WWTP processes is still unknown. Researchers [39, 73, 101-108] have investigated the potential toxicity of FQ-Me complexes to microorganisms and generally, complexes have similar activity as FQs. In some cases, such as $[Co(CIP)_2(H_2O)_2]\cdot 9H_2O$ [39], $Fe(ENR)_3$ [101] or Co-LEVO [107], they exhibit enhanced toxicity. Complexes, i.e. $[Ni/Co(LOME)(H_2O)_4]Cl_2\cdot H_2O$ [106] or GTI-Me (Me=Ca^{2+}, Cd^{2+}, Fe^{3+}, Co^{2+}, Ni^{2+}, Co^{2+}, Zn^{2+}) [108], may also exhibit antifungal potency. Hence, so far knowledge of FQs-Me complexes strongly signifies that FQs-metal complexes may also contribute to the dissemination of antibiotic-resistant bacteria and/or genes. Further, FQs-Me complexation was promoting the FQs transport among different environmental compartments such as water, sediment, and soils by adsorption, desorption and ionization processes. And these interactions depend on the present condition and composition of the environmental matrices.

Acknowledgment(s)

The authors are sincerely thankful to the Natural Sciences and Engineering Research Council of Canada (Discovery Grant 355254and NSERC Strategic Grant) and Ministère des Relations Internationales du Québec (coopération Québec-Catalanya 2012-2014- project 07.302).

References

[1] O. Koba, O. Golovko, R. Kodesova, M. Fer, R. Grabic, Environ Pollut, 220 (2017) 1251-1263.

[2] J. Chen, X.D. Wei, Y.S. Liu, G.G. Ying, S.S. Liu, L.Y. He, H.C. Su, L.X. Hu, F.R. Chen, Y.Q. Yang, Sci Total Environ, 565 (2016) 240-248.

[3] J. Xu, Y. Xu, H. Wang, C. Guo, H. Qiu, Y. He, Y. Zhang, X. Li, W. Meng, Chemosphere, 119 (2015) 1379-1385.

[4] L.H. Santos, A.N. Araujo, A. Fachini, A. Pena, C. Delerue-Matos, M.C. Montenegro, J Hazard Mater, 175 (2010) 45-95.

[5] X. Li, N. Watanabe, C. Xiao, T. Harter, B. McCowan, Y. Liu, E.R. Atwill, Environ Monit Assess, 186 (2014) 1253-1260.

[6] C. Stange, J.P. Sidhu, A. Tiehm, S. Toze, Int J Hyg Environ Health, 219 (2016) 823-831.

[7] S.H. Zhang, X. Lv, B. Han, X. Gu, P.F. Wang, C. Wang, Z. He, Environ Sci Pollut Res Int, 22 (2015) 11412-11421.

[8] T. Schwartz, W. Kohnen, B. Jansen, U. Obst, FEMS Microbiol Ecol, 43 (2003) 325-335.

[9] I. Rosas, E. Salinas, L. Martinez, A. Cruz-Cordova, B. Gonzalez-Pedrajo, N. Espinosa, C.F. Amabile-Cuevas, Curr Microbiol, 71 (2015) 490-495.

[10] L.J. Zhou, G.G. Ying, J.L. Zhao, J.F. Yang, L. Wang, B. Yang, S. Liu, Environ Pollut, 159 (2011) 1877-1885.

[11] P.C. Sharma, A. Jain, S. Jain, Acta Pol Pharm, 66 (2009) 587-604.

[12] J.F. Gerster, in, Google Patents, 1975.

[13] T. Irikura, in, Google Patents, 1979.

[14] M. Pesson, in, Google Patents, 1981.

[15] K. Grohe, H.J. Zeiler, K.G. Metzger, in, Google Patents, 1987.

[16] I. Hayakawa, T. Hiramitsu, Y. Tanaka, in, Google Patents, 1983.

[17] V. Niddam-Hildesheim, N. Gershon, E. Amir, S. Wizel, in, Google Patents, 2003.

[18] K. Masuzawa, S. Suzue, K. Hirai, T. Ishizaki, in, Google Patents, 1990.

[19] K.D. Grohe, H.J.D. Zeiler, K.G.D. Metzger, in, Google Patents, 1984.

[20] I. Laponogov, M.K. Sohi, D.A. Veselkov, X.-S. Pan, R. Sawhney, A.W. Thompson, K.E. McAuley, L.M. Fisher, M.R. Sanderson, Nat Struct Mol Biol, 16 (2009) 667-669.

[21] A. Jia, Y. Wan, Y. Xiao, J. Hu, Water res, 46 (2012) 387-394.

[22] K. He, A.D. Soares, H. Adejumo, M. McDiarmid, K. Squibb, L. Blaney, J Pharm Biomed Anal, 106 (2015) 136-143.

[23] G.C. Ghosh, T. Okuda, N. Yamashita, H. Tanaka, Water Sci Technol, 59 (2009) 779-786.

[24] N.M. Vieno, T. Tuhkanen, L. Kronberg, J Chromatogr A, 1134 (2006) 101-111.

[25] H. Nakata, K. Kannan, P.D. Jones, J.P. Giesy, Chemosphere, 58 (2005) 759-766.

[26] X.S. Miao, F. Bishay, M. Chen, C.D. Metcalfe, Environ Sci Technol, 38 (2004) 3533-3541.

[27] H.B. Lee, T.E. Peart, M.L. Svoboda J, Chromatogr A, 1139 (2007) 45-52.

[28] G. Chen, X. Liu, D. Tartakevosky, M. Li, Ecotoxicol Environ Saf, 133 (2016) 18-24.

[29] F. Tamtam, F. Mercier, B. Le Bot, J. Eurin, Q. Tuc Dinh, M. Clément, M. Chevreuil, Sci Total Environ, 393 84-95.

[30] J. Gibs, H.A. Heckathorn, M.T. Meyer, F.R. Klapinski, M. Alebus, R.L. Lippincott, Sci Total Environ, 458 (2013) 107-116.

[31] R.M.P. Leal, R.F. Figueira, V.L. Tornisielo, J.B. Regitano, Sci Total Environ, 432 (2012) 344-349.

[32] A. Karci, I.A. Balcioglu, Sci Total Environ, 407 (2009) 4652-4664.

[33] Public Health Agnecy of Canada, Canadian Antimicrobial Resistance Surveillance System Report 2016, 2016

https://www.canada.ca/en/public-health/services/publications/drugs-health-products/canadian-antimicrobial-resistance-surveillance-system-report-2016.html (accessed: 17.01.24)

[34] European Medicines Agency, Sales of veterinary antimicrobial agents in 26 EU/EEA countries in 2013. Fifth ESVAC report, 2015

http://www.ema.europa.eu/docs/en_GB/document_library/Report/2015/10/WC500195687.pdf (accessed: 17.01.25)

[35] G.G. Zhanel, A. Walkty, L. Vercaigne, J.A. Karlowsky, J. Embil, A.S. Gin, D.J. Hoban, Can J Infect Dis, 10 (1999) 207-238.

[36] V.M.F. Frade, M. Dias, A.C.S.C. Teixeira, M.S.A. Palma, Braz J Pharm Sci, 50 (2014) 41-54.

[37] European Centre for for Disease Prevention and Control, Antimicrobial resistance surveillance in Europe. Annual report of the European Antimicrobial Resistance Surveillance Network (EARS-Net) 2015, 2015

https://ecdc.europa.eu/sites/portal/files/media/en/publications/Publications/antimicrobial-resistance-europe-2015.pdf (accessed: 17.01.25)

[38] World Health Organisation, Critically important antibacterial agents for human medicine for risk management stategies of non-human, 2005,

http://apps.who.int/iris/bitstream/10665/43330/1/9241593601_eng.pdf?ua=1&ua=1 (accessed: 17.01.26)

[39] M.P. Lopez-Gresa, R. Ortiz, L. Perello, J. Latorre, M. Liu-Gonzalez, S. Garcia-Granda, M. Perez-Priede, E. Canton, J Inorg Biochem, 92 (2002) 65-74.

[40] Y. Zhang, X. Cai, X. Lang, X. Qiao, X. Li, J. Chen, Environ Pollut, 166 (2012) 48-56.

[41] J.S. Mohler, T. Kolmar, K. Synnatschke, M. Hergert, L.A. Wilson, S. Ramu, A.G. Elliott, M.A. Blaskovich, H.E. Sidjabat, D.L. Paterson, G. Schenk, M.A. Cooper, Z.M. Ziora, J Inorg Biochem, 167 (2017) 134-141.

[42] S.A. Breda, A.F. Jimenez-Kairuz, R.H. Manzo, M.E. Olivera, Int J Pharm, 371 (2009) 106-113.

[43] G. Hoffken, K. Borner, P.D. Glatzel, P. Koeppe, H. Lode, Eur J Clin Microbiol, 4 (1985) 345.

[44] G.G. Mohamed, M.H. Soliman, Spectrochim Acta A Mol Biomol Spectrosc, 76 (2010) 341-347.

[45] H.-R. Park, K.-Y. Chung, H.-C. Lee, J.-K. Lee, K.-M. Bark, Bull Korean Chem Soc, 21 (2000) 849-854.

[46] G. Psomas, D.P. Kessissoglou, Dalton Trans, 42 (2013) 6252-6276.

[47] R. Pulicharla, R.K. Das, S.K. Brar, P. Drogui, S.J. Sarma, M. Verma, R.Y. Surampalli, J.R. Valero, Sci Total Environ, 532 (2015) 669-675.

[48] Y.J. Wang, D.A. Jia, R.J. Sun, H.W. Zhu, D.M. Zhou, Environ Sci Technol, 42 (2008) 3254-3259.

[49] Y. Zhao, J. Geng, X. Wang, X. Gu, S. Gao, J Colloid Interface Sci, 361 (2011) 247-251.

[50] M. Graouer-Bacart, S. Sayen, E. Guillon, Ecotoxicol Environ Saf, 122 (2015) 470-476.

[51] W.R. Chen, C.H. Huang, Environ Sci Technol, 43 (2009) 401-407.

[52] M.C. Cuquerella, A. Belvedere, A. Catalfo, M.A. Miranda, J.C. Scaiano, G. de Guidi, J Photochem Photobiol B, 101 (2010) 295-303.

[53] P. Villegas-Guzman, J. Silva-Agredo, D. Gonzalez-Gomez, A.L. Giraldo-Aguirre, O. Florez-Acosta, R.A. Torres-Palma, J Environ Sci Health A Tox Hazard Subst Environ Eng, 50 (2015) 40-48.

[54] C. Ribeiro, S.C. Lopes, P. Gameiro, J Membr Biol, 241 (2011) 117-125.

[55] I. Turel, Coord Chem Rev, 232 (2002) 27-47.

[56] V. Uivarosi, Molecules, 18 (2013) 11153-11197.

[57] X. Van Doorslaer, J. Dewulf, H. Van Langenhove, K. Demeestere, Sci Total Environ, 500-501 (2014) 250-269.

[58] N. Janecko, L. Pokludova, J. Blahova, Z. Svobodova, I. Literak, Environ Toxicol Chem, 35 (2016) 2647-2656.

[59] L.A. Mitscher, Chem Rev, 105 (2005) 559-592.

[60] S. Kim, P.A. Thiessen, E.E. Bolton, J. Chen, G. Fu, A. Gindulyte, L. Han, J. He, S. He, B.A. Shoemaker, J. Wang, B. Yu, J. Zhang, S.H. Bryant, Nucleic acids res, 44 (2016) D1202-1213.

[61] D.S. Wishart, C. Knox, A.C. Guo, S. Shrivastava, M. Hassanali, P. Stothard, Z. Chang, J. Woolsey, Nucleic acids res, 34 (2006) D668-672.

[62] J.M. Blondeau, Clin Ther, 21 (1999) 3-40; discussion 41-42.

[63] A. Wohlkonig, P.F. Chan, A.P. Fosberry, P. Homes, J. Huang, M. Kranz, V.R. Leydon, T.J. Miles, N.D. Pearson, R.L. Perera, A.J. Shillings, M.N. Gwynn, B.D. Bax, Nat Struct Mol Biol, 17 (2010) 1152-1153.

[64] A.I. Drakopoulos, P.C. Ioannou, Anal Chim Acta, 354 (1997) 197-204.

[65] K. Takacs-Novak, B. Noszal, I. Hermecz, G. Kereszturi, B. Podanyi, G. Szasz, J Pharm Sci, 79 (1990) 1023-1028.

[66] K. Drlica, X. Zhao, Microbiol Mol Biol Rev, 61 (1997) 377-392.

[67] S. Tornaletti, A.M. Pedrini, Biochimica et biophysica acta, 949 (1988) 279-287.

[68] G. Palù, S. Valisena, G. Ciarrocchi, B. Gatto, M. Palumbo, Proc Natl Acad Sci U S A, 89 (1992) 9671-9675.

[69] I. Turel, P. Živec, A. Pevec, S. Tempelaar, G. Psomas, Eur J Inorg Chem, 2008 (2008) 3718-3727.

[70] D.R. Xiao, E.B. Wang, H.Y. An, Z.M. Su, Y.G. Li, L. Gao, C.Y. Sun, L. Xu, Chemistry, 11 (2005) 6673-6686.

[71] Z.-F. Chen, R.-G. Xiong, J.-L. Zuo, Z. Guo, X.-Z. You, H.-K. Fun, Journal of the Chemical Society, Dalton Transactions, (2000) 4013-4014.

[72] P. Drevensek, J. Kosmrlj, G. Giester, T. Skauge, E. Sletten, K. Sepcic, I. Turel, J Inorg Biochem, 100 (2006) 1755-1763.

[73] P. Drevensek, I. Turel, N. Poklar Ulrih, J Inorg Biochem, 96 (2003) 407-415.

[74] T.R. Blower, B.H. Williamson, R.J. Kerns, J.M. Berger, Proc Natl Acad Sci U S A, 113 (2016) 1706-1713.

[75] X.-y. Yuan, J. Qin, L.-l. Lu, Spectrochim Acta A Mol Biomol Spectrosc, 75 (2010) 520-524.

[76] M.A. Ragheb, M.A. Eldesouki, M.S. Mohamed, Spectrochim Acta A Mol Biomol Spectrosc, 138 (2015) 585-595.

[77] A. Serafin, A. Stańczak, Russian Journal of Coordination Chemistry, 35 (2009) 81-95.

[78] M.S. Refat, Spectrochim Acta A Mol Biomol Spectrosc, 68 (2007) 1393-1405.

[79] S. Lecomte, M.H. Baron, M.T. Chenon, C. Coupry, N.J. Moreau, Antimicrob Agents Chemother, 38 (1994) 2810-2816.

[80] F. Gao, P. Yang, J. Xie, H. Wang, J Inorg Biochem, 60 (1995) 61-67.

[81] L.M.M. Vieira, M.V.d. Almeida, H.A.d. Abreu, H.A. Duarte, R.M. Grazul, A.P.S. Fontes, Inorg Chim Acta, 362 (2009) 2060-2064.

[82] S.A. Sadeek, J Mol Struct, 753 (2005) 1-12.

[83] M.S. Refat, G.G. Mohamed, J Chem Eng Data, 55 (2010) 3239-3246.

[84] M.S. Refat, G.G. Mohamed, R.F. de Farias, A.K. Powell, M.S. El-Garib, S.A. El-Korashy, M.A. Hussien, J. Therm. Anal. Calorim., 102 (2010) 225-232.

[85] A.W. Coats, J.P. Redfern, Nature, 201 (1964) 68-69.

[86] I. Turel, N. Bukovec, E. Farkas, Polyhedron, 15 (1996) 269-275.

[87] M. Sakai, A. Hara, S. Anjo, M. Nakamura, J Pharm Biomed Anal, 18 (1999) 1057-1067.

[88] B. Urbaniak, Z.J. Kokot, Anal Chim Acta, 647 (2009) 54-59.

[89] S. Creager, 3 - Solvents and Supporting Electrolytes A2 - Zoski, Cynthia G, in: Handbook of Electrochemistry, Elsevier, Amsterdam, 2007, pp. 57-72.

[90] D.L. Ross, C.M. Riley, Int J Pharm, 83 (1992) 267-272.

[91] Z. Zhao, J. Wang, Y. Han, J. Chen, G. Liu, H. Lu, B. Yan, S. Chen, Environ Pollut, 220 (2017) 909-918.

[92] B. Li, T. Zhang, Environ Sci Technol, 44 (2010) 3468-3473.

[93] M. Tobajas, V. Verdugo, A.M. Polo, J.J. Rodriguez, A.F. Mohedano, Environ Technol, 37 (2016) 713-721.

[94] C. Girardi, J. Greve, M. Lamshoft, I. Fetzer, A. Miltner, A. Schaffer, M. Kastner, J Hazard Mater, 198 (2011) 22-30.

[95] T.A. Gad-Allah, M.E. Ali, M.I. Badawy, J Hazard Mater, 186 (2011) 751-755.

[96] T. An, H. Yang, W. Song, G. Li, H. Luo, W.J. Cooper, J Phys Chem A, 114 (2010) 2569-2575.

[97] G. Marquez, E.M. Rodriguez, F.J. Beltran, P.M. Alvarez, Chemosphere, 113 (2014) 71-78.

[98] L. Fink, I. Dror, B. Berkowitz, Chemosphere, 86 (2012) 144-149.

[99] Z.-H. Diao, X.-R. Xu, D. Jiang, G. Li, J.-J. Liu, L.-J. Kong, L.-Z. Zuo, J Hazard Mater, 327 (2017) 108-115.

[100] J.D. Maul, L.J. Schuler, J.B. Belden, M.R. Whiles, M.J. Lydy, Environ Toxicol Chem, 25 (2006) 1598-1606.

[101] E.K. Efthimiadou, A. Karaliota, G. Psomas, Polyhedron, 27 (2008) 1729-1738.

[102] E.K. Efthimiadou, Y. Sanakis, M. Katsarou, C.P. Raptopoulou, A. Karaliota, N. Katsaros, G. Psomas, J Inorg Biochem, 100 (2006) 1378-1388.

[103] E.K. Efthimiadou, Y. Sanakis, C.P. Raptopoulou, A. Karaliota, N. Katsaros, G. Psomas, Bioorg Med Chem Lett, 16 (2006) 3864-3867.

[104] A.R. Shaikh, R. Giridhar, M.R. Yadav, Int J Pharm, 332 (2007) 24-30.

[105] F. Ahmadi, M. Saberkari, R. Abiri, H.M. Motlagh, H. Saberkari, Appl Biochem Biotechnol, 170 (2013) 988-1009.

[106] H.F. Abd el-Halim, G.G. Mohamed, M.M. el-Dessouky, W.H. Mahmoud, Spectrochim Acta A Mol Biomol Spectrosc, 82 (2011) 8-19.

[107] N. Sultana, M.S. Arayne, S.B.S. Rizvi, U. Haroon, M.A. Mesaik, Med Chem Res, 22 (2013) 1371-1377.

[108] N. Sultana, A. Naz, M.S. Arayne, M.A. Mesaik, J Mol Struct, 969 (2010) 17-24.

[109] A. Levina, D.C. Crans, P.A. Lay, Coord Chem Rev, (2017).

[110] M. Tümer, H. Köksal, M.K. Sener, S. Serin, Transit Metal Chem, 24 (1999) 414-420.

[111] P.K. Panchal, H.M. Parekh, P.B. Pansuriya, M.N. Patel, J Enzyme Inhib Med Chem, 21 (2006) 203-209.

[112] A. Mora Carpio, A. Climaco, Candidiasis, Fungemia, in: StatPearls, StatPearls Publishing, StatPearls Publishing LLC., Treasure Island (FL), 2017.

[113] M. Parniske, Nat Rev Microbiol, 6 (2008) 763-775.

[114] C.H. Robinson, J. Dighton, J.C. Frankland, P.A. Coward, Plant and Soil, 151 (1993) 139.

[115] H. Setala, M.A. McLean, Oecologia, 139 (2004) 98-107.

[116] J.M. Pages, C.E. James, M. Winterhalter, Nat Rev Microbiol, 6 (2008) 893-903.

[117] X. Zhao, J. Yang, B. Zhang, S. Sun, W. Chang, Front Microbiol, 8 (2017) 1300.

[118] P. Gao, S. He, S. Huang, K. Li, Z. Liu, G. Xue, W. Sun, Appl Microbiol Biotechnol 99 (2015) 3971-3980.

[119] D. Mao, S. Yu, M. Rysz, Y. Luo, F. Yang, F. Li, J. Hou, Q. Mu, P.J. Alvarez, Water res, 85 (2015) 458-466.

[120] X. Ji, Q. Shen, F. Liu, J. Ma, G. Xu, Y. Wang, M. Wu, J Hazard Mater, 235-236 (2012) 178-185.

[121] J.A. Lemire, J.J. Harrison, R.J. Turner, Nat Rev Microbiol, 11 (2013) 371-384.

[122] K.R. Mahendran, M. Kreir, H. Weingart, N. Fertig, M. Winterhalter, J Biomol Screen, 15 (2010) 302-307.

[123] T. Mach, P. Neves, E. Spiga, H. Weingart, M. Winterhalter, P. Ruggerone, M. Ceccarelli, P. Gameiro, J Am Chem Soc, 130 (2008) 13301-13309.

[124] M.J. Feio, I. Sousa, M. Ferreira, L. Cunha-Silva, R.G. Saraiva, C. Queiros, J.G. Alexandre, V. Claro, A. Mendes, R. Ortiz, S. Lopes, A.L. Amaral, J. Lino, P. Fernandes, A.J. Silva, L. Moutinho, B. de Castro, E. Pereira, L. Perello, P. Gameiro, J Inorg Biochem, 138 (2014) 129-143.

[125] M. Ferreira, P. Gameiro, J Membr Biol, 248 (2015) 125-136.

[126] C. Ribeiro, S.C. Lopes, P. Gameiro, J Membr Biol, 241 (2011) 117-125.

[127] F. Kang, Q. Wang, W. Shou, C.D. Collins, Y. Gao, Environ Pollut, 220 (2017) 112-123.

[128] G. Blanco, A. Junza, D. Segarra, J. Barbosa, D. Barron, Chemosphere, 144 (2016) 1536-1543.

[129] G. Blanco, A. Junza, D. Barron, Sci Total Environ, 135 (2017) 292-301.

[130] L. Gao, Y. Shi, W. Li, J. Liu, Y. Cai, J Environ Monit, 14 (2012) 1248-1255.

[131] Q.M. Xiao, J.W. Wang, Y.L. Tang, Ying yong sheng tai xue bao = The journal of applied ecology, 23 (2012) 2708-2714.

[132] J. Wang, H. Lin, W. Sun, Y. Xia, J. Ma, J. Fu, Z. Zhang, H. Wu, M. Qian, J Hazard Mater, 304 (2016) 49-57.

[133] L.M. Peruchi, A.H. Fostier, S. Rath, Chemosphere, 119 (2015) 310-317.

[134] F.J. Peng, L.J. Zhou, G.G. Ying, Y.S. Liu, J.L. Zhao, Environ Toxicol Chem, 33 (2014) 776-783.

[135] R.M. Leal, L.R. Alleoni, V.L. Tornisielo, J.B. Regitano, Chemosphere, 92 (2013) 979-985.

[136] P. Kulshrestha, R.F. Giese, Jr., D.S. Aga, Environ Sci Technol, 38 (2004) 4097-4105.

[137] Q.L. Fu, J.Z. He, L. Blaney, D.M. Zhou, Chemosphere, 159 (2016) 103-112.

[138] L. Aristilde, G. Sposito, Environ Toxicol Chem, 29 (2010) 90-98.

[139] D. Vasudevan, G.L. Bruland, B.S. Torrance, V.G. Upchurch, A.A. MacKay, Geoderma, 151 (2009) 68-76.

[140] Q. Wu, Z. Li, H. Hong, K. Yin, L. Tie, Appl Clay Sci, 50 (2010) 204-211.

[141] C. Gu, K.G. Karthikeyan, Environ Sci Technol, 39 (2005) 9166-9173.

[142] H. Chen, L.Q. Ma, B. Gao, C. Gu, J Hazard Mater, 262 (2013) 805-811.

[143] H. Chen, L.Q. Ma, B. Gao, C. Gu, J Hazard Mater, 252-253 (2013) 375-381.

[144] M. Graouer-Bacart, S. Sayen, E. Guillon, J Colloid Interface Sci, 408 (2013) 191-199.

[145] Y. Tan, Y. Guo, X. Gu, C. Gu, Environ Sci Pollut Res Int, 22 (2015) 609-617.

[146] Z. Pei, X.Q. Shan, J. Kong, B. Wen, G. Owens, Environ Sci Technol, 44 (2010) 915-920.

[147] X. Qin, F. Liu, G. Wang, L. Weng, L. Li, Colloids Surf B Biointerfaces, 116 (2014) 591-596.

[148] X. Kong, S. Feng, X. Zhang, Y. Li, J Environ Sci (China), 26 (2014) 846-854.

[149] A.M. Jacobsen, B. Halling-Sørensen, F. Ingerslev, S.H. Hansen, J . Chromatogr A, 1038 (2004) 157-170.

[150] D.d.G.J. Batista, P.B. da Silva, L. Stivanin, D.R. Lachter, R.S. Silva, J. Felcman, S.R.W. Louro, L.R. Teixeira, M.d.N.C. Soeiro, Polyhedron, 30 (2011) 1718-1725.

[151] D.A. Martins, L.R. Gouvea, D. da Gama Jean Batista, P.B. da Silva, S.R. Louro, C.S.M. de Nazare, L.R. Teixeira, Biometals, 25 (2012) 951-960.

[152] G.S. Bisacchi, M.R. Hale, Curr Med Chem, 23 (2016) 520-577.

[153] A. Ahmed, M. Daneshtalab, J Pharm Pharm Sci, 15 (2012) 52-72.

[154] I. Turel, J. Kljun, F. Perdih, E. Morozova, V. Bakulev, N. Kasyanenko, J.A.W. Byl, N. Osheroff, Inorg Chem, 49 (2010) 10750-10752.

[155] J. Kljun, A.K. Bytzek, W. Kandioller, C. Bartel, M.A. Jakupec, C.G. Hartinger, B.K. Keppler, I. Turel, Organometallics, 30 (2011) 2506-2512.

[156] R. Hudej, J. Kljun, W. Kandioller, U. Repnik, B. Turk, C.G. Hartinger, B.K. Keppler, D. Miklavčič, I. Turel, Organometallics, 31 (2012) 5867-5874.

[157] J. Kljun, I. Bratsos, E. Alessio, G. Psomas, U. Repnik, M. Butinar, B. Turk, I. Turel, Inorg Chem, 52 (2013) 9039-9052.

[158] Y. Fu, Y. Yang, S. Zhou, Y. Liu, Y. Yuan, S. Li, C. Li, Int J Oncol, 45 (2014) 2092-2100.

[159] U.K. Komarnicka, R. Starosta, A. Kyziol, M. Jezowska-Bojczuk, Dalton Trans, 44 (2015) 12688-12699.

[160] U.K. Komarnicka, R. Starosta, M. Plotek, R.F. de Almeida, M. Jezowska-Bojczuk, A. Kyziol, Dalton Trans, 45 (2016) 5052-5063.

[161] C. Sun, H. Ping, M. Zhang, H. Li, F. Guan, Spectrochim Acta A Mol Biomol Spectrosc, 82 (2011) 375-382.

[162] C. Guo, A. Lang, L. Wang, W. Jiang, J Lumin, 130 (2010) 591-597.

[163] M.J. Schneider, L. Yun, S.J. Lehotay, Food Addit Contam Part A Chem Anal Control Expo Risk Assess, 30 (2013) 666-669.

[164] J. Zdunek, E. Benito-Pena, A. Linares, A. Falcimaigne-Cordin, G. Orellana, K. Haupt, M.C. Moreno-Bondi, Chemistry, 19 (2013) 10209-10216.

[165] N.A. Alarfaj, M.F. El-Tohamy, Luminescence, 30 (2015) 1403-1408.

[166] M. Kamruzzaman, A.M. Alam, K.M. Kim, S.H. Lee, Y.S. Suh, Y.H. Kim, S.H. Kim, S.H. Oh, J Nanosci Nanotechnol, 12 (2012) 6125-6130.

[167] M.S. Attia, A.A. Essawy, A.O. Youssef, M.S. Mostafa, J Fluoresc, 22 (2012) 557-564.

[168] S.H. Lee, S.M. Wabaidur, Z.A. Alothman, S.M. Alam, Luminescence, 26 (2011) 768-773.

[169] L. Wang, C. Guo, B. Fu, L. Wang, J Agric Food Chem, 59 (2011) 1607-1611.

[170] M. Kamruzzaman, A.N. Faruqui, M.I. Hossain, S.H. Lee, Luminescence, 30 (2015) 1077-1082.

[171] T. Wu, B. Fang, L. Chang, M. Liu, F. Chen, Luminescence, 28 (2013) 894-899.

Tables

Table 1. Structures, medical use and physicochemical properties of fluoroquinolones representatives. Data obtained from PubChem Compound Database [60]

Quinolone structure	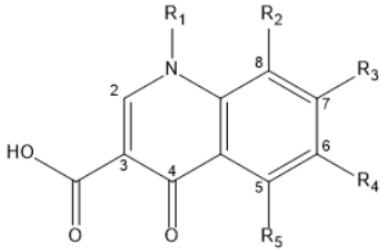										
Compound name	Medical use	R_1	R_2	R_3	R_4	R_5	PubChem CID	Molecular weight [g/mol]	$\log K_{ow}$	pK_a	Solubility (in water) [mg/L]
Ciprofloxacin (CIP)	Human medicine: urinary tract infections, acute uncomplicated cystitis, chronic bacterial prostatitis, lower respiratory tract infections, acute sinusitis, skin and skin structure infections, bone and joint infections, complicated intra-abdominal infections (used in combination with metronidazole), infectious diarrhea, typhoid fever (enteric fever), uncomplicated		-H	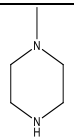	-F	-H	2764	331.347	0.28	pK_{a1}=6.09 pK_{a2}=8.74	30.0 (20°C)

Quinolone structure	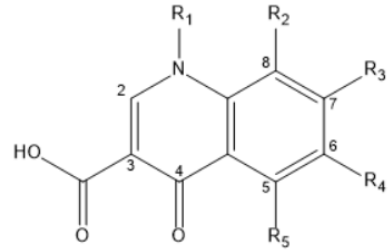										
Compound name	Medical use	R_1	R_2	R_3	R_4	R_5	PubChem CID	Molecular weight [g/mol]	$\log K_{ow}$	pK_a	Solubility (in water) [mg/L]
	cervical and urethral gonorrhea, and inhalational anthrax (post-exposure)										
Enrofloxacin (ENR)	Veterinary med: treatment of individual pets and domestic animals (U.S.)		-H	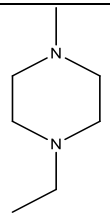	-F	-H	71188	359.401	0.83*	pK_{a1} = 5.88 - 6.06 pK_{a2}= 7.70 - 7.74	>53.9 [μg/mL]
Gatifloxacin (GTI)	Human med: bronchitis, sinusitis, community-acquired pneumonia, and skin infections (abscesses, wounds)		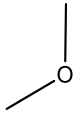	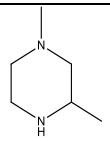	-F	-H	5379	375.4	2.6	pK_{a1}=5.69** pK_{a2}=8.73**	60 (at pH4)

Quinolone structure	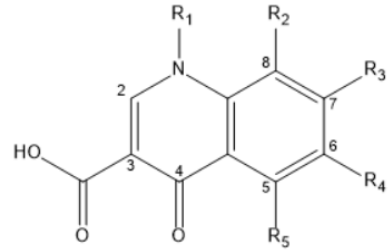										
Compound name	Medical use	R_1	R_2	R_3	R_4	R_5	PubChem CID	Molecular weight [g/mol]	$\log K_{ow}$	pK_a	Solubility (in water) [mg/L]
Levofloxacin (LEVO)	Human med: acute bacterial sinusitis, pneumonia, urinary tract infections, chronic prostatitis, some types of gastroenteritis; addition to other drugs - tuberculosis, meningitis, or pelvic inflammatory disease	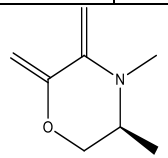		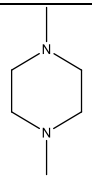	-F	-H	149096	361.373	-0.39	pK_{a1}=6.24	Insoluble (>54.2 [μg/mL])
Lomefloxacin (LOME)	Human med: bronchitis and urinary tract infections	-CH_2CH_3	-F	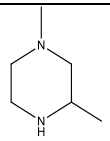	-F	-H	3948	351.354	-0.3	pK_{a1}=5.64*** pK_{a2}=8.70***	27.2

Quinolone structure	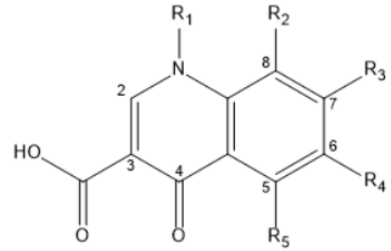										
Compound name	Medical use	R_1	R_2	R_3	R_4	R_5	PubChem CID	Molecular weight [g/mol]	$logK_{ow}$	pK_a	Solubility (in water) [mg/L]
Norfloxacin (NOR)	Human med: urinary tract infections, prostatitis, and sexually transmitted diseases (syphilis)	-CH_2CH_3	-H	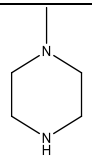	-F	-H	4539	319.336	0.46	pK_{a1}= 6.34 pK_{a2}=8.75	0.28 (25°C) *Solubility in water is pH dependent, increasing sharply at pH<5 or pH >10*
Ofloxacin (OFL)	Human medicine: respiratory tract, kidney, skin, soft tissue infections, urinary tract infections, urethral and cervical gonorrhea	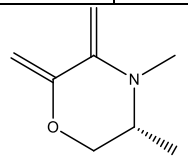		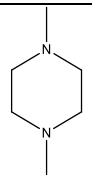	-F	-H	4583	361.373	-0.39	pK_{a1}= 5.97 pK_{a2}=9.28	28.3

Quinolone structure	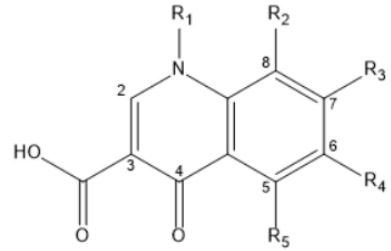										
Compound name	Medical use	R_1	R_2	R_3	R_4	R_5	PubChem CID	Molecular weight [g/mol]	$\log K_{ow}$	pK_a	Solubility (in water) [mg/L]
Sparfloxacin (SPR)	Human med: pneumonia, bronchitis (withdrawn from the U.S. market)		-F	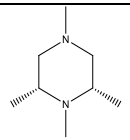	-F	-NH_2	60464	392.407	2.5	pK_{a1}= 5.75** pK_{a2}= 8.79 **	Practically insoluble

** Data obtained from DrugBank Database [61]

*** Data obtained from He K. et. al (2015) [22]

Table 2. Thermodynamic parameters of decomposition process of norfloxacin (NOR) metal complexation

Compound	**Temperature range [K]**	**E^* [kJ mol^{-1}]**	**ΔS^* [JK^{-1}mol^{-1}]**	**ΔH^* [kJ mol^{-1}]**	**ΔG^* [kJ mol^{-1}]**	**Ref.**
NOR	336–458 537–735 844–996	4.43 12.6 17.5	-1.78 -1.73 -1.74	4.11 12.1 16.7	1.1 2.25 3.28	[82]
$[Mn(NOR)_2](OAc)_2 \cdot 8H_2O$	305–369 727–827	3.65 24.5	-1.74 -0.26	3.38 23.9	0.91 2.19	
$[Fe(NOR)_3]Cl_3 \cdot 12H_2O$	316-383 597-694	9.33 15.3	-0.007 -0.526	9.05 14.8	0.903 1.81	
$[Co(NOR)_2]SO_4\ 8H_2O$	312-372 706-909	8.02 11.1	-0.399 -1.63	7.44 10.04	0.907 2.4	
$[Cd(NOR)_2]Cl_2 \cdot 2H_2O$	303-413 413-843 843-1273	37.98 27.96 71.28	-129.2 -87.45 -104.4	37.48 25.31 65.29	45.23 53.30 140.5	[84]
$[Cd(NOR)_2](NO_3)_2$	373-696 696-1173	71.66 56.79	-133.0 -96.26	68.67 51.14	116.6 116.6	
$[Hg(NOR)_2]Cl_2$	323-423 423-693 693-923	116.2 59.40 49.82	-83.50 -146.8 -69.82	115.6 57.15 45.74	109.7 96.79 93.18	
$[Hg(NOR)_2](NO_3)_2$	323-773	17.24	-67.41	14.17	39.11	
$[Zn(NOR)_2]Cl_2 \cdot 2H_2O$	303-413 473-583	46.75 113.6	-116.5 -80.39	46.21 111.0	53.78 136.7	
$[Zn(NOR)_2]Br_2$	423–1273	205.0	-67.52	16.34	50.10	
$[Cr(H\text{-}NOR)_2(Cl)_2]Cl \cdot \cdot 3H_2O$	303-586	53.43	-95.32	53.21	112.21	[83]
$[Mn(H\text{-}NOR)_2(Cl)_2]$	303-909	101.5	-142.6	81..65	177.20	
$[Mn(NOR)_2(H_2O)_2]$	303-593	208	-51.21	93.44	88.94	
$[Ni(H\text{-}NOR)_2(Cl)_2]$	303-903	60.42	-151.24	58.34	96.22	
$[Ni(H\text{-}NOR)_2(SO_4)]$	303-303	50.11	-97.44	51.22	92.46	

Table 3. Overall stability constants logβ of FQs-metal complexes received via potentiometric titration experiment, pH 2-11, ionic strength I= 0,1 M NaCl, under gaseous nitrogen atmosphere, at 22 ◦C, and analyzed by Hyperquad programe. Data obtained from [88]

$pMe+qFQ+rH \rightarrow Me_pFQ_qH_r$ $$log\beta = \frac{[Me_pFQ_qH_r]}{[Me]^p[FQ]^q[H^r]}$$						
Metal ions	Ca^{2+}	Cu^{2+}	Mg^{2+}	Zn^{2+}	Fe^{3+}	Al^{3+}
CIP						
Me(FQ)H	11.24	14.89	11.88	12.74	18.86	16.27
$Me(FQ)_2H_2$	-	29.06	-	24.84	-	29.67
$Me(FQ)_3H_3$	-	-	-	-	48.63	43.53
ENR						
Me(FQ)H	-	12.73	10.11	13.26	17.58	15.14
$Me(FQ)_2H_2$	-	25.73	-	23.70	-	27.36
$Me(FQ)_3H_3$	-	-	-	-	44.63	44.28
LEVO						
Me(FQ)H	9.93	13.74	11.88	12.90	18.98	18.90
$Me(FQ)_2H_2$	-	26.25	-	23.87	-	31.17
$Me(FQ)_3H_3$	-	-	-	-	46.92	40.85
LOME						
Me(FQ)H	10.66	15.94	10.90	10.90	25.44	18.95
$Me(FQ)_2H_2$	-	28.61	-	-	-	23.36
$Me(FQ)_3H_3$	-	-	-	-	51.60	45.55
NOR						
Me(FQ)H	10.65	14.75	11.80	12.90	15.80	15.36
$Me(FQ)_2H_2$	-	28.45	-	25.35	-	29.47
$Me(FQ)_3H_3$	-	-	-	-	47.80	42.79
OFL						
Me(FQ)H	9.89	14.21	11.11	14.64	20.32	17.56

pMe+qFQ+rH→$Me_pFQ_qH_r$ $$log\beta = \frac{[Me_pFQ_qH_r]}{[Me]^p[FQ]^q[H^r]}$$						
Metal ions	Ca^{2+}	Cu^{2+}	Mg^{2+}	Zn^{2+}	Fe^{3+}	Al^{3+}
$Me(FQ)_2H_2$	-	26.25	-	24.40	-	28.84
$Me(FQ)_3H_3$	-	-	-	-	48.32	41.11
SPR						
Me(FQ)H	10.97	14.41	11.54	13.16	-	17.68
$Me(FQ)_2H_2$	-	28.44	-	25.91	-	29.47
$Me(FQ)_3H_3$	-	-	-	-	50.54	42.53

Abbreviations: [Me] – metal concentration, [FQ] – fluoroquinolone concentration, [H] – protons concentration, [MeFQH] – complex concentration, p, q, r – molar ratios of metal, fluoroquinolone and protons repsectvely, CIP – ciprofloxacin, ENR – enrofloxacin, LEVO – levofloxacin, LOME -lomefloxacin, NOR – norfloxacin, OFL – ofloxacin, SPR – sparfloxacin

Table 4 Minimal inhibition concentration of fluoroquinolone-metal complexes [μg/mL]

Compound	Minimal inhibitory concentration [μg/mL]											Additional information (media composition, pH)	References
	Bacteria Gram+					Bacteria Gram-							
	S.aureus	*M.luteus*	*B. subtilis*	*S. epidermidis*	*E. faecalis*	*E. coli*	*P. aeugrinosa*	*S. enteriditis*	*K..pneumoniae*	*S. liquefaciens*	*C. freundii*		
CIP	0.25	-	0.03	0.12	1	0.12	0.12	-	0.12	0.004	0.004	Agar incorporation method; media: Mueller Hinton broth/agar (Difco) - Beef extract 2 g/L, Acid digest of Casein 17.5 g/L, Starch 1.5 g/L, Calcium: 2.9–5.9 mg/L; Magnesium: 3.2–5.2 mg/L, pH (2.1% solution, 25°C): 7.3 ± 0.1	[39]
$[Co(CIP)_2(H_2O)_2]\cdot 9H_2O$	0.25	-	0.06	0.06	1	0.03	0.12	-	0.12	0.008	0.12		
$[Zn(CIP)_2(H_2O)_2]\cdot 8H_2O$	0.25	-	0.03	0.12	1	0.03	0.12	-	0.06	0.008	0.004		
$Ni(CIP)_2\cdot 10H_2O$	0.5	-	0.03	0.12	1	0.03	0.12	-	0.12	0.001	0.004		
$Cu(CIP)_2\cdot 6H_2O$	0.25	-	0.03	0.06	1	0.12	0.12	-	0.06	0.004	0.001		
ENR	8	-	-	-	-	1	1	-	-	-	-	Broth dilution method; media: minimal medium salts broth - 1.5% w/v glucose, 0.5% w/v NH_4Cl, 0.5% w/v K_2HPO_4, 0.1% w/v NaCl, 0.01% w/v $MgSO_4\cdot 7H_2O$ and 0.1% w/v yeast extract	[101]
$Mn(ENR)_2(H_2O)_2$	8	-	-	-	-	1	1	-	-	-	-		
$Fe(ENR)_3$	2	-	-	-	-	0.25	0.25	-	-	-	-		
$Co(ENR)_2(H_2O)_2$	2	-	-	-	-	1	1	-	-	-	-		
$Ni(ENR)_2(H_2O)_2$	8	-	-	-	-	1	1	-	-	-	-		
$Zn(ENR)_2(H_2O)_2$	2	-	-	-	-	1	1	-	-	-	-		

Compound	Minimal inhibitory concentration [μg/mL]											Additional information (media composition, pH)	References
	Bacteria Gram+					Bacteria Gram-							
	S.aureus	*M.luteus*	*B. subtilis*	*S. epidermidis*	*E. faecalis*	*E. coli*	*P. aeugrinosa*	*S. enteriditis*	*K..pneumoniae*	*S. liquefaciens*	*C. freundii*		
$Cd(ENR)_2(H_2O)_2$	8	-	-	-	-	1	1	-	-	-	-		
$Cu(ENR)_2(H_2O)$	4	-	-	-	-	0.125	0.125	-	-	-	-		[102]
LEVO	-	7	0.3	0.3	4	0.15	3	0.3	0.25	-	-	Agar diffusion method; media: Lauria Broth nutrient agar - 0.5% (w/v) yeast extract, 1% (w/v) tryptone, 1% (w/v) NaCl; FQs-Me complexes diluted in 50 mM Tris HCl buffer pH 7.4	[72]
$[Mg(LEVO)(H_2O)_2]\cdot 2H_2O$	-	10	0.5	0.6	4	0.15	5	0.6	0.5	-	-		
NOR	0.06	-	-	0.04	-	0.05	-	-	0.075	-	-	Agar diffiusion method; media: Mueller Hinton broth/agar (Difco) - Beef extract 2 g/L, Acid digest of Casein 17.5 g/L, Starch 1.5 g/L, Calcium: 2.9–5.9 mg/L; Magnesium: 3.2–5.2 mg/L, pH (2.1% solution, 25°C): 7.3 ± 0.1	[104]
$Bi(NOR)_4(H_2O)_2$	0.045	-	-	0.03	-	0.025	-	-	0.06	-	-		
NOR	-	-	-	-	0.001	0.002	0.002	-	-	-	-		[105]

Compound	Minimal inhibitory concentration [μg/mL]											Additional information (media composition, pH)	References
	Bacteria Gram+					Bacteria Gram-							
	S.aureus	*M.luteus*	*B. subtilis*	*S. epidermidis*	*E. faecalis*	*E. coli*	*P. aeugrinosa*	*S. enteriditis*	*K..pneumoniae*	*S. liquefaciens*	*C. freundii*		
Zn-NOR	-	-	-	-	$3 \cdot 10^{-5}$	0.001	0.002	-	-	-	-	Broth dilution method; media: Mueller Hinton broth/agar (Difco) - Beef extract 2 g/L, Acid digest of Casein 17.5 g/L, Starch 1.5 g/L, Calcium: 2.9–5.9 mg/L; Magnesium: 3.2–5.2 mg/L, pH (2.1% solution, 25°C): 7.3 ± 0.1	
OFL	-	12	0.5	0.75	10	0.2	7	0.75	0.7	-	-	Agar diffusion method; media: Lauria Broth nutrient agar - 0.5% (w/v) yeast extract, 1% (w/v) tryptone, 1% (w/v) NaCl; FQs-Me complexes diluted in 50 mM Tris HCl buffer pH 7.4	[72]
$[Mg(R/S\text{-}OFL)(H_2O)_2] \cdot 2H_2O$	-	20	0.8	1	15	0.25	10	1	1	-	-		
H-SPR	0.5	-	-	-	-	8.0	0.25	-	-	-	-	-	[103]
$Cu(SPR)_2$	1.0	-	-	-	-	2.0	0.25	-	-	-	-		

Abbreviations: *S. aureus – Staphylococcus aureus; M. luteus - Micrococcus luteus; B. subtilis - Bacillus subtilis; S. epidermidis – Staphylococcus empidermidis; E. faecalis - Enterecoccus faecalis; E. coli – Escherichia coli; P. aeugrinosa - Pseudomonas aeruginosa; S. enteriditis - Salmonella enteriditi; Klebsiella pneumoniae – K. pneumoniae; Serratia liquefaciens - S. liquefaciens, Citrobacter freundi – C. freundi*

1. Efthimiadou, E.K., A. Karaliota, and G. Psomas, *Mononuclear metal complexes of the second-generation quinolone antibacterial agent enrofloxacin: Synthesis, structure, antibacterial activity and interaction with DNA.* Polyhedron, 2008. **27**(6): p. 1729-1738.

Table 5 Antimicrobial activity tested via Dish Diffusion Testing

Compound	Bacteria Gram+				Bacteria Gram-					Fungi			
	S.aureus	*C. hoffmannii*	*B. subtilis*	*E. faecalis*	*P. mirabilis*	*E. coli*	*P. aeugrinosa*	*S. enteriditis*	*K..pneumoniae*	*C. albicans*	*A. niger*	*A. flavus*	*S. cerevisiae*
Inhibition zone diameter [mm/ml sample] [106] – media: Lauria Broth nutrient agar - 0.5% (w/v) yeast extract, 1% (w/v) tryptone, 1% (w/v) NaCl;													
LOME	48	-	-	-	-	43	-	-	-	11	-	NA	-
$[Cr(LOME)(H_2O)_4]\cdot Cl_3$	38	-	-	-	-	36	-	-	-	12	-	NA	-
$[Mn(LOME)(H_2O)_4]\cdot Cl_2$	48	-	-	-	-	43	-	-	-	11	-	NA	-
$[Fe(LOME)(H_2O)_4]Cl_3\cdot H_2O$	46	-	-	-	-	40	-	-	-	13	-	NA	-
$[Co(LOME)(H_2O)_4]\cdot Cl_2$	44	-	-	-	-	40	-	-	-	20	-	NA	-
$[Ni(LOME)(H_2O)_4]Cl_2\cdot H_2O$	40	-	-	-	-	40	-	-	-	21	-	NA	-
$[Cu(LOME)(H_2O)_4]Cl_2\cdot 2H_2O$	43	-	-	-	-	42	-	-	-	12	-	NA	-
$[Zn(LOME)(H_2O)_4]\cdot Cl_2$	47	-	-	-	-	42	-	-	-	12	-	NA	-
Inhibition zone diameter [mm] [107]– media: Nutrient Agar - agar 15 g/L, meat extract 1 g/L, peptone 5 g/L, NaCl 5 g/L, yeast extract 2 g/L; 7.1±0.2 (25 °C)													
LEVO	12	10	12	-	12	16	14	-	16	-	-	-	-
Mn-LEVO	13	10	13	-	14	17	12	-	18	-	-	-	-
Co-LEVO	18	11	16	-	11	15	12	-	14	-	-	-	-
Ni-LEVO	15	12	13	-	12	16	15	-	17	-	-	-	-
Cu-LEVO	14	9	13	-	13	16	13	-	17	-	-	-	-
Zn-LEVO	14	11	14	-	13	15	16	-	17	-	-	-	-
[108]; Compound activity: +++++ = 150–200% inhibition; ++++, 90–100% inhibition; +++, 75–85% inhibition; ++, 50–60% inhibition; +, 20–30% inhibition													

Compound	Bacteria Gram+				Bacteria Gram-					Fungi			
	S.aureus	*C. hoffmannii*	*B. subtilis*	*E. faecalis*	*P. mirabilis*	*E. coli*	*P. aeugrinosa*	*S. enteriditis*	*K..pneumoniae*	*C. albicans*	*A. niger*	*A. flavus*	*S. cerevisiae*
GTI	++++	-	+++	-	++++	++++	++++	-	++++	++++	-	-	NA
$Mg(GTI)_2$	+++++	-	+++	-	+++++	++++	++++	-	++++	NA	-	-	NA
$Ca(GTI)_2$	++++	-	+++	-	+++	+++++	+++++	-	+++++	+++++	-	-	NA
$Cr(GTI)_2$	++++	-	+++	-	+++++	+++	+++	-	+++++	+++++	-	-	NA
$Mn(GTI)_2$	++++	-	+++	-	+++++	+++++	+++++	-	++++	NA	-	-	NA
$Fe(GTI)_2$	++++	-	+++	-	+++++	++++	++++	-	+++++	+++++	-	-	NA
$Co(GTI)_2$	++++	-	+++	-	+++	++++	+++++	-	+++++	+++++	-	-	NA
$Ni(GTI)_2$	+++++	-	+++	-	+++++	+++	++++	-	+++++	+++++	-	-	NA
$Cu(GTI)_2$	++++	-	+++	-	++++	++++	+++	-	+++++	+++++	-	-	NA
$Zn(GTI)_2$	+++++	-	+++	-	++++	++	++++	-	+++++	+++++	-	-	NA
$Cd(GTI)_2$	++++	-	+++	-	+++	+++	+++	-	+++++	+++++	-	-	NA

Abbreviations: NA – no activity; *S. aureus – Staphylococcus aureus; C. hoffmannii - Corynebacterium hoffmannii B. subtilis - Bacillus subtilis; E. faecalis - Enterecoccus faecalis; P. mirabilis - Proteus mirabilis; E. coli – Escherichia coli; P. aeugrinosa - Pseudomonas aeruginosa; S. enteriditis - Salmonella enteriditi; Klebsiella pneumoniae – K. pneumoniae; C. albicans – Candida albicans; A. niger - Aspergillus niger; A. flavus- Aspergillus flavus; S. cereisiae – Saccharomyces cerevisiae*

Figures

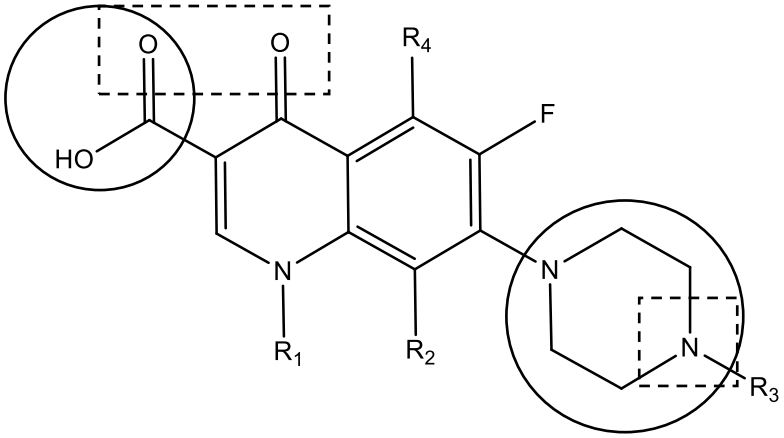

Figure 1 Structure of Fluroquinones with possible binding sites (marked in rectangles) and position of ionizable groups, responsible for pK_a values (marked in circles)

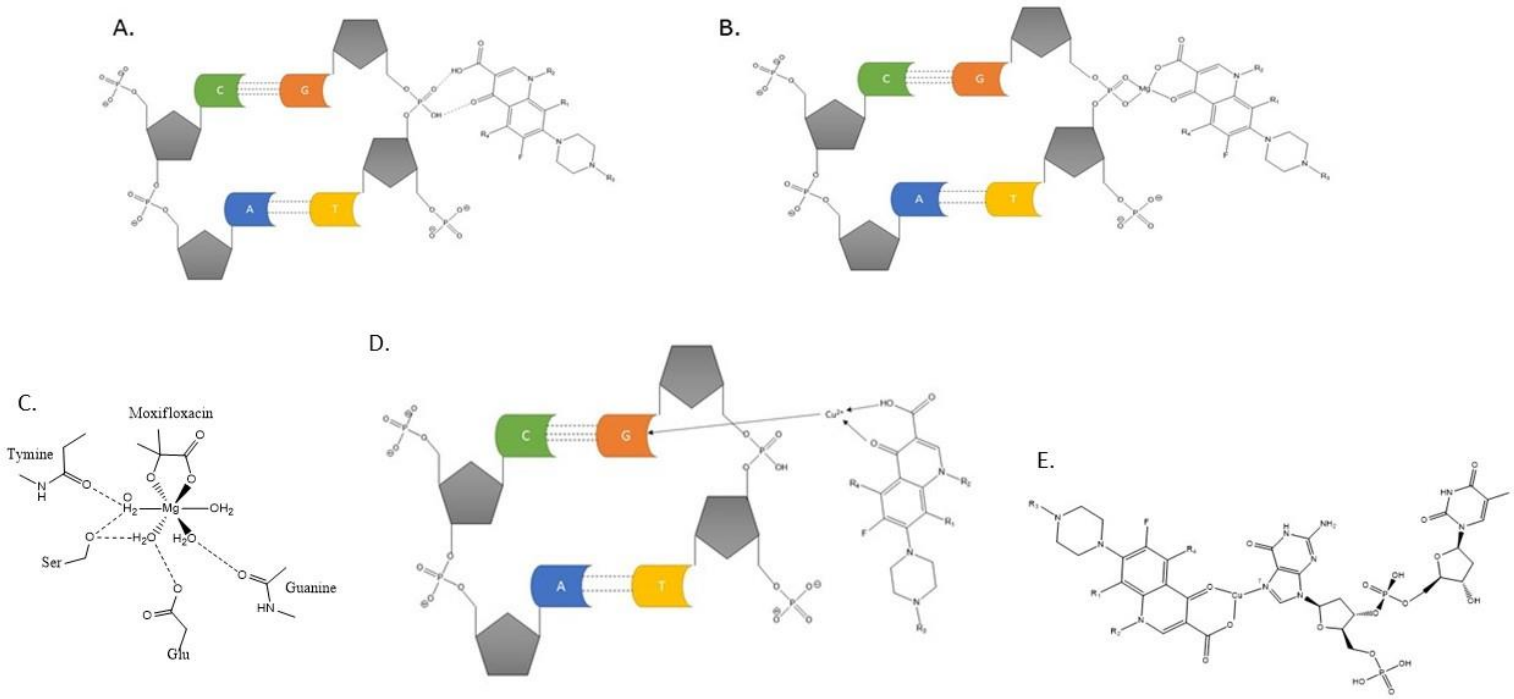

Figure 2 Schematic binding between DNA and A. fluoroquinolone; B. fluoroquinolone via magnesium bridge; C. Coordination sphere around Mg^{2+} based on the crystal structure of complex of moxifloxacin, DNA and magnesium ions [56]; D. fluoroquinolone via transition ion as a mediator; E. binding between N-7 at guanine and fluoroquinolone, when transition ion acts as mediator – the presence of ion facilities the binding of fluoroquinolone

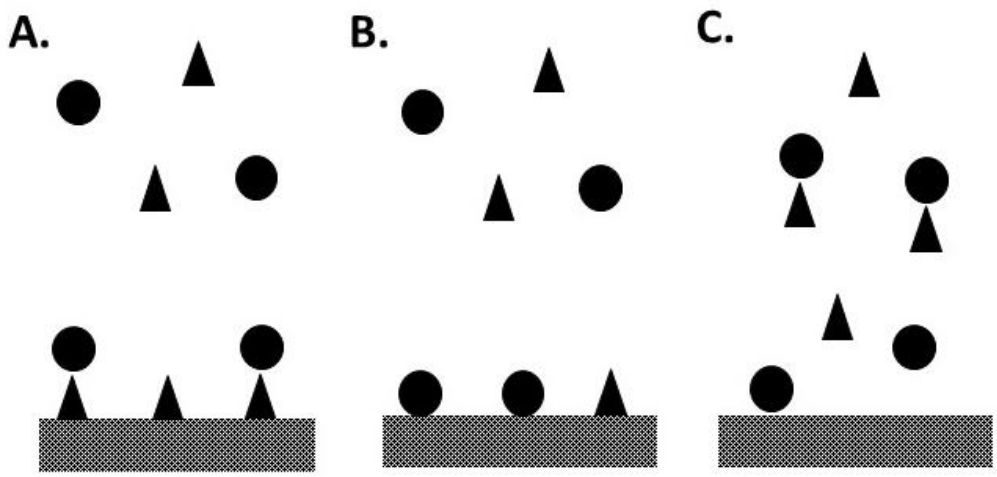

Figure 3. Key interactions between soils, metals, and fluoroquinolones, where circle is fluoroquinolone and triangle is metal ion; A. metal ion acts as metal bridge between antibiotic and soil; B. metal ion and fluoroquinolone compete for binding sites in soil; C. formation of fluoroquinolone and metal complexes, which inhibits sorption onto soil

ANNEX B

Minimal inhibitory concentration – protocol

Firstly, the stock solutions of the tested MI-CIP complexes were prepared as described in section 2. The final concentrations of components were 10 mg/L of CIP, 0.4 of MI and 10 mg/L of HS, when they toxicity of antibiotic complex was investigated in the presence of HS. Then the serial dilutions were prepared with the final volume of 1 ml.

The agar was prepared. It was sterilized and then cooled down to 50˚C in a water bath. About 19 ml of liquid agar was added to the tubes with a diluted solution of MI-CIP. They were mixed carefully and then poured into the Petri plates. The plates were left at ambient temperature to solidify. The inoculum of both bacteria was diluted in 0.85% w/v saline solution to obtain 107 colony-forming unit/ml. Then, the plates were inoculated with diluted strains onto the dried plates. The plates were incubated in the conditions given before.

The minimal inhibitory concentration of the CIP complexes was estimated by the evaluation of the growth of the bacteria on the plates which contained a decreasing concentration of the complex. A single colony or thin haze within the area of the inoculated spot was disregarded. The Figure S1 presents the example of the investigated concentration of CIP-Cu. The 1st plate has few single colonies, which were discarded during the evaluation step. The growth of bacteria had an increasing trend with the decreasing CIP-Cu concentration, hence the authors concluded that the minimal inhibitory concentration, in this case, is represented by the first plate.

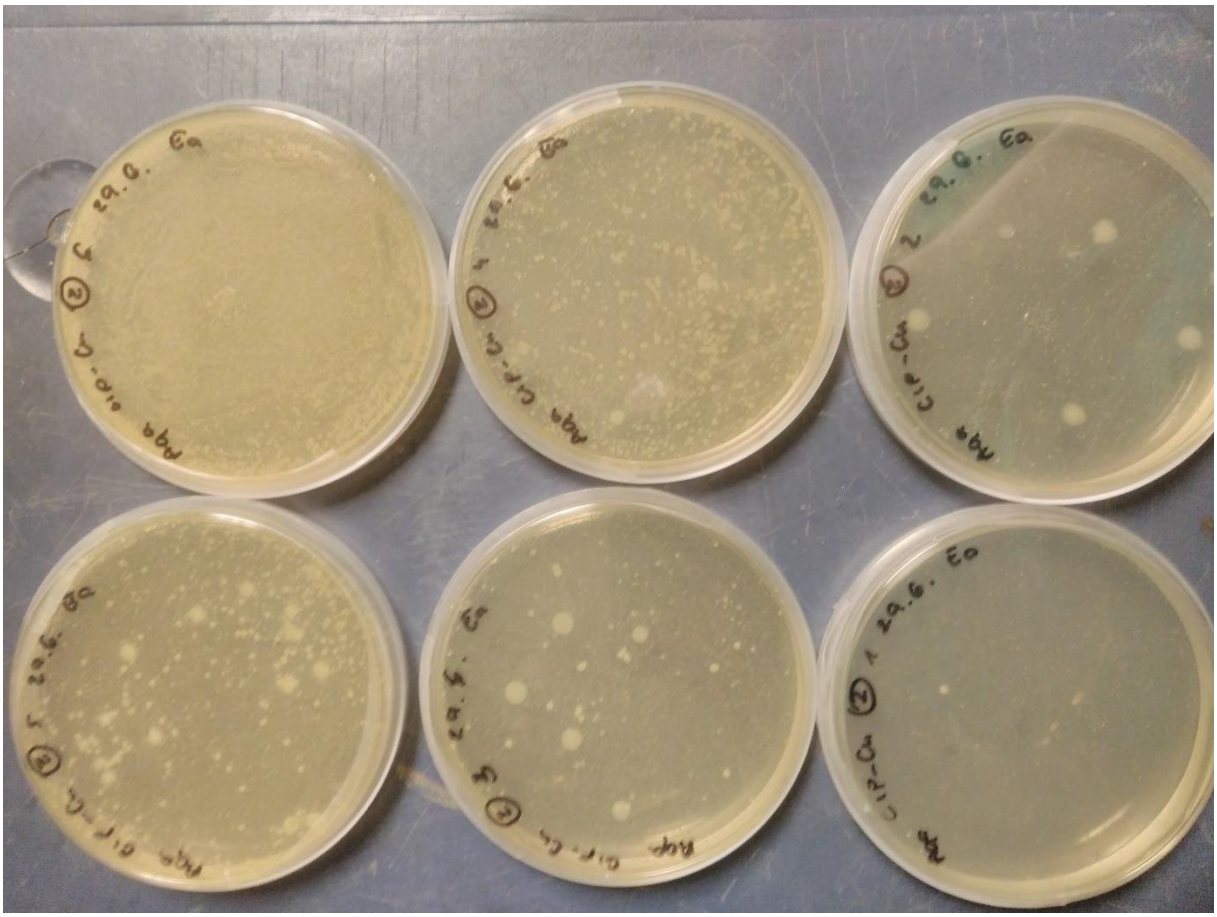

Figure S1. The example of agar dilution results for the estimation of MIC of Cu-CIP for E. aeruginosa; the plate with number 1 has the highest tested concentration, whereas the 6th plate has the lowest

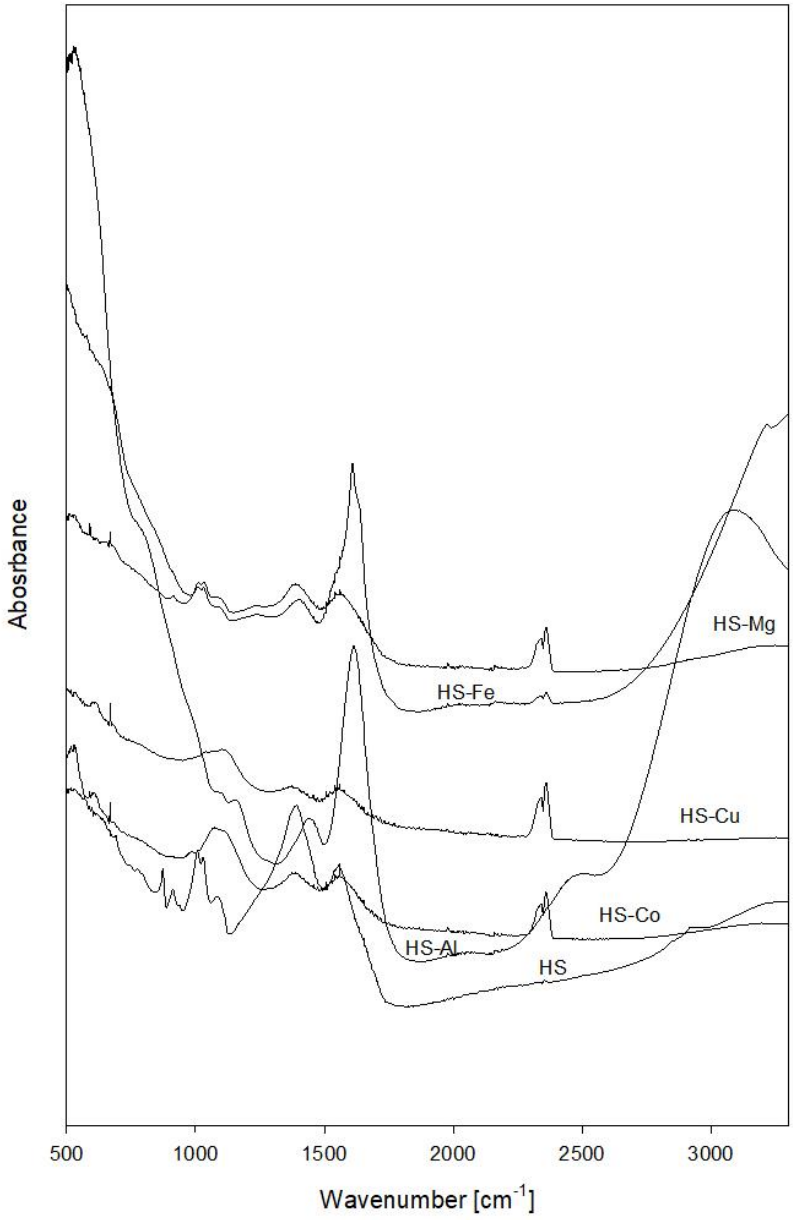

Figure S2. The FTIR spectra of complexes between humic substances and metal ions

ANNEX C

Methodology

1. ICP-AES

Calibration standards were prepared in 10% HNO_3 and 30% HCl. To all standards and samples, Y 5mg/L + CsCl 10 g/L in 1% HNO_3 was added as the internal standard. Randomly chosen samples were spiked with a known concentration of elements; the recovery of all tested elements was 100±2%.

2. CTC and CIP sludge extraction

    a. Pressurized hot water extraction

The extraction of CIP and CTC from sludge was performed via PHWE using Dionex ASE 350 accelerated solvent extractor (Dionex, Sunnyvale, CA, USA). The procedure described by Carretero et al. (2008) was used with some modifications [1]. A 0.5 g of lyophilized sludge was placed in the mortar and gently blended with the dispersing agent (EDTA-washed or not washed diatomaceous earth). Subsequently, the mixture was packed into a 34 mL stainless steel cell. The circular glass microfiber filters (1.98 cm diameter, Dionex) were placed on the top and bottom of the cell. Any void space that remained after packing, was filled with the dispersing agent (diatomaceous earth). The heating cell time was set at 5 min, the pressure was kept at 1500 psi, the time of purging with nitrogen was 60 s, the flushing volume of water with respect to the cell size was 40%. Tested parameters were the static time of solvent in contact with the samples (5, 10 and 15 min) and the temperature (70, 90 and 100 ˚C).

    b. Ultrasonic extraction

USE was carried out in an ultrasonic water bath (Fisher, FB 15069, Mississauga, Ontario) at a frequency of 37 kHz. The procedure was based on the protocol described by Martínez-Carballo et al. (2007) with some changes [2]. Lyophilized sludge sample (0.5 g) was transferred into a 50 mL Falcon tube (Fisher Scientific, Canada), followed by addition of 5 mL of solvent and vortexed. Different solvents, i.e. EDTA-McIlwaine buffer, pH 4.0; EDTA-McIlwaine buffer, pH 3.0; acetonitrile: acetic acid pH 4.0; acetonitrile: trichloroacetic acid pH 3.5 were used to optimize the best simultaneous recovery for CTC and CIP. The sonication was carried out for 20 min, then the samples were centrifuged (12,000 x g, 15 min), the supernatant was collected. The extraction process was repeated twice for each sample. The supernatants were combined and preconcentrated via solid-phase extraction.

Results

Method development for simultaneous detection of CTC and CIP from WW and WWS

The quantification of CTC and CIP was successfully achieved by LC-ESI-MS/MS method. The calibration curve of CIP and that of CTC exhibited a good linear correlation in the tested concentration range (20 – 200 µg/L) with a correlation coefficient (R^2) of 0.9975 and 0.9951 respectively. The limit of detection was found to be 8 µg/L and 15 µg/L for CIP and CTC respectively whereas the limit of quantification was 24 µg/L and 45 µg/L for CIP and CTC respectively.

Due to their diverse chemical structures, antibiotics exhibited specific interactions in the wastewater matrix and the tested solvents even though both are hydrophilic and amphoteric compounds. To simultaneously extract both antibiotics, the extraction methods were adapted from Ferhi et al. [3]. Based on the overall recovery results shown in Table S1 (Annex C), the elution carried out with MeOH: TCA (8:2) was chosen as a suiTable SPE eluent. The recoveries above 100% (Table S1, Annex C) may have been due to the differences between the extracted matrix and calibration matrix. The addition of Na_2EDTA to liquid samples before SPE as the chelating agent was found essential due to minimized weak ion complexation by CTC and CIP [4] as characterized by decreases in recovery efficiency, which dipped to around 50% in absence of Na_2EDTA addition (data not shown), which confirms the importance of EDTA addition from previous reports [4, 5]. Moreover, EDTA-metal complexes might have prevented the competitive interaction between the antibiotics and other metal ions over adsorbing sites of C18 cartridge [5]. On the other hand, the study of Lee et al. (2007) reported that addition of chelating agents in spiked sewage samples resulted in a substantial decrease of fluoroquinolone recovery (<40%) [6], which is similar to our results or dissimilar to our recoveries. The recoveries of CIP and CTC in selected wastewater matrixes are shown in Table S2 (Annex C). As can be seen, the elution of CTC/CIP from wastewater gives recoveries up to >85%. CTC has higher extraction efficiency in water samples than in spiked deionized water, which may suggest that compounds present in this matrix facilitated the extraction.

The extraction of targeted antibiotics via PHWE was unsuccessful, as the recoveries were less than 10% for both the compounds. As for USE, a few extraction solvents were tested, and the results are presented in Table S3. One of the highest extraction efficiency was obtained with McIlvaine-EDTA buffer, pH 3.0 (90% for CTC and 50% for CIP), thereafter all the sludge extractions were carried out using this method. The recovery studies showed that extraction efficiency depends on the type of sample (Table S2) [7].

Tables

Table S1. Mean percent of SPE recoveries for CIP and CTC in deionized water

Compound	MeOH pH 3.0 [%]	MeOH pH 4.0 [%]	MeOH:AA 9:1, pH 4.0 [%]	MeOH:AA 9:1, pH 3.0 [%]	MeOH:AA 8:2, pH 4.0 [%]	MeOH:AA 8:2, pH 3.0 [%]	MeOH:TCA 8:2, pH 4.0 [%]	MeOH:TCA 8:2, pH 3.0 [%]

CTC	48±7	80±2	51±4	32±9	24±0.3	38±13	56±7	38±14
CIP	85±11	50±16	126±5	126±17	92±15	123±9	118±12	30±4

Table S2. Mean percent recoveries for CIP and CTC in the selected spiked matrix

Compound	Deionized water [%]	Influent [%]	Screening unit [%]	Effluent [%]	Primary sludge [%]	Secondary sludge [%]	Thickened sludge [%]
CTC	56±7	90±0.3	123±4	85±0.02	25±5	45±2	90±14
CIP	118±12	98±0.2	135±2	85±2	28±5	50±4	50±4

Table S3. Mean percent of USE recoveries for CIP and CTC in thickened sludge

Solvent	Acetonitrile + acetic acid pH 4.0 [%]	Acetonitrile + trichloroacetic acid pH 3.5 [%]	EDTA-McIlvaine buffer pH 4.0 [%]	EDTA-McIlvaine buffer pH 3.0 [%]
CTC	<10	<10	65±11	90±14
CIP	<10	<10	43±6	50±4

Figures

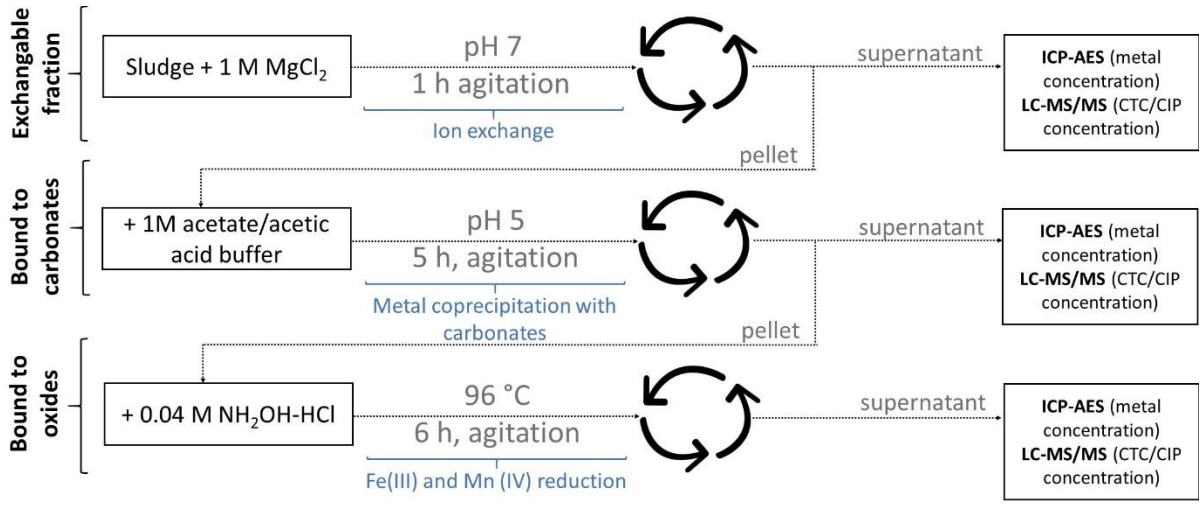

Figure S1. Schematic procedure of fractionable extraction

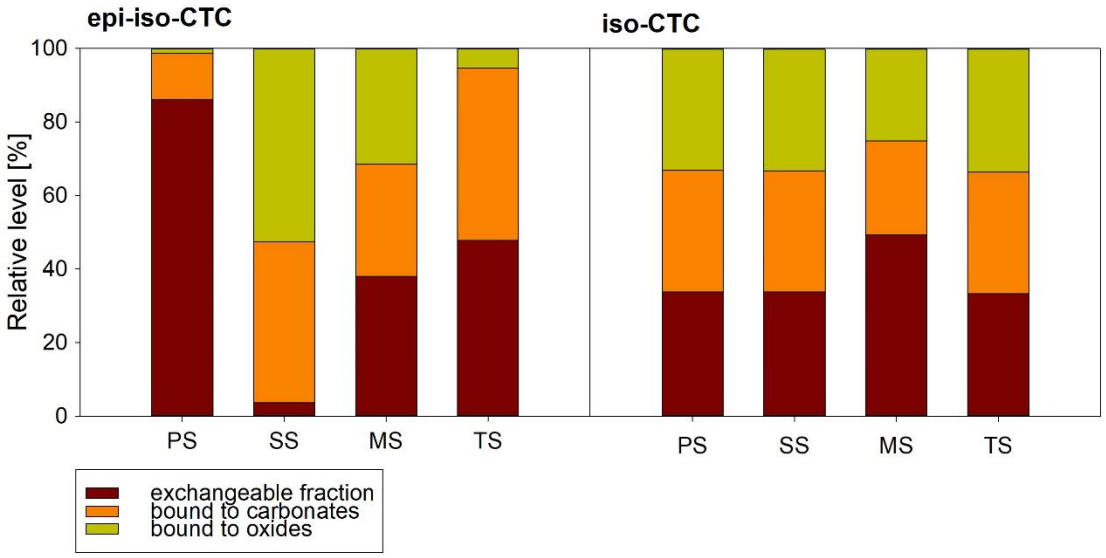

Figure S2. Distribution of chlortetracycline (CTC) isomers, i.e. epi-iso-CTC and iso-CTC in waster sludges; PS – primary sludge; SS – secondary sludge; MS – mixed sludge; TS – thickened sludge

ANNEX D

Tables

Table S1. Characterization of wastewater effluent

Parameter	Value
Total solids [g/L]	0.49 ± 0.013
Total suspended solids [g/L]	0.071 ± 0.0041
Volatile solids [g/L]	0.037 ± 0.022
Total organic carbon [mg/L]	6.15±0.25
Chemical oxygen demand [mg/L]	49
pH	7.53
CIP [μg/L]	2.85 ±0.62

Table S2. Cost of materials used in the study

Material	Cost [USD/kg]
Sodium sulfate	0.3
Laccase	20
Syringaldehyde	20

Figures

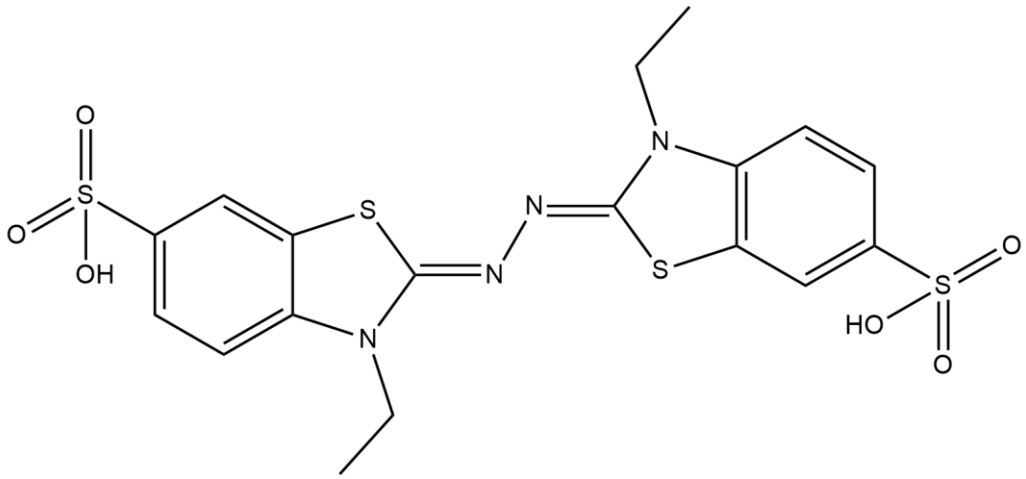

ABTS

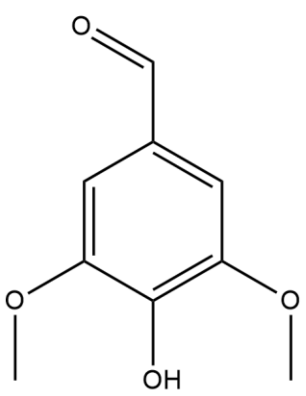

Syringaldehyde

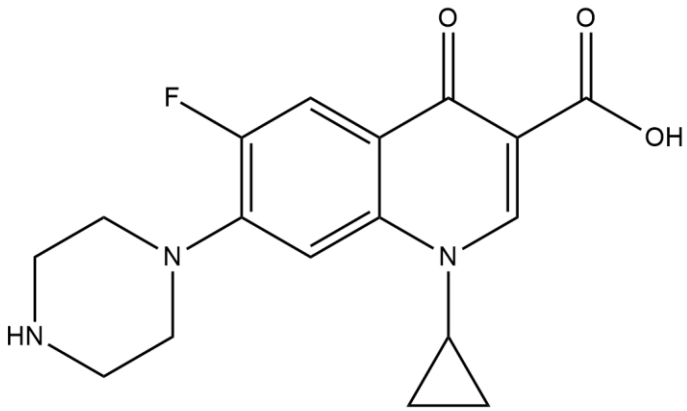

Ciprofloxacin

Figure S1. Chemical structures of compound used in the study

ANNEX E

Table S1 Estimation of the costs related to the production of the crude enzyme and water treatment

Material	Material cost	Material cost to treat 1 m^3 of wastewater
	[USD/kg]	[USD/m^3]
Apple pomace	0.00*	-
Tween 80	2.57	-
Na_2HPO_4	0.47	-
NaH_2PO_4	1.13	-
Syringaldehyde	20	2.90
Pure laccase	105 000	42 000
Crude laccase	-	10 000

	Equipment	Equipment price [USD]	Energy consumption to treat 1 m3 of wastewater [kWh]	Cost to treat 1 m3 of wastewater [USD/m^3]
Solid state fermentation	Incubator (e.g. ThermoFisher Herotherm™, capacity 747 L)	6,200	468	-
Enzyme extraction	Liquid mixer (e.g. LIANHE Chemical Machinery, capacity 100-10000 L)	2,000	50	-
	Centrifuge (e.g. PKII Ultracentrifuge Alfa Wassermann; 100 L in 4 hours)	12,000	14	-
Water treatment	Liquid mixer (e.g. LIANHE Chemical Machinery, capacity 100-10000 L)	10,000	0.09	0.14

***** The haulage cost is non-significant to the overall cost of material procurement in case of scaled-up process

ANNEX F

Table S1. Metals concentration leached from biochars and CH-BB. All concentrations are given in µg/L

Metal	PM-BC	PW-BC	AS-BC	CH-BB
Al	ND	ND	ND	356.9
As	9.7	8.7	6.4	3.9
Be	2.2	1.3	1.6	0.9
Ca	1185.0	2670.7	ND	ND
Cd	0.6	0.3	0.2	0.3
Co	1.2	0.8	0.6	0.4
K	127566.3	15123.3	250530.9	ND
Mg	2933.9	386.2	621.5	914.7
Mn	ND	188.6	ND	8.1
Mo	2121.2	4564.8	2607.4	6451.5
Na	16112.1	ND	ND	5107.7
Ni	1.5	5.4	4.0	9.3
P	4003.4	405.8	2377.1	72.6
Se	88.9	99.6	8.2	90.1
Sr	5.9	14.5	2.9	2.1

Abbreviations: PM-BC – pig manure biochar; PW-BC – pinewood biochar; AS-BC – almond shell biochar; CH-BB – chitosan-biochar beads; ND – not detected

Table S2. Kinetic and adsorption models and their parameters

Model	Equation	Linearized form	Parameters
Pseudo-first order	$\frac{dq_t}{dt} = k_1(q_e - q_t)$	$\log(q_e - q_t) = log q_e - \frac{k_1}{2.303}$	b_T [J/mol]: the Temkin constant related to the heat of adsorption C_0 [mg/L]: initial concentration of pollutant I: thickness of the boundary layer k_1 [1/h]: the rate constant of pseudo-first-order adsorption k_2 [g/mg h]: the rate constant of pseudo-second-order adsorption K_F [(mg/g)(L/mg)$^{1/n}$]: the Freundlich adsorption constant
Pseudo-second order	$\frac{dq_t}{dt} = k_2(q_e - q_t)^2$	$\frac{t}{q_t} = \frac{1}{k_2 q_e^2} + \frac{1}{q_e}t$	
Intraparticle diffusion	$q_t = k_p t^{1/2} + C$	$q_t = k_p t^{1/2} + I$	
Langmuir	$q_e = \frac{q_m K_L C_e}{1 + K_L C_e}$	$\frac{C_e}{q_e} = \frac{1}{q_m K_L} + \frac{C_e}{q_m}$ $R_L = \frac{1}{1 + K_L C_{0,max}}$	

Model	Equation	Linearized form	Parameters
Freundlich	$q_e = K_F C_e^{1/n}$	$lnq_e = lnK_F + \frac{1}{n} lnC_e$	K_L [L/mg]: the Langmuir adsorption constant k_p [mg/g $h^{1/2}$): the intraparticle diffusion rate constant K_T [L/mg]: the Temkin constant related to the equilibrium binding energy *n*: the empirical parameter relating the adsorption intensity, which varies with the heterogeneity of the material (dimensionless) q_e [mg/g]: the adsorption capacity at equilibrium q_m [mg/g]: complete monolayer adsorption capacity q_t [mg/g]: the adsorption capacity at time *t* *R* [8.314 J/(mol K)]: the gas constant R_L : equilibrium parameter *T* [K]: the absolute temperature *t* [h]: contact time
Temkin	$q_e = Bln(K_T C_e)$	$q_e = BlnK_T + BlnC_e$ $B = \frac{RT}{b_T}$	

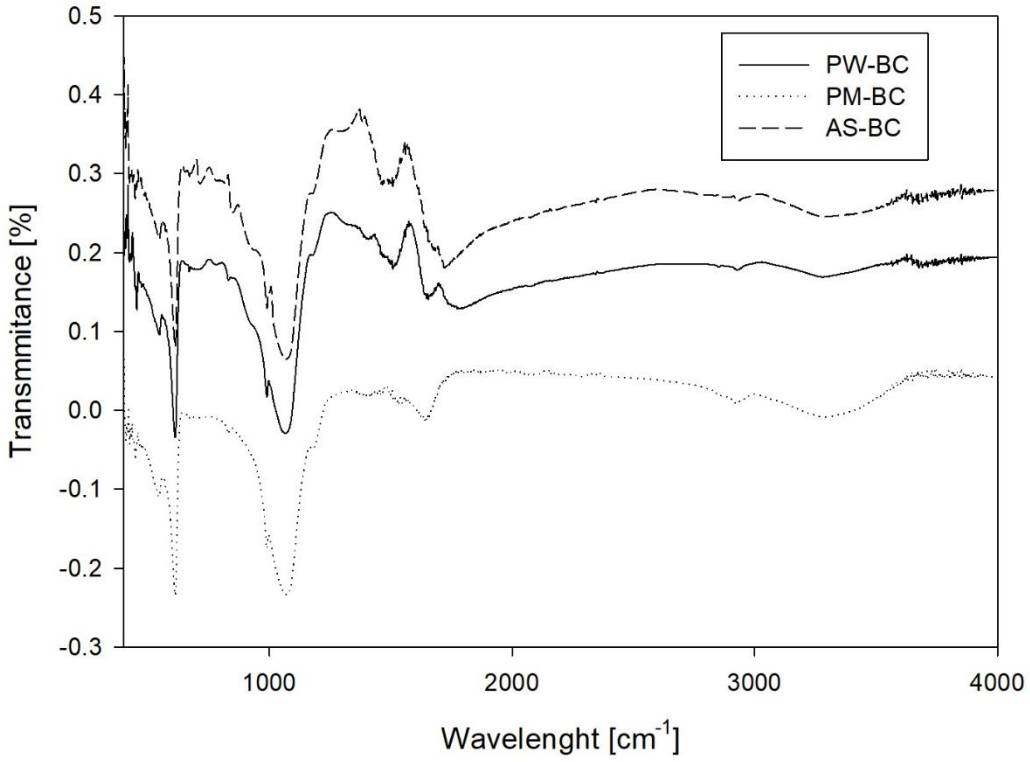

Figure S1. FTIR Spectra of tested biochars

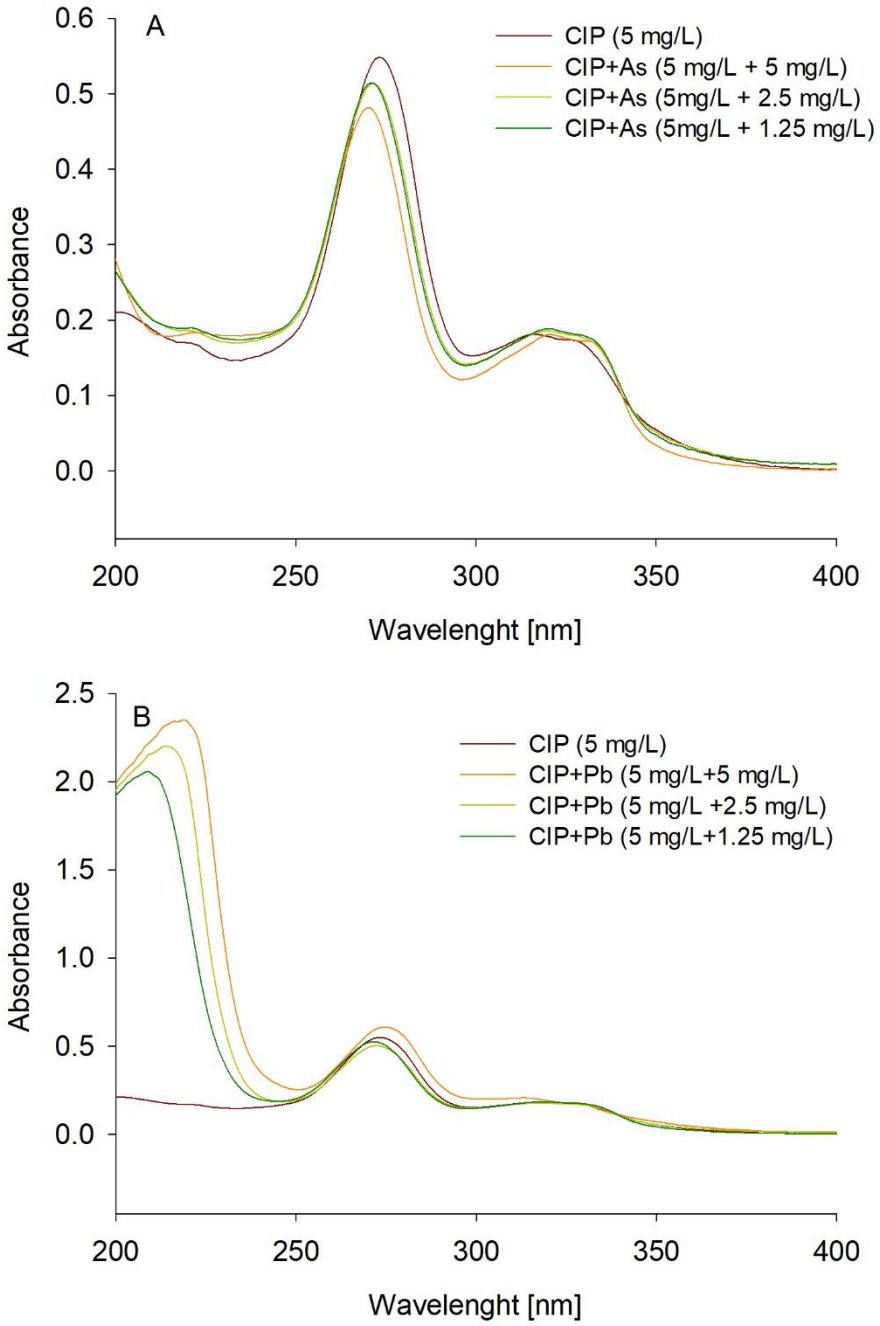

Figure S2. UV-Vis absorption spectra of ciprofloxacin (CIP) in the presence of different concentrations of A. As; B. Pb

1. Carretero, V., C. Blasco, and Y. Picó, *Multi-class determination of antimicrobials in meat by pressurized liquid extraction and liquid chromatography–tandem mass spectrometry.* Journal of Chromatography A, 2008. **1209**(1): p. 162-173.

2. Martínez-Carballo, E., et al., *Environmental monitoring study of selected veterinary antibiotics in animal manure and soils in Austria.* Environmental Pollution, 2007. **148**(2): p. 570-579.

3. Ferhi, S., et al., *Factors influencing the extraction of pharmaceuticals from sewage sludge and soil: an experimental design approach.* Analytical and Bioanalytical Chemistry, 2016. **408**(22): p. 6153-6168.

4. Castiglioni, S., et al., *A multiresidue analytical method using solid-phase extraction and high-pressure liquid chromatography tandem mass spectrometry to measure pharmaceuticals of different therapeutic classes in urban wastewaters.* Journal of Chromatography A, 2005. **1092**(2): p. 206-215.

5. Puicharla, R., et al., *A persistent antibiotic partitioning and co-relation with metals in wastewater treatment plant—Chlortetracycline.* Journal of Environmental Chemical Engineering, 2014. **2**(3): p. 1596-1603.

6. Lee, H.B., T.E. Peart, and M.L. Svoboda, *Determination of ofloxacin, norfloxacin, and ciprofloxacin in sewage by selective solid-phase extraction, liquid chromatography with fluorescence detection, and liquid chromatography--tandem mass spectrometry.* J Chromatogr A, 2007. **1139**(1): p. 45-52.

7. Jacobsen, A.M., et al., *Simultaneous extraction of tetracycline, macrolide and sulfonamide antibiotics from agricultural soils using pressurised liquid extraction, followed by solid-phase extraction and liquid chromatography–tandem mass spectrometry.* Journal of Chromatography A, 2004. **1038**(1): p. 157-170.